NASA CR-145369

FINAL REPORT– Volume I

STUDY OF FUEL SYSTEMS FOR LH_2-FUELED SUBSONIC TRANSPORT AIRCRAFT

by G. D. Brewer
R. E. Morris
G. W. Davis
E. F. Versaw
G. R. Cunnington, Jr.
J. C. Riple
C. F. Baerst
G. Garmong

July, 1978
Prepared under Contract NAS 1-14614

for

NASA

Langley Research Center
National Aeronautics and Space Administration

by

Lockheed – California Company
Burbank, California

supported by

Lockheed Missiles and Space Company, Inc.
AiResearch Divisions of the Garrett Corporation
Rocketdyne Division of Rockwell International

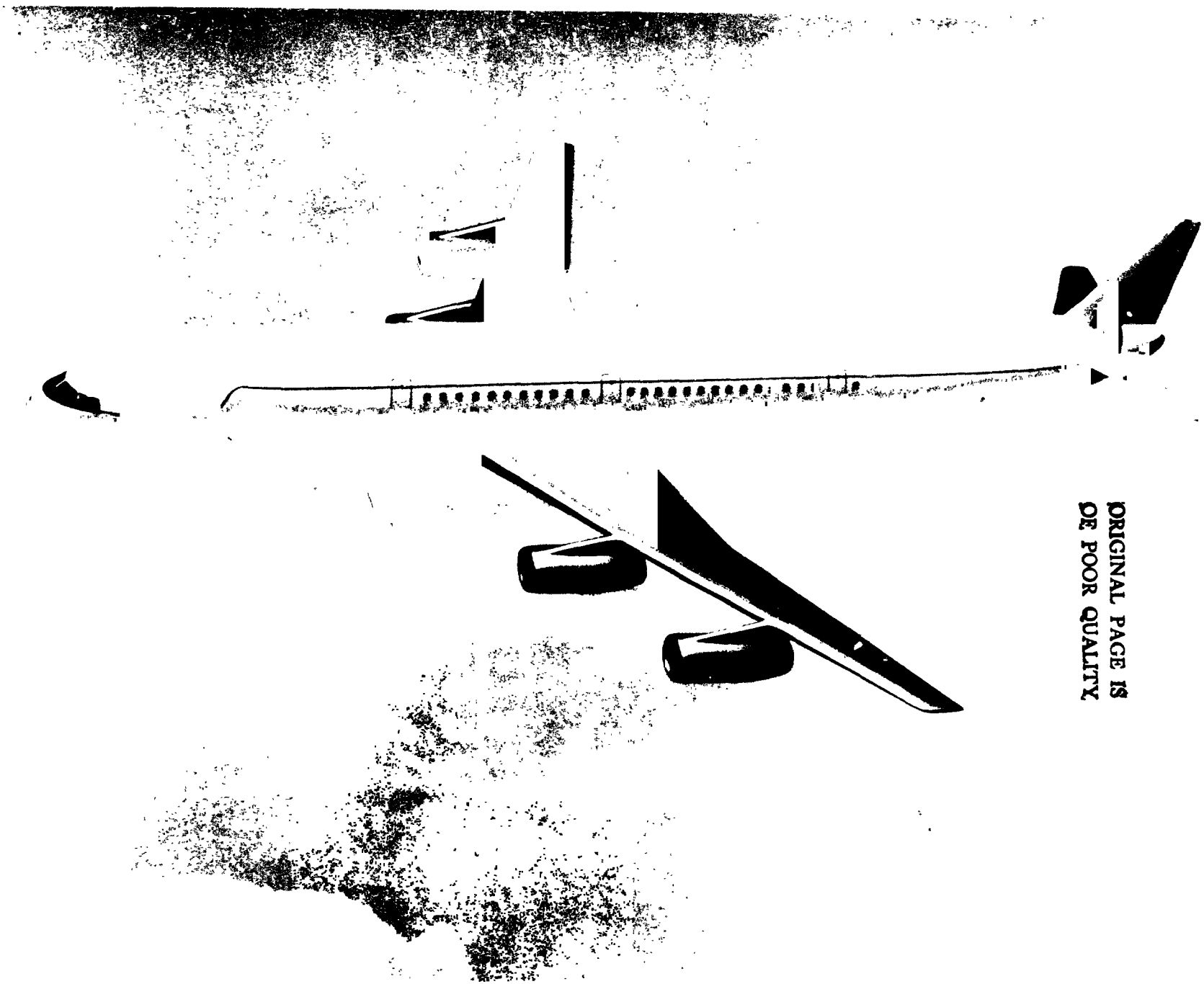

Frontispiece: Subsonic LH_2 fueled Transport

FOREWORD

This is the final report of a study made under Contract NAS 1-141614 for NASA-Langley Research Center, Hampton, Virginia. Mr. Robert D. Witcofski of the Aeronautical Systems Division at NASA-Langley Research Center was technical monitor for the study. The report presents results of work performed during the 14 month period, October 1976 through November 1977. Volume I contains Sections 1 through 6; Volume II contains Sections 7 through 10, and Appendixes A through G.

The Lockheed-California Company was the prime contractor to NASA and the work was performed in the Commercial Advanced Design Division at Burbank, California. In addition, important segments of the work which required special expertise were subcontracted to the following organizations. The individuals named were principal contributors.

LOCKHEED-CALIFORNIA COMPANY

G. Daniel Brewer, Study Manager

Robert E. Morris, Project Engineer

George Davis, Structures

Edward Versaw, Fuel Systems

Roger Jensen, Weights

Roy Adamson, Propulsion

Dalen Horning, DOC Analysis

LOCKHEED MISSILES AND SPACE COMPANY, INC.

George Cunnington, Jr., Tank Insulation

Richard Parmley, Tank Insulation

Jorgen Skogh, Tank Stress Analysis

Richard Cima, Heat Transfer Analysis

AIRESEARCH DIVISION OF THE GARRETT CORP.

James C. Riple, Engine Pump and Fuel Control System

Carl F. Baerst, LH_2 Engine Design

ROCKETDYNE DIVISION OF ROCKWELL INTERNATIONAL

Greg Garmong, Engine Fuel Supply System

William R. Bissell, Boost Pump

Ron Tobin, Fuel Feed Lines

TABLE OF CONTENTS

TABLE OF CONTENTS (Continued)

TABLE OF CONTENTS (Continued)

TABLE OF CONTENTS (Continued)

STUDY OF FUEL SYSTEMS FOR LH_2-FUELED SUBSONIC TRANSPORT AIRCRAFT

G. D. Brewer, R. E. Morris, G. W. Davis, E. F. Versaw
G. R. Cunnington, Jr.,* J. C. Riple,** C. F. Baerst,** G. Garmong,***

Lockheed-California Company
Burbank, California

SUMMARY

Concern for the potential short supply of petroleum-base fuels has led to a series of studies sponsored by NASA which have explored the technological aspects and established the potential of using liquid hydrogen (LH_2) for fuel in advanced commercial transport aircraft. Previous studies have investigated most promising methods of producing hydrogen, processes for liquefying the gas, aircraft configurations, and air terminal design and operations as they would be affected by introduction of LH_2-fueled aircraft.

The present study was directed at exploring the design problems presented by the fuel system of a representative LH_2-fueled transport. This encompasses everything required in the aircraft to contain, control, or handle the fuel. Although hydrogen fuel systems have been developed for space mission applications, the requirements for aircraft are so different in regard to mission duration, system life, operating cycles, and safety aspects that entirely different design problems are presented. The experience with LH_2 systems in the U.S. Space Program did, however, provide valuable reference data and serve as a point of departure in establishing designs for some of the aircraft components.

An aircraft design from a previous study performed by Lockheed for NASA (Reference 1) was used as basis for developing the fuel system design. The aircraft is shown in the frontispiece. It carries 400 passengers 10 190 km (5500 n.mi.) at a cruise speed of Mach 0.85. A design guideline was that the technology should represent initial operational capability in 1990-1995.

In order to provide maximum competence in all aspects of the study Lockheed-California Company was supported by Lockheed Missiles and Space Company, Inc., the California and Arizona AiResearch Divisions of the Garrett Corporation, and the Rocketdyne Division of Rockwell International in the performance of the work.

An initial task in the study was to define an efficient engine cycle, one which would take best advantage of the unique properties of hydrogen. Five ideas for exploiting the advantages offered by the large heat capacity and the low temperature of hydrogen were explored. These included precompressor cooling, compressor interstage cooling, cooling of the turbine cooling air, regenerative

---

*Lockheed Missiles and Space Company

**AiResearch Divisions of the Garrett Corporation

***Rocketdyne Division of Rockwell International

heating of the hydrogen fuel by the core exhaust, and use of an expansion cycle in connection with exhaust heat regeneration to provide power for engine accessories. In addition, two levels of turbine rotor inlet temperatures, 1482 and 1760°C (2700 and 3200°F), were evaluated, each in conjunction with an appropriate range of values of cycle pressure ratios and fan pressure ratios to permit selection of a preferred set of those parameters. All of this work was based on a definition of engine component performance and efficiencies agreed upon as representative of technology which can be developed for operational use by 1990.

The selected engine cycle was based on the following characteristics at sea level static, standard day conditions.

Rotor Inlet Temperature	1482°C (2700°F)
Cycle Pressure Ratio	35
Fan Pressure Ratio (tip)	1.594
Bypass Ratio	10.25

The design uses hydrogen to cool the turbine cooling air, the engine oil and ECS air, and also provides for heating the fuel to 677°K (1219°R) in an exhaust regenerator before injection into the combuster.

The engine fuel supply system and the engine delivery and control system received significant attention. The engine fuel supply system takes the LH_2 out of the tanks and delivers it to the inlet of the engine high pressure pump. It consists, in main, of the boost pumps, valves, and fuel delivery lines. For reasons of reliability, each of the four tank compartments in the airplane is provided with a cluster of three boost pumps. The pumps are three-stage, variable speed, centrifugal designs which are driven by 270 Vdc motors. They are designed to be line replacable units (LRU's) for ready removal from the airplane in case they malfunction.

Fuel delivery lines are stainless steel, 2.54 cm dia x 0.406 mm wall (1.0 in. x 0.016 in.). The lines are enclosed in 3.81 cm (1.5 in.) of closed cell foam insulation, which is itself contained in a 10.16 cm dia. x 0.406 mm wall (4 in. x 0.016 in.) aluminum tube which serves as a vapor barrier and provides mechanical protection.

The engine delivery and control system consists of the engine-mounted high pressure pump, heat exchangers, and the fuel control system, all mounted in the engine nacelle. The engine pump is a two-stage centrifugal design, shaft driven at a fixed speed ratio. It is designed to take saturated liquid hydrogen (0 NPSH) at 345 kPa (50 psia) and provide a flow of 0.454 kg/sec (1.0 lb/sec) at a pressure rise of 4813 kPa (698 psi). Its design rotational speed is 50 000 rpm.

The engine fuel control system employs electronic control circuitry and has a flowmeter and a flow-modulating and shut-off valve located just ahead of the engine combustor to control fuel flow to the engine. These units are located downstream of the heat exchangers to avoid lag in response which would otherwise result from the capacities of the heat exchangers.

Fuel subsystems which were designed include the following: Fueling/Defuel, Vent and Pressurization, Fuel Transfer, and Fuel Jettison. The design requirements of each of these subsystems was established, then the designs were created so weights and costs could be estimated and operational requirements assessed.

An extensive analytical study was carried out to determine the best design for the fuel containment system. This consisted of investigation of various tank structural concepts and 15 different tank insulation systems. The structural investigation included analysis of both integral and nonintegral tank designs, plus several parametric studies involving consideration of

- dome shape
- pressure stabilization
- pressure level
- design life
- tank support methods

The tank insulation study consisted of a concept screening phase in which 15 designs were investigated, followed by selection and more detailed examination of four preferred candidates, two each for integral and nonintegral tank structural designs. These four candidates were each treated as a basis for a separate airplane design so the comparison and final choice could be made in terms of parameters of primary interest to aircraft operators.

Tank insulation concepts which originally entered the concept screening phase included representatives of all conceivable types including active systems dependent on reasonably hard vacuum [0.0133 Pa (1×10^{-4} Torr)] ; some which were self evacuating by a process of cryopumping an included gas; and those which were completely passive.

The fuel containment system which ranked highest in the overall rating scheme was a design which used an integral tank and an insulation system consisting of tiny, hollow borosilicate spheres (microspheres) contained in an annulus enclosing the tank which is pumped to a soft vacuum. The design pressure in the annular space is 13.33 Pa (0.1 Torr). A very close second choice in the final evaluation was a design which also used an integral tank but the insulation system was a wrap of closed cell plastic foam around the tank, with a vapor barrier then wrapped around that to prevent air from penetrating the foam. These two insulation systems were so close in the ratings it is recommended both be further developed. The nonintegral tank designs were eliminated because of their inherent tendency to be both heavier and thicker.

Following the design of all elements of the aircraft LH_2 fuel system it was required that a comparison be made between the LH_2 and a corresponding Jet A-fueled aircraft. To do this it was necessary to generate a Jet A engine design which matched the component performance used in the subject LH_2 engine. This was accomplished and LH_2-fueled and Jet A-fueled aircraft designs were then established so the comparison of their characteristics could be made. A summary of some of the significant parameters is presented in the following table.

		LH_2	Jet A	Ratio $\left(\frac{\text{Jet A}}{LH_2}\right)$
Gross weight	kg	168 829	232 056	
	(lb)	(372 200)	(511 600)	1.37
Operating empty wt	kg	103 305	107 363	
	(lb)	(227 750)	(236 700)	1.04
Block fuel weight	kg	21 621	72 365	
	(lb)	(47 670)	(159 540)	3.35
Thrust per engine	N	135 000	184 900	
	(lb)	(30 350)	(41 567)	1.37
Wing area	m^2	296.8	380.3	
	(ft^2)	(3195)	(4093)	1.28
Span	m	51.7	58.5	
	(ft)	(169.6)	(191.9)	1.13
Body length	m	65.7	60.0	
	(ft)	(215.6)	(197.0)	0.914
Aircraft price	$\$10^6$	43.39	44.53	1.03
DOC*	¢/seat km	0.869	0.907	
	(¢/seat n.mi.)	(1.609)	(1.679)	1.04
Energy utilization	kJ/seat km	636	759	
	(Btu/seat n.mi)	(1118)	(1334)	1.19

*Calculated for baseline prices of each fuel; \$5.69/GJ (\$6/10^6Btu) for LH_2 and \$4.74/GJ (\$5/10^6 Btu) for synthetic Jet A, assuming both fuels are made from coal.

The LH_2-fueled design is superior in nearly every parameter. In fact, the advantages are greater than those calculated originally as presented in Reference 1. This is due primarily to a more conservative appraisal of some engine component efficiencies, reflected in engines using both fuels; however, through exploitation of the properties of hydrogen, the specific fuel consumption of the LH_2 design was nearly restored to its original value. At the baseline price for synthetic Jet A, a price differential amounting to an additional \$1.59 per GJ (\$1.67/10^6 Btu) can be paid for LH_2 fuel and still provide equal DOC.

A list of 12 items is recommended for development of technology or to provide information needed in order for LH_2-fueled aircraft to become a viable possibility. The items are arranged in order of priority according to scheduling requirements. Development of an aircraft tank and insulation system and LH_2 pumps is considered top priority.

NOMENCLATURE

NOTE: Computations in this analysis were performed in U.S. Customary units and then converted to S.I. units.

AR	=	Aspect Ratio
ATA	=	Air Transport Association
BPR	=	Bypass Ratio
CPR	=	Cycle Pressure Ratio
DOC	=	Direct Operating Cost
E_c	=	Young's Modules of Elasticity (compression)
E_t	=	Young's Modules of Elasticity (tension)
ECS	=	Environmental Control System
FAR	=	Federal Air Regulation
FCS	=	Fuel Containment System
fg	=	Fiberglass
F_N	=	Net Thrust
FPR	=	Fan Pressure Ratio
F_{t_u}	=	Ultimate fiber stress, tension
H	=	Head in feet
HC	=	Honeycomb
HP	=	High Pressure
H.P.EXT	=	Horsepower Extraction
I	=	Integral
IGV	=	Inlet Guide Vanes
IOC	=	Initial Operational Capability
Jet A	=	Conventional Hydrocarbon fuel
KEAS	=	Knots Equivalent airspeed
L/D	=	Lift-to-Drag ratio
LH_2	=	Liquid Hydrogen
LHV	=	Fuel Lower Heating Value
LP	=	Low Pressure
M	=	Mach Number
M_D	=	Design Mach Number

NOMENCLATURE (Continued)

N	=	Rotational speed, rpm
NI	=	Nonintegral
NPSH	=	Net Positive Suction Head
OPR	=	Overall Pressure Ratio
OEW	=	Operating Empty Weight
P	=	Pressure
PLA	=	Positive Low Angle of Attack
P_{T_2}	=	Average Fan Face Total Pressure
P_{T_0}	=	Freestream Total Pressure
Q	=	Heating rate or Volumetric flow rate in gpm
QEC	=	Quick Engine Change Nacelle
RIT	=	Rotor Inlet Temperature
S	=	Wing Reference Area
SLS	=	Sea Level Static
TOGW	=	Takeoff Gross Weight
T/W	=	Thrust to Weight Ratio
TCA	=	Turbine Cooling Air
TIT	=	Turbine Inlet Temperature
VjP	=	Primary exhaust jet velocity
VjD	=	Fan Duct exhaust jet velocity
Vo	=	Flight velocity
Vr	=	Takeoff rotate Velocity
Vs	=	stall Velocity
$\dot{w}$	=	Flow rate
$\dot{w}_a \frac{\sqrt{\theta_{T_2}}}{\delta_{P_2}}$	=	Engine corrected airflow
W_{pod}	=	Engine pod weight
W/S	=	Wing Loading = $\frac{\text{Aircraft weight}}{\text{wing area}}$
ZFW	=	Zero Fuel Weight
α	=	Angle of Attack
δ_{P_2}	=	Delta $P_2 = P_{T_2}$ (PSIA/14.7)

NOMENCLATURE (Continued)

θ_{T_2}	=	Theta $T_2 = T_{T_2}$ ($^{o}K/288.2$)
η	=	efficiency
ρ	=	density
ϵ	=	heat exchanger effectiveness

1. INTRODUCTION

As a result of serious concern regarding the potential short supply of petroleum-base fuels, in 1973 the National Aeronautics and Space Administration instigated a program to investigate alternate fuels for commercial transport aircraft.

Liquid hydrogen (LH_2), liquid methane (LCH_4), and synthetic Jet A (synjet), all manufactured from coal and water, are leading alternate fuel candidates. To date, attention has been focused primarily on liquid hydrogen and on synjet, assuming the synthetic jet fuel would have the same properties as the present fuel for commercial airliners, Jet A or Jet A-1. Aircraft designs based on use of both of these alternate fuels have been created and compared (Reference 1), and the facilities, equipment, and operations needed at representative major air terminals to service liquid hydrogen-fueled aircraft have been studied (References 2 and 3).

The LH_2-fueled aircraft design from the previous study (Reference 1) was a conceptual design in which advanced technology features were incorporated representing an initial operational capability in the 1990 decade. The aircraft was sized to carry 400 passengers 10 190 km (5500 n.mi.) at a cruise speed of Mach 0.85. Necessarily, many assumptions were mad concerning the characteristics of the LH_2-fueled engine, the fuel containment system, the engine fuel supply system, and other elements of the complete aircraft fuel system.

In the present work, attention was focused on precisely those items so that a more realistic evaluation of the potential of a hydrogen fueled transport aircraft could be obtained. The objectives of this study were as follows:

- Define the characteristics of a preferred design of fuel system for the specified LH_2-fueled transport aircraft.
- Establish the size, weight, cost and performance of the LH_2-fueled aircraft using the final fuel system design.
- Compare the LH_2-fueled aircraft with an equivalent technology Jet A-fueled design.
- Identify related research and technology development requirements for the LH_2 fuel system.

An outline of the approach taken in performing this study is described in Section 2.

2. TECHNICAL APPROACH

2.1 Team Organization

The wide scope of technical expertise required to define adequately a practical fuel system for a liquid hydrogen-fueled aircraft led to formation of a team, the members of which were selected for their competence in specified technical areas. Lockheed-California Company reached agreement with the following companies to participate in the study on a subcontract basis to provide special skills and innovative thinking in the areas indicated:

- Lockheed Missiles and Space Company, Inc. - For analysis, design, and evaluation of cryogenic insulation systems, and for specialized tank structural analysis

- Airesearch Divisions of the Garrett Corporation - For analysis and design of an advanced design LH_2-fueled turbofan engine, a fuel control system, pumps and other specific components

- Rocketdyne Division of Rockwell International - For analysis and design of the LH_2 engine fuel supply system, and for boost pump design

This team provided an ideal combination of basic knowledge and familiarity with the reference aircraft design, plus experience with technology developed in the U.S. Space Program on cryogenic fuel systems in general, and use of LH_2 in particular.

2.2 Work Plan

A schematic representation of the study work plan is shown in Figure 1. The work was performed in four phases. Phase I involved compilation of input data needed in the remainder of the study. These items are described in Section 3.

Phase II, System Studies, was the focus of the principal effort of the study. In this phase, the designs of the LH_2-fueled turbofan engine, the engine fuel supply system, the fuel subsystems, and the fuel containment system were established. In essence, these tasks involved examining the requirements, originating design concepts for evaluation, and choosing preferred designs for each of these elements of the fuel system of an LH_2-fueled aircraft. In addition, a comparable design of Jet A-fueled turbofan engine was also established to provide a basis for equivalent comparison of aircraft operated with the respective fuels.

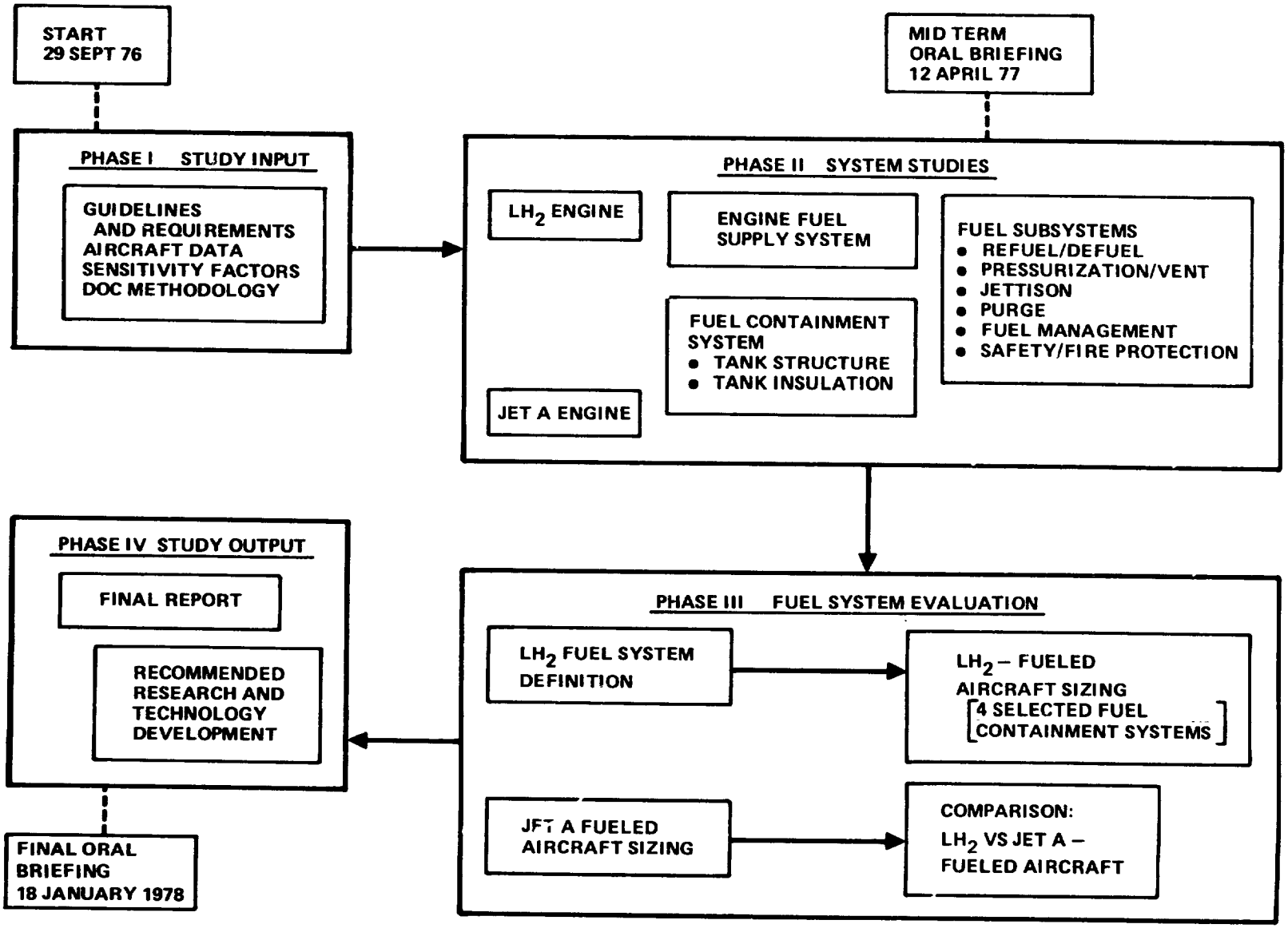

Figure 1. – Study work plan.

Phase III was an evaluation of the fuel system design which resulted from the work of Phase II. Drawings of the engine fuel supply system, the pressurization/vent system, and the fueling/defuel system, plus principal components of each of these, were prepared so weight, reliability, maintenance, and operational requirements could be assessed.

Four designs of fuel containment systems (tank structure, insulation system, and support structure) were selected from 15 candidates originally conceived and studied. These four selected designs were evaluated using the Lockheed Aircraft System Synthesis Evaluation Technique (ASSET) computer program to establish the potential of each in terms of aircraft size, weight, performance, and cost. Direct operating cost (DOC) was the principal measure of merit used in selecting the final preferred design.

The characteristics of the aircraft with the preferred fuel containment system, which also used the LH_2 engine and fuel system designs from Phase II, were compared with those of an equivalent technology Jet A-fueled aircraft. The Jet A design was subjected to the same optimization procedure using ASSET as the LH_2-fueled design so that the comparison would be on an equitable basis.

Phase IV consisted of summarizing the results of the work and preparing the final report. A recommended research and technology development program for critical LH_2 fuel system elements was formulated as a part of this effort.

3. STUDY GUIDELINES AND INITIAL DATA

Information required to perform analyses of the LH_2-fueled engine and fuel system components was generated or assembled as an initial step in the program. This work included reaching agreement with NASA on specific guidelines and requirements to be met; compiling basic data from Reference 1 on the baseline aircraft into a convenient package; generating sensitivity factors so that the benefit or liability of changes in key aircraft parameters could be assessed, and thus provide help in guiding design decisions; and finally, formulating a procedure for calculating direct operation cost (DOC) for the subject aircraft which would reflect a reasonable approximation of current airline practices, and which would also account for differences between LH_2-fueled and conventionally fueled aircraft.

3.1 Guidelines and Requirements

The guidelines and requirements which were established for use during the study are listed in Table 1. These items were either originally specified by NASA as a basis for the study, or were perceived during the early stages of the program as being necessary for validity and consistency of results.

3.2 Basic Data

Basic information on the reference LH_2-fueled aircraft, and its design mission, which was needed to establish a starting point for the fuel system design requirements and analysis was derived, for the most part, from Reference 1. Some additional information was generated by making special runs of the ASSET computer program, and by separate analyses. In all, the following items were assembled and transmitted to all study team members and to the NASA Technical Monitor as preliminary data:

- Drawing CL 1317-1-1, General Arrangement - LH_2 M 0.85, 400 PAX, 10 190 km (5500 n.mi.)
- Drawing CL 1317-1-4, Engine Feed System - LH_2 Subsonic Transport (preliminary draft)
- Drawing CL 1317-1-5, Fueling/Vent System - LH_2 Subsonic Transport (preliminary draft)
- Design Mission Fuel Flow Schedule (shown in Appendix A).

TABLE 1. - GUIDELINES AND REQUIREMENTS

Baseline aircraft: Final design in Reference 1: 400 passengers, 10 190 km (5500 n.mi.) range, Mach 0.85 cruise speed. See Figure 2.

Initial Operational Capability: 1990 - 1995

Baseline fuel costs:

LH_2 = \$5.69 per GJ (\$6 per 10^6 Btu = 31¢/lb)

Synjet = \$4.74 per GJ (\$5 per 10^6 Btu = 9.2¢/lb = 62.2¢/gal)

DOC basis:

1967 ATA equations updated to 1976 cost experience and modified to more accurately reflect airline practice, as well as differences resulting from use of alternate fuels. Assume production of 350 aircraft and 3600 engines.

Evaluation criteria:

DOC to be final measure of merit. All concepts must meet safety, reliability, maintainability, and operational requirements.

Safety:

Equal to or better than conventionally fueled commercial transport.

Design criteria:

Meet all applicable or anticipated regulatory requirements including FAR 25.

- LH_2 Turbofan Engine Thrust and Fuel Flow
- Fuel Flow Envelope - LH_2 Turbofan
- Design mission flight profile
- Lockheed LH_2 engine characteristics, component efficiencies, and installation factors (inlet recovery, installation drag, bleed air requirements, power extraction requirements).

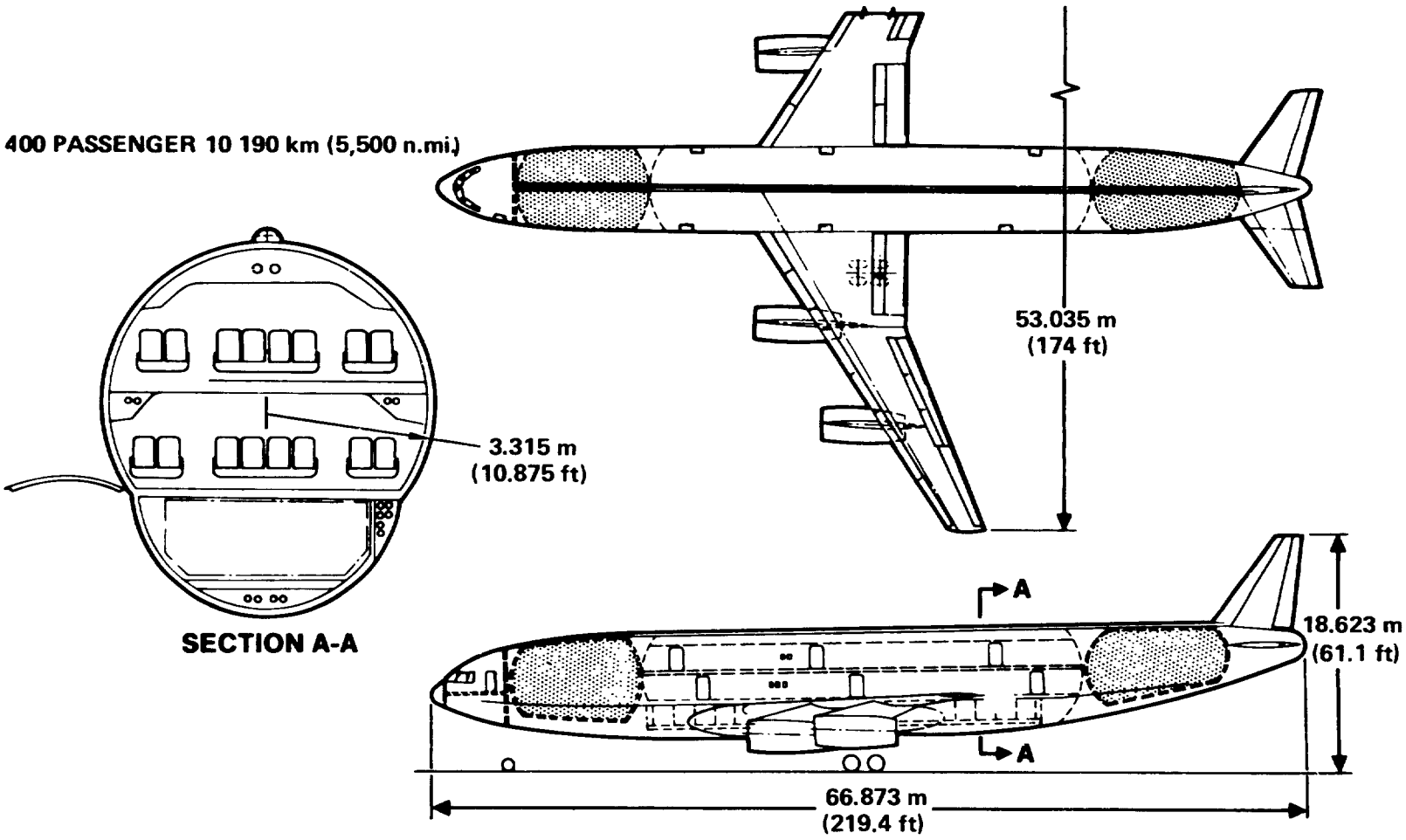

Figure 2. - Baseline LH_2-fueled passenger transport.

3.3 Sensitivity Factors

Sensitivity factors were generated for the reference LH_2-fueled airplane to provide a basis for evaluation of the effect of changes from the baseline design. For example, in the study of the LH_2 engine design, a given option may have offered a few percent reduction in specific fuel consumption (SFC), but at the expense of an increase in inert weight. Sensitivity factors were a means of evaluating the net benefit which might be realized by incorporating that option in the design of the engine. Note that the sensitivity factors were used merely as an evaluation procedure to assist in screening attractive candidates. Evaluation of final design concepts was made by incorporating appropriate data in the ASSET aircraft synthesis program.

The sensitivity factors, or exchange ratios as they are sometimes called, were established by using the ASSET computer program to define optimized vehicles for each of a series of deviations from the nominal value of items like specific fuel consumption (SFC), vehicle inert weight (W_i), and thickness of fuel tank insulation system. The results were then plotted vs various airplane characteristics so the slope of the curve through the design point represented the sensitivity of those characteristics to small changes in the parameter being studied.

An example of this process is presented in Table 2 and Figure 3. The effect of 10 percent and 20 percent changes in SFC, both above and below the nominal value, on takeoff gross weight (TOGW), fuel weight (W_f), operating empty weight (OEW), manufacturer's empty weight (MEW), engine size, airplane cost, and direct operating cost (DOC) were all evaluated. The aircraft represented by each column in Table 2 are real in the sense that they have been sized using the ASSET program so that they represent a minimum gross weight design to perform the required mission, and that they meet all the specified design constraints.

The results as plotted in Figure 3 illustrate the effect changes in SFC would have on TOGW, OEW, W_f, and DOC. The slope of the curve at the design point, shown for each case, is the sensitivity factor. It is accurate in representing the effect on the various airplane characteristics of small deviations in the subject parameter. If large deviations are contemplated, their effect must be read from the curves, or a separate evaluation must be performed.

Similar data are tabulated and plotted in Table 3 and Figure 4 to illustrate the effect changes in inert weight of the aircraft would have on certain characteristics assuming the design has not been frozen. This assumption allows design characteristics of the aircraft such as wing loading and thrust-to-weight ratio to be changed to accommodate the inert weight variations in the most efficient manner.

TABLE 2. - EFFECT OF CHANGE IN SPECIFIC FUEL CONSUMPTION

(Reference SFC_{cruise} = 0.203 (kg/hr)/daN (0.199 $\frac{lb}{hr}$/lb))

SFC Basis		80%	90%	Reference	110%	120%
TOGW	kg	162 440	169 467	177 672	186 717	196 510
	(lb)	(358 120)	(373 610)	(391 700)	(411 640)	(433 230)
Fuel wt.	kg	21 287	24 400	27 946	31 792	35 929
	(lb)	(46 930)	(53 880)	(61 610)	(70 090)	(79 210)
OEW	kg	101 242	105 111	109 810	115 008	120 660
	(lb)	(223 200)	(231 730)	(242 090)	(253 550)	(266 010)
MEW	kg	92 106	95 894	100 498	105 592	111 135
	(lb)	(203 060)	(211 410)	(221 560)	(232 790)	(245 010)
Thrust per Engine	N	116 677	121 748	127 619	134 114	141 142
	(lb)	(26 230)	(27 370)	(28 690)	(30 150)	(31 730)
Cost/aircraft	(10^6)	38.96	40.25	41.81	43.53	45.39
DOC	¢/S km	0.862	0.922	0.990	1.063	1.143
	(¢/S n.mi.)	(1.597)	(1.707)	(1.833)	(1.969)	(2.116)
	(% of ref.)	87.1	93.1	100	1.07	1.15

TABLE 3. - EFFECT OF CHANGE IN INERT WEIGHT VARIATION

Inert Wt. kg(lb)		-9 072 (-20 000)	-4 536 (-10 000)	Reference	+4 536 (+10 000)	+9 072 (+20 000)
TOGW	kg	159 306	168 918	177 672	187 365	197 304
	(lb)	(351 210)	(372 400)	(391 700)	(413 070)	(434 980)
Fuel wt.	kg	26 150	27 238	27 946	29 039	30 218
	(lb)	(57 650)	(60 050)	(61 610)	(64 020)	(66 620)
OEW	kg	93 240	101 763	109 810	118 410	127 169
	(lb)	(205 560)	(224 350)	(242 090)	(261 050)	(280 360)
MEW	kg	83 983	92 474	100 498	109 062	117 789
	(lb)	(185 150)	(203 870)	(221 560)	(240 440)	(259 680)
Thrust per Engine	N	114 453	121 347	127 619	134 603	141 720
	(lb)	(25 730)	(27 280)	(28 690)	(30 260)	(31 860)
Cost/aircraft	(10^6)	35.77	38.88	41.81	44.90	48.02
DOC	¢/S km	0.908	0.952	0.990	1.033	1.079
	(¢/S n.mi.)	(1.681)	(1.763)	(1.833)	(1.914)	(1.998)
	(% of ref.)	91.7	96.2	100	104	109

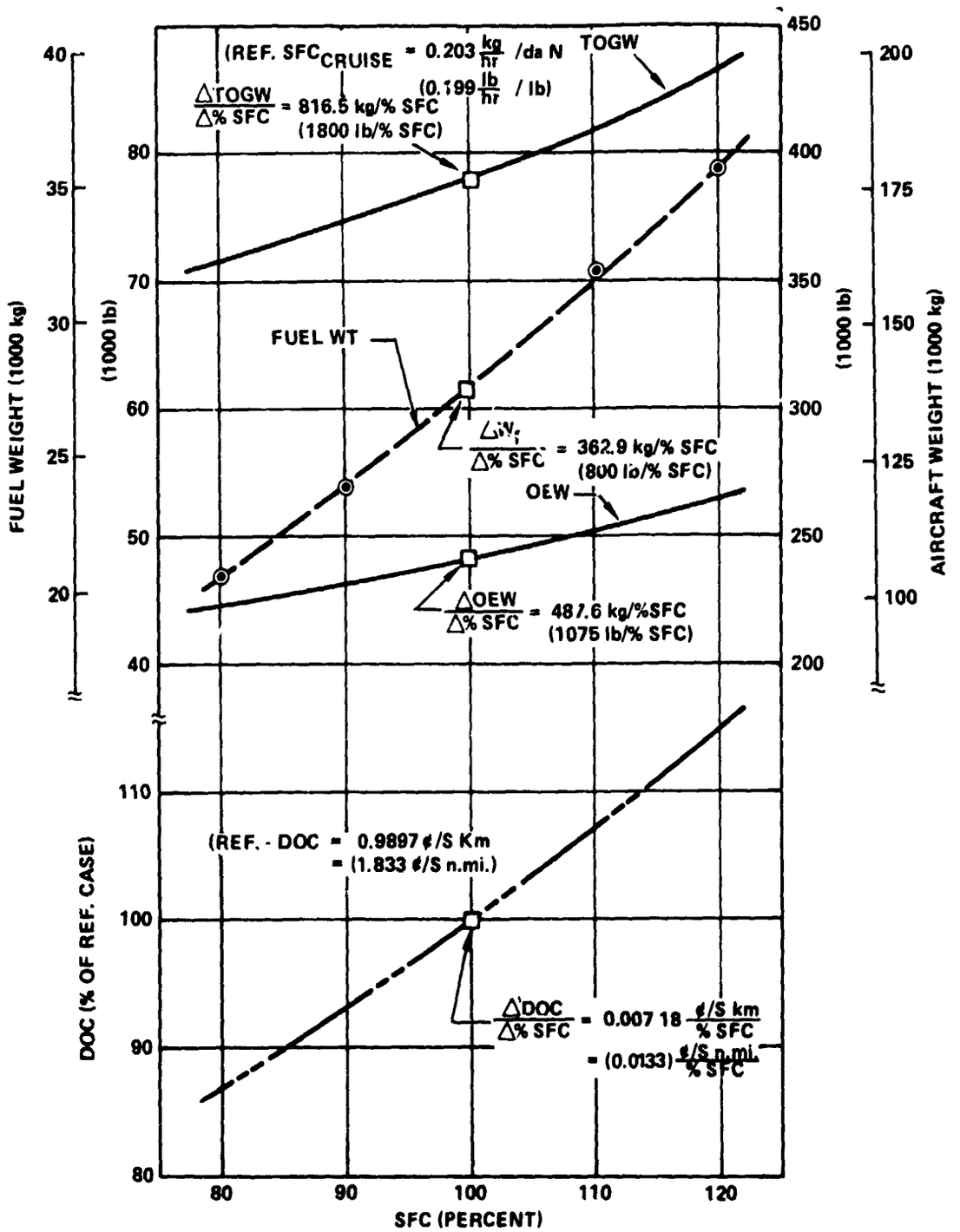

Figure 3. - Sensitivity of CL 1317-1 aircraft to changes in specific fuel consumption.

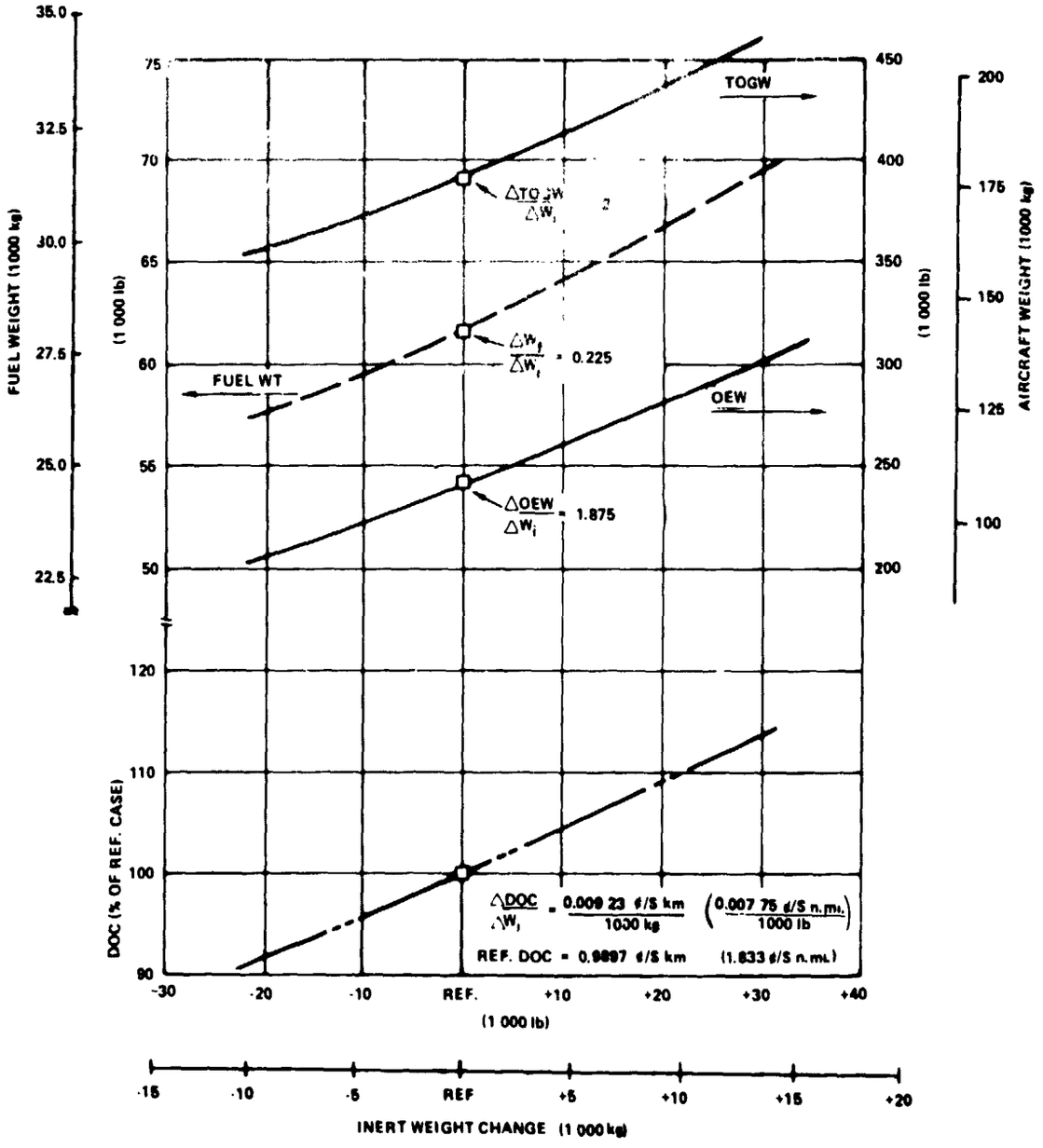

Figure 4. - Sensitivity of CL 1317-1 aircraft to inert weight change.

Sensitivity factors for these two parameters, SFC and W_i, in addition to the effect of variation in thickness of fuselage tank insulation systems and the resulting influence this would have an fuselage length, were the primary tools needed to evaluate design or concept trade-offs throughout Phase II. The following are some of the specific trade-off relationships which were developed for application during this part of the program. (Note that these sensitivity relationships were derived on the basis of U.S. Customary units. If SI units are employed, constants and coefficients in the equations will require reevaluation.)

3.3.1 Sensitivity of DOC to engine weight, SFC, and maintenance cost. - The following procedure permitted trade-offs to be made of engine cycles or concepts in which, for example, a more complex, heavier engine might deliver a reduced SFC. To use this evaluation method, it was necessary that preliminary estimates be made of the installed SFC, weight and maintenance requirements of the proposed engine relative to equivalent values for the baseline engine.

$$DOC = K\left(0.89 + 0.11\,\frac{Maint}{Maint_{bl}}\right)$$

where:

DOC is evaluated in $\frac{¢}{S\ n.mi.}$

$$K = 1.8334 + \frac{7.75}{10^6}\left[W_{prop} - W_{prop_{bl}}\right] + 1.332\left[\frac{\overline{SFC}}{\overline{SFC}_{bl}} - 1\right]$$

$\frac{Maint}{Maint_{bl}}$ = Estimated maintenance manhours and material relative to the baseline engine based on complexity, operating temperatures, pressures, etc.

$W_{prop} - W_{prop_{bl}}$ = Change in weight of the proposed engine(s) or propulsion system compared to the following baseline values:

F_{SLS}(installed) = 28 694 lb per engine

Weight (for 4 engines):

Engines	22 141 lb
Exhaust (including thrust rev.)	2006 lb
Inlets	2558 lb
Nacelles	6559 lb
Start system	33 686 lb

Installed $\frac{thrust}{weight} = \frac{4 \times 28694}{33686} = 3.41$

(Note that the proposed engine thrust level must be the same as the baseline engine for a valid comparison.)

$\frac{\overline{SFC}}{SFC_{bl}}$ = Estimated SFC of the proposed engine relative to values for the baseline engine.

The scaling limits of this method are: $\pm$15% SFC

$\pm$4536 kg ($\pm$10 000 lb) weight

3.3.2 Sensitivity of DOC to fuel pumping system power and weight. - This trade-off was for purposes of assessing the relative benefit (or liability) of weight vs power requirements of candidate pumping systems. ASSET vehicle synthesis data were used, together with the baseline engine characteristics, to obtain an approximation of the horsepower-weight trade-off of tank-mounted aircraft fuel pumping systems. It was assumed that the pumps were driven by electric, hydraulic, or other suitable power source extracted from the engine accessory drive. The approach used was to compare systems on the basis of the incremental change in direct operating cost (DOC) as shown:

$$DOC = \frac{3.22}{10^5} \Sigma hp_{cruise} + \frac{7.75}{10^6} \left[W_{system} + 6 \Sigma hp_{max} \right]$$

where:

DOC is expressed in $\frac{¢}{S \text{ n.mi.}}$

Σhp_{cruise} = total input horsepower to all pumps running during cruise flight

W_{system} = total weight of pumping system including pumps, drives, installation, plumbing, etc.

$6 \Sigma hp_{max}$ = factor to account for the aircraft system installed weight penalty to provide the necessary input power. This is based on the total maximum horsepower of tank-mounted pumps.

EXAMPLE:

Drive type	System No. 1 Electric	System No. 2 Hydraulic
Σ hp max	80	70
Σ hp cruise	50	40
Wt. pumps - lb	40	40
Wt. drives	58	90
Wt. installation	20	30
Wt. lines	100	120
W_{system}	218	280

$$DOC_{Sys\ No.\ 1} = 0.0000322 \times 50 + \frac{7.75}{10^6} (218 + 6 \times 80)$$

$$= 0.0016 + 0.00541$$

$$= 0.00702 \frac{¢}{S\ n.mi.}$$

$$DOC_{Sys\ No.\ 2} = 0.000322 \times 40 + \frac{7.75}{10^6} (280 + 6 \times 70)$$

$$= 0.00129 + 0.00543$$

$$= 0.00672 \frac{¢}{S\ n.mi.}$$

System No. 2 has the lowest increment of DOC and would be favored over No. 1. However, since this evaluation does not address the important aspects of reliability and maintenance, it can only be considered as a screening

means to eliminate the least likely candidates or to measure the relative impact of power consumption and weight trade-offs on the aircraft.

3.3.3 Sensitivity of DOC to volume and weight of fuel containment system. - The various candidate tank insulation systems and tank structural concepts offer trade-offs of thickness "t" (measured from inside surface of tank to exterior surface of aircraft) and weight. As thickness varies, the aircraft fuselage length must change to provide the required fuel volume within the fixed fuselage cross section. The following procedure, and associated values of influence coefficients, was derived from a matrix of ASSET cases which were run to simulate all reasonable combinations of fuel containment system thicknesses and weights. As noted earlier, all aircraft represented by the combinations of thickness and weight in the matrix are real in that they are sized to perform the design mission while meeting necessary design constraints.

1. Determine total fuel boiloff for the 10 190 km (5500 n.mi.) mission for the insulation concept and thickness being evaluated.

2. Calculate the fuel tank volume required using the following allowances:

	Integral Baseline Case	New Case
• Ullage	2.00%	2.00%
• Net tank contraction due to cooling*, plus expansion due to pressurization	0.90	0.90
• Structure and equipment	0.64	0.64
• Trapped and unusable fuel	1.60	1.60
Subtotal	5.14	5.14
• Boiloff:		
Pressurant gas	1.00	As
Vented gas	2.56	Calculated
Total Allowance (percent)	8.70	5.14 + % Boiloff

*where insulation is on outside of tank

$$\text{Total Vol}/_{\text{tank}} = \frac{61\ 630}{2} \times \frac{\dfrac{1}{\rho_{H_2}\ \text{(Sat. liq. at 21 psia)}}}{1 + \dfrac{\text{Total allowance (\%)}}{100}}$$

For baseline case:

$$\text{(Ref.)} = \frac{61\ 630}{2} \times \frac{\dfrac{1}{4.325}}{1.087} = 7746\ \text{ft}^3/_{\text{tank}}$$

3. From Figure 5, find the aircraft fuselage length (L_{fus}) knowing "t".

4. Calculate the installed weight of the total fuel containment system (ΣW_{fcs}). Assume weight of forward tank is same as aft tank.

   NOTE: Installed weight includes tank, tank supports, shell structure (nonintegral), insulation, adhesive, vapor barrier protective cover, etc. For nonintegral tanks add the weight of the fuselage shell structure in the tank region and the tank removal provisions. Assume forward tank shell specific weight is the same.

5. Calculate DOC using the following equation:

$$\text{DOC} = 1.8334 + \frac{7.75}{10^6}\left(\Sigma W_{fcs} + \Sigma W_{H_2} - 82\ 294\right)$$

$$+ \frac{3540}{10^6}\left(L_{fus} - 224.3\right)$$

where:

1.8334 = Baseline aircraft DOC - ¢/S n.mi. (fuel cost = $\$6/10^6$ Btu)

$\frac{7.75}{10^6}$ = Wt. influence coefficient

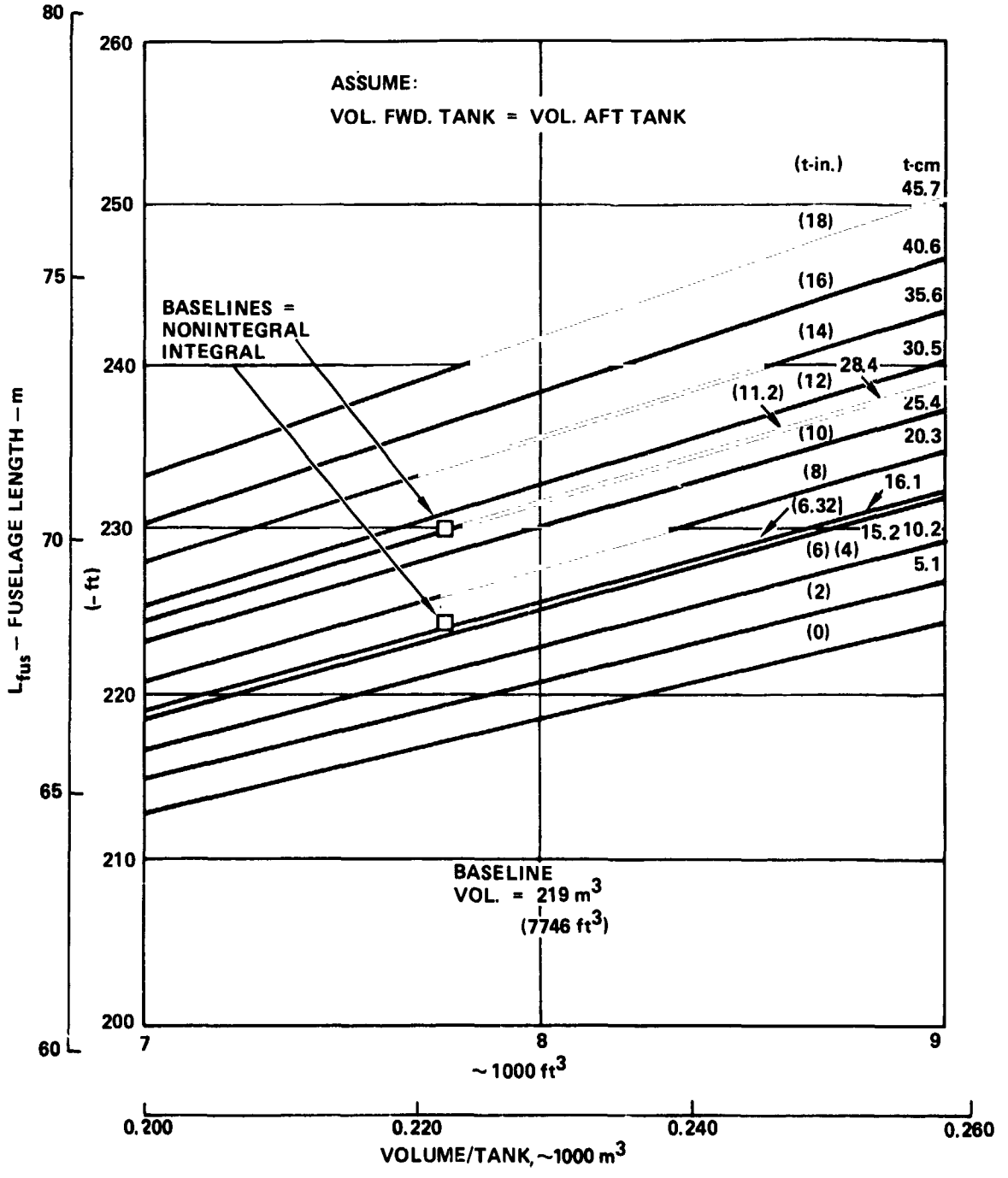

Figure 5. - Fuselage length vs fuel containment system thickness and tank volume.

$\frac{3540}{10^6}$ = Length influence coefficient

224.3 = Fuselage length (feet) for baseline integral tank (with t = 6.32 in.)

82 294 = $\Sigma W_{fcs} + \Sigma W_{H_2}$ for the baseline integral tank design

ΣWH_2 = Weight of tanked liquid plus both pressurization and vented gas.

3.3.4 Sensitivity of DOC to aircraft ground losses. - The choice of fuel containment concept is influenced by the fuel boiloff losses during tank refueling and by the boiloff during the daily out-of-service periods. In the LH_2 Airport Requirements Study (Reference 2) the economic desirability of collecting this vent gas for reliquefaction was established. The following method of analyzing the worth of capturing and reliquefying this ground boiloff hydrogen was derived to provide a basis for comparing competitive fuel containment system concepts. The assessment is in terms of DOC.

Assumptions:

1. The vapor is returned via a vacuum jacketed collection header and insulated surge tank to the hydrogen liquefier at a point just upstream of heat exchanger X-8 (stream no. 56) as shown in Figure 7 of the report "Survey Study of the Efficiency and Economics of Hydrogen Liquefaction" (Reference 4). It enters at a pressure of 103 to 110 kPa (15 to 16 psia) and a temperature of approximately 70°K (126°R). It then passes through the heat exchanger and, in turn, through the H_2 flash and recycle compressors.

2. The cost of reliquefaction is assumed to consist of the cost of the electric power at 2¢/kWh used in recompression, and a prorated share of the storage, distribution and plant costs using the discounted cash flow (DCF) method of accounting described on page 45 of Reference 2.

   On this basis the estimated cost of reliquefaction is:

	($/lb)
Electric power	0.05
Share of plant costs	0.027
Total	0.077

The cost of the original GH_2 feedstock was, of course, included in the cost of the liquid hydrogen.

The effect of hydrogen boiloff losses on DOC of the baseline aircraft with a utilization of 4000 hours/year is:

$$\Delta DOC_{grnd.} = \frac{\Sigma W_{H_2\ grnd.}}{day} \times 3.75 \times 10^{-6} \left(\frac{¢}{S\ n.mi.}\right)$$

where:

$\Sigma W_{H_2\ grnd.}$ = total of all daily ground boiloff losses

3.4 Calculation of Direct Operating Cost

Direct Operating Cost (DOC) was used as a primary selection criteria in evaluation of design options for the LH_2 transport aircraft, and as a basis for comparing the economic performance of liquid hydrogen fueled aircraft of advanced design with that of conventionally fueled counterparts.

The 1967 ATA DOC equations (Reference 35) were used as a starting point in the derivation of an improved method for calculating LH_2 and Jet A aircraft DOC. The 1967 ATA equations do not accurately reflect operation of either current or advanced technology aircraft and therefore required considerable modification. To provide a basis for reasonable evaluation of DOC for the subject LH_2 and Jet A aircraft, an extensive survey of airline operational practices was made, actual CAB data analyzed, and Lockheed and engine manufacturer's specialists consulted regarding probable maintenance requirements of the LH_2 aircraft. The information derived as a result of this work was used to formulate modifications to the 1967 ATA formulas in terms of January 1976 dollars for international trunk operation.

3.4.1 Background. - The DOC elements, and variables which affect their evaluation as reflected in the standard ATA formula, are listed in Table 4.

The airline surveys involved a series of meetings with four major U.S. air carriers to determine the elements which are of significance to them and the parameters and methods which they conventionally use in determining DOC. The following airline representatives cooperated in the investigation and contributed valuable data and advice:

TABLE 4. - COST ELEMENTS AND VARIABLES IN 1967 ATA FORMULAS

Element	Evaluated as Functions of the Following Variables
Crew cost	GTOW
Fuel and oil	Lbs fuel, fuel cost, non-revenue flying
Maintenance	
Airframe	
Labor	Airframe weight, speed, labor rate
Material	Airplane cost
Engine	
Labor	Thrust, labor rate
Material	Engine cost
Burden	Ratio of maintenance labor cost
Insurance	% of airplane cost
Depreciation	Cost of airplane, life, residual

American Airlines	-	Mr. Jack Graef
	-	Mr. Keith Grayson
Pan American World Airways	-	Mr. William Hibbs
Trans World Airlines	-	Mr. Walt Sherwood
United Airlines	-	Mr. John Curry

The participation of these airlines was solicited to provide representation of a spectrum of route structures, operational procedures, and financial practices.*

*It should be noted that each of the airlines consulted has its own methodology for determining DOC according to its individual requirements. The method and procedure described herein should not be construed as representing that of any one of the cooperating airlines. Rather, the method presented in this report is the result of an attempt by Lockheed to represent nominal industry values.

Statistical analyses of 1973, 1975, and 1976 CAB airline operating data were made in order to provide realistic parameters in addition to those provided by the airlines. Various statistical techniques, including multiple regression, were used to identify trends in the data. The CAB data were also used to identify and quantify variations between domestic and international trunk operation, variations between airlines, and variations between types of airframes and engines. The variations between 1973, 1975, and 1976 data were used to evaluate and define trends and to provide escalation factors. Consultations with both airframe and engine specialists were used to determine relative engine life, spares requirements, and maintenance values for LH_2 operation.

Evaluation of DOC for the subject aircraft study was performed within the Lockheed ASSET computer program which was used to develop aircraft configurations and mission performance, as well as cost data. Airframe and engine costs were derived from detailed parametric formulas within ASSET using values for aircraft and engine parameters which were developed for the subject aircraft.

3.4.2 Parameters required for DOC evaluation. - The following paragraphs present the basis for evaluation of the parameters involved in determination of DOC for the subject study.

3.4.2.1 Weight: Weight is a primary factor in developing aircraft cost and DOC. Formulas containing weight as a parameter are based upon weight-cost relationships resulting from current technology aircraft. When advanced materials such as composites are introduced, the historical weight-cost relationships are no longer valid and must be modified. These modifications were made by using weights equivalent to current technology aircraft rather than calculated weights. Equivalent weights were used for weight-related parameters such as density.

3.4.2.2 Aircraft cost: Airframe cost and schedule were based upon a five aircraft development program and a 345-aircraft production for a total of 350 aircraft. A maximum production rate of four aircraft per month was used. Most labor costs were estimated in terms of hours with applicable Lockheed-California Company January 1976 direct and overhead rates applied. Warranty costs and a profit of 15 percent were added.

Engine costs were based upon use of the engine in two separate aircraft production programs requiring a total of 3600 engines.

Airframe and engine spare costs were estimated as a percentage of the engine or airframe cost. These percentages were derived from curves provided by TWA which relate percentage of spares to fleet size. A fleet size of 20 was selected: 12 percent was used for airframe; 29 percent was used for the conventional

engine, and 21 percent used for the LH_2 engine. The reduction for the LH_2 engines is considered appropriate because of an expected 30 percent increase in life for engines using that fuel. Precedent for this assumption lies in experience using gas turbine engines fueled with natural gas to drive electrical generators and compressors in pipeline installations (Reference 44). In these applications with natural gas (85 percent methane) it has been observed that engine life and maintenance requirements are both improved by about 20 to 25 percent compared to the same engines fueled with aviation kerosene.

Theoretical justification for the additional improvement expected with hydrogen stems from considerations such as (1) gaseous hydrogen and air mix very rapidly and thoroughly in the combustion chamber, which results in a very uniform temperature profile, thereby minimizing thermal stresses; (2) the very low emissivity of H_2/air combustion gases minimizes metal temperatures for a given temperature of the working fluid; (3) there are no carbon compounds to form coke or lacquer in the fuel lines, on the combustor walls, or in the turbine section; and (4) there is no sulfur or any other impurity in the fuel to cause either erosion or corrosion.

3.4.2.3 Mission characteristics: An average stage length (ASL) of 2187 nautical miles was selected from prior route studies. This agrees very closely with Lockheed formulas for deriving ASL for an international route. Block and flight times were calculated in ASSET based upon the mission profile for the ASL. Block time equals flight time plus ground time. A utilization of 3993 block hours/year (10.9 block hours/day) is estimated from the Lockheed developed formula:

$$U = 2942.75 \times (\text{block time})^{0.191}$$

3.4.2.4 DOC elements:

- Crew Cost. - An international crew cost of $450/block hour was estimated from Lockheed-developed formula for 1973 domestic crew cost times a percentage for international bonus and adjusted for inflation from 1973 to January 1976. The formula and adjustment factors were derived from CAB data.

$$\text{DCC (1976)} = 38.38 \times \text{ASL}^{0.12} \times \text{OEW}^{0.202}$$

$$\text{ICC (1973)} = \text{DCC (1973)} \times 1.10$$

$$\text{ICC (JAN 1976)} = \text{ICC (1973) escalated at 12.7\%/year}$$

Where

DCC = Domestic Crew Cost

ICC = International Crew Cost

OEW = Operating Empty Weight

- Fuel Cost. - Fuel costs were given by NASA (see Table I, Guidelines and Requirements), assuming both fuels are produced from coal and water in the 1990's.

LH_2 = \$5.69 per GJ (\$6/10^6 Btu = 31¢/lb = 18.3¢/gal)

JET A = \$4.74 per GJ (\$5/10^6 Btu = 9.2¢/lb = 62.2¢/gal)

Block fuel usage is calculated by ASSET.

A factor of 1.23 percent for nonrevenue flying was applied, based upon average airline operations from CAB data.

- Maintenance Cost. - A maintenance labor rate of \$9.00/hour was used as representative of the rates reported by the airlines from the airline survey. A maintenance burden factor of 2.27 was applied to maintenance labor. The burden factor was developed from a selected average for 1975 escalated at 3 percent per year to January 1976.

The correction factors for the various elements of maintenance are summarized in Table 5.

- Insurance. - An average insurance rate over the life of the aircraft of 0.304 is estimated from an LCC-developed formula.

$$\text{Avg. Rate} = (-1357.9 + 1359 \times \text{Years}^{0.001})/\text{LIFE}$$

- Depreciation. - Estimated average aircraft cost, including spares less residual value, is divided by the estimated life of the aircraft. A 4-percent residual value for wide body was derived from the airline survey. The 16-year life is normal for current large aircraft.

TABLE 5. - MAINTENANCE FACTORS FOR DOC CALCULATION

Maintenance Element	Maintenance Correction Factors				
	① Equiv. Weight	x ② ATA-to-Actual	x ③ LH_2 Cmplxty	x ④ Intntl DMSTC	= Total Factor Applied to ATA Formula
Airframe Labor					
Jet A	1.408	0.52	1.0	1.07	0.783
LH_2	1.388	0.52	1.02	1.07	0.788
Airframe Material	(Uses cost)		(Incl. in cost)		
Jet A	-	0.68	-	1.07	0.728
LH_2	-	0.68	-	1.07	0.717
Engine Labor	(Uses thrust)				
Jet A	-	0.62	1.0	1.07	0.663
LH_2	-	0.62	0.7532	1.07	0.50
Engine Material	(Uses cost)				
Jet A	-	1.31	1.0	1.07	1.402
LH_2	-	1.31	0.7382	1.07	1.035

① - Airframe weight is used in airframe labor only. The equivalent weight factor adjusts the weight of advanced technology materials to an equivalent current technology weight.

② - The ATA-to-actual ratio reflects a factor which must be applied to the ATA formulas to adjust to actual experience on wide body airframes and high bypass engines.

③ - The LH_2 complexity factor accounts for variations between a Jet A-fueled aircraft and an LH_2-fueled aircraft. A detailed maintenance analysis of each subsystem indicated a net 2 percent increase in airframe labor for the LH_2-airframe. Engine maintenance for the LH_2 is reduced 30 percent from the Jet A-engine maintenance for the same reasons discussed previously to account for longer life with LH_2 engines.

④ - The international/domestic adjustment is required because ATA-to-actual factors were developed on domestic trunk operation only and CAB data indicates a relatively higher cost for international maintenance.

4. LH_2 ENGINE DEFINITION

The objective of the engine definition task was to establish a viable baseline concept for a liquid hydrogen-fueled transport engine considering the requirements of the aircraft, i.e., mission profile and performance requirements, and the unique properties of the liquid hydrogen fuel. The work was performed as follows:

- The first element of this task addressed a feasibility investigation of various schemes to exploit the properties of hydrogen.
- The second element consisted of parametric engine investigations oriented toward selecting cycle variables and the engine configuration which minimized direct operating cost. The factors considered in evaluating direct operating cost were specific fuel consumption and engine weight.
- The third element of the engine definition task was the detailed definition of the selected engine design. The definition included determining engine performance throughout the flight envelope; weight and geometry; scaling laws; engine estimated cost; noise and emission levels; and operating limits and capabilities.
- The final element consisted of formulating a list of technology development requirements.

It is appropriate to point out that this task was not originally identified as a major activity in the study. Although definition of an optimum design of a LH_2-fueled engine is a topic deserving of serious effort, it served the purposes of the present study to limit the work to a preliminary investigation. Accordingly, the results are presented with the reservation that many of the design choices were made, necessarily, with less than rigorous technical justification. A much more comprehensive design study is recommended to fully explore the potential of LH_2 as a fuel for advanced turbofan engines.

4.1 Feasibility Studies - Hydrogen Exploitation

The objective of this task was to determine if the unique properties of hydrogen could be capitalized on to provide engine performance and/or weight benefits. The concepts which were selected for evaluation included:

- Compressor air precooling
- Compressor air intercooling

- Cooling of turbine cooling air
- Regenerative fuel heating
- Expander cycle

4.1.1 Approach. - The approach used in the feasibility studies was to select a turbofan cycle compatible with the requirements of the liquid hydrogen-fueled transport and to investigate the effects of the selected concepts on this baseline. Previous Lockheed work (Reference 1) resulted in the definition of a turbofan cycle for a liquid hydrogen-fueled transport. Characteristics of this cycle are shown in Table 6. The data shown in Table 6 were derived using AiResearch analysis and modeling techniques and, therefore, differ slightly from Lockheed results as reported in Reference 1. AiResearch reviewed this cycle and found it to be generally consistent with technology projections for 1990. The bypass ratio and fan pressure ratio selected appeared to be high and low, respectively, but the detailed parameterics required to select optimum values were not completed until later in the study. Therefore, this cycle was used as a baseline for the hydrogen exploitation feasibility studies. The high bypass ratio and low fan pressure ratio had little or no effect on the results of the feasibility studies.

TABLE 6. - BASELINE ENGINE

Parameter	Takeoff SLS, Std	Maximum Climb 10 668 m (35 000 feet) M = 0.85
Rotor inlet temperature, ^{o}C (^{o}F)	1416 (2580)	1379 (2514)
Cycle pressure ratio	35.2:1	41.13
Fan pressure ratio	1.51:1	1.634
Core pressure ratio	23.3:1	25.17
Nozzle-to-core-velocity ratio	1.022	1.17
Bypass ratio	12.95:1	13.0:1
Net thrust, N (lb)	127 664 (28 700)	26 689 (6 000)
Specific fuel consumption (kg/hr)/daN ((lb/hr)/lb)	0.096 (0.094)	0.2022 (0.1983)
Specific thrust, N/(kg/sec) (lb/(lb/sec))	256 (26.10)	119 (12.14)

Two notable changes were made to the cycle shown in Table 6 during the course of the feasibility studies. The first change adjusted the cycle for the low temperature of the hydrogen fuel as it entered the combustor. The second change debited the cycle for the effects of turbine cooling air. Cycle and performance characteristics associated with these changes are shown in Table 7.

The effects of turbine cooling air were incorporated only for the investigation of the concept where compressor discharge air was cooled by the hydrogen fuel before it entered the turbine blades. Since the analysis method required evaluation of differential effects only, for all other concepts, zero turbine cooling air was assumed. The Lockheed-defined cycle assumed the use of sodium-potassium (NaK) fluid to cool the turbine. The NaK was cooled by the hydrogen fuel.

TABLE 7. - BASELINE ENGINE CHARACTERISTICS

(Maximum Climb, 10 668 m (35 000 ft), M = 0.85)

Cycle and Performance Characteristics	Adjusted for Fuel Temperature	Adjusted for Turbine Cooling
Rotor inlet temperature, ^{o}C (^{o}F)	1379 (2514)	1379 (2514)
Bypass ratio	13:1	13:1
Fan pressure ratio	1.634:1	1.634:1
Core pressure ratio	25.17:1	25.17:1
Nozzle-to-core velocity ratio	1.19	1.10
Fuel temperature to combustor, ^{o}K (^{o}R)	50 (90)	50 (90)
Net thrust, N (lb)	26 689 (6000)	26 689 (6000)
Specific fuel consumption, (kg/hr)/daN ((lb/hr)/lb)	0.2082 (0.2042)	0.2129 (0.2088)
Specific thrust, N/(kg/sec) (lb/(lb/sec))	120 (12.20)	112 (11.47)
Horsepower extraction	125	125
Aircraft systems bleed extraction, %	4.1	4.1
Inlet total pressure recovery	0.991	0.991
Nozzle thrust coefficients	0.995	0.995

All concepts were evaluated at the initial cruise flight conditions of 10 668m (35 000 feet), Mach 0.85. This flight condition determined engine sizing and was also typical of the cruise condition where the majority of fuel is consumed.

The criteria used for evaluation of the concepts was direct operating cost. The sensitivity of direct operating cost to changes in specific fuel consumption and engine weight was based on a relationship presented in Section 3.3. The relationship used in the engine study was:

$$\Delta DOC\ (\%) = \frac{\frac{7.75}{10^6}\ (\Delta \text{engine weight}) + 1.332\ \left(\frac{SFC}{SFC_{base}} - 1\right)}{DOC_{base}} \times 100$$

The change in specific fuel consumption was evaluated using a design point thermodynamic routine which allowed the various concepts to be modeled. Engine weight for the various concepts was determined by adding the weight of the components associated with each concept to the baseline weight and adjusting the baseline weight for changes in airflow, bypass ratio and turbine design considerations.

For all cycle investigations thrust, cycle pressure ratio, turbine inlet temperature, and fan pressure ratio were held constant. Specific thrust (F_N/W_a) was held nearly constant by fixing the energy extraction of the low pressure turbine. This was accomplished by specifying a constant jet nozzle velocity ratio (V_{core}/V_{fan}) in addition to the other constant parameters. Holding specific thrust approximately constant allows the effects of the various concepts to be observed independently of propulsive efficiency changes. It should be noted that holding the jet nozzle velocity ratio and fan pressure ratio constant does not hold specific thrust exactly constant, but it results in only very minor changes in specific thrust and the analytical procedure is greatly simplified. The jet nozzle velocity ratio selected was 1.19 which was based on the original Lockheed cycle.

Installation effects that were included in the analysis were bleed and horsepower extraction for aircraft systems, inlet total pressure recovery, and exhaust system losses including fan scrubbing drag. Freestream cowl drag and inlet spillage drag were not included. To a first approximation, freestream cowl drag is a function of specific thrust and therefore, for this analysis, is a constant. Spillage drag at the design point condition is insignificant.

Other important assumptions included the temperature of the liquid hydrogen fuel at the fuel pump outlet, the specific heat of hydrogen, and the temperature of the fuel into the combustor. The fuel pump outlet temperature of 50°K (90°R) was calculated based on an assumed temperature rise through fuel

system lines and the temperature rise across the engine high pressure fuel pump. Over the range of temperatures encountered, the specific heat of LH_2 is not constant but can be approximated by a constant 3.5 Btu/lb/^{o}R. The fuel temperature into the combustor was assumed equal to the temperature out of the last engine heat exchanger for all concepts except the expander cycle. For that concept it was assumed equal to the temperature out of the hydrogen expansion turbine.

4.1.2 Compressor air precooling. - The concept incorporating compressor air precooling is shown in Figure 6. An annular heat exchanger is required in the core stream in front of the compressor. Fuel would be routed to the heat exchanger, entering at a temperature of approximately 50^{o}K (90^{o}R) and, after passing through the heat exchanger, to the burner at an increased temperature. Precooling the compressor inlet air results in less compression work required and the benefit is a reduced gas generator size. A second benefit is the fuel heating effect. As discussed, LH_2 would typically enter the combustor at 50^{o}K (90^{o}R) and part of the heat of combustion is required to heat the fuel to compressor discharge temperature. The elevated temperature of the fuel at the heat exchanger outlet minimizes this penalty. The benefit achieved is limited by the effectiveness and the air side pressure drop of the heat exchanger.

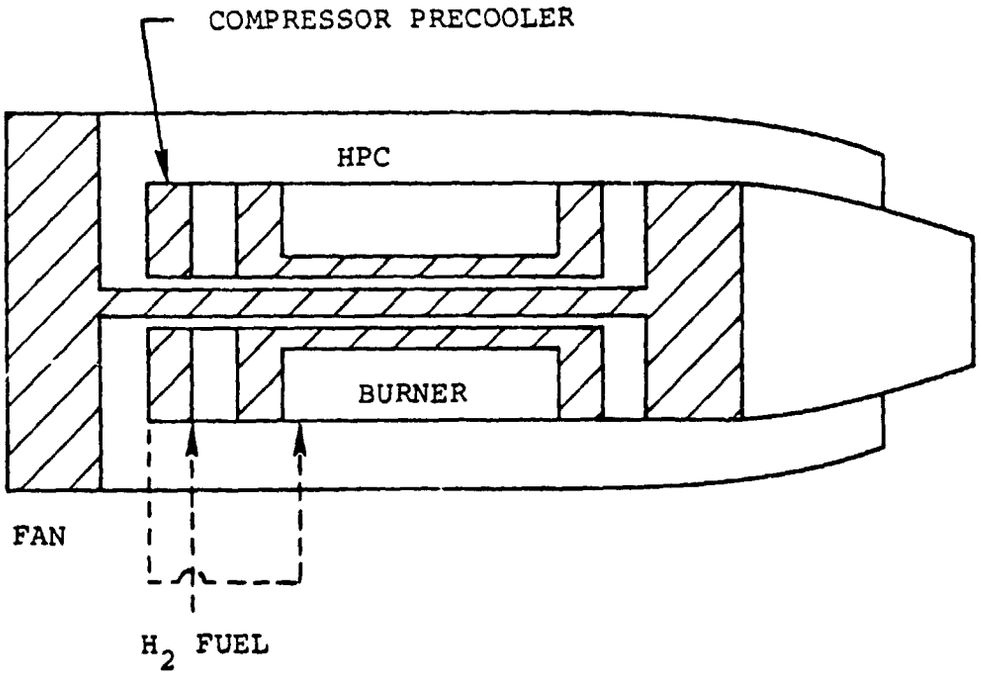

Figure 6. - Schematic of engine cycle with compressor precooling with H_2 fuel.

The results of this investigation are shown in Figure 7 in terms of specific fuel consumption versus precooler heat exchanger effectiveness and precooler air side pressure drop, all for an exhaust nozzle velocity ratio of 1.19.

Preliminary heat exchanger design analysis indicated that an effectiveness (H_2 side) of 0.8 and air side pressure drop of 6 percent was feasible. This combination results in a 1.86 percent improvement in specific fuel consumption. Basic engine weight decreased 29 kg (63 lb) but the heat exchanger added 34 kg (75 lb). The net effect was an improvement in DOC of 1.33 percent

Detailed heat exchanger design conducted later in the study indicated a severe air side freezing problem. Recirculation of warm fuel was investigated but did not solve the problem. Potential damage due to foreign object ingestion was also identified as a serious problem associated with this concept.

4.1.3 Compressor intercooling. - The potential performance improvement due to intercooling the compressor air at an intermediate point in its compression process with the H_2 fuel was evaluated. The benefit to the cycle was expected to result from a reduction in core size due to compressor horsepower reduction per pound of core airflow and decrease in fuel flow due to heating of the fuel. An offsetting effect, as with compressor precooling, is the pressure drop on the air side of the intercooling heat exchanger.

The cycle with compressor intercooling is illustrated in Figure 8. The point in the compression process selected for the heat exchanger was chosen as one giving approximately equal enthalpy rise in the compression process prior to and following intercooling.

The results of this study are presented in Figure 9 in terms of specific fuel consumption versus intercooling effectiveness and pressure drop, all for an exhaust nozzle velocity ratio of 1.19.

Preliminary heat exchanger design indicated that an effectiveness (H_2 side) of 0.8 and an air side pressure drop of 4 percent was feasible. This combination results in a 1.0 percent improvement in SFC relative to the baseline cycle. Basic engine weight decreased 18 kg (40 lb) but the heat exchanger added 45 kg (100 lb). The net effect was an improvement in DOC of 0.57 percent.

NOTES:

10 668 m (35 000 ft), M = 0.85, Max Cruise Thrust

FPR = 1.634 Nozzle Vel. Ratio = 1.19

TIT = 1379°C (2514°F) Net Thrust = 26 698 N (6000 lb)

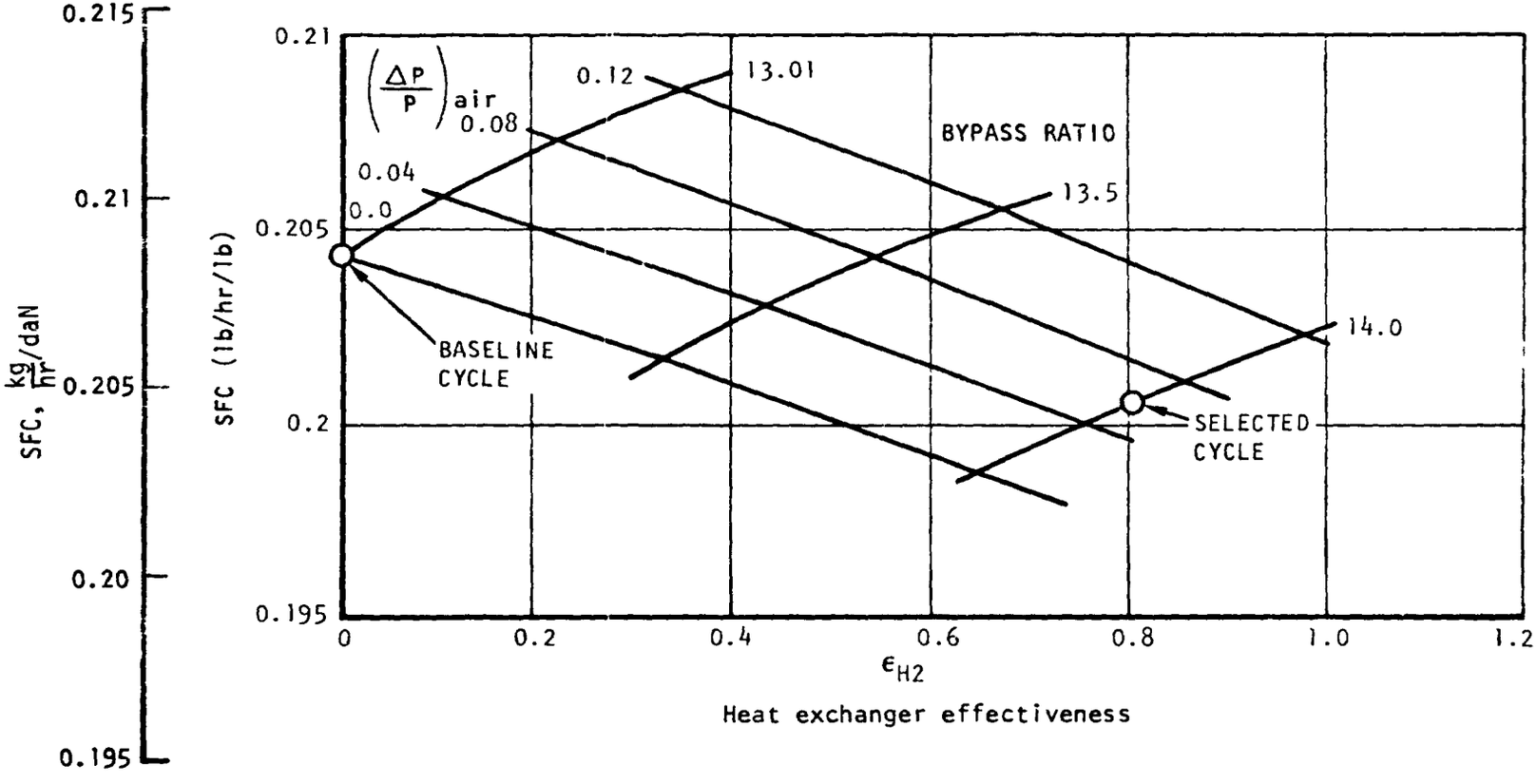

Figure 7. - Engine performance with precooling.

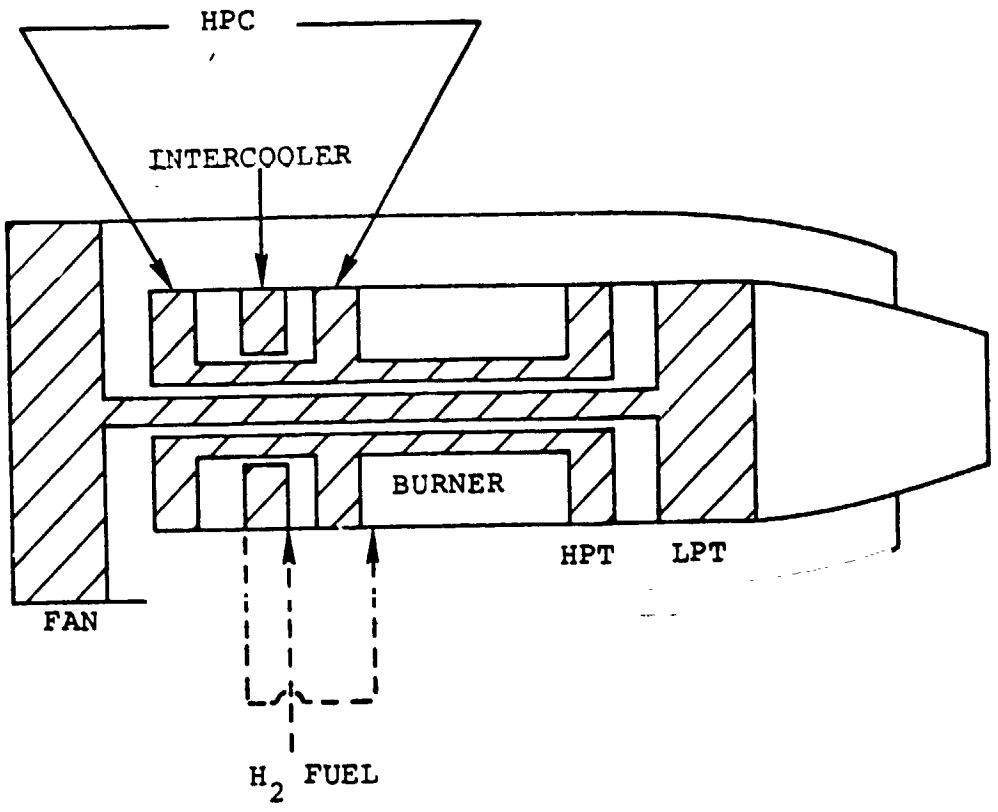

Figure 8. - Schematic of engine cycle with compressor intercooling with H_2 fuel.

4.1.4 Hydrogen cooling of turbine cooling air. - An evaluation was made of the potential benefit which might be derived from cooling the HP turbine blade cooling air with the hydrogen fuel. Hydrogen cooling of the turbine cooling air would reduce the quantity of turbine cooling air extracted from the compressor and, simultaneously, would heat the hydrogen fuel.

A schematic of this concept is illustrated in Figure 10. Air for cooling the turbine hub is extracted from the compressor and routed to the turbine by conventional means. Hub cooling air is not cooled by the hydrogen as the flow requirements are set by the pumping characteristics of the turbine disks and not by heat transfer requirements. If there was no flow of cool air through the cavities in front of or behind a disk, the air in the cavity would quickly reach the temperature of the main stream. This is due to a significant recirculation between the cavity air that is pumped in a toroidal flow pattern by the rotating disk and the high velocity main stream air. To maintain the cavity air at an acceptable level, cool air must be introduced into the cavity to avoid recirculation, or at least limit it. The quantity required is set by the rotating flow process more than by the temperature of the air. If some recirculation were allowed, cooling the cavity purge

NOTES:

10 668 m (35 000 ft), M = 0.85, Max Cruise Thrust

FPR = 1.634 Nozzle Vel. Ratio = 1.19

TIT = 1379°C (2514°F) Net Thrust = 26 689 N (6000 lb)

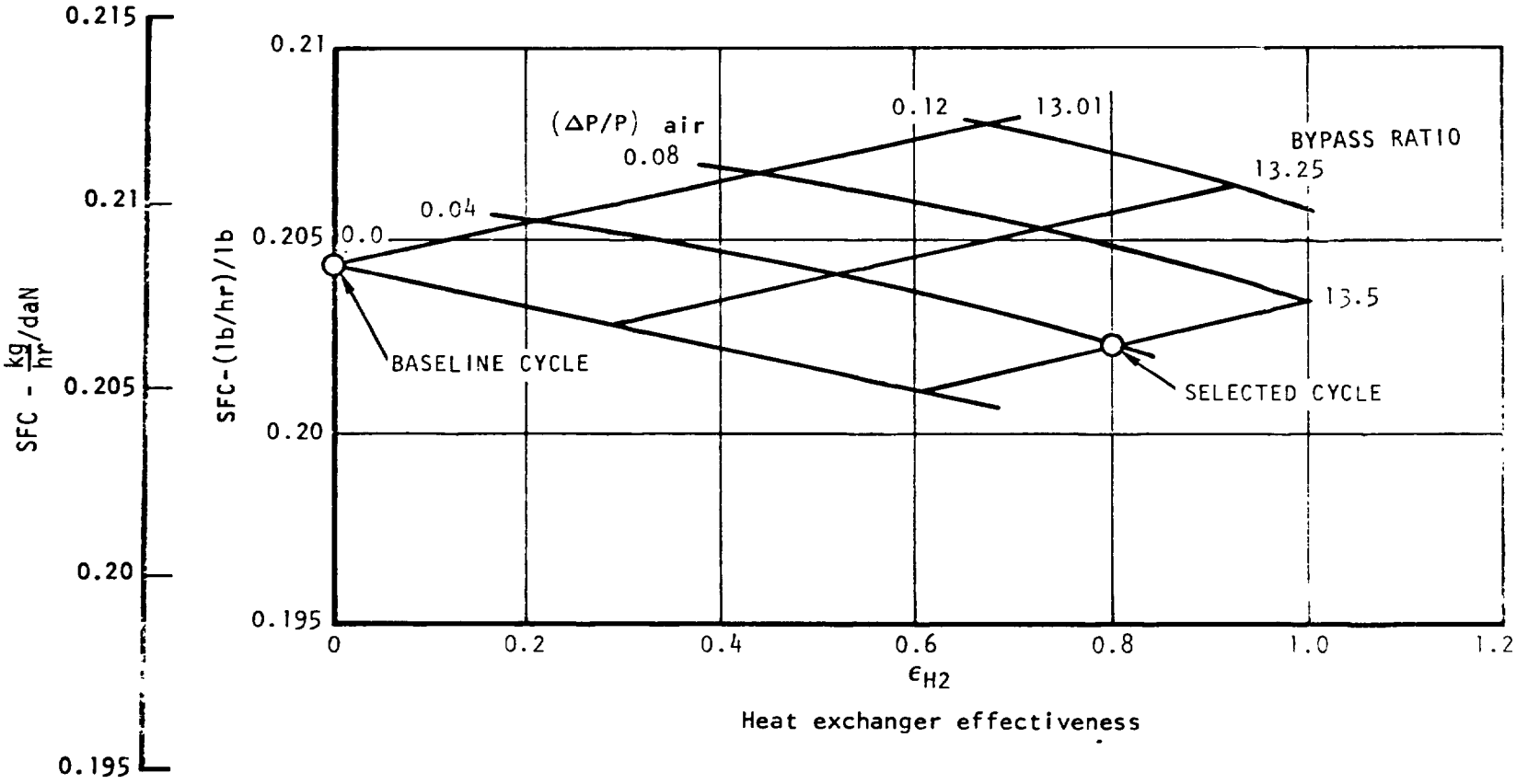

Figure 9. - Engine performance with intercooling.

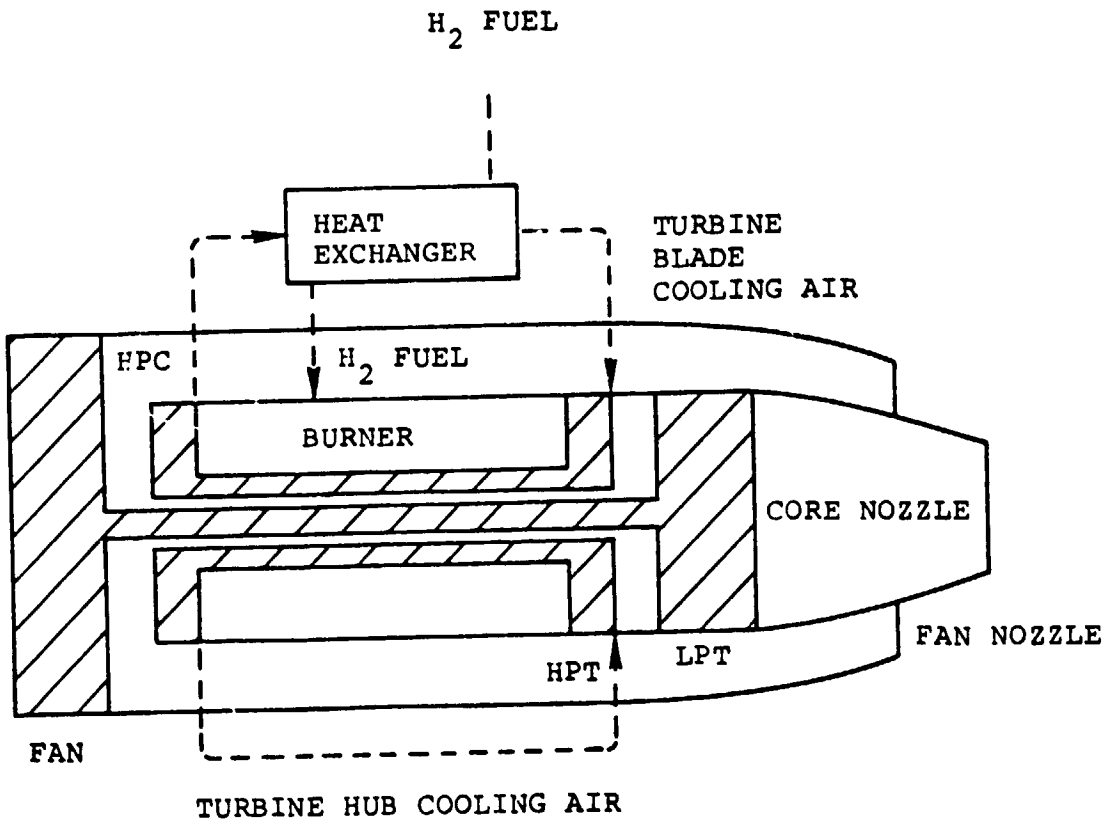

Figure 10. - Schematic of cooled turbine cooling air cycle.

air could reduce the flow. However, design standards which account for worn seals, varying engine power levels, and allowable disk temperature environment would need to be established. Furthermore, different approaches to routing of the air to the disks would have to be established.

Turbine blade cooling air is extracted from the compressor and directed to a heat exchanger and from there to the HP turbine at a temperature lower than compressor discharge temperature. The air used to cool the HP turbine vanes does not bypass any work producing stages and, therefore, is considered nonchargeable provided that the turbine inlet temperature is quoted at the rotor inlet rather than the combustor outlet. (For an explanation of the terms chargeable and nonchargeable, see Paragraph 4.2.3.1.4.) Cooling of the vane cooling air would reduce the amount of air required, but it would not impact the cycle. Another reason for cooling the cooling air would be to reduce the vane flow in order to diminish the effect of cooling flow on

turbine efficiency. As the vane cooling flow exits, it disrupts the vane flow field. At high flows, this effect can be significant. However, for the time period specified and at the turbine inlet temperature level assumed, the vane cooling flow is low enough to preclude significant efficiency penalties.

The analytical method used to evaluate the effects of cooling was to penalize the turbine efficiency for pumping losses, etc., and to assume that the blade and hub cooling air do no work in the turbine being cooled and re-enter the cycle behind the HP turbine. This assumption is valid only in the case of a single-stage turbine. For a multistage turbine, cooling air bypasses only the stage being cooled and reenters the cycle behind that stage. Turbine vanes in multistage turbines also require different handling. The cooling air to a second stage vane bypasses the first turbine stage and therefore, must be considered as chargeable cooling air.

Turbine efficiency was penalized for the amount of cooling air required. In other words, turbine efficiency increased as required blade cooling decreased. The efficiency penalty schedule used was 0.2 points of efficiency for each percent cooling air.

The results of this study are summarized in Figures 11, 12, and 13. Presented in Figures 11 and 12, are curves of specific fuel consumption, bypass ratio, and specific net thrust as functions of jet nozzle velocity ratio and heat exchanger effectiveness. Figure 13 presents curves of HP turbine efficiency, and HP turbine cooling airflow versus heat exchanger effectiveness.

At a jet nozzle velocity ratio of 1.19 and a heat exchanger effectiveness of 0.8, the maximum benefit to the cycle was approximately 0.53 percent improvement in specific fuel consumption. This improvement was relative to the baseline cycle with cooling air (see earlier discussion of baselines). Basic engine weight decreased 12.2 kg (27 lb) per engine but the heat exchangers added 4.5 kg (10 lb) per engine. The net improvement in DOC was 0.41 percent. The benefit to the cycle was small because the projected blade cooling air requirement for the 1985-1990 time frame is small.

Although the benefit to the cycle was small, hydrogen cooling of the blade cooling air seemed promising from other aspects. It suggested that the combined benefit of higher turbine inlet temperature plus inexpensive cooling might be attractive. Accordingly, a more detailed study was conducted at 1760°C (3200°F) turbine inlet temperature. The results of this study will be discussed in a subsequent section.

4.1.5 Fuel heating with exhaust gas. - The concept of regenerative fuel heating was suggested because of the effect of the low temperature fuel at the combustor inlet. As noted earlier, the introduction of low temperature

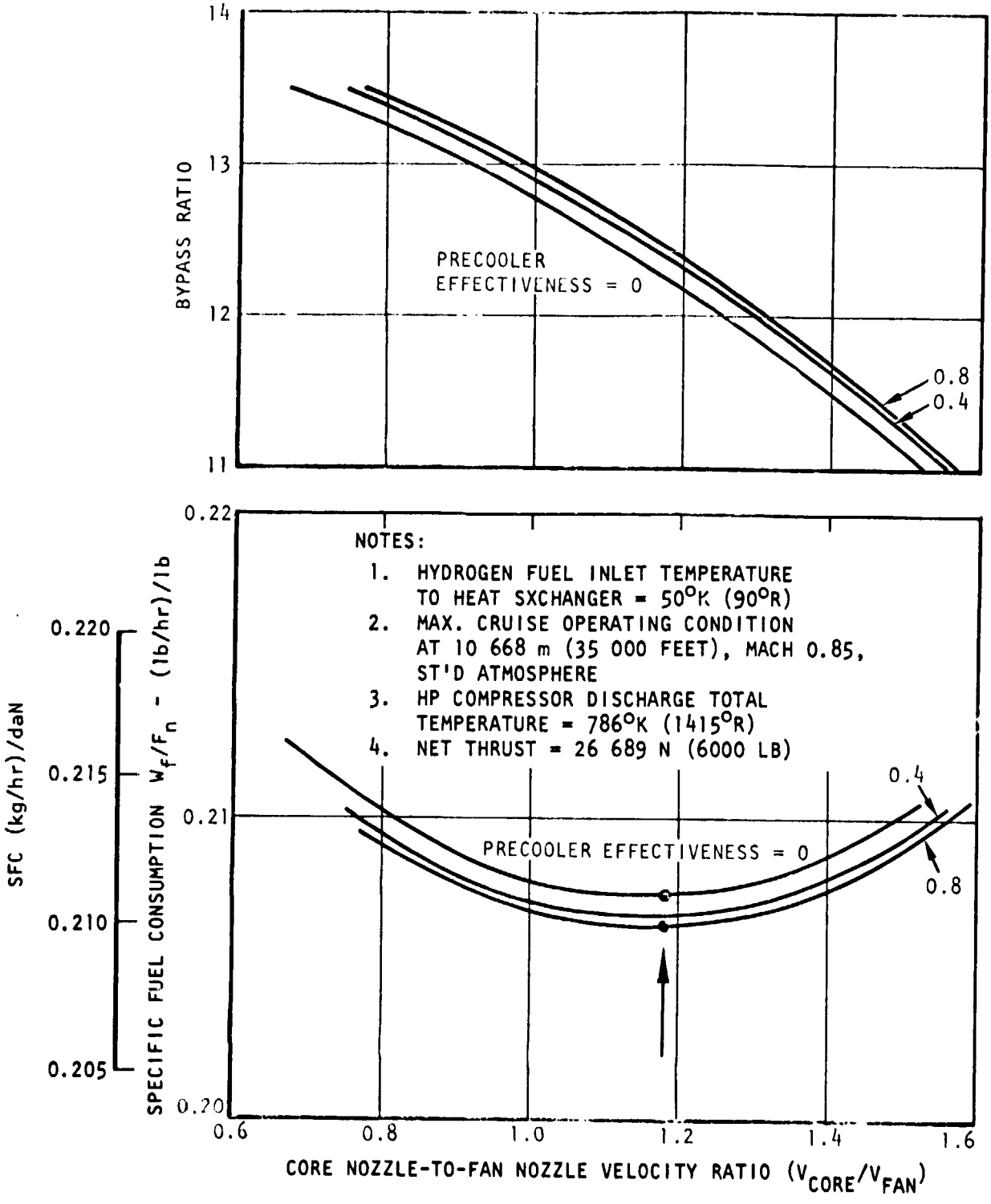

Figure 11. - Effect on SFC of cooling turbine cooling air with fuel at max. cruise.

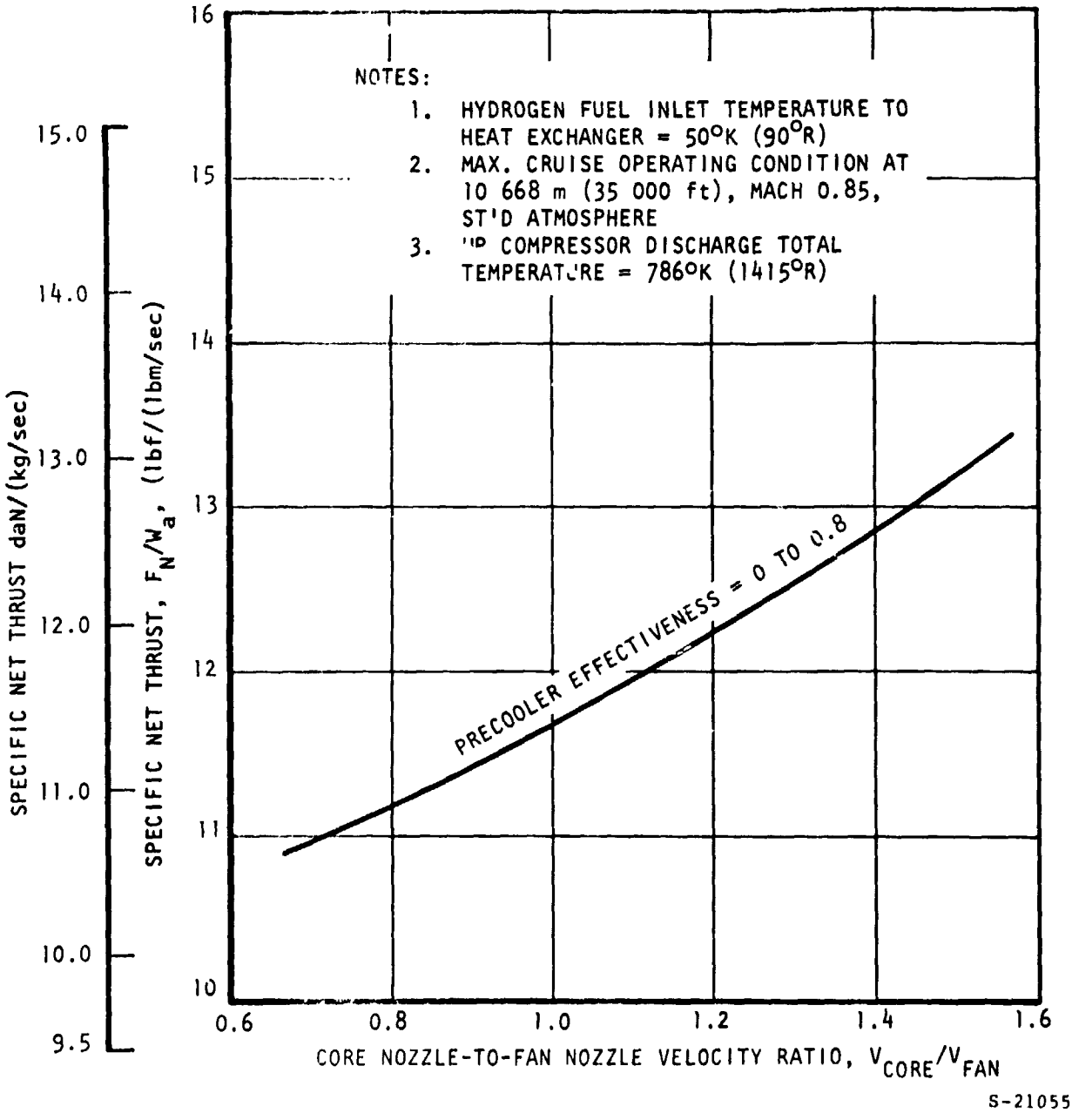

Figure 12. - Effect on specific net thrust of cooling turbine cooling air with fuel at max. cruise.

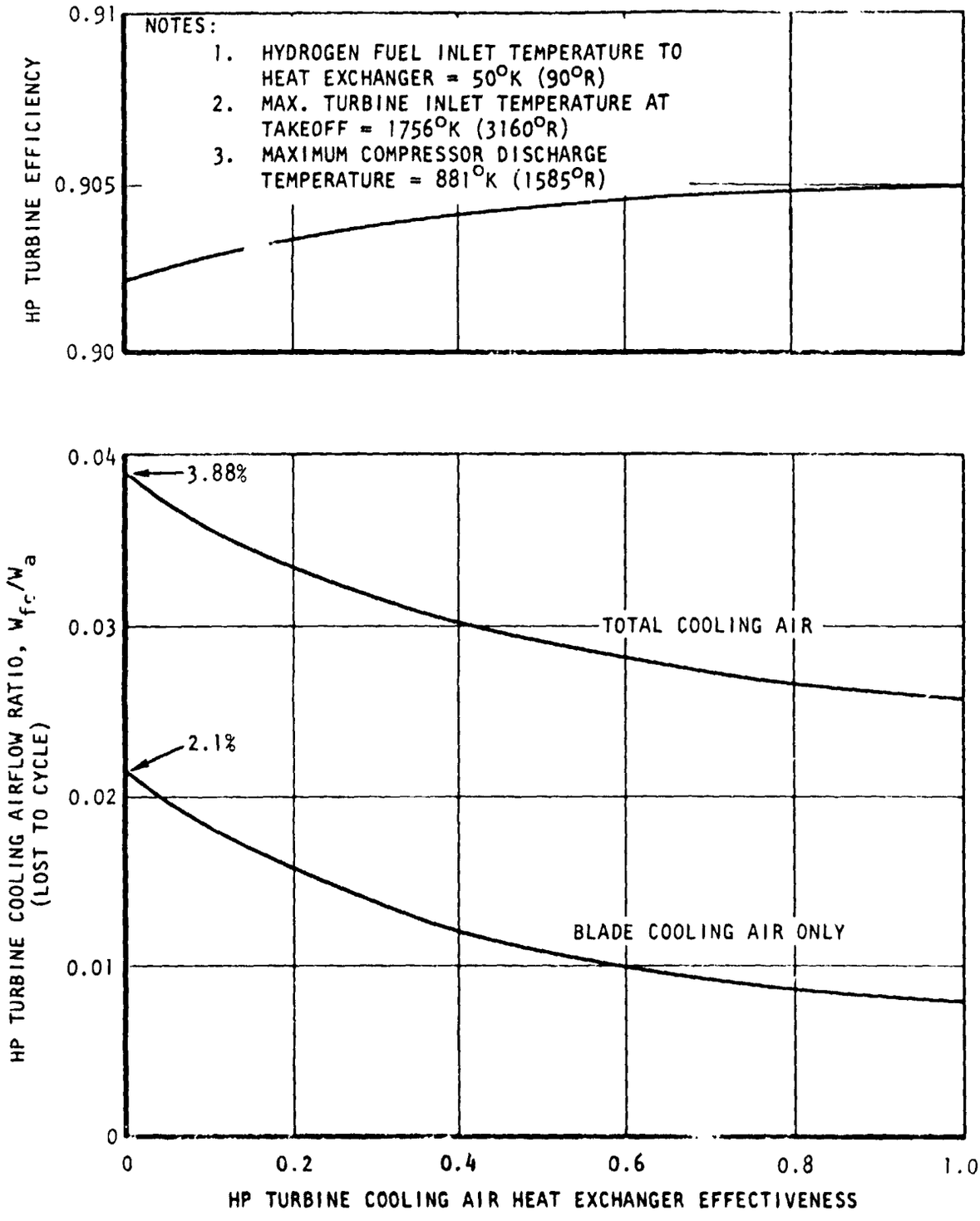

Figure 13. - HP turbine efficiency and cooling air schedules used in study of fuel cooling of turbine cooling air.

fuel into the combustor results in a performance penalty when compared with the fuel temperatures typical of conventional kerosene type fuels. The scheme is essentially a regenerative gas turbine cycle except that the energy is added to the fuel rather than the air. It is illustrated in Figure 14. Parenthetically it is interesting to note that, with the high pressure ratio cycles being evaluated, regeneration of the compressor discharge air would not be feasible because its temperature is higher than that of the exhaust gas.

The results of this study are presented in Figures 15, 16, and 17. Presented are curves of specific net thrust, and specific fuel consumption as functions of exhaust heat exchanger effectiveness (H_2 side) and exhaust nozzle velocity ratio. Figure 15 is for the case where the exhaust gas side pressure drop is zero, Figure 16 shows 4 percent, and Figure 17 shows 8 percent.

The results indicate that this scheme offers the maximum benefit of any of the concepts evaluated. The improvement in specific fuel consumption at a combination of 0.80 effectiveness and 4 percent pressure drop at a 1.19 jet nozzle velocity ratio is 4.31 percent, relative to the reference value as shown on Figure 16. Engine weight increased 12 kg (27 lb) and the heat exchanger added an additional 112 pounds. The net improvement in DOC was 2.9 percent relative to the baseline cycle where the fuel was introduced into the combuster at 50K (90R).

The decrease in engine effectiveness which would normally result from removing heat from the exhaust is more than made up by the increase in work output from both the fan and core engine section as a result of the increase in enthalpy of the fuel/air combustion products applied to both the high- and low-pressure turbine stages, and as a result of the multiplying factor stemming from the 10:1 bypass ratio.

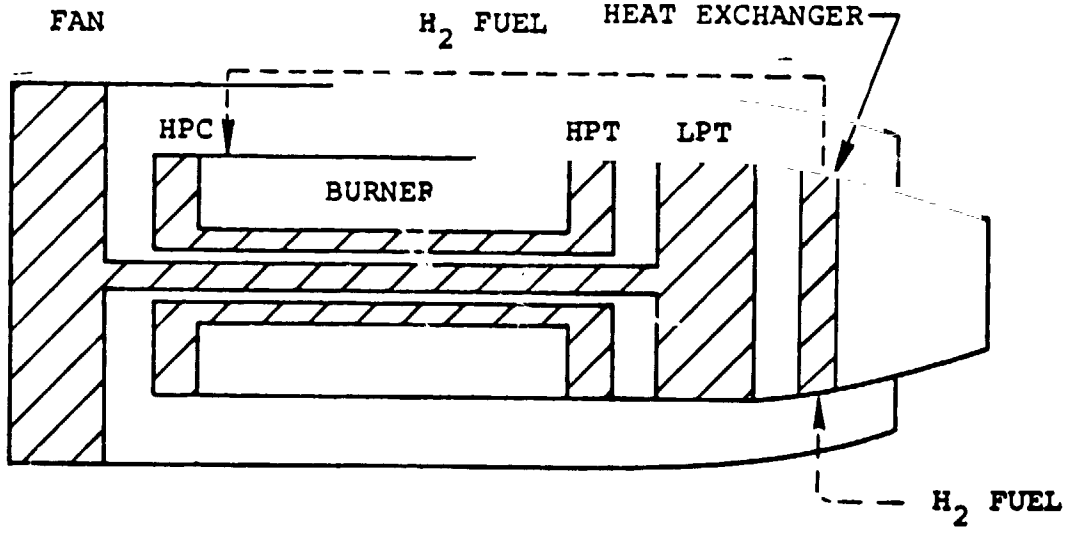

Figure 14. - Schematic of engine cycle with exhaust gas heating of H_2 fuel.

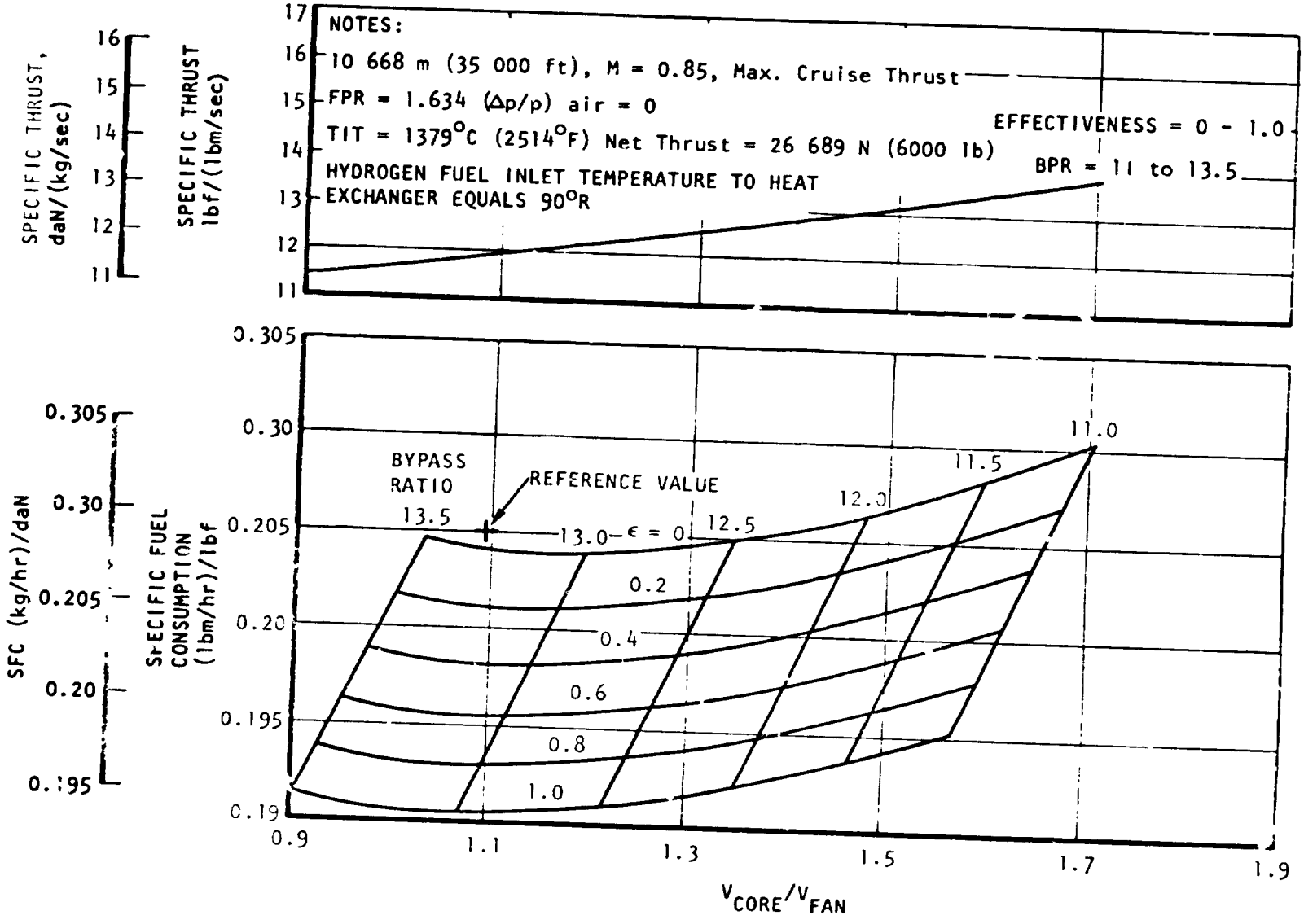

Figure 15. - Effect of exhaust heating on fuel at max. cruise (ΔP/P = 0).

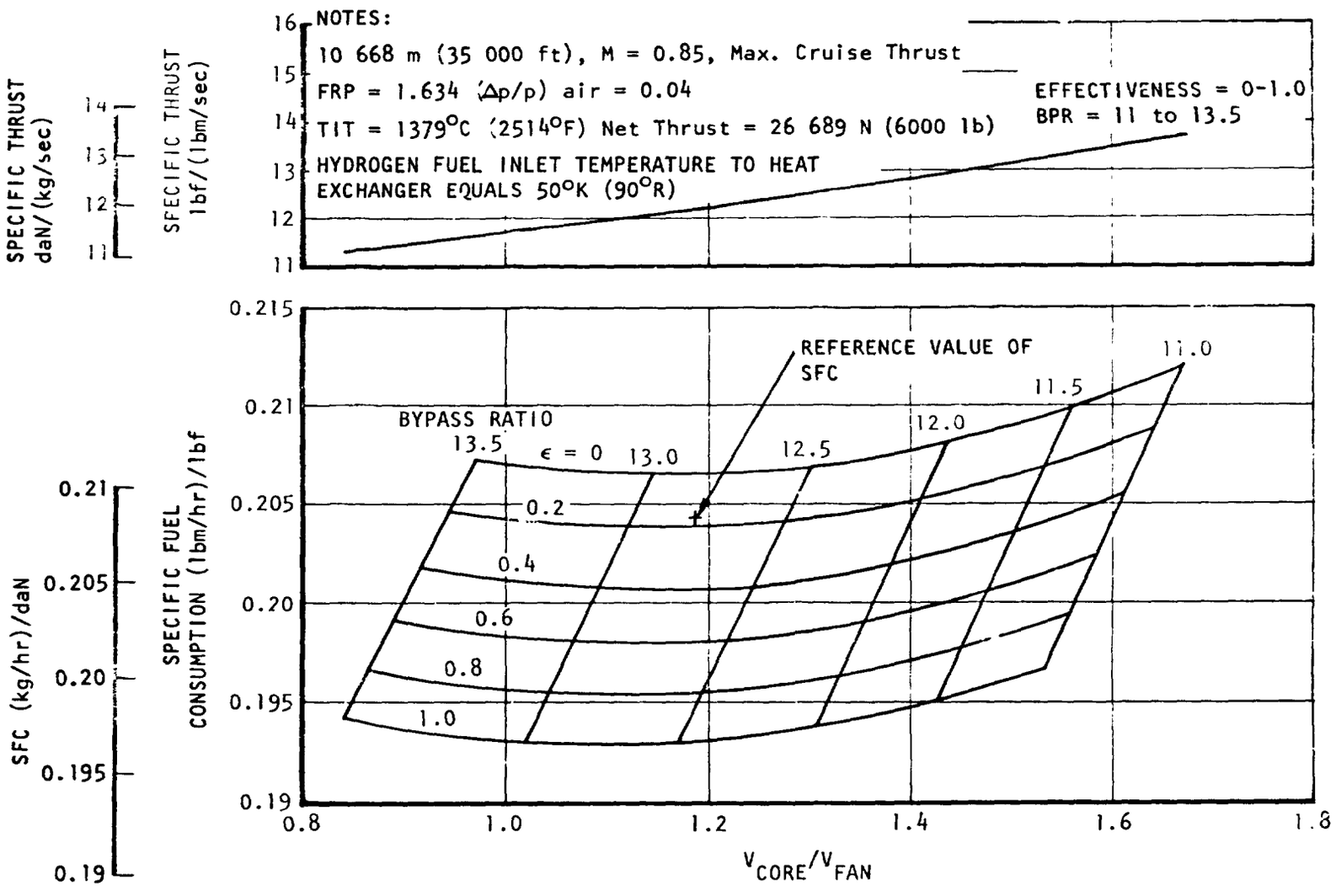

Figure 16. - Effect of exhaust heating of fuel at max. cruise (ΔP/P = 0.04).

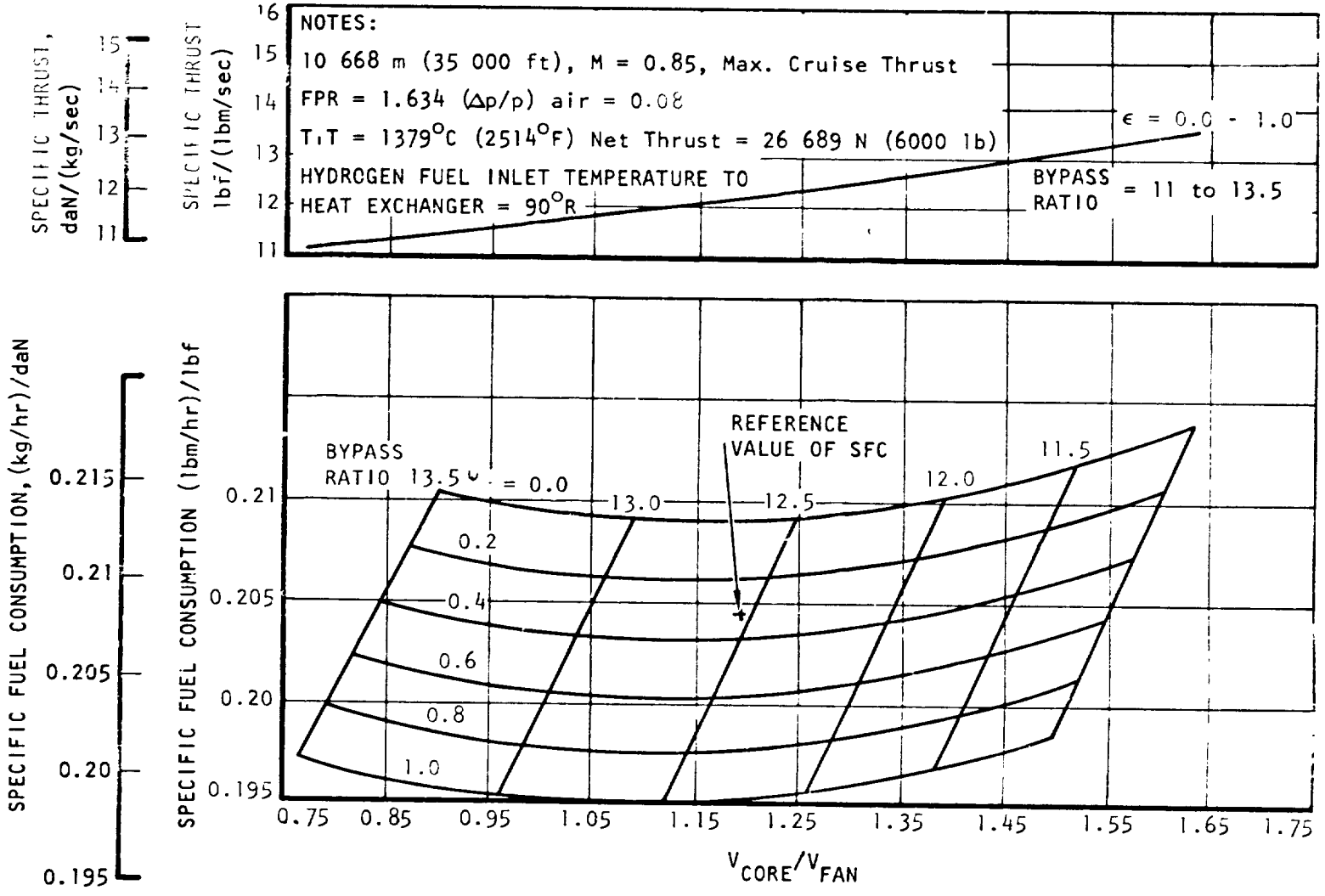

Figure 17. - Effect of exhaust heating of fuel at max. cruise (ΔP/P = 0.08).

4.1.6 H_2 expander cycle. - A study was completed to evaluate the performance improvement which might be obtained by providing aircraft accessory horsepower using a hydrogen expansion turbine rather than extracting it from the engine through a gearbox. Originally, it was hoped that the expander cycle could provide some of the fan or compressor horsepower requirements. However, preliminary calculations showed that the fuel would have to be pumped to very high pressures to provide significant amounts of power relative to the requirements of the fan and compressor. For example 13 790 kPa, (2000 psi) is required to obtain 580 hp, which is only 5 percent of the compressor horsepower. Further increases in power would require higher hydrogen pressures since the turbine flow rate which is the engine fuel flow rate, and the heat addition from the exhaust stream is constant. It is believed that the increase in engine complexity required to use the hydrogen expansion turbine to provide only a small amount of the compression horsepower requirements is unwarranted.

The emphasis shifted to the investigation of providing aircraft accessory horsepower requirements. The expander cycle is illustrated in Figure 18. This scheme consists of pumping the hydrogen fuel to a pressure level above that required for delivery to the engine, heating it in an exhaust gas heat exchanger, and expanding it through a turbine. The benefit to the cycle was

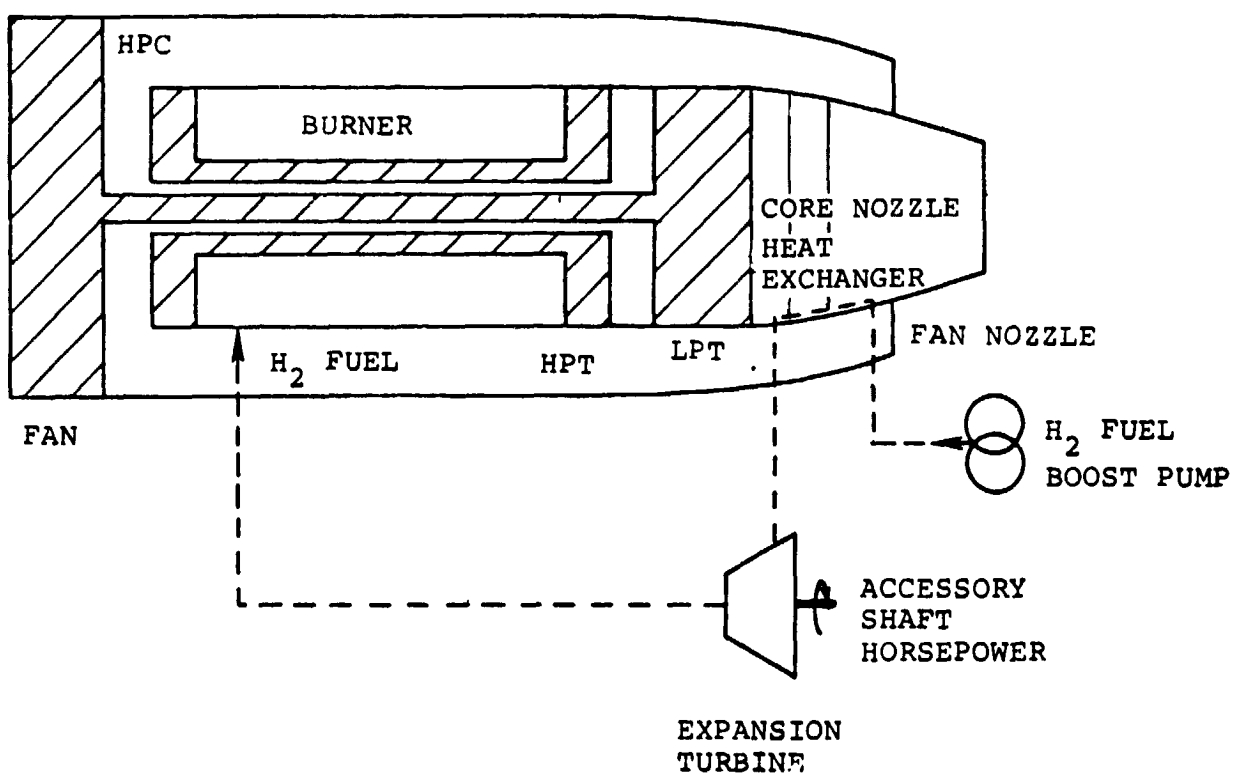

Figure 18. - Schematic of expander cycle.

expected to result from the elimination of the accessory power load and the decrease in fuel flow due to fuel heating. There would also be a decrease in engine weight associated with a smaller engine gearbox, but it was assumed that was offset by the increased weight of the fuel pump and the additional weight of the hydrogen turbine and the associated gearing.

The heat exchanger effectiveness and pressure drop ($\Delta P/P$) selected were 0.8 and 0.04, respectively. The pressure to which the fuel must be pumped to yield a net output of 125 hp for the aircraft accessories was calculated. Only the power required to pump the hydrogen to pressures above 2482 kPa (360 psia) was charged to the expander cycle.

The relationship of net horsepower available to the aircraft accessories and the hydrogen turbine inlet pressure is shown in Figure 19. The fuel pump efficiency was selected as 65 percent and hydrogen turbine efficiency including mechanical losses was assumed to be 80 percent. The fuel temperature out of the fuel pump was calculated as a function of fuel pressure rise. The hydrogen temperature into the H_2 turbine was calculated using all the engine exhaust flow and the effectiveness of 0.8. The hydrogen was expanded across the turbine to the required combustor inlet pressure of 360 psia. The H_2 temperature at the outlet of the turbine was calculated based on a 90 percent adiabatic efficiency. Engine performance was based on the fuel temperature at the turbine outlet and includes the effects of exhaust gas pressure drop and cooling in the heat exchanger. Specific fuel consumption and core jet-to-fan duct velocity ratio are shown versus bypass ratio in Figure 20. The specific fuel consumption at a core-to-fan nozzle velocity ratio of 1.19 is 0.1993 (kg/hr)/daN (0.1954 (lb/hr)/lb which is a 4.31 percent improvement over the baseline SFC of 0.2042 (lb/hr)/lb listed in Table 7. The regenerator weight is 51 kg (112 lb) engine and the decrease in engine weight is 12.2 kg (27 lb)/engine. The improvement in DOC is 2.9 percent.

4.1.7 Selection of preferred concepts. - A summary of the feasibility studies is included as Table 8. The concepts which yield the largest reduction in DOC are fuel heating and the expander cycle. The fuel heating concept was recommended for use in the study as it is less complex and provides an equal DOC benefit. As noted earlier, however, hydrogen cooling of the turbine cooling air is attractive in many respects and offers advantages if higher turbine inlet temperatures were selected. This concept is further discussed in section 4.2.3.1.

4.2 Cycle Definition and Configuration Definition

The cycle definition and configuration work was accomplished in three parts. The first part was a review of prior studies of advanced turbofan engines. The second part was selection of the initial cycle for a LH_2-fueled engine. It relied heavily on these prior studies and cycle variables were

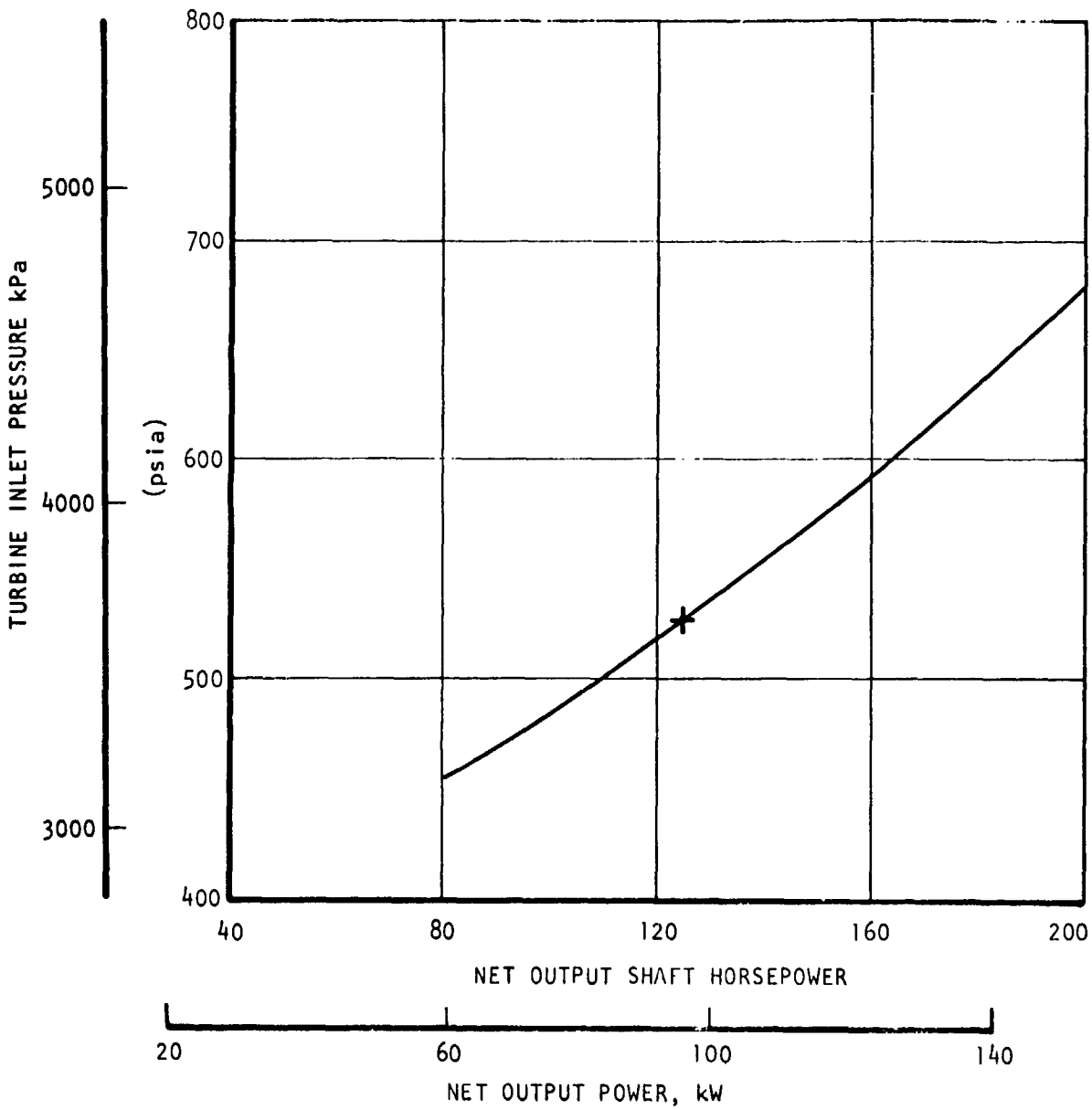

Figure 19. - Net output shaft horsepower vs turbine inlet pressure.

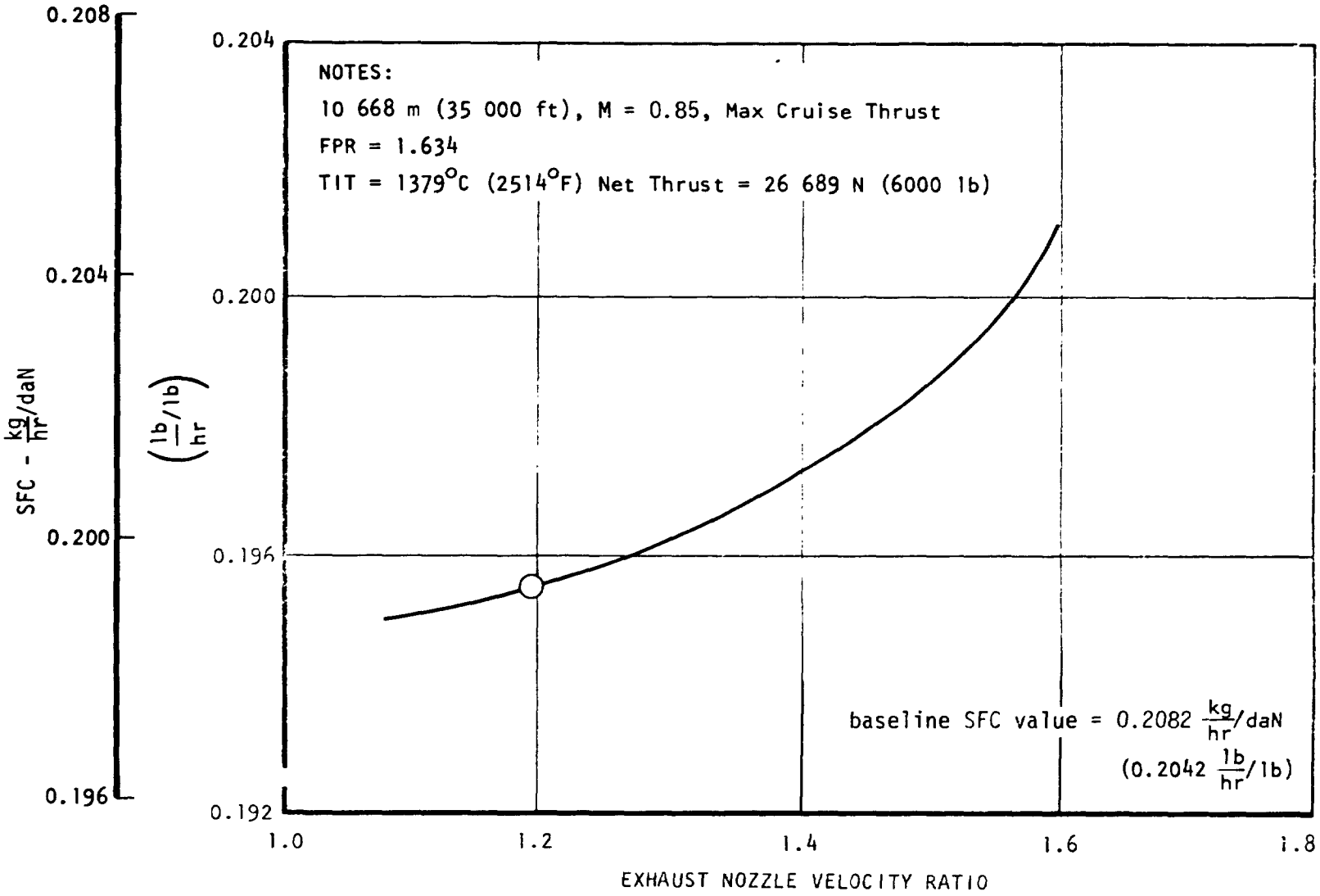

Figure 20. - Engine performance - expander cycle.

TABLE 8. - HYDROGEN EXPLOITATION SUMMARY

	ϵ_{H2}	$\frac{\Delta P}{P_{air}}$	ΔSFC** %	Engine Δwt	HX Δwt	ΔDOC* %
Precooling	0.8	0.06	-1.86	-63	+ 75	-1.33
Inter cooling	0.8	0.04	-0.93	-40	+100	-0.57
Cooled turbine cooling air	0.8	N/A	-0.53	-27	+ 10	-0.41
Fuel heating	0.8	0.04	-4.31	+27	+112	-2.90
H_2 Expander cycle	0.8	0.04	-4.31	+27	+'12	-2.90

**Relative to the baseline SFC = 0.2042 $(\frac{lb}{hr})/lb$

$$*\Delta DOC(\%) = \frac{\frac{7.75}{10^6}(\Delta wt) + 1.332\ \frac{SFC}{SFC_{61}} - 1}{DOC_{base}} \times 100$$

selected consistent with them. In the third part, a more detailed study was made of a high temperature, high pressure ratio cycle. Work completed in the second part was updated and compared to the results of the high temperature study.

4.2.1 Review of previous studies. - In a previous LH_2 transport study (Ref. 1), Lockheed established a baseline engine cycle which is defined in Table 6. More recently, the General Electric Company and Pratt and Whitney Aircraft have studied turbofan engines designed for low fuel consumption under contract to NASA Lewis. The work is reported in References 36, 37, and 38. These studies were reviewed in detail as they represent the latest engine cycle and configuration studies for conventionally fueled subsonic transports which might become operational in the late 1980's, and because they were of a much greater depth and scope than the engine studies accomplished in the subject program. The aircraft used in these studies are very similar to the LH_2-fueled transport in mission and payload. It was considered that cycle and configuration characteristics for LH_2-fueled transport engines should be very similar to the cycle characteristics selected by G.E. and P&W in the E^3 (Energy Efficient Engine) study. A brief summary of the results of the General Electric and Pratt and Whitney Studies is given in the following sections.

4.2.1.1 Turbine temperature and cycle pressure ratio: General Electric found that low-pressure turbine (LPT) cooling requirements became the overriding factor at rotor inlet temperatures greater than 1538°C (2800°F). Minimum SFC occurred at 1427°C (2600°F) for cycle pressure ratios from 32:1 to 45:1. Minimum engine weight occurred at approximately 1538°C (2800°F) for cycle pressure ratios from 32:1 to 45:1. Minimum DOC occurred between 1482 and 1510°C (2700 and 2750°F) for cycle pressure ratios from 32:1 to 45:1.

GE selected a 1427°C (2600°F) takeoff rotor inlet temperature and a cycle pressure ratio of 38:1.

Following similar logic, Pratt and Whitney selected a 1427°C (2600°F) maximum combustor outlet temperature and a cycle pressure ratio of 45:1.

4.2.1.2 Fan pressure ratio and bypass ratio: General Electric's results showed that higher fan pressure ratios (up to 1.8:1) yielded improved direct operating cost (DOC). GE selected a fan pressure ratio of 1.7:1 for initial rating with possible growth to 1.8:1. For a separate flow exhaust system, an exhaust nozzle velocity ratio of approximately 1.5 yielded minimum DOC.

Pratt and Whitney found that the lower SFC possible at low fan pressure ratio and higher bypass ratios was offset completely by increased propulsion system weight. Nacelle drag drives high bypass ratio engines to more compact, high fan pressure ratio levels. A fan pressure ratio of 1.7:1 and a bypass ratio of 8.0:1 was selected.

4.2.1.3 Engine configuration: The General Electric Energy Efficient Engine is comprised of a single-stage fan driven by a 4-1/2 stage low-pressure turbine; a three-stage low-pressure ratio compressor providing a pressure ratio of 1.7 driven by the LPT; a nine-stage high-pressure compressor providing a pressure ratio of approximately 14:1 driven by a single-stage cooled axial turbine; a double-annular combustor; and a mixed flow exhaust system.

The selected P&W engine consists of a high-speed, single-stage 1.7 pressure ratio fan, a three-stage low-pressure compressor with a pressure ratio of 1.53, and a two-stage, 18.2:1 pressure ratio high-pressure compressor. A low emission, two-stage vortex combustor with aerating pilot nozzles is included to provide a 1427°C (2600°F) maximum average combustor exit temperature. The compression system is powered by a two-stage, cooled high-pressure turbine and a five-stage low-pressure turbine. The exhaust system consists of a fan nozzle and a core nozzle.

4.2.2 Initial LH_2 engine cycle selection. - The initial LH_2 engine cycle selection proceeded on the basis that a rotor inlet temperature of 1427°C (2600°F) to 1538°C (2800°F) was optimum. The assumption was based on findings that show temperatures above this level require cooling for the low-pressure turbine vanes and blades. Cooling the low-pressure turbine results in significant performance penalties and is expensive. This assumption was tested later in the study through the investigation of a 1760°C (3200°F) engine that used hydrogen to cool the turbine cooling air and thereby minimize the performance penalty. The results of this investigation are covered in a subsequent section.

4.2.2.1 Baseline engine description: The baseline engine chosen for the initial cycle selection study is a two-spool, separately exhausted turbofan consisting of the following components:

- Single-stage fan
- Two-stage low-pressure compressor (booster stages)
- Ten-stage high-pressure compressor
- Annular combustor
- Axial cooled HP turbine (single stage)
- Axial uncooled fan turbine (4-6 stages)
- Exhaust regenerator (for fuel heating)
- Separate fan and core convergent exhaust nozzles

The cycle characteristics of the baseline engine were selected to approximate the cycle used in the feasibility studies discussed in 4.1; however, additional intercomponent pressure drops, cooling flows and leakage were added. A definition of the baseline cycle for the cycle selection studies is provided in Table 9. Also shown in Table 9 are three other cycles which provide a summary of how the cycle was changed from the initial Lockheed cycle to the baseline cycle derived for the cycle selection studies. The cycle labeled 4 is the baseline cycle used in the hydrogen exploitation feasibility, studies and is quite close to the original Lockheed cycle (see 4.1.1). Cycle number 3 resulted when the exhaust regenerator was added for fuel heating. A 4.3 percent improvement in specific fuel consumption resulted when the exhaust regenerator was added.

There was some optimism in cycle 3, however, and cycle number 2 incorporated the following changes:

- HP turbine efficiency was reduced 1 point to 0.90 to allow for losses due to cooling.
- LP turbine efficiency was reduced 3 points to 0.88 as a result of turbine preliminary design.
- 21 horsepower allowed for bearing losses, etc., and to drive engine accessories.
- Fan duct and intercompressor pressure drops were modified.
- 3.5 percent turbine cooling air was added.

The net effect of these changes was to increase specific fuel consumption 7.8 percent with respect to the cycle number 3.

The baseline cycle for cycle selection studies resulted from flow path and component analysis. The core compressor ratio of 25.17 postulated for cycles 2, 3, 4 was considered too high. Extensive variable geometry (all stages) would be required and the turbine work levels for a single stage

TABLE 9. - BASELINE ENGINE CYCLE, INITIAL CYCLE SELECTION

	1 Baseline	2 Adjusted Cycle	3 Exhaust Heating Study	4 Baseline Feasibility Studies
FAN				
Inlet Corrected Flow, kg/sec (lb/sec)	684 (1507)	659 (1453)	618 (1362)	619 (1364)
Pressure Ratio	1.6	1.6	1.634	1.634
Adiabatic Efficiency	0.892	0.892	0.889	0.889
Bypass Ratio	12.0:1	12.0:1	12.5:1	13.0:1
LP Compressor (Booster)				
Pressure Ratio	1.3	-	-	-
Adiabatic Efficiency	0.865	-	-	-
HP Compressor				
Pressure Ratio	19.5	25.17	25.17	25.17
Adiabatic Efficiency	0.862	0.862	0.862	0.862
Combustor				
Efficiency	1.0	1.0	1.0	1.0
Pressure Drop, $\Delta P/P$	0.045	0.045	0.045	0.045
Hp Turbine				
Rotor Inlet Total Temperature, ^{o}C (^{o}F)	1379 (2514)	1379 (2514)	1379 (2514)	1379 (2514)
Adiabatic Efficiency	0.90	0.90	0.91	0.91
Horsepower Extraction	125	125	125	125
LP Turbine				
Inlet Total Temperature, ^{o}C (^{o}F)	959 (1758)	948 (1738)	975 (1787)	978 (1793)
Adiabatic Efficiency	0.88	0.88	0.91	0.91
Horsepower Extraction	21	21	0	0
Exhaust Regenerator				
Effectiveness	0.8	0.8	0.8	-
Gas Side Pressure Drop ($\Delta P/P$)	0.04	0.04	0.04	-
Core Nozzle Thrust Coefficient	0.988	0.988	0.995	0.995
Fan Nozzle Thrust Coefficient	0.98	0.98	0.995	0.995
Fan Duct Pressure Loss, $\Delta P/P$	0.015	0.015	0.03	0.03
LPC-HPC Pressure Loss $\Delta P/P$	0.015	0.015	0	0
LPT-Nozzle Pressure Loss, $\Delta P/P$	0.005	0.005	0.005	0.005
Aircraft Bleed Extraction, Percent	4.1	4.1	4.1	4.1
Turbine Cooling Air, Percent	3.5	3.5	0	0
Leakage, Percent	1.0	0	0	0
Net Thrust, N (lb)	29 687 (6674)	29 576 (6649)	29 687 (6674)	29 687 (6674)
Specific Fuel Consumption, (kg/hr)/daN (lb/hr)/lb)	0.2183 (0.2141)	0.2148 (0.2106)	0.1993 (0.1954)	0.2082 (0.2042)
Net Thrust, N (lb) (Includes Nacelle Drag)	26 689 (6000)	26 689 (6000)	26 689 (6000)	26 689 (6000)
SFC, (kg/hr)/daN (lb/hr)/lb) (Includes Nacelle Drag)	0.2428 (0.2381)	0.2379 (0.2333)	0.2217 (0.2174)	0.2317 (0.2272)

high-pressure turbine were considered excessive. To maintain cycle pressure ratio at 40:1 with a lower core pressure ratio, booster stages were added to the fan spool. Provisions for seal leakage (1 percent) were also incorporated. This resulted in a 1.7 percent increase in specific fuel consumption with respect to cycle number 2.

With respect to the cycle defined by Lockheed in the previous study, specific fuel consumption was higher by 7.7 percent, including the effect of the exhaust regenerator.

The flight condition chosen for the cycle selection studies was for initial cruise at 10 788m (35 000 feet), M = 0.85, maximum climb power setting. The studies were made on the basis of installed performance and included the effects of cowl drag but not inlet spillage drag.

The selection criteria for all investigations was minimum DOC. DOC was evaluated using the equation given in 4.1.1.

4.2.2.2 Selection of rotor inlet temperature and cycle pressure ratio: As stated earlier, turbine inlet temperature was limited to a restricted range 1427-1538°C (2600-2800°F). The G.E. Energy Efficient Engine study showed minimum DOC occuring between 1482-1510°C (2700-2750°F). A maximum rotor inlet temperature of 1482°C (2700°F) was selected on the basis of the prior studies.

Cycle pressure ratio was selected primarily on the basis of utilizing a single stage high pressure turbine. Although extensive tradeoff studies could be made addressing single and two stage HP turbines, AiResearch experience has shown that a single stage turbine minimizes turbine cooling required and that minimizing the number of cooled stages results in lower engine cost.

The actual maximum turbine work level is based on tip speed, flow path, cooling and stresses, but for cycle selection a value of 488.1 kJ/kg (210 Btu/lb) at the temperature selected is a reasonable maximum. Likewise, the maximum core compressor ratio is rightfully the subject of a detailed study but for this program, the selection of a 20:1 maximum core pressure ratio is reasonable and avoids consideration of mismatch and stability problems.

Shown in Figure 21 is the relationship of high pressure turbine work, fan pressure ratio and high pressure compressor pressure ratio. A maximum turbine inlet temperature of 1482°C (2700°F) and a booster pressure ratio of 1.30:1 was assumed. Within the constraints of 488.1 kJ/kg (210 Btu/lb) turbine work and core compressor ratio, an overall pressure ratio of 45:1 is reached only with high fan pressure ratios. At an overall pressure ratio of 40:1, fan pressure ratio can be approximately 1.55 to 2.0:1. Furthermore, a cycle pressure ratio of 40:1 achieves most of the benefit of high cycle pressure ratio. Based on these considerations, cycle pressure ratio was selected at 40:1.

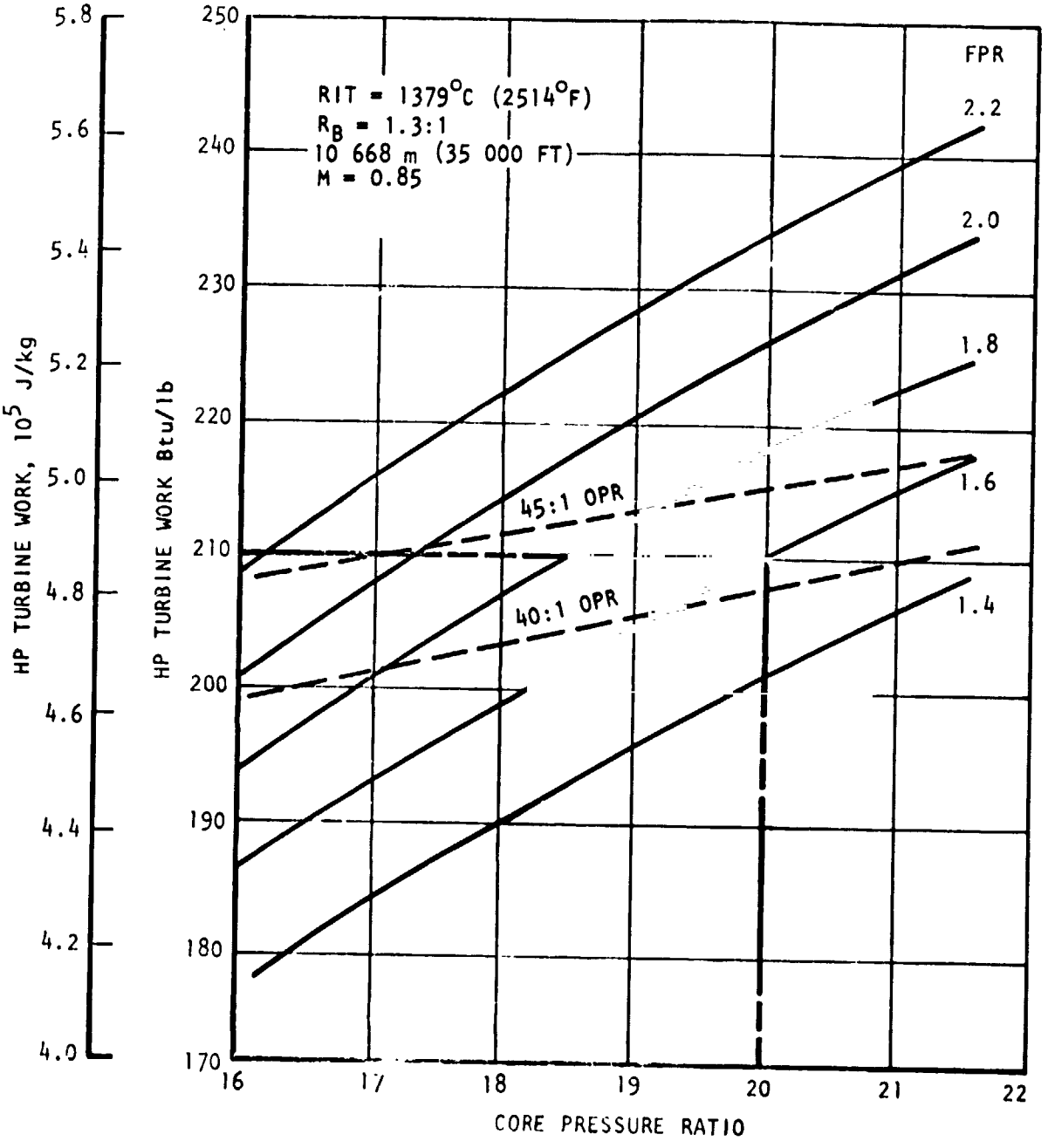

Figure 21. - Selection of cycle overall pressure ratio.

4.2.2.3 Fan pressure ratio and bypass ratio selection: Fan pressure ratios from 1.4 to 2.2 were studied. The turbine inlet temperature of 1482°C (2700°F) maximum (1379°C (2514°F) cruise) and the maximum cruise cycle pressure ratio of 40:1 were held constant in this portion of this study. Primary stream energy extraction was varied by considering a range of bypass ratios.

Fan pressure ratio was selected on the basis of minimum DOC which includes the effects of specific fuel consumption and engine weight. Maintenance was not included.

The baseline engine is as described in 4.2.2.1. Figure 22 shows specific fuel consumption versus exhaust nozzle velocity ratio for the range of fan pressure ratios considered. Figure 23 shows bypass ratio versus fan pressure ratio and exhaust nozzle velocity ratio. Figure 24 shows estimated engine relative weight versus fan pressure ratio and bypass ratio.

The trends in DOC are shown in Figure 25. Each fan pressure ratio has a minimum DOC. The curve of minimum DOC and fan pressure ratio is shown in Figure 26. Based on this curve, the fan pressure ratio for minimum DOC is 1.7:1. The related bypass ratio is 9.3:1 as shown in Figure 27.

4.2.3 High temperature investigation. - As the results of the hydrogen exploitation studies and the initial cycle selection work became available, it was apparent that some benefit might accrue to a high temperature cycle which used hydrogen to cool the cooling air and thereby minimize the cooling penalty for both the high and low pressure turbines. In order to take full advantage of the higher turbine inlet temperatures, higher cycle pressure ratios are required and a two-stage, high pressure turbine becomes necessary. At a fan pressure ratio of 1.6, for example, high pressure compressor pressure ratio would be between 21.5:1 and 26:1 at cycle pressure ratios between 50:1 and 60:1 respectively. Attaining these pressure ratios in a reasonable number of stages and avoiding mismatch and stability problems is quite a formidable task without even considering weight, complexity and cost penalties.

The introduction of a two-stage high pressure turbine and a cooled fan turbine required a more detailed turbine cooling flow analysis.

Turbine inlet temperature was held constant at 1760°C (3200°F). This temperature was arbitrarily selected but is representative of the maximum turbine inlet temperature feasible in the study time period. Cycle pressure ratios of 40, 50, and 60 were investigated. Fan pressure ratio was also varied although it was believed that changes from the fan pressure ratio selected in the earlier investigation would be second order.

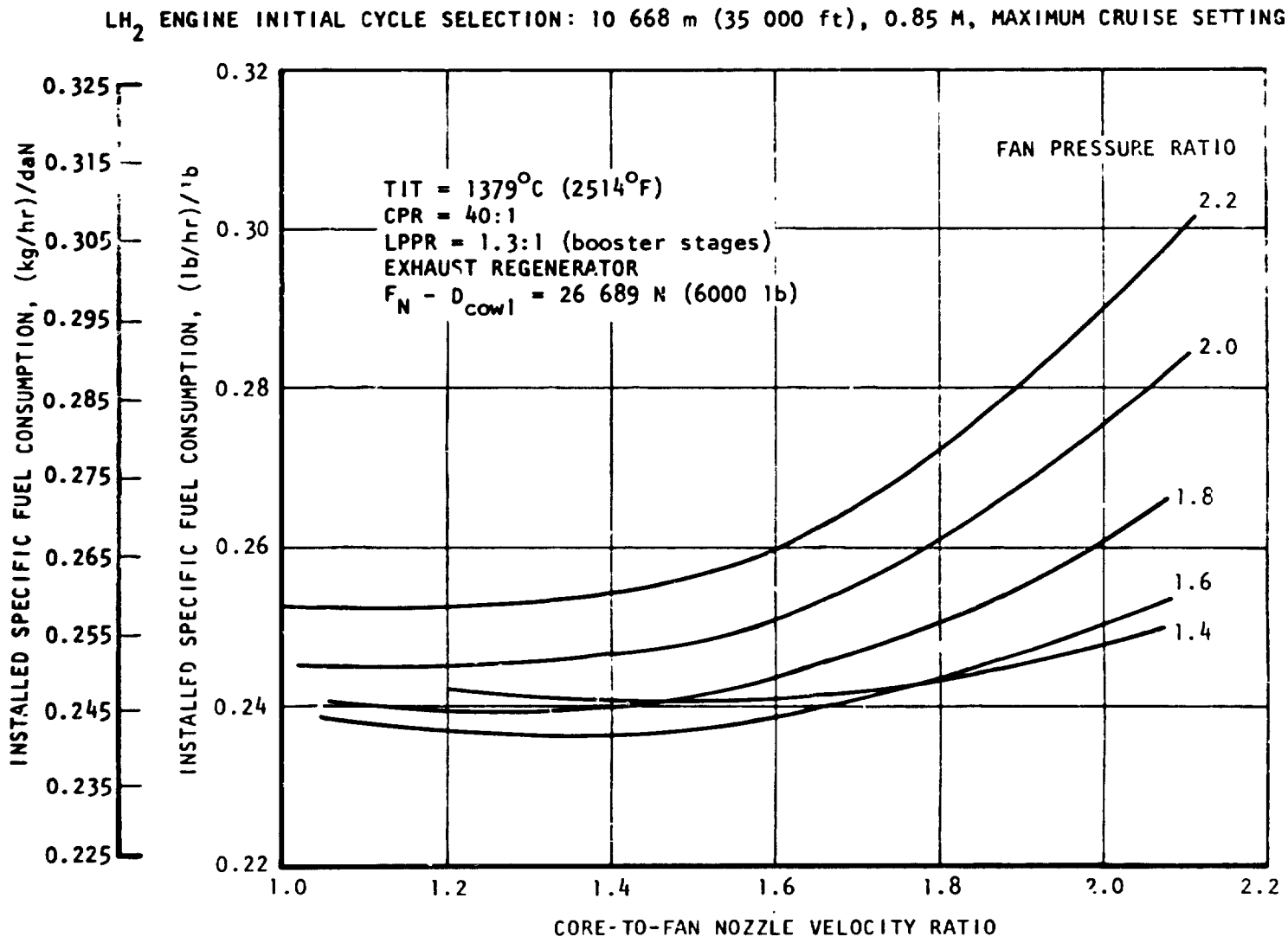

Figure 22. - Effect of fan pressure ratio and nozzle velocity ratio on engine performance.

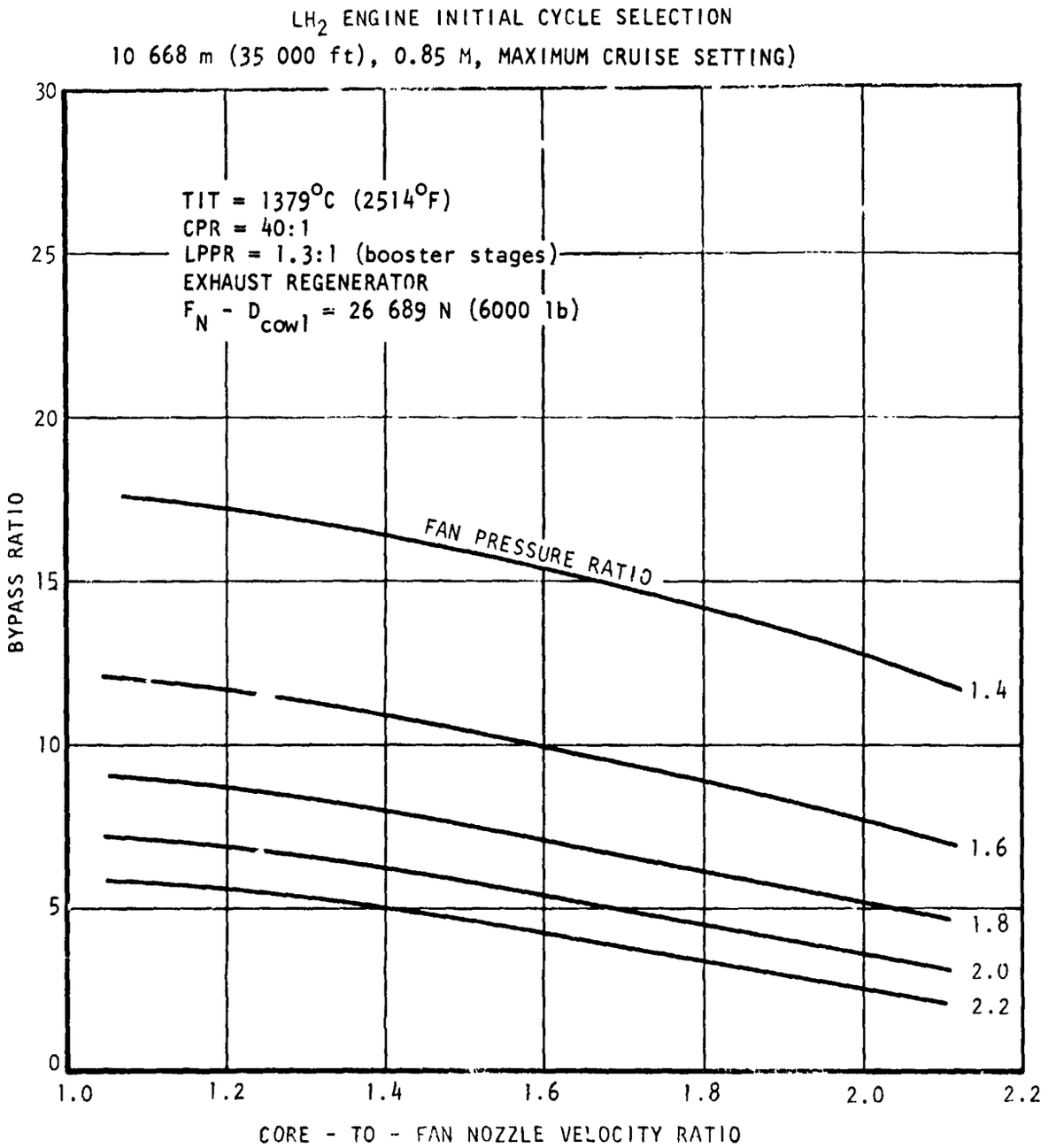

Figure 23. - Effect of fan pressure ratio and nozzle velocity ratio on bypass ratio.

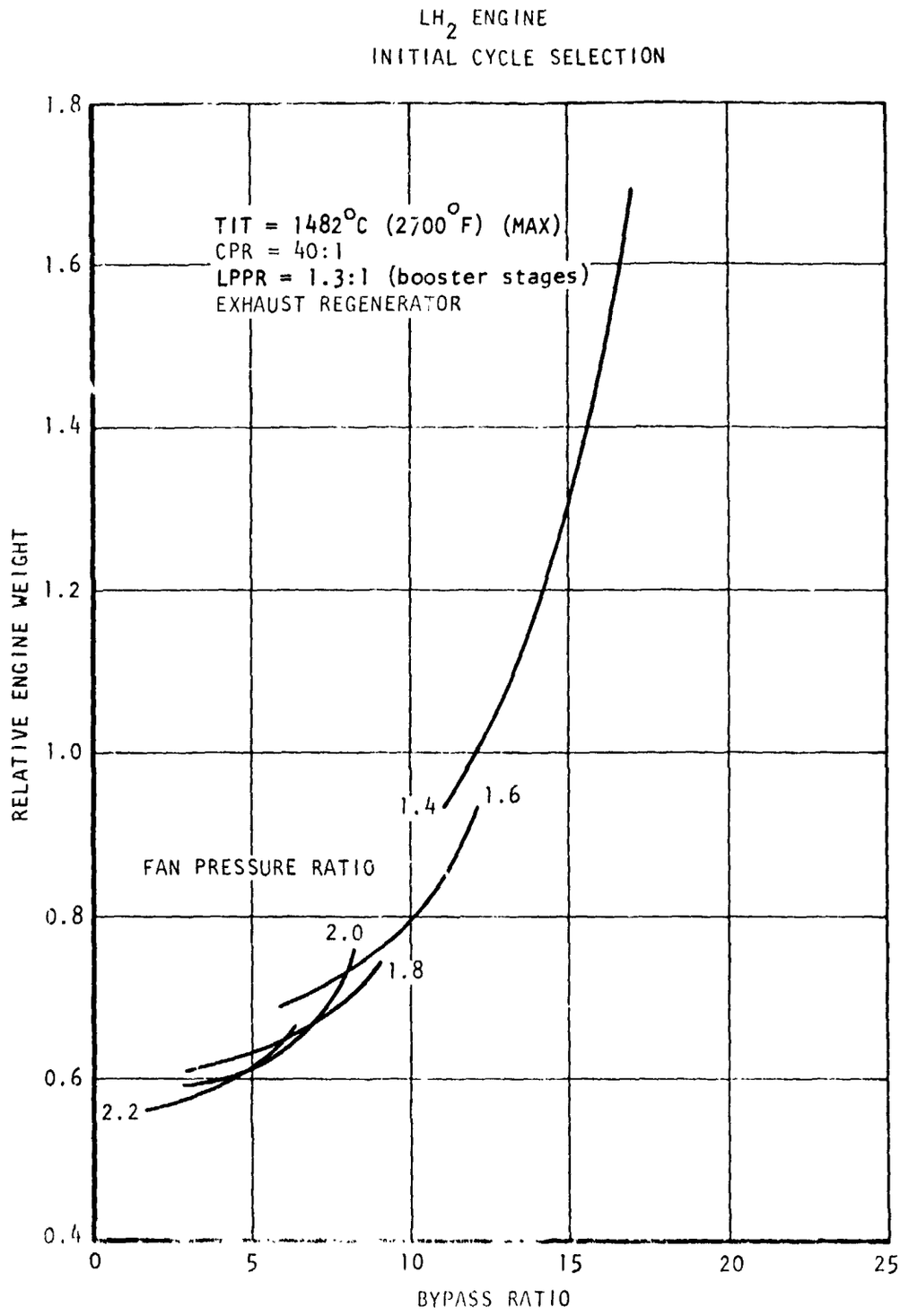

Figure 24. - Effect of fan pressure ratio and bypass ratio on engine weight.

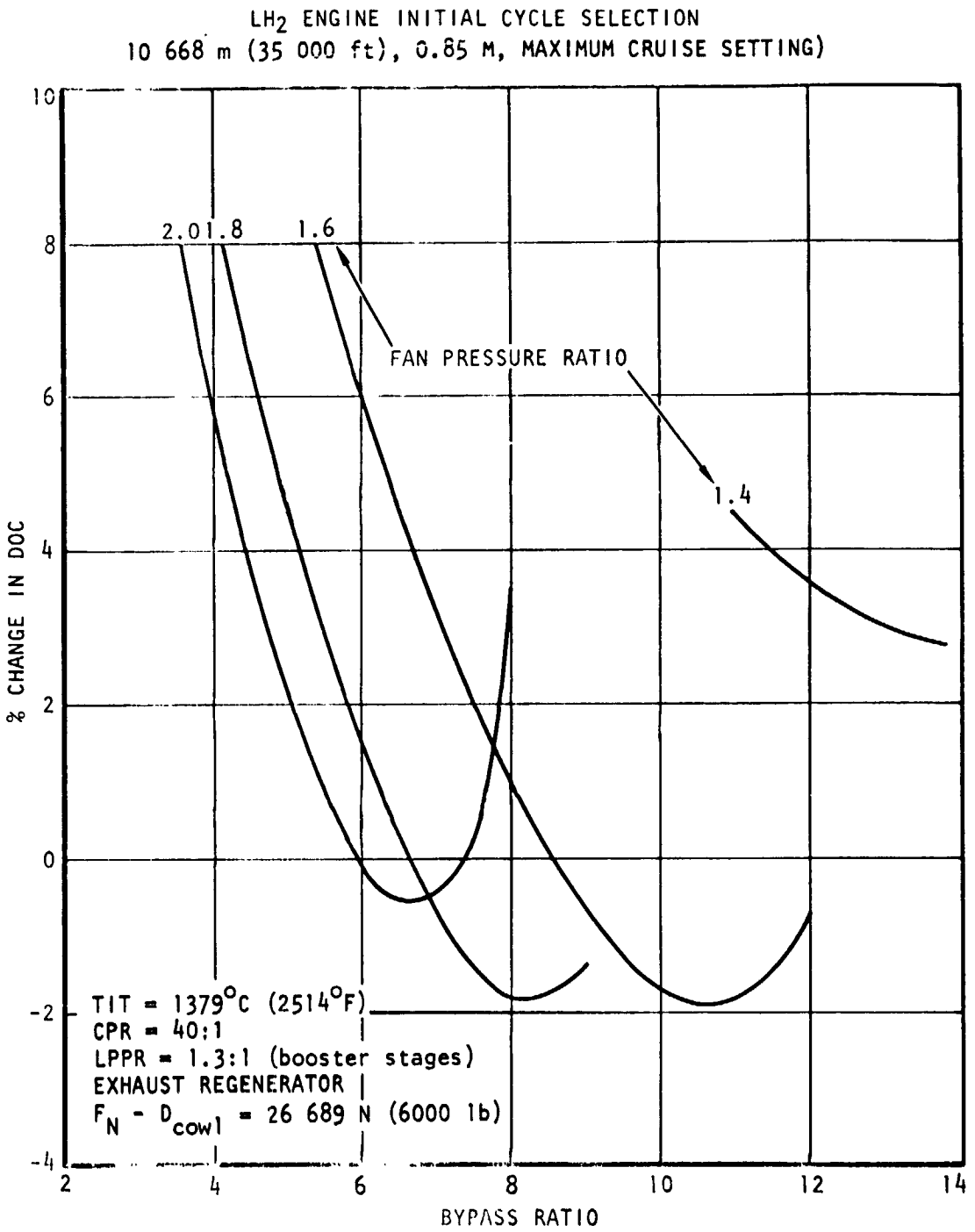

Figure 25. - Effect of fan pressure ratio and bypass ratio on direct operating cost.

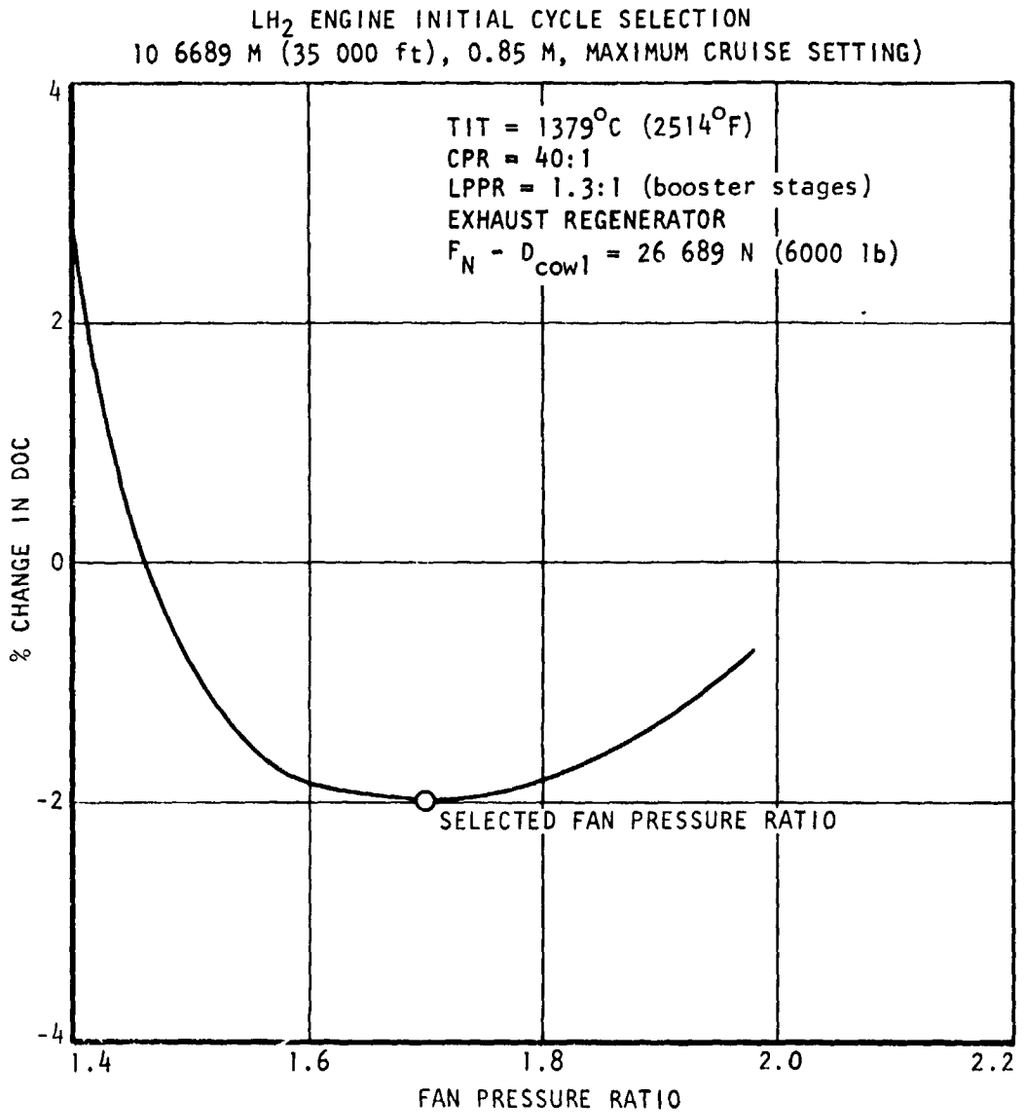

Figure 26. - Effect of fan pressure ratio on change in direct operating cost.

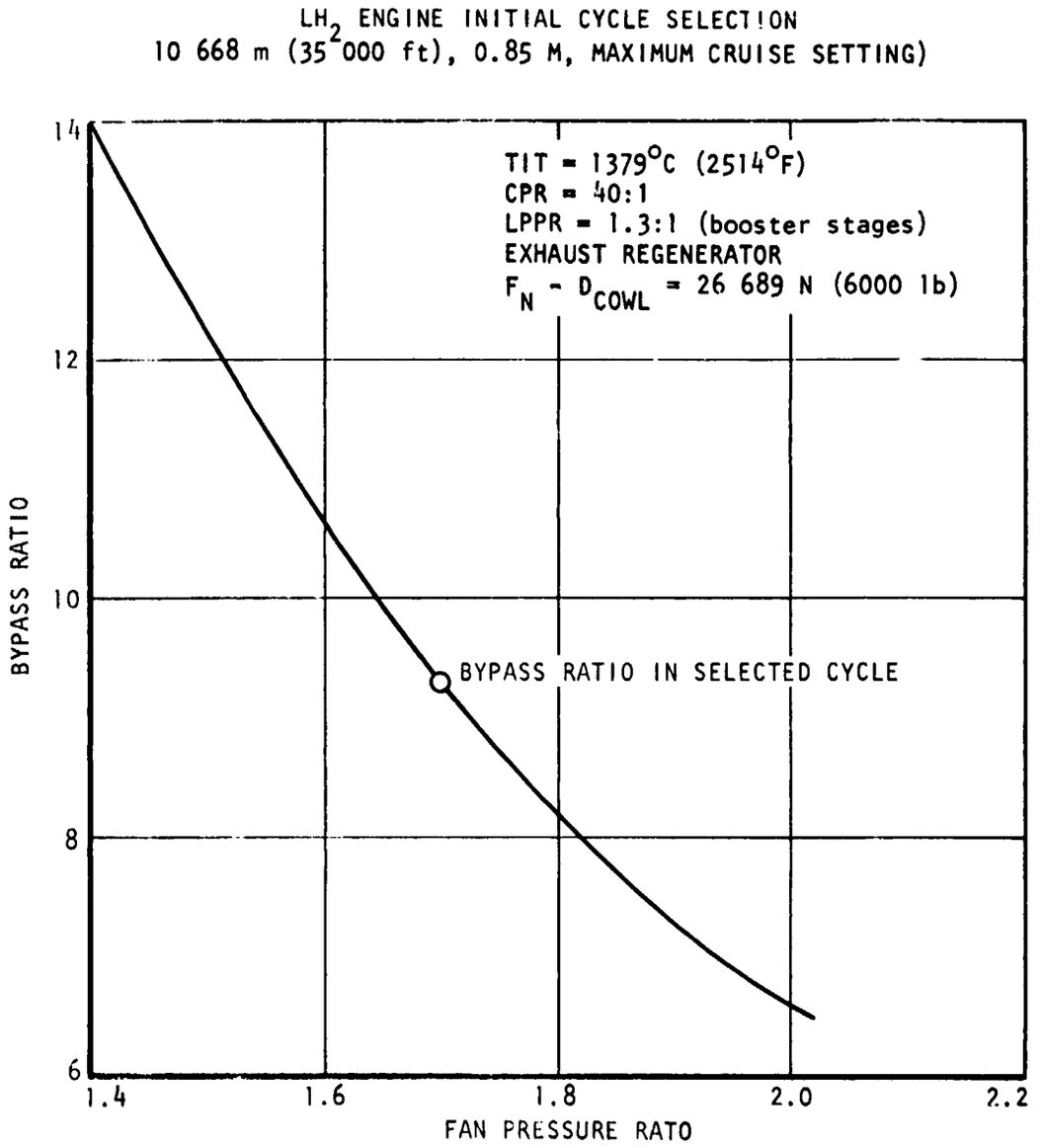

Figure 27. - Bypass ratio vs fan pressure ratio.

The flight condition, installation factors, and other related assumptions were identical to those assumed earlier. The baseline engine is identical to that described in 4.2.2.1.

Cooling flow requirements were defined at maximum power, hot day, sea level. An engine having a fan pressure ratio of 1.7:1 and a bypass ratio of 9.3:1 was assumed in computing the cooling flow requirements. A schematic representation of the hydrogen cooling of the turbine cooling air was shown previously in Figure 10.

4.2.3.1 Turbine cooling requirements:

4.2.3.1.1 Engine operating conditions: Turbine cooling requirements were established for hot day, sea level, maximum power conditions. Cycle temperatures are related to temperatures at the cruise conditions using ratios established in prior studies. The temperatures that are important are compressor discharge temperature, combustor outlet temperature, high pressure rotor inlet temperature, and low pressure turbine inlet temperature. These locations are shown schematically in Figure 28. The temperatures used in this study are shown in Table 10.

Temperatures at turbine stations other than those listed in Table 10 were calculated based on equal temperature drop across each turbine stage. For example, if the ΔT across the low pressure turbine is 1000^{o} and there are four stages, tne temperature drop across each stage is assumed to be 250^{o}. The temperatures between each blade or vane row are based c the mass averaged temperatures of the gas stream and the cooling flows. Also, combustor outlet temperature is that required to provide the rated rotor inlet temperature after mixing of the first high pressure turbine vane cooling air.

TABLE 10. - INTERNAL CYCLE TEMPERATURES (SEA LEVEL, HOT DAY, TAKEOFF THRUST)

	Cycle Pressure Ratio		
Station	40:1	50:1	60:1
Compressor Discharge T_3	859 (1546)	916 (1648)	968 (1742)
Combustor Outlet $T_{3.9}$	2087 (3756)	2087 (3756)	2087 (3756)
HP Rotor Inlet T_4	2033 (3660)	2033 (3660)	2033 (3660)
LP Turbine Inlet $T_{4.2}$	1617 (2910)	1577 (2838)	1537 (2766)

Temperatures in ^{o}K (^{o}R)

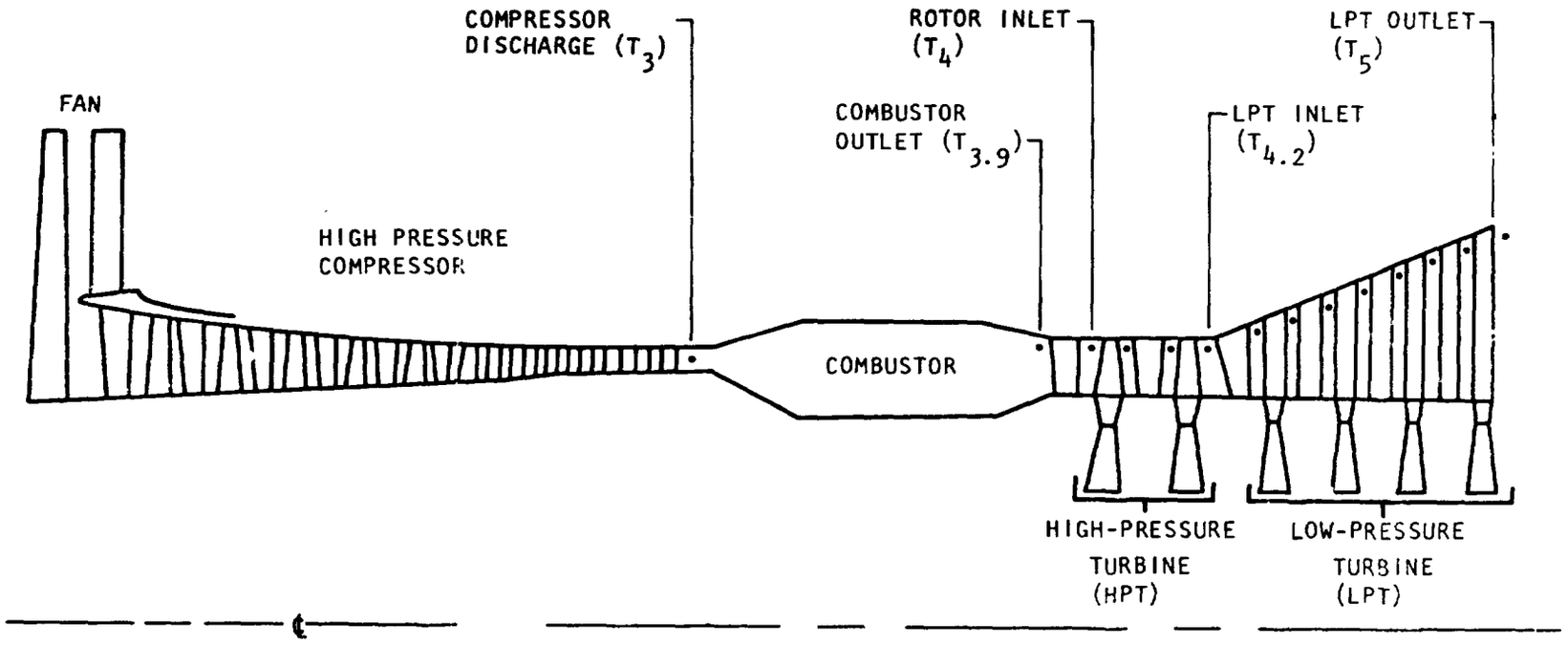

Figure 28. - Engine station designations.

4.2.3.1.2 Turbine cooling air heat exchanger: The turbine cooling air heat exchanger is similar to those used in prior work which has been discussed earlier. At first, it was assumed that the heat exchanger had an effectiveness of 0.8. Further study indicated that the resulting cooling air outlet temperature was approximately 211°K (380°R). Heat exchanger freezing would be a problem at this temperature and cooling air outlet temperature was limited to 311°K (560°R) to avoid this problem. A bypass arrangement or a lower effectiveness heat exchanger is required. (Refer to heat exchanger design, Section 4.3.6.)

4.2.3.1.3 Turbine design criteria: Minimum design criteria were established to allow the determination of turbine cooling requirements. The criteria established included the following:

- Allowable metal temperatures
- Combustor pattern factor
- Blade and vane heat transfer effectiveness
- Blade relative gas temperature
- Turbine work limits
- Turbine cooling efficiency penalties

The allowable metal temperatures assumed for this study are shown in Table 11. They are based on the results and projections of turbine material technology programs and are applicable to long-life transport engines.

TABLE 11. - ALLOWABLE METAL TEMPERATURE LIMITS

	Temperature Limit
High Pressure Turbine Vanes	1204°C (2200°F)
High Pressure Turbine Blades	1093°C (2000°F)
Low Pressure Turbine Vanes	1149°C (2100°F)
Low Pressure Turbine Blades	1093°C (2000°F)

The combustor pattern factor $(T_{3.9max} - T_{3.9avg})/T_{3.9avg} - T_3)$ determines the peak temperature that the turbine vanes feel. Blades are not influenced by the pattern factor as their rotation tends to average the temperatures to which they are exposed. The combustor pattern factor persists throughout the turbine, although it is attenuated and tends to shift both radially and circumferentially. Hydrogen-fueled engines will have lower pattern factors than Jet A fueled engines. However, the inherent lower pattern factor can be traded to some extent for smaller combustor volumes. The pattern factors assumed for the study are shown in Table 12. They are significantly better than can be achieved with conventional fuels and are consistent with the combustor size selected. Further improvement would be possible if a larger combustor were selected; however, the combustor was sized based on flowpath, weight and cost considerations which generally favor small size.

Blade and vane cooling requirements were calculated on the basis of simple effectiveness correlations, a simplified approach. To establish cooling flows precisely requires consideration of a number of factors not included in the simple effectiveness correlations and is beyond the scope of this study. Two levels of effectiveness versus cooling flow were used. One, used for the higher pressure turbine, reflects a sophisticated, high effectiveness, high cost approach. The second is a lower effectiveness, lower cost approach which was used for the low pressure turbine.

The temperature environment of the rotating blade is a function of the stage work, mean blade speed and the gas temperature. For this study, it was assumed that the temperature felt by the blade was 90 percent of the gas temperature for high pressure turbine blades and 93 percent of the gas temperature for the low pressure turbine.

An analysis of the turbine work required to drive the high pressure compressor in the 40:1, 50:1 and 60:1 cycle pressure ratio engines indicated that the 40:1 engine required a single-stage turbine and the 50:1 and 60:1 cycles required two-stage high pressure turbines.

TABLE 12. - LH_2 COMBUSTOR PATTERN FACTORS

Turbine Vane	Pattern Factor
First High Pressure Vane	0.15
Second High Pressure Vane	0.15
First Low Pressure Vane	0.125
Second Low Pressure Vane	0.10

Turbine cooling flow leaving the turbine blades or vanes disrupts the flow field and causes losses. These losses are small when trailing edge discharge is feasible. However, to achieve the high effectiveness cooling schemes required, film cooling is required and efficiency penalties are incurred. Baseline turbine efficiencies were, therefore, adjusted to reflect the type of cooling air discharge and the quantity of cooling air.

4.2.3.1.4 Turbine cooling flow quantities: Turbine cooling flow requirements are shown in Table 13 for the three pressure ratios being investigated. As just stated, a single-stage high pressure turbine is satisfactory for the 40:1 pressure ratio cycle, but a two-stage high pressure turbine is required for the 50:1 and 60:1 pressure ratio cycles.

The flow requirements are separated into cooled chargeable, uncooled chargeable, and, in the case of the high pressure turbine, nonchargeable cooling air. Cooled chargeable air is cooling flow that is cooled by hydrogen and which bypasses one or more work producing stages of the turbines. It therefore reduces horsepower produced by the turbine. Uncooled chargeable air is cooling flow that is not cooled by the hydrogen and which bypasses one or more work producing stages. Nonchargeable air is the air used to cool the first high-pressure vane. First high-pressure vane cooling air does not bypass any work producing stage and, therefore, does not diminish horsepower produced by the turbine. First vane cooling air does have an

TABLE 13. - TURBINE COOLING AIR FLOW REQUIREMENTS
1760°C (3200°F) ROTOR INLET TEMPERATURE

Cycle Pressure Ratio	HP Turbine*			LP Turbine*	
	Cooled Chargeable	Uncooled Chargeable	Nonchargeable (1st Vane	Cooled Chargeable	Uncooled Chargeable
40:1 (1 STG HPT)	3.0	1.8	3.0	5.0	2.4
50:1 (2 STG HPT)	6.2	2.3	3.0	4.1	2.4
60:1 (2 STG HPT)	5.0**	2.3	3.0	2.7	2.4

*Cooling flow expressed in percent of compressor flow. Includes coolant for blades, vanes, shroud, and disks, plus leakage.

**Note that cooling flow requirements are lower for the 60:1 pressure ratio design due to the lower inlet temperature at the second stage of the high pressure turbine and at the inlet of the low pressure turbine. These lower temperatures result from the greater work extraction at higher pressure ratios.

effect on the temperature of the gas entering the first turbine rotor. However, all cycle calculations are based on the mixed temperature at the first rotor inlet. Therefore, the gas temperature at the first vane inlet (combustor outlet) is higher than the temperature at the first rotor inlet. The amount of cooling flow to the vane is only important in determining the temperature environment of the vane and the efficiency of the turbine. High vane cooling can effect the efficiency of the turbine as discussed earlier. To minimize the amount of vane cooling and the efficiency penalty, hydrogen cooling of the vane cooling air is utilized. Cooling air for the second high pressure turbine vane and the low pressure turbine vane is chargeable as it bypasses one or more work producing stages.

As described in Paragraph 4.1.4, disk cooling air is not cooled by the hydrogen.

4.2.3.1.5 Thermodynamic accountability of turbine cooling air: Turbine cooling air results in two penalties to the cycle. The first is a reduction in turbine efficiency due to disturbing the blade and vane flow fields. This has been covered in earlier discussion. The penalty assessed was 0.2 points in efficiency for every percent cooling air used. The second penalty results from bypassing one or more work producing stages of the turbine. In the thermodynamic model of the engine, flow to any of the blade or vane rows, other than the first vane, is assumed to completely bypass the high pressure turbine. This is also true for all air going to the low pressure turbine. This approach simplifies the model considerably but results in a more severe penalty than is actually incurred. For example, vane cooling to the second vane of the HPT bypasses only one stage of the HPT. To account for this, the actual cooling air to any cascade row was reduced by the ratio of the number of work producing stages it bypasses and the total number of stages in the turbine. This is a simplification which is considered satisfactory for this investigation.

4.2.3.2 Cycle selection: The cooling flows listed in Table 13 were used in the cycle selection studies for the high-temperature investigation. Rotor inlet temperature was held constant at 1760°C (3200°F) and cycle pressure ratio, fan pressure ratio and bypass ratio were varied. Booster pressure ratio was held constant at 1.45:1. All engine cycles were evaluated at 10 668M (35 000 ft), Mach 0.85. Engine thrust minus cowl drag was held constant at 26 689 N (6000 lb). The exhaust regenerator was included in the cycle. Figures 29 through 34 show the results of the investigation for the range of cycle pressure ratios and fan pressure ratios investigated. The weight and performance data shown in Figures 29 through 34 were used to determine ΔDOC relative to the baseline. Trends of DOC versus fan pressure ratio and bypass ratio are shown in Figures 35, 36, 37 for the three selected values of cycle pressure ratio. The minimum DOC at each fan pressure ratio and cycle pressure ratio is shown in Figure 38. Figure 38 also shows the bypass ratios as a function of fan pressure ratio and cycle pressure ratio.

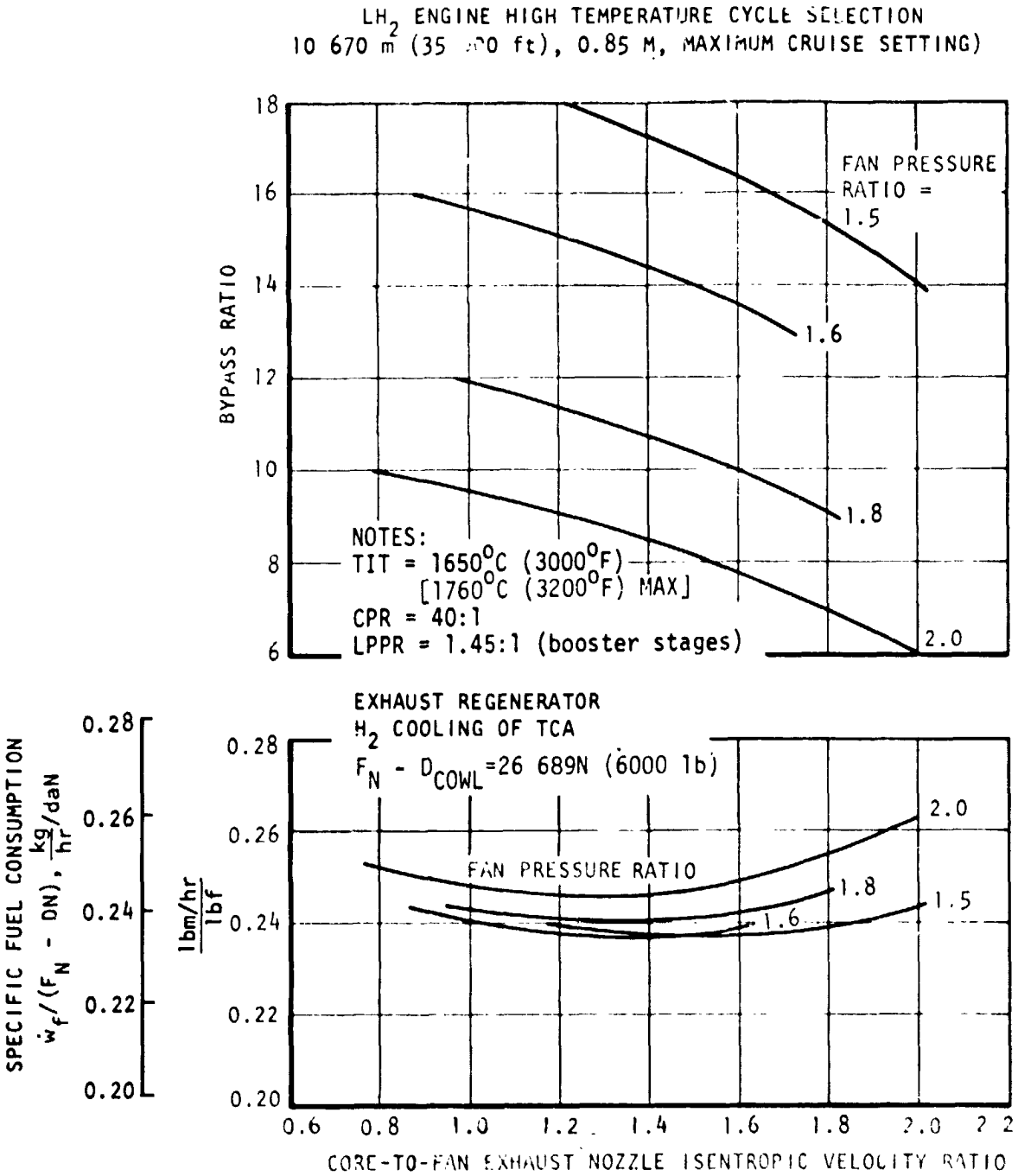

Figure 29. - Effect of core energy extraction and fan pressure ratio on SFC and bypass ratio (CPR = 40).

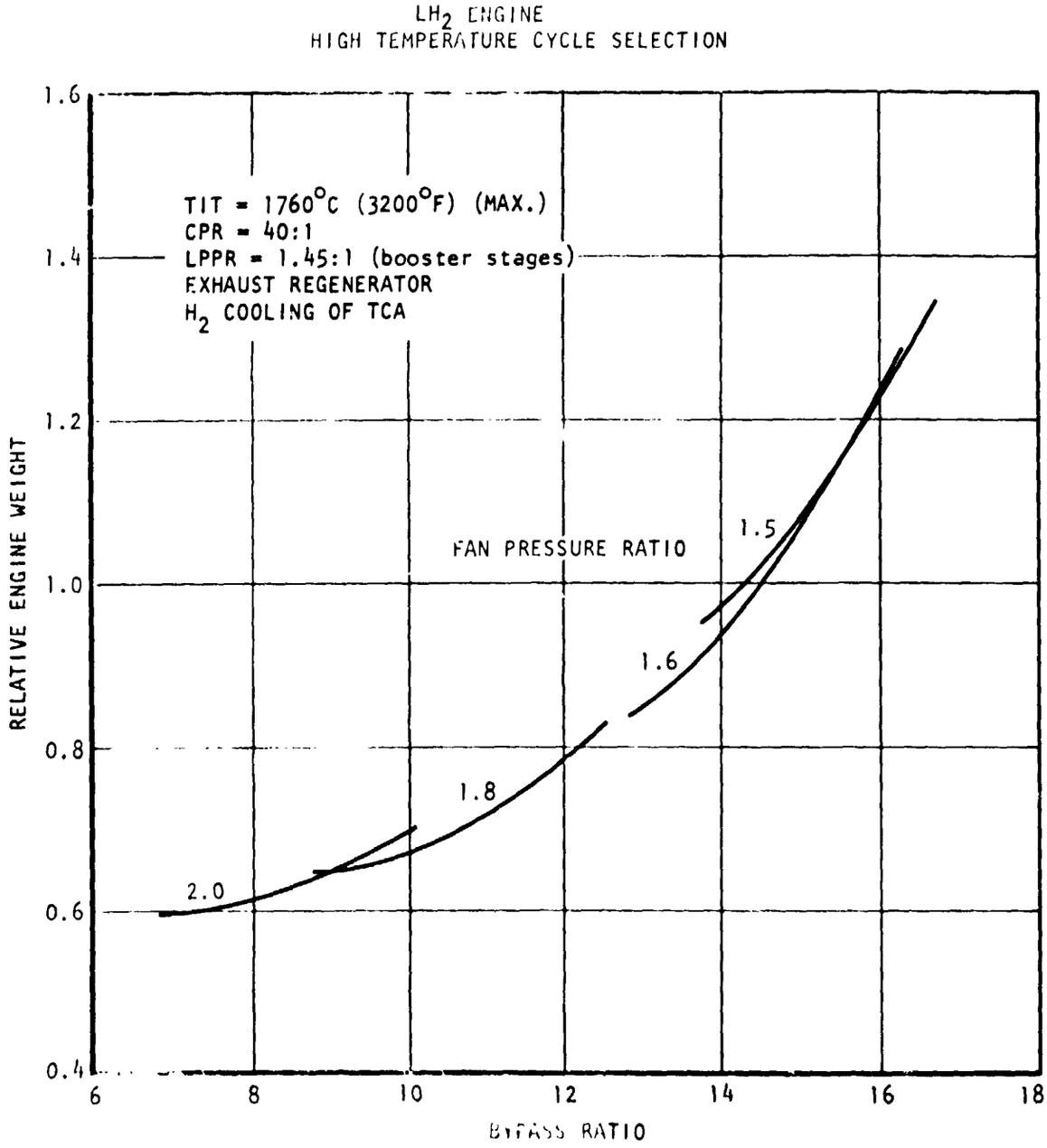

Figure 30. - Effect of fan pressure ratio and bypass ratio on engine weight (CPR = 40).

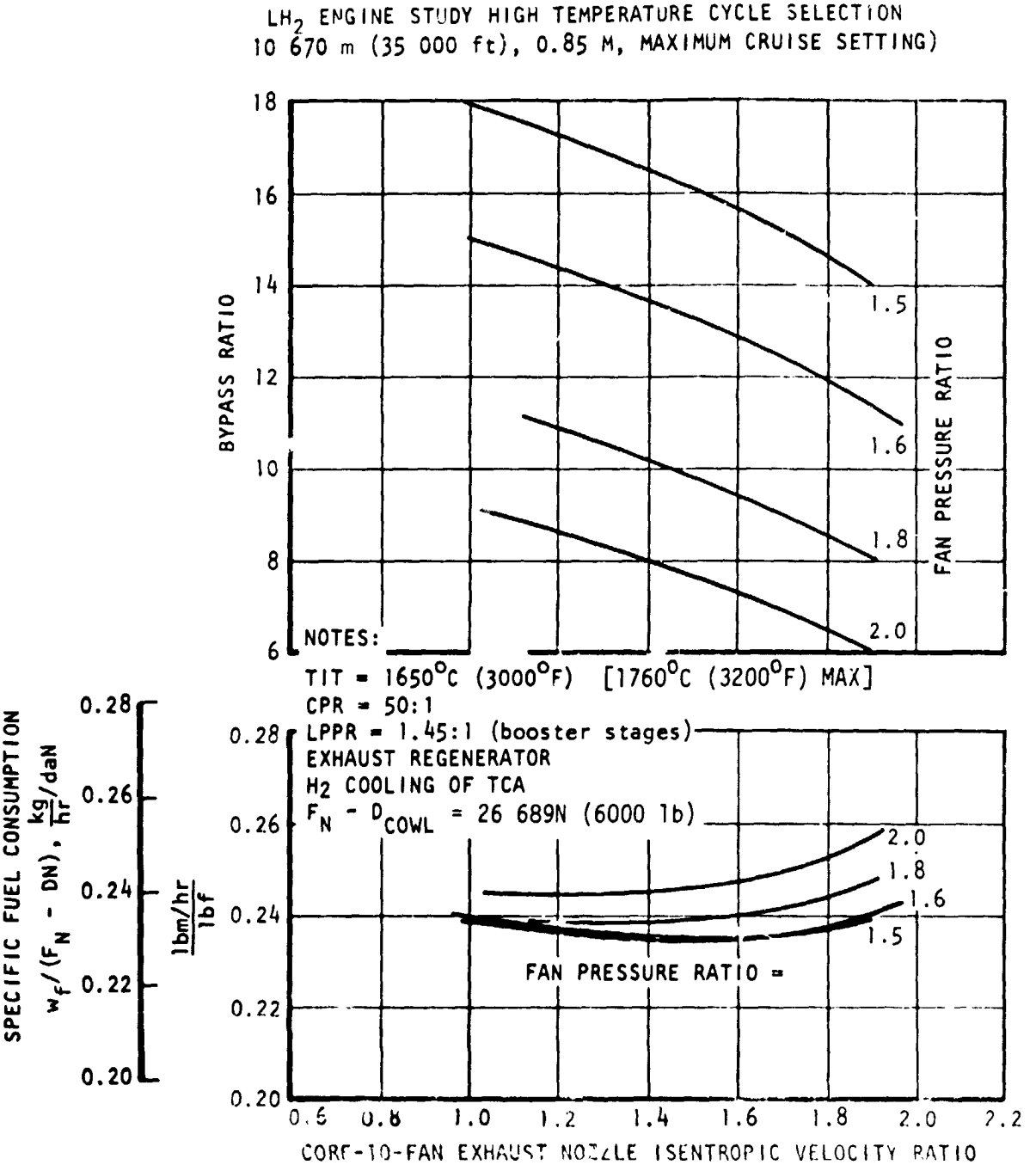

Figure 31. - Effect of core energy extraction and fan pressure ratio on SFC and BPR (CPR = 50).

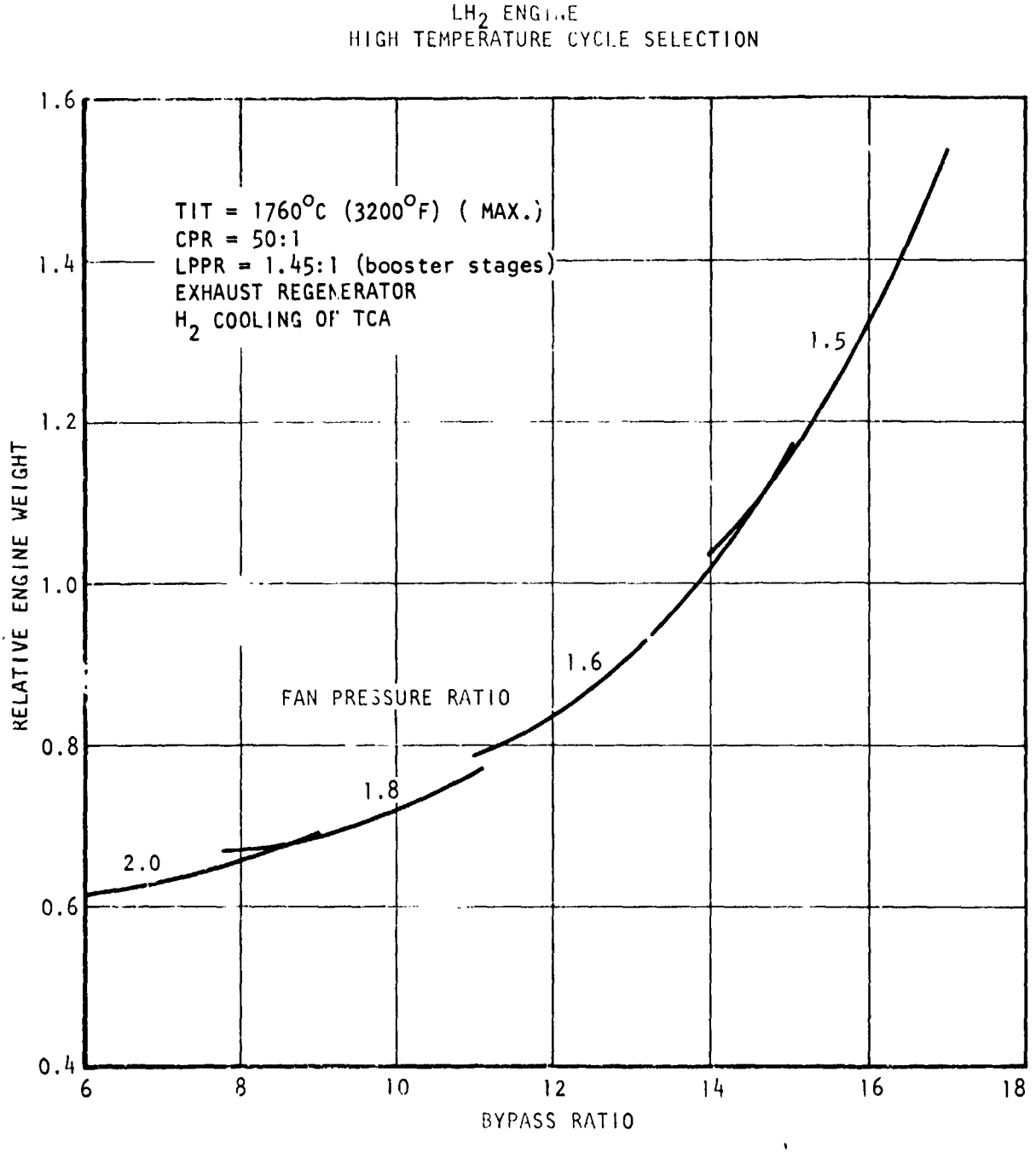

Figure 32. - Effect of fan pressure ratio and bypass ratio on engine weight (CPR = 50).

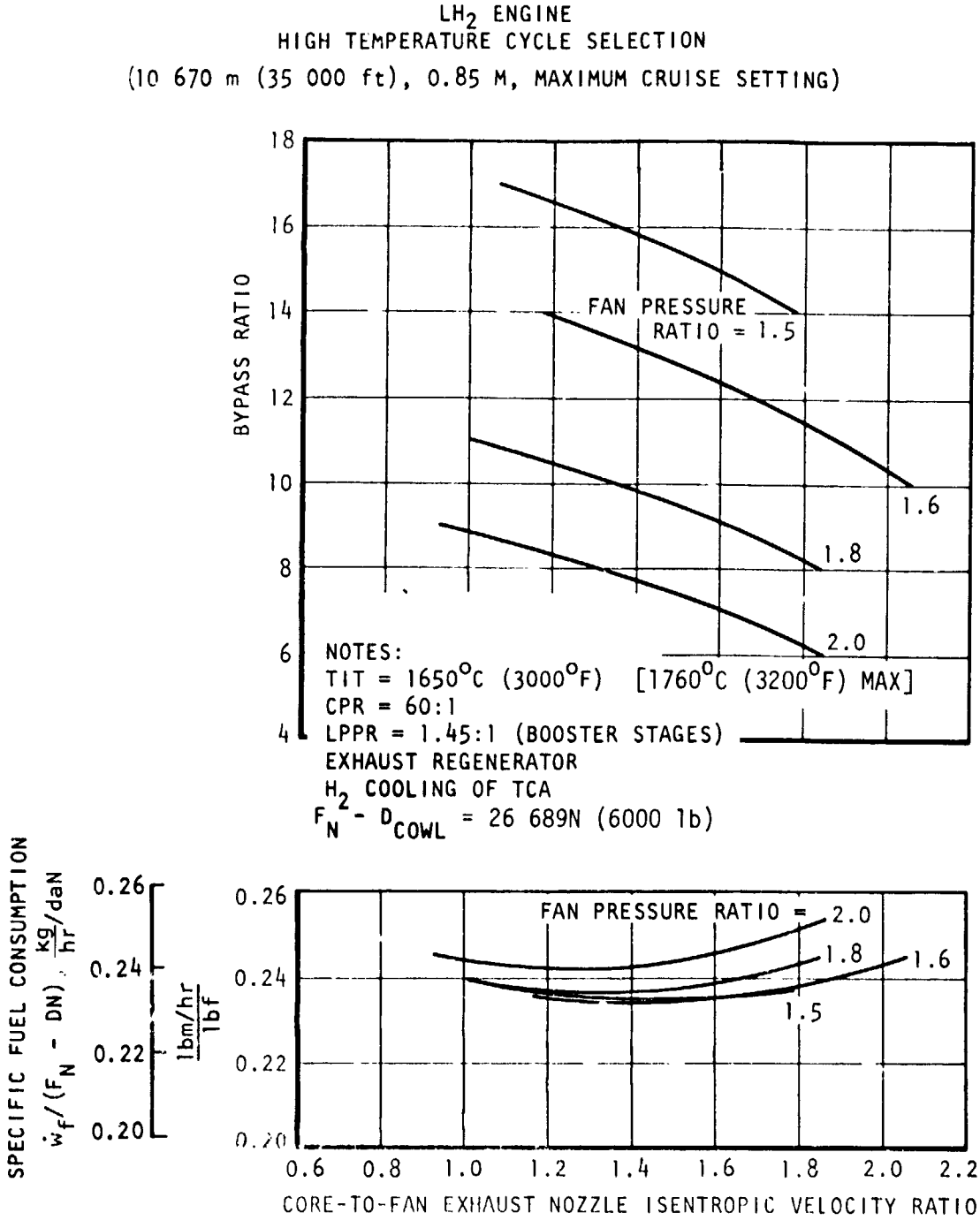

Figure 33. - Effect of core energy extraction and fan pressure ratio on SFC and BPR (CPR = 60).

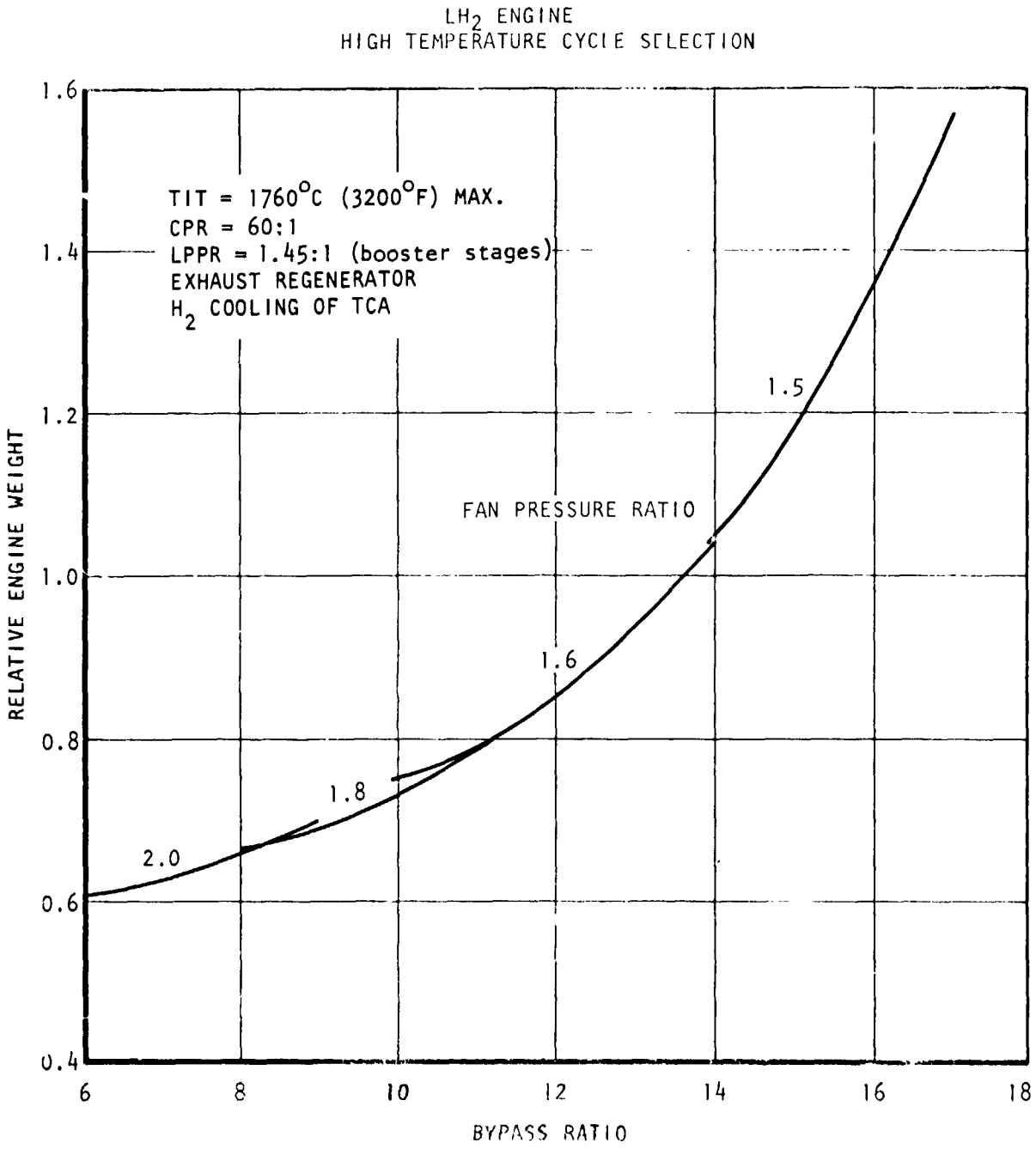

Figure 34. - Effect of fan pressure ratio and bypass ratio on engine weight (CPR = 60).

LH_2 ENGINE
HIGH TEMPERATURE CYCLE SELECTION
(10 668 m (35 000 ft), 0.85 M, MAXIMUM CRUISE SETTING)

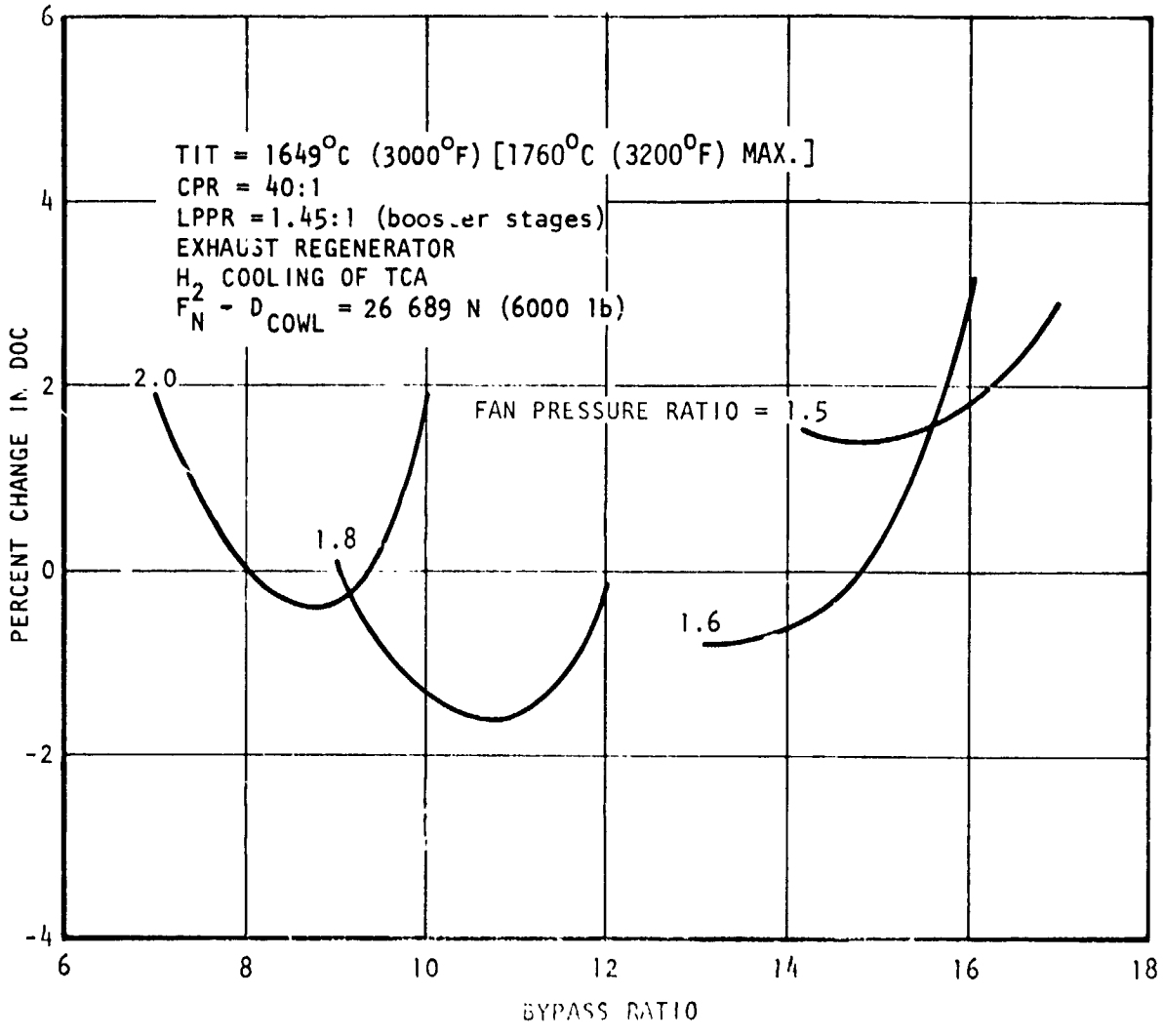

Figure 35. - Effect of bypass ratio and FPR on DOC for CPR = 40.

LH_2 ENGINE
HIGH TEMPERATURE CYCLE SELECTION
(10 668 m (35 000 ft), 0.85 M, MAXIMUM CRUISE SETTING)

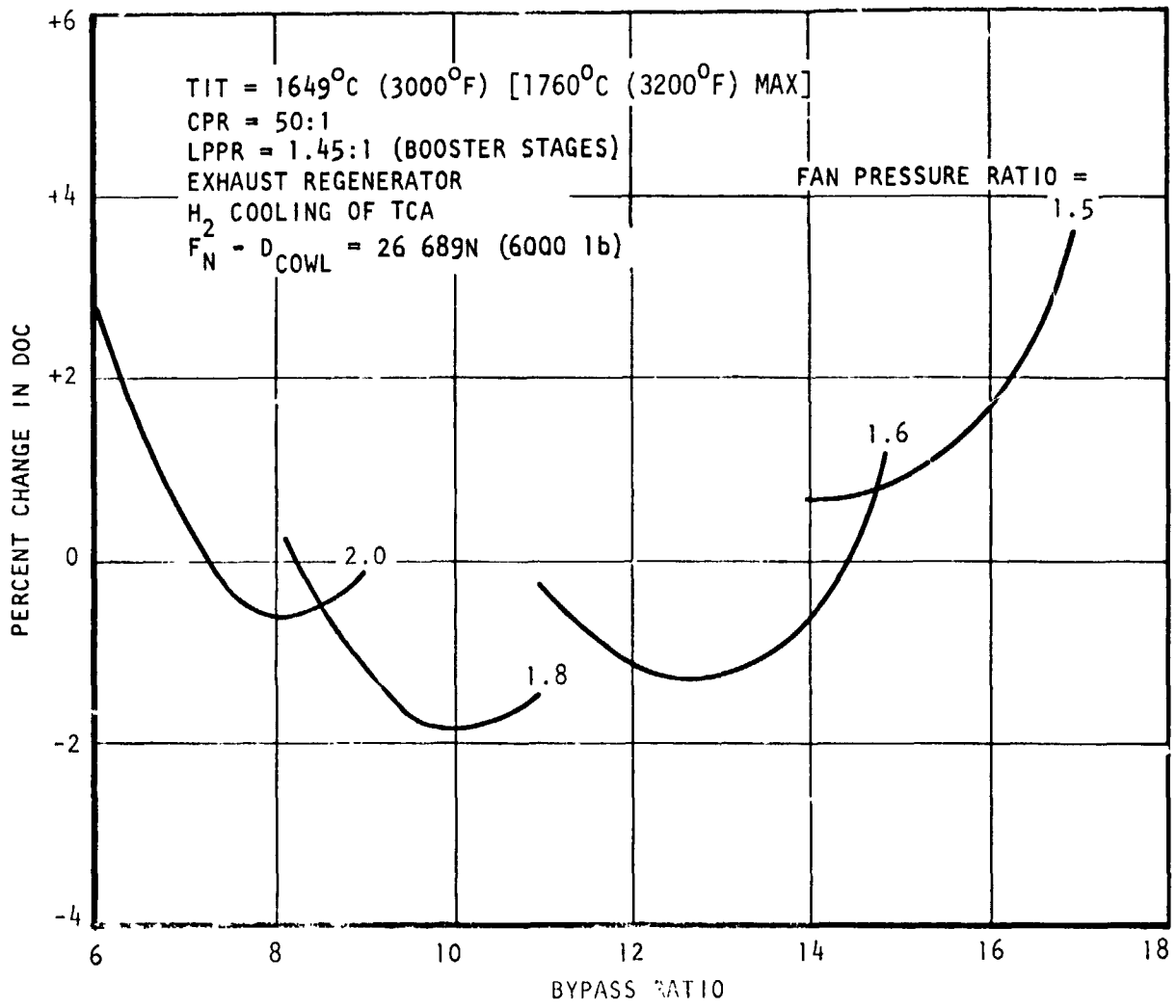

Figure 36. - Effect of bypass ratio and FPR on DOC for CPR = 50.

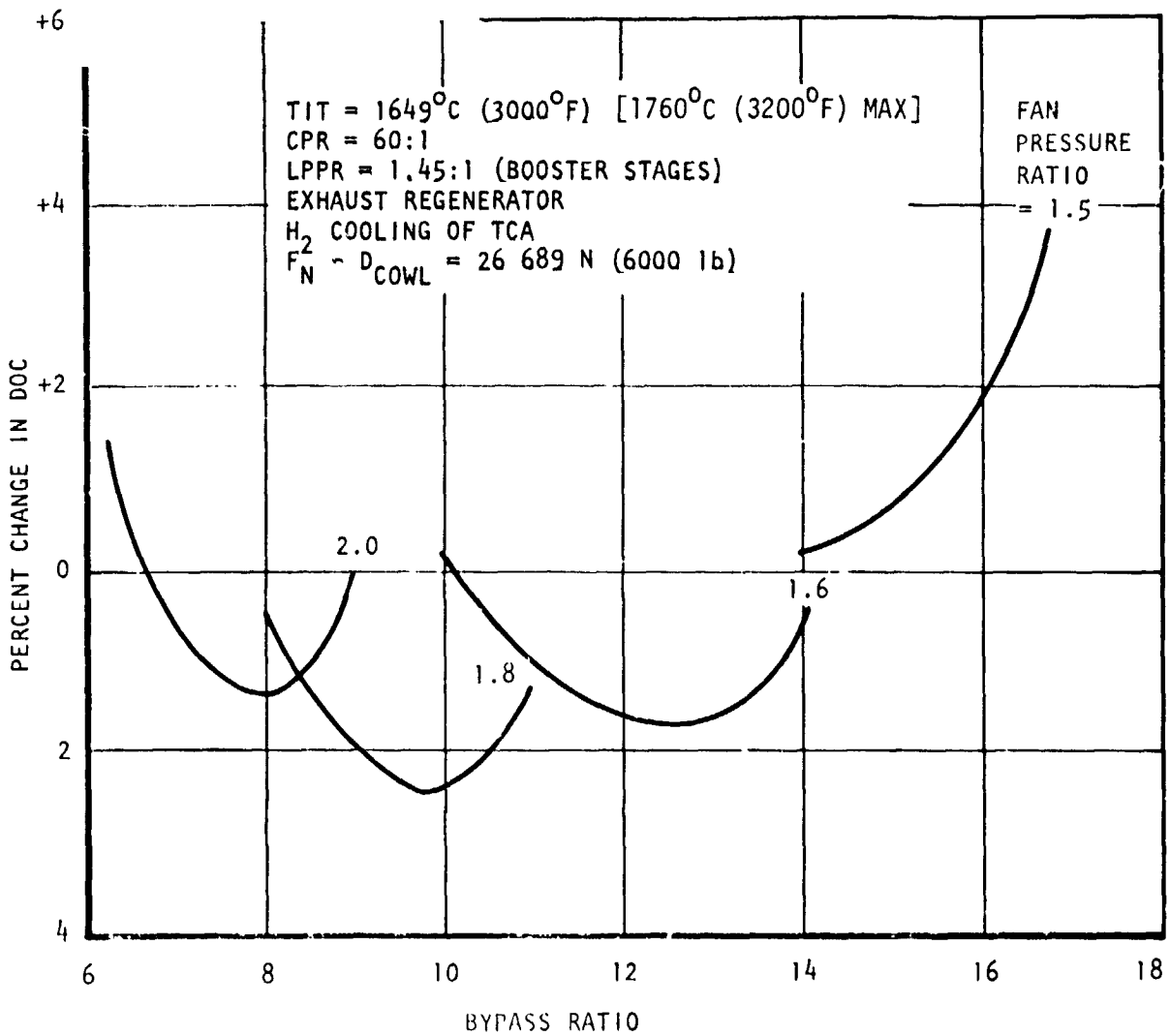

Figure 37. - Effect of bypass ratio and FPR on DOC for CPR = 60.

LH_2 ENGINE
HIGH TEMPERATURE CYCLE SELECTION
(10 668 m (35 000 ft), 0.85 M, MAXIMUM CRUISE SETTING)

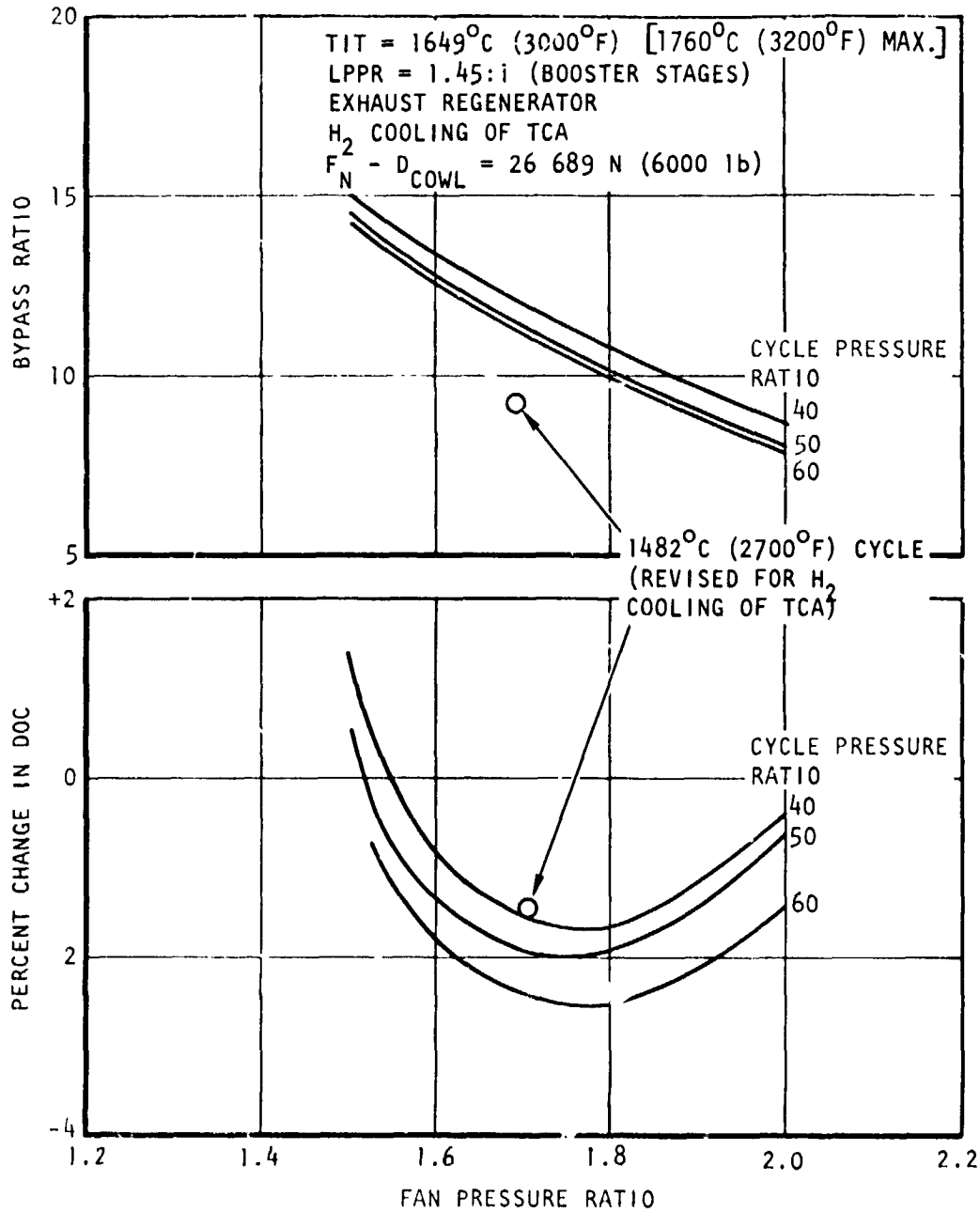

Figure 38. - Effect of fan pressure ratio and cycle pressure ratio on DOC and bypass ratio.

Minimum DOC occurs at a fan pressure ratio of approximately 1.75:1 for all three cycle pressure ratios and a 60:1 cycle pressure ratio yields the most improvement. There is approximately 0.8 percent difference in DOC between a cycle pressure ratio of 40:1 and 60:1. This small difference in DOC was not believed to be high enough to justify the significant complexity and cost penalties associated with the very high pressure ratio engine.

The 1482°C (2700°F) cycle initially selected offered a ΔDOC of 2 percent. However, cooling flows were calculated on a different basis and hydrogen cooling was not utilized. Accordingly, cooling flows were calculated on the basis of the revised methodology (4.2.3.1) and weight and SFC recalculated. The ΔDOC for this cycle is shown in Figure 38.

The 1482°C (2700°F), 40:1 cycle pressure ratio engine incorporating hydrogen cooling of the turbine cooling air and the exhaust regenerator was selected as the cycle to represent technology and performance appropriate for the subject LH_2 fuel system study. This selection results in a DOC approximately 1 percent higher than the 60:1, 1760°C (3200°F) cycle. The high-temperature, high-pressure ratio engine would be significantly higher in cost than the selected engine. If the cost were more than 6 percent higher, which is very likely, the DOC advantage would be negated.

4.3 Selected Engine Concept

The final cycle selected as a result of the hydrogen exploitation studies and cycle selection investigations has the following significant features at the engine design point (maximum cruise power, 10 668 m (35 000 ft) M 0.85):

- Fan pressure ratio of 1.7:1 and a bypass ratio of 10:1
- A booster pressure ratio of 1.45:1
- A compressor pressure ratio of 16.5:1
- A rotor inlet temperature of 1379°C (2514°F) [1482°C (2700°F) maximum] rotor inlet temperature
- A cycle pressure ratio of 40:1

4.3.1 Description and performance. - The selected engine is a twin spool, direct drive, separately exhausted turbofan. A single stage fan and two booster stages are driven by a multistage, uncooled, axial turbine. The gas generator consists of a 10-stage axial compressor, a through-flow circular combustor and a single-stage cooled axial turbine. The spool shafts are concentric and the low pressure spool shaft passes through the high pressure shaft.

Four heat exchangers are included as part of the engine to provide (a) hydrogen cooling of the turbine cooling air, (b) engine oil cooling, (c) hydrogen cooling of the aircraft environmental control system air and (d) fuel heating. They are described in Section 4.3.6.

Basic cycle and performance data are listed in Table 14 at the engine design point and at sea level static takeoff conditions. The performance includes the effects of inlet pressure recovery, horsepower extraction, aircraft bleed extraction and fan stream scrubbing drag. Freestream cowl drag and inlet spillage drag is not included. The cycle and performance characteristics shown in Table 14 are the final results of cycle optimization. They reflect final estimates of component performance, pressure losses, cooling flows, etc. The primary refinements included increases in low pressure turbine efficiency and nozzle thrust coefficients, compared to those used in the early part of the study. Typical engine performance curves are presented in Appendix G.

4.3.2 Weight, geometry, and scaling relationships. - An envelope drawing of the selected engine is included as Figure 39. Dimensions, mount locations, accessory gearbox and thrust reverser details are shown.

The estimated dry weight of the bare baseline-size engine is 1715 kg (3780 lb). This weight includes engine accessories, i.e., fuel control, fuel pump, lubrication pumps, heat exchangers and accessory gearbox. Aircraft accessories, inlet, nozzles, fan thrust reverser and noise suppression are not included. The estimated weight of the inner and outer fan ducts, fan and core nozzles, and fan thrust reverser is 367 kg (809 lb). The total dry weight of the engine exclusive of inlet, aircraft accessories and noise suppression is 2082 kg (4589 lb).

The engine may be scaled within ± 25 percent of its base size according to the following relationships:

$$\text{Scaled Weight} = W_{bl} \left(\frac{\text{Scaled Thrust}}{\text{Base Thrust}} \right)^{1.0}$$

$$\text{Scaled Length} = L_{bl} \left(\frac{\text{Scaled Thrust}}{\text{Base Thrust}} \right)^{0.25}$$

$$\text{Scaled Diameter} = D_{bl} \left(\frac{\text{Scaled Thrust}}{\text{Base Thrust}} \right)^{0.5}$$

TABLE 14. - CYCLE AND INSTALLED PERFORMANCE CHARACTERISTICS - SELECTED LH_2-FUELED BASELINE ENGINE

	SLS, Std Day	M 0.85 10 668 m (35 000 ft)
Power setting	Takeoff	Max. cruise
Net thrust N, (lb)	136 587 (30 706)	29 100 (6542)
SFC, (kg/hr)/daN ((lb/hr)/lb)	0.1045 (0.1025)	0.2054 (0.2014)
Bypass ratio	10.25	10.0
Fan airflow, kg/sec (lb/sec)	483.7 (1066.4)	217.2 (478.8)
Fan pressure ratio (tip)	1.594	1.7
Fan pressure ratio (hub)*	2.26	2.466
Compressor pressure ratio	15.5	16.5
Rotor inlet temperature, ^{o}C, (^{o}F)	1482^{o}C (2700)	1379^{o}C (2514)

*Hub pressure ratio includes booster stages

4.3.3 Engine cost. - Engine cost was established using techniques developed for estimating the cost of Jet A-fueled engines, with suitable allowances made for the differences between Jet A-fueled engine technology and H_2-fueled engine technology. These differences include the previously discussed provisions for cooling the turbine cooling air, the engine oil, and the cabin air; heating the hydrogen in a core exhaust heat exchanger; and the fuel control and delivery system. Costs were developed for the base engine, and also for the installation of nozzles and thrust reverser. The cost data were in 1976 dollars, and were provided as input to the ASSET computer program.

4.3.4 Noise and emissions. -

4.3.4.1 Noise: It is estimated that the engine selected for the LH_2 transport will allow the requirements of FAR36 minus 10 EPNdB to be met. The penalty to specific fuel consumption to meet these requirements is estimated to be negligible. The penalty to engine weight and cost is estimated to be less than two percent.

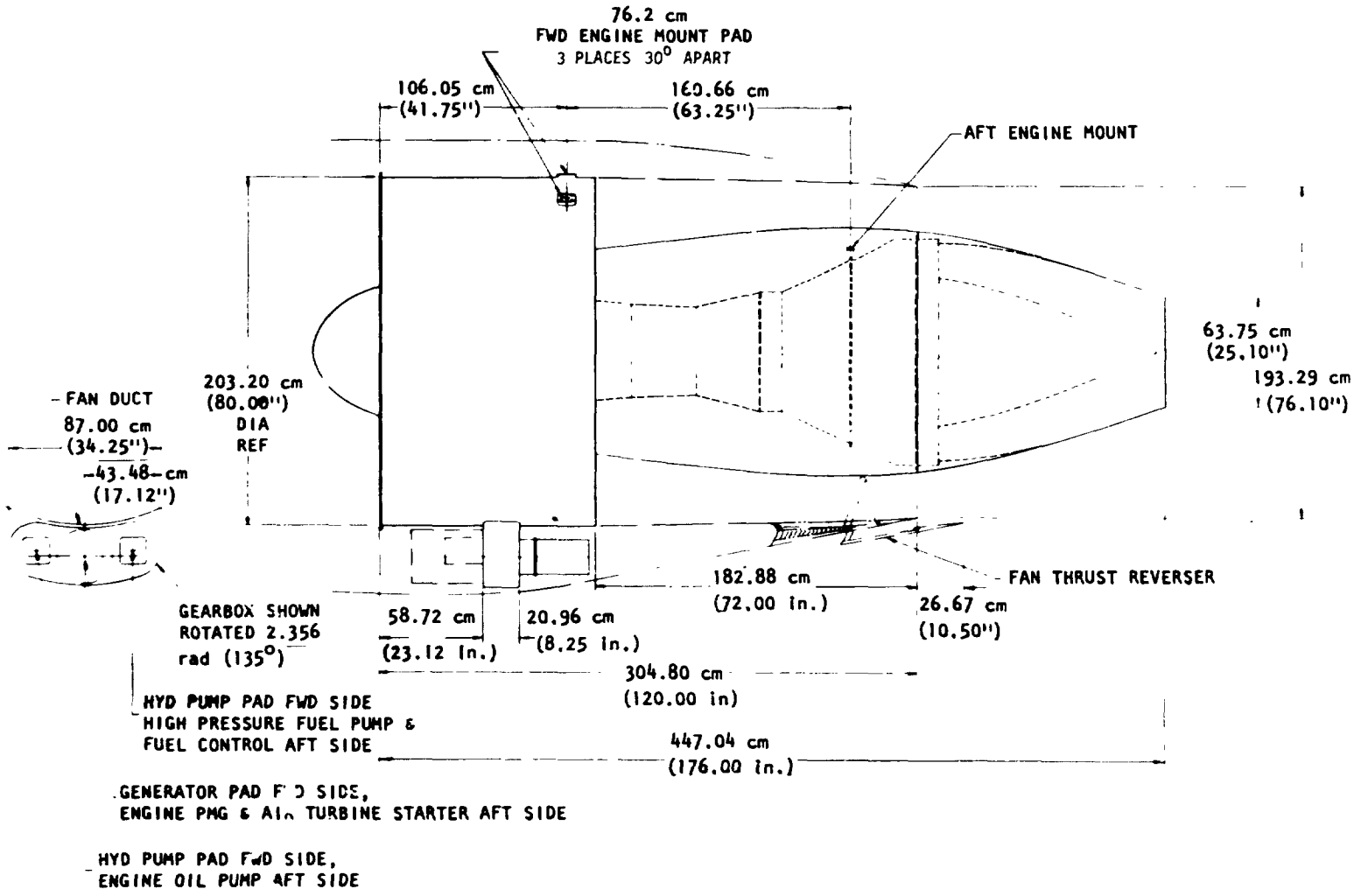

Figure 39. - Envelope drawing - selected baseline LH_2 engine.

Noise reduction in the following areas will be necessary:

- Fan source noise through improved airfoil design and proper blade-to-stator spacing
- Combustor noise
- Turbine source noise through optimization of blade and vane numbers and spacing

It is anticipated that the technology for achieving the reduction in the areas listed above will be available by the 1990 time period. The acoustical treatment of the inlet, fan duct and turbine exhaust will continue to be a requirement. With respect to noise, there is no difference between equivalent Jet A- and LH_2-fueled engines.

4.3.4.2 Emissions: The use of liquid hydrogen as a fuel simplifies the emissions problem as products of combustion do not include hydrocarbons, carbon monoxide, or impurities such as sulfur or carbon. The exhaust from a LH_2-fueled engine is basically water vapor. The only pollutant that will be produced are some oxides of nitrogen (NO_x) as a result of nitrogen and oxygen from the air combining at the high combustion temperatures encountered in aircraft jet engines. The NO_x output is an exponential function of temperature and residence time in the combustor.

Hydrogen, injected in gaseous form into the combustor, has the characteristic of diffusing rapidly into the air so that mixing occurs thoroughly and very quickly. Combustion of H_2/air also occurs at a high rate so the result is smooth, complete burning with a much more uniform temperature profile than is characteristic with Jet A fuel. Elimination of the high temperature peaks, which occur with Jet A, and reduction of the residence time can significantly reduce the production of NO_x from a LH_2-fueled engine, even though the average temperature in the combustion chambers of comparable engines is the same.

4.3.5 Operational characteristics. -

4.3.5.1 Rated performance: Performance ratings for the baseline-size engine are shown in Tables 15, 16, and 17. The performance shown includes the effects of 125 horsepower extraction and 3.2 percent bleed air extraction. It also includes the effects of internal nozzle performance, inlet recovery, and fan stream scrubbing drag.

TABLE 15. - INSTALLED PERFORMANCE RATINGS AT U.S. STANDARD ATMOSPHERE SEA-LEVEL STATIC CONDITIONS

Power Setting	Net Thrust daN (lb)	Specific Fuel Consumption kg/hr/daN (lb/hr/lb)	Turbine Inlet Temperature °C (°F)	Low Pressure Spool Speed rpm	High Pressure Spool Speed rpm
Takeoff (5 minutes)	13 659, (30 706)	0.1045 (0.1025)	1482 (2700)	4059	17 297
Maximum Climb	13 045, (29 327)	0.1032 (0.1012)	1454 (2650)	3984	17 09[illegible]

TABLE 16. - INSTALLED PERFORMANCE RATINGS AT 34.2°C (93.6°F) SEA-LEVEL STATIC CONDITIONS

Power Setting	Net Thrust daN (lb)	Specific Fuel Consumption kg/hr/daN (lb/hr/lb)	Turbine Inlet Temperature °C (°F)	Low Pressure Spool Speed rpm	High Pressure Spool Speed rpm
Takeoff (5 minutes)	11 443, (25 724)	0.1048 (0.1028)	1482 (2700)	3902	17 104

TABLE 17. - INSTALLED PERFORMANCE RATINGS AT U.S. STANDARD ATMOSPHERE 10 688 m (35 000), 0.85 MACH

Power Setting	Net Thrust daN (lb)	Specific Fuel Consumption kg/hr/daN (lb/hr/lb)	Turbine Inlet Temperature °C (°F)	Low Pressure Spool Speed rpm	High Pressure Spool Speed rpm
Maximum Climb	3236, (7275)	0.2096 (0.2055)	1454 (2650)	4300	17 341
Max[illegible]um Cruise	2910, (6542)	0.2054 (0.2014)	1379 (2514)	4127	16 886

4.3.5.2 Capabilities and limits:

4.3.5.2.1 Engine flight envelope: The engine flight operating envelope is shown in Figure 40.

4.3.5.2.2 Flight-maneuver loads: The flight maneuver operating load diagrams are shown in Figure 41.

4.3.5.2.3 Starting: The engine shall be capable of groundstarts at altitudes from sea level to 4572 m (15 000 ft). The air start envelope in terms of altitude and Mach number is shown on Figure 37. The ambient temperature range for ground starting is from -40°C (-40°F) to 51°C (125°F).

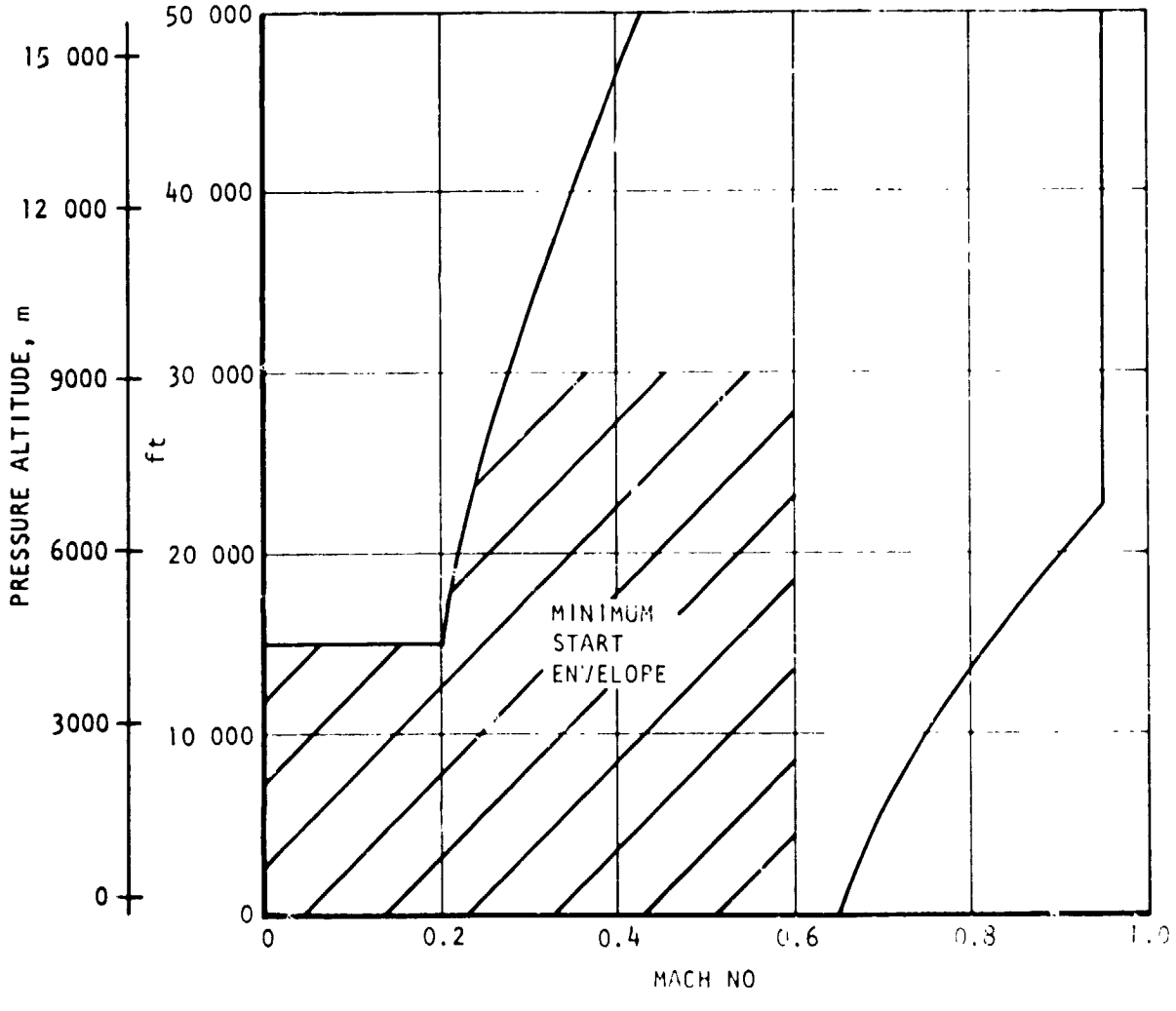

Figure 40. - LH_2 engine flight operating envelope.

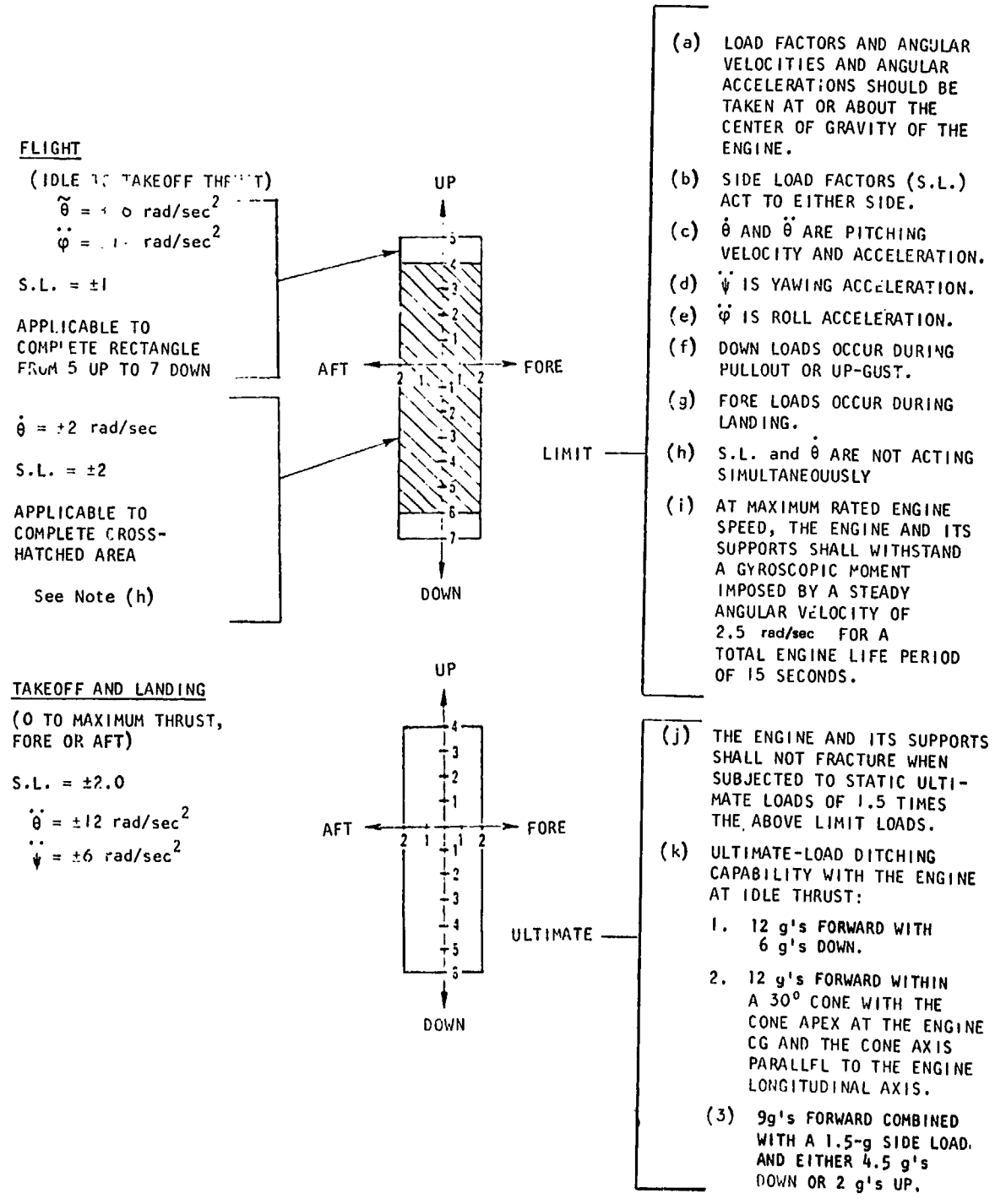

Figure 41. - LH_2 engine operating load limits.

C-2

4.3.5.2.4 Ambient temperature limits: The engine ambient temperature flight envelope is as shown on Figure 42.

4.3.5.2.5 Engine speed limits: Maximum low pressure spool (fan) speed is 4430 rpm and maximum high pressure spool (compressor) speed is 17 860 rpm.

4.3.6 Description of engine-mounted heat exchangers. - Based upon the engine analysis, problem statements for the four-engine mounted heat exchangers were prepared, and heat exchanger preliminary designs were established to meet these requirements. Engine-mounted heat exchangers are required to perform the following functions:

- An air to hydrogen heat exchanger to cool compressor bleed air for use in cooling the HP turbine vanes and rotor blades.
- An oil to hydrogen heat exchanger to cool the engine oil.
- An air to hydrogen heat exchanger to cool compressor bleed air for use in the aircraft environmental control system.
- An exhaust gas to hydrogen heat exchanger, located in the engine flow path downstream of the low-pressure turbine and upstream of the exhaust nozzle, to transfer heat from the engine exhaust gas to the hydrogen fuel.

Design point data for the four heat exchangers are presented in Table 18.

Because of the high hydrogen inlet pressure 2758 kPa (400 psia), only tubular heat exchangers were considered for these applications. The heat exchangers were designed to eliminate freezing problems which can occur when moisture is condensed out of the air as it is cooled and is then exposed to tube wall temperatures below $0^{o}C$ ($32^{o}F$).

To provide compact heat exchanger designs and eliminate freezing problems, the turbine cooling air heat exchanger and the aircraft ECS heat exchanger both utilize finned tubes and hydrogen recirculation. The fins provide high thermal conductance to the air and the recirculation preheats the hydrogen to raise the tube wall temperature above the freezing point.

The engine lubrication oil heat exchanger is also in the recirculation loop and was designed as a shell and tube heat exchanger. An ejector (jet pump) is used to produce the hydrogen recirculation flow with only a small additional pressure drop in the hydrogen. The turbine cooling air heat exchanger, the engine lubrication oil cooler, and the aircraft ECS air heat exchanger heat the hydrogen in series from $50^{o}K$ ($90^{o}R$) to a temperature of $264.1^{o}K$ ($475.4^{o}R$) to eliminate freezing problems in the engine exhaust gas heat exchanger. The turbine cooling air heat exchanger was arranged in a pattern as shown in Figure 43. The engine lubrication oil cooler was

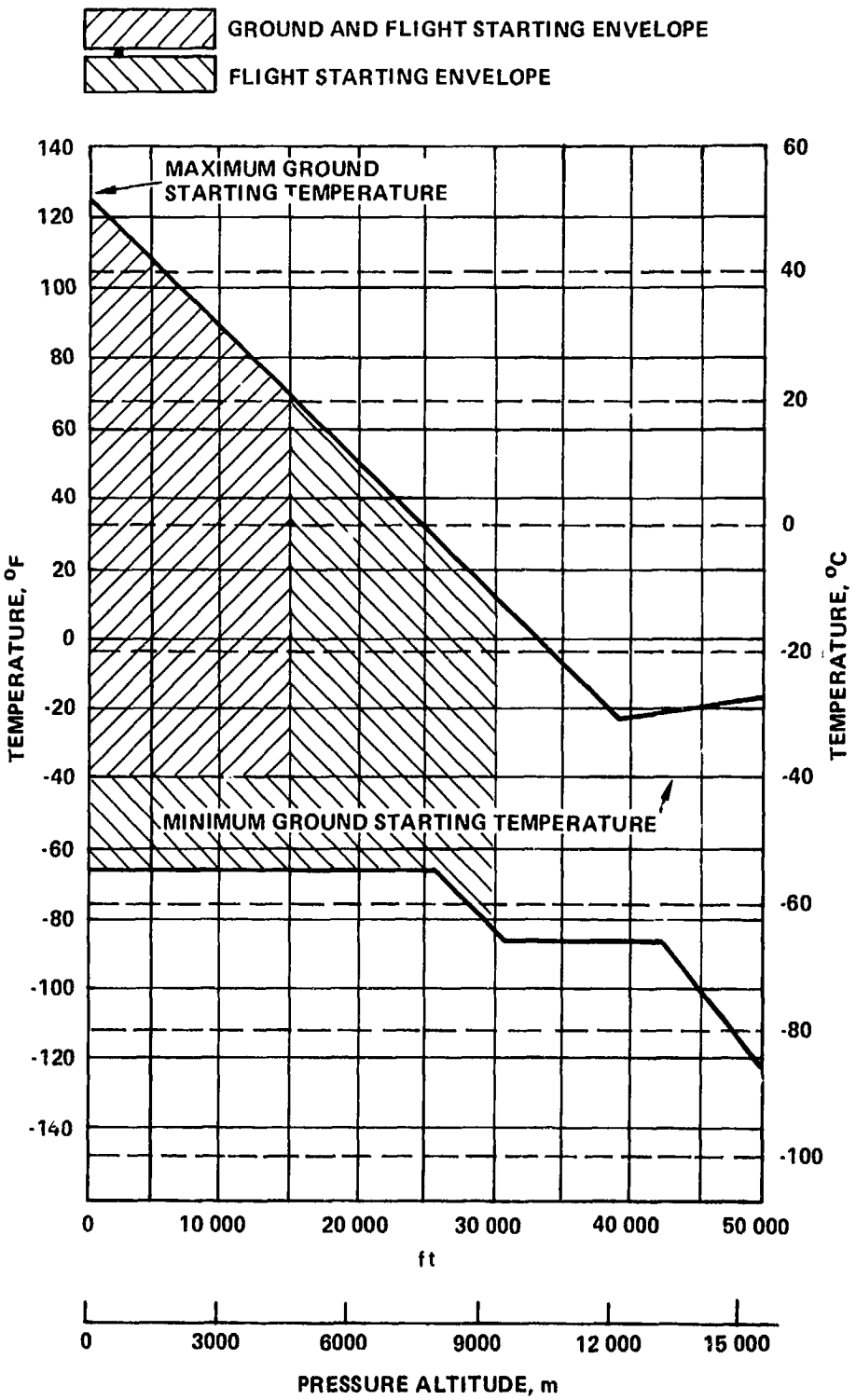

Figure 42. - LH_2 engine ambient flight and starting temperature envelope.

TABLE 18. LIQUID HYDROGEN FUELED ENGINE HEAT EXCHANGER DESIGN CONDITIONS

	Turbine Cooling Air HX	Oil Cooler	ECS Bleed HX	Engine Exhaust HX
Total Heat Transferred, kJ/min (Btu/min)	26628 (25219)	4012 (3800)	1921 (1819)	60422 (57225)
Shell Side Air (Oil) Flow, kg/min (lb/min	49.9 (110)	57.6 (127)	48.4 (106.7)	1144 (2523)
Air (Oil) Inlet Temp., ^{o}K (^{o}R)	791 (1423)	378 (680)	336 (604)	778 (1400)
Air (Oil) Outlet Temp., ^{o}K (^{o}R)	303 (546)	343 (617.3)	297 (535)	733 (1319)
Air Inlet Pressure, kPa (psia)	1515.5 (219.8)		92.05 (13.35)	40.04 (5.81)
Air Pressure Drop $\Delta P/P$ inlet	0.04		0.074	0.032
Oil Pressure Drop, kPa (psi)		83 (12)		
Shell Side Effectiveness	0.825	0.276	0.502	0.0873
Tube Side Hydrogen Flow, kg/min (lb/min)	32.59 (71.85)*	32.59 (71.85)*	32.59 (71.85)*	9.95 (21.94)
Hydrogen Inlet Temperature, ^{o}K (^{o}R)	200 (360)	251 (452)	260 (468)	264 (475)
Hydrogen Outlet Temperature, ^{o}K (^{o}R)	251 (452)	260 (468)	264 (475)	677 (1219)
Hydrogen Pressure Drop, kPa (psi)	2.76 (0.4)	26.2 (3.8)	2.14 (0.31)	45.5 (6.6)
Tube Side Effectiveness	0.0873	0.0686	0.0509	0.8043

*Recirculation flow of 22.637 kg (49.905 lb/min) hydrogen required to prevent water condensate freezing. Hydrogen temperature before mixing recirculation flow is $50^{o}K$ ($90^{o}R$).

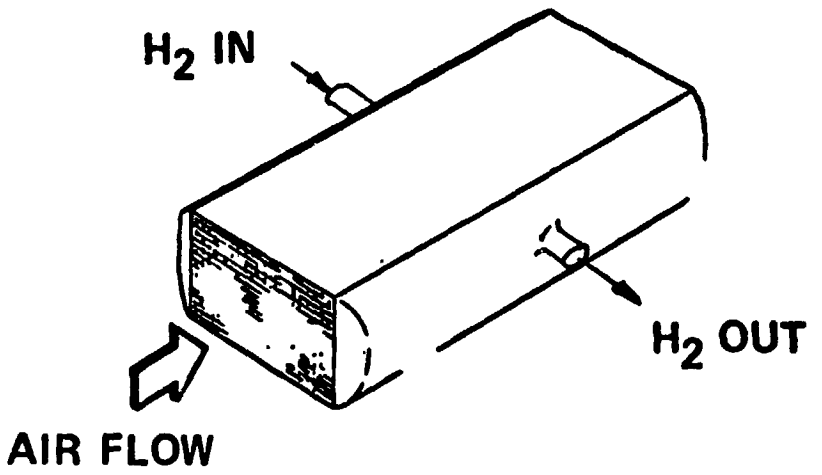

AIRFLOW LENGTH	48.59 cm (19.13 in.)
WIDTH	12.7 cm (5.0 in.)
HEIGHT	9.42 cm (3.71 in.)
FINNED TUBES	
TUBE O.D.	0.64 cm (0.25 in.)
TUBE WALL	0.04 cm (0.016 in.)
TUBE MATERIAL	304 CRES
FIN O.D.	1.27 cm (0.50 in.)
FIN SPACING	0.06 cm (0.025 in.)
FIN THICKNESS	0.010 cm (0.004 in.)
FIN MATERIAL	OFHC COPPER
FIN AND TUBE COATING	NiCr
TOTAL NUMBER TUBES	308
NUMBER HYDROGEN PASSES	1
TUBE WEIGHT	7.4 kg (16.3 lb)
TOTAL HEAT EXCHANGER WT	18 kg (40 lb)

Figure 43. - Turbine cooling air to hydrogen heat exchanger.

designed as shown in Figure 44. The aircraft ECS air cooler was arranged as shown in Figure 45.

The engine exhaust gas heat exchanger heated the hydrogen for entry to the combustor. This heat exchanger is exposed to a large flow rate of air (exhaust gas) and had to be designed with low air pressure drop in a location with limited air flow area. To satisfy these requirements, an inline tubular heat exchanger such as used by Pratt and Whitney in the 304 engine was selected. The proposed design has involute curved tubes running from a 56.4 cm (22.2 in.) inner diameter to a 126.5 cm (49.8 in.) outer diameter air passage. The involute tubes are arranged in a pattern as shown in Figure 46.

4.4 Technology Development Required

The technology postulated for the LH_2-fueled engine is representative of that which would be incorporated in an engine entering service in the 1990 time period. Much of the technology is not, however, unique to use of LH_2 fuel. Much of the aerodynamics, materials, mechanical design and manufacturing processes, while advanced, are equally applicable to future kerosene-fueled advanced transport engines.

Elements which are unique to the LH_2 fueled engine are:

- Combustor
- H_2 cooling of the turbine cooling air
- Heat exchangers
- Fuel control

The fuel control system is discussed in section 5.5 of this report.

4.4.1 Combustor. - Technology development is required to take advantage of the properties of hydrogen and to execute a combustor design which is smaller, provides an improved pattern factor, and is low in oxides of nitrogen emissions.

The design of hydrogen combustion systems is particularly amenable to analysis relative to conventional kerosene combustion systems. The kinetic schemes and reaction rates are well established except for turbulent flow. Therefore, a technology program to develop a hydrogen combustion system could consist of analytical design augmented by an experimental program to provide turbulent flow kinetics and to verify the analytical design.

4.4.2 H_2 cooling of turbine cooling air. - There are two problems introduced when hydrogen cooling of turbine cooling air is incorporated in an engine.

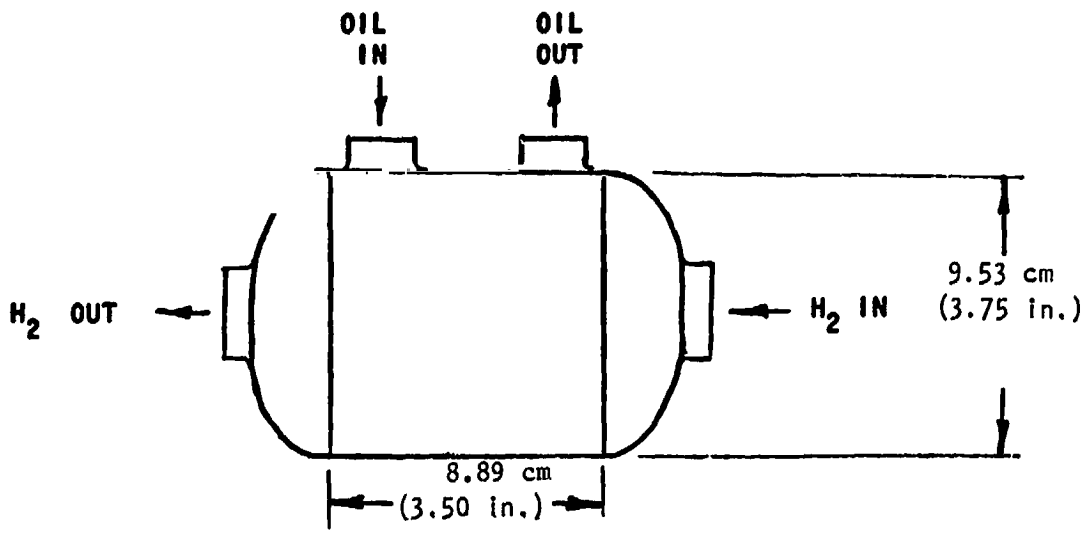

TUBES	
TUBE O.D.	0.32 cm (0.125 in.)
TUBE WALL	0.030 cm (0.012 in.)
TUBE MATERIAL	304 CRES
TOTAL NUMBER OF TUBES	600
NUMBER OF HYDROGEN PASSES	1
NUMBER OF OIL PASSES	2
TUBE WEIGHT	1.2 kg (2.6 lb)
TOTAL HEAT EXCHANGER WEIGHT	2.6 kg (5.75 lb)

Figure 44. - Engine oil to hydrogen heat exchanger.

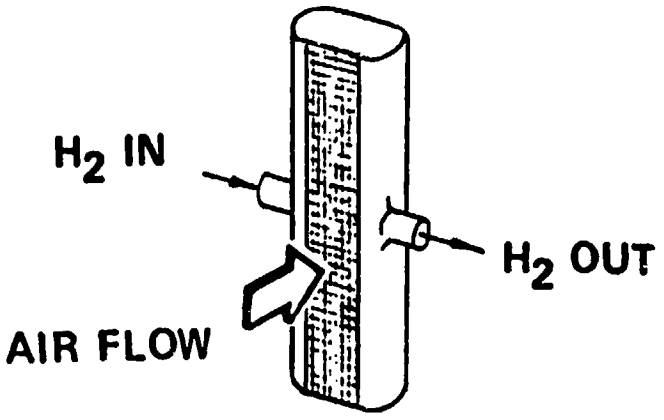

AIR FLOW LENGTH	7.9 cm (3.1 in.)
WIDTH	7.6 cm (3.0 in.)
HEIGHT	60.7 cm (23.9 in.)
FINNED TUBE	
TUBE O.D.	0.64 cm (0.25 in.)
TUBE WALL	0.041 in. (0.016 in.)
TUBE MATERIAL	304 CRES
FIN O.D.	1.27 cm (0.50 in.)
FIN SPACING	0.064 cm (0.025 in.)
FIN THICKNESS	0.010 cm (0.004 in.)
FIN MATERIAL	OFHC COPPER
FIN AND TUBE COATING	NiCr
TOTAL NUMBER TUBES	315
NUMBER HDYROGEN PASSES	1
TUBE WEIGHT	4.5 kg (10.0 lb)
TOTAL HEAT EXCHANGER WEIGHT	11.3 kg (25.0 lb)

Figure 45. - ECS bleed air to hydrogen heat exchanger.

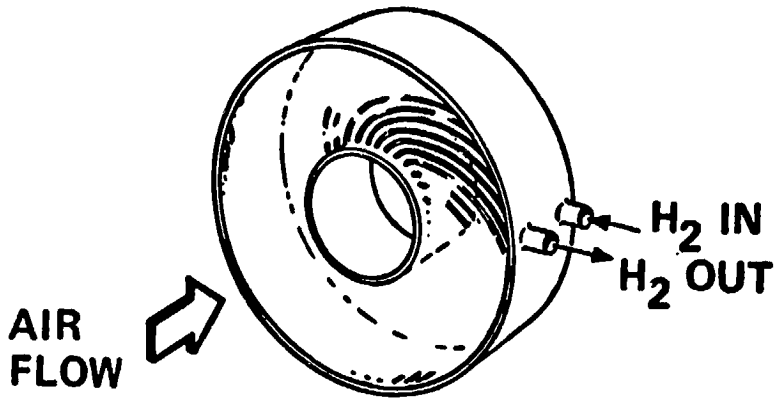

OUTSIDE DIAMETER	126.5 cm (49.8 in.)
INSIDE DIAMETER	56.4 cm (22.2 in.)
AIR FLOW LENGTH	19.1 cm (7.5 in.)
INVOLUTE TUBE LENGTH	56.9 cm (22.4 in.)
CIRCUMFERENTIAL TUBE SPACING	6 DIAMETERS
AXIAL TUBE SPACING	1.25 DIAMETERS
TUBE O.D.	0.478 cm (0.188 in.)
TUBE WALL	0.030 cm (0.012 in.)
TUBE MATERIAL	304 CRES
TOTAL NUMBER OF TUBES	1984
NUMBER OF HYDROGEN PASSES	8
TUBE WEIGHT	38.3 kg (84.5 lb)
TOTAL HEAT EXCHANGER WEIGHT	77.1 kg (170 lb)

Figure 46. - Engine exhaust fuel heater.

The first is a design problem. Normally turbine cooling air is routed internally through the engine from the compressor to the cooled turbine. The routing is different when the turbine cooling air is hydrogen cooled. Complex design problems would have to be addressed but the task could be best undertaken concurrently with engine design.

The second problem is caused by the lower temperatures of the turbine cooling air. Thermal gradients in the blades would be more severe than presently experienced for a similar blade heat transfer system. These high thermal gradients can result in low cycle fatigue damage. In order to realize the advantages of H_2 cooling of the turbine cooling air, it is recommended that parallel technology programs be undertaken to

1. Develop heat transfer systems which produce more uniform temperatures

2. Extend development of single crystal turbine blades which have higher cyclic fatigue strength.

5. ENGINE FUEL SUPPLY SYSTEM

5.1 Candidate System Concepts

5.1.1 Concept descriptions. - The basic fuel system performance requirement is that a pump or combination of pumps must supply fuel according to a specified flow-pressure schedule. The schedule shown in Table 19 was used for initial design considerations. Additionally, a tank-mounted pump must be included in the system, to provide a pressure higher than the vapor pressure to the fuel lines and the engines. The wide range of pumping systems that could achieve these requirements is constrained by cost considerations, as expressed through the ΔDOC equation applied in Section 5.1.2. The objective of the concept selection was to determine the general arrangement of the fuel supply system which could most efficiently meet the basic requirements of the system.

Two concepts for the arrangement of pumps in the engine fuel supply subsystem were considered initially. In concept 1, a low-pressure-rise (nominally 50 psi rise) boost pump would be in the tank and a high-pressure rise main pump would be on the engine. The boost pump would provide a positive pressure to move LH_2 from the tank to the engine and would meet main pump inlet pressure requirements. In concept 2, the main pump on the engine would be eliminated, with the total flow-pressure requirements of the engine met by a single tank-mounted pump. The analytical concept selection procedure described below (Section 5.1.2) also included evaluation of a concept 1-1/2 pump arrangement. Here, an engine-mounted main pump and a tank-mounted boost pump would be performance matched so that the boost pump would supply some intermediate pressure rise (determined as a parameter of the analysis) and the main pump would supply the balance of the pressure rise. In such an arrangement, the performance requirements of the main pump (and hence its weight and power requirements) could be reduced and conceivably provide benefits to the overall system.

5.1.2 Results of evaluation. - The concept selection process utilized a parametric trade-off study approach based upon the ΔDOC sensitivity equation appropriate to the fuel subsystem. With this approach, the entire range of system configurations could be evaluated. In performing this analysis, both the pump concept and the optimum fuel line diameter were selected. Pressure dropline diameter and calculated line diameter-line weight data (see Sec. 5.2.1) were introduced into the analysis at the appropriate points. For example, as the line diameter was decreased, the line weight decreased but the pressure drop necessarily overcome by the tank-mounted pump increased, thus increasing the required size and weight of the boost pump.

TABLE 19. - LH_2 TURBOFAN ENGINE NET THRUST, FUEL FLOW AND FUEL PRESSURE SCHEDULE FOR INITIAL DESIGN CONSIDERATIONS

Condition	Altitude m (1000 ft)	Mach	$\dot{w}$/Engine kg/sec (lb/sec)	Net Thrust/Eng. N (lb)	Comp. Discharge Pressure-kPa (psia)
Max SLS	0	0	0.340 (0.749)	127 664 (28 700)	4875 (707)
Takeoff	0	0	0.340 (0.750)	127 664 (28 700)	4875 (707)
Climb	0	0.38	0.351 (0.774)	83 538 (18 780)	5068 (735)
	610 (2)	0.39	0.342 (0.755)	80 246 (18 040)	
	1 219 (4)	0.41	0.332 (0.732)	76 243 (17 140)	
	1 829 (6)	0.42	0.313 (0.690)	71 172 (16 000)	
	2 438 (8)	0.44	0.301 (0.664)	67 124 (15 090)	
	3 048 (10)	0.46	0.288 (0.635)	63 832 (14 350)	4165 (604)
	3 048 (10)	0.64	0.303 (0.667)	56 715 (12 750)	4392 (637)
	4 572 (15)	0.71	0.278 (0.613)	50 354 (11 320)	
	6 096 (20)	0.78	0.251 (0.553)	44 705 (10 050)	3730 (541)
	7 620 (25)	0.85	0.226 (0.498)	38 655 (8 690)	
	9 144 (30)	0.85	0.195 (0.429)	32 828 (7 380)	3061 (444)
	10 668 (35)	0.85	0.158 (0.348)	27 357 (6 150)	2668 (387)
Cruise	10 668 (35)	0.85	0.159 (0.351)	26 689 (6 000)	2641 (383)
	11 582 (38)	0.85	0.132 (0.292)	23 576 (5 300)	2448 (355)
Flight Idle	10 668 (35)	0.85	0.029 (0.063)	-912 (-205)	1551 (225)
	11 582 (38)	0.85	0.023 (0.051)	-730 (-164)	
	0	0.4	0.078 (0.171)	3 648 (820)	
Ground Idle	0	0	0.039 (0.085)	8 140 (1 830)	1868 (271)
	1 524 (5)	0	0.032 (0.071)	6 761 (1 520)	
Ground Start	0	0	0.011 (.024)	-	152 (22)

Concept selection was translated into a problem of optimization of the tank-mounted boost pump pressure rise. If the optimum rise were small, concept 1 would be chosen; if large, concept 2; and if some intermediate pressure rise were found optimum, concept 1-1/2 would be chosen.

An analysis based on ΔDOC was conducted to determine the optimum design pressure rise (at maximum flow) for the boost pump. If the engine-mounted main pump efficiency (η_m) is assumed to be a constant 45 percent regardless of the boost pump pressure rise, and if the main pump weight is assumed to be

a constant 25 pounds, the minimum direct operating cost occurs at the lowest possible boost-pump pressure rise. The reason for this is shown by an investigation of the ΔDOC sensitivity equation.

$$DOC \times 10^5 = 3.22 \sum hp_c + 0.775 \left(W_s + 6 \sum hp_{max}\right)$$

where

DOC is expressed in $\frac{¢}{\text{seat n.mi.}}$

$\sum hp_c$ = horsepower at cruise for all pumps (tank and engine mounted)

W_s = total weight

6 = coefficient approximating the aircraft weight penalty to provide and transmit the required horsepower

$\sum hp_{max}$ = maximum horsepower into pump drives that are tank mounted (not engine mounted)

Parameters on the right-hand side were related to pressure rise ΔP through the relations $HP \propto P$ and $W_{pump} \propto P^{0.6}$, the latter equation being based on extensive Rocketdyne experience with cryogenic pumps. Results of the analysis are shown in Figure 47. For this case of constant main pump weight, increasing the boost pump pressure rise decreases HP_c slightly because the boost pump is more efficient than the main pump. However, this factor is far outweighed by the increased boost pump weight (which increases W_s) and the $6 \sum hp_{max}$ term, which is directly proportional to boost-pump pressure rise. The net effect is that, for constant main pump weight, the minimum feasible ΔDOC occurs at the minimum boost pump pressure rise that will provide sufficient pressure to the main pump inlet.

If, as is usually the case, the main pump design speed is assumed to be NPSH limited (resulting in a weight that decreases with increasing boost-pump pressure rise), the optimum ΔDOC is shown to occur at a boost pump pressure rise of 317 kPa (46 psi). An investigation of the ΔDOC relation shows the reason for this. At boost pump pressure rises (ΔP_B) below 276 kPa (40 psia), the main pump NPSH is so low that the main pump weight becomes large and consequently dominates the ΔDOC equation. This causes ΔDOC to increase with decreasing ΔP_B. If, on the other hand, ΔP_B is greater than 345 kPa (50 psi), the main pump NPSH is so large that the main pump weight reduction has little effect. However, the boost pump power is directly proportional to ΔP_B and, therefore, the tank-mounted pump power term ($6 \sum hp_{max}$) becomes the dominant factor. As a result, ΔDOC increases with increasing ΔP_B if ΔP_B is greater than 345 kPa (50 psi).

These results show that it is not economical to increase the boost pump design pressure rise much above 46 psi. Therefore, the concept 1-1/2 approach does not appear to be practical. This, in combination with the even higher ΔDOC for concept 2 (main pump in the tank) resulted in the selection of concept 1, with a minimum boost pump design pressure rise, for the hydrogen-fueled aircraft. These parametric results were verified by preliminary calculations using several system configurations. Again, concept 1 with a pressure rise of 46 psi was found to be favored.

5.1.3 Characteristics of selected systems. - Figure 48 depicts the selected engine feed system concept. This figure, together with the flow-pressure schedule found in Table 19 defined the requirements for the selected boost pump/drive system described in Section 5.3 and the engine-mounted fuel pump described in Section 5.4.

5.2 Engine Fuel Supply Lines

Selection of the configuration of the engine fuel supply lines that carry the fuel from the tank to the engines involves determination of two basic factors. First, the diameter of the lines which contain the fuel must be selected. Second, the appropriate insulation system for the cryogenic lines must be found. Diameter affects system performance in establishing both fuel-line pressure drop that must be overcome by the tank-mounted boost pump, and also line weight. The choice of insulation enters the system calculation in weight and heat leakage. Qualitative insulation effects such as safety and fabricability must also be considered. This section presents the results of the feed-lines portion of this investigation and the methods used.

5.2.1 Size Selection. - The line diameter for the fuel-feed lines was optimized in the concept selection analysis described in Section 5.1.2 above. As a precursor to that calculation, it was first necessary to determine the line pressure loss as a function of line diameter. Feed Line No. 4 (aft tank to right-hand outboard engine), was selected as the most severe configuration in terms of total line length and number of bends. Total line length, including a growth factor of 1.2, was calculated to be 54 m (176 ft). Line losses for eight right-angle bends were calculated assuming utilization of optimum line bend radius ratio (r/d_{tube}) of about three to five. This results in loss coefficients (K_L) of about 0.2 for a 1.57 rad (90 deg) bend. The results of a conventional analysis for the flow of incompressible liquid hydrogen in pipes are summarized in Figure 49 for the maximum engine fuel flow rate condition of 351 kg/sec (0.774 lb/sec), Table 19. It has been assumed that: (1) vapor/liquid ratio of the fluid delivered to the engine must be zero at maximum flow, and (2) low loss valves have been utilized in the system, so that line loss due to valves is approximately equal to their equivalent line length. Ball valves when used in liquid hydrogen systems satisfy this assumption. A nominal one-inch diameter line results in a pressure loss of 97 kPa (14 psi) at max. flow.

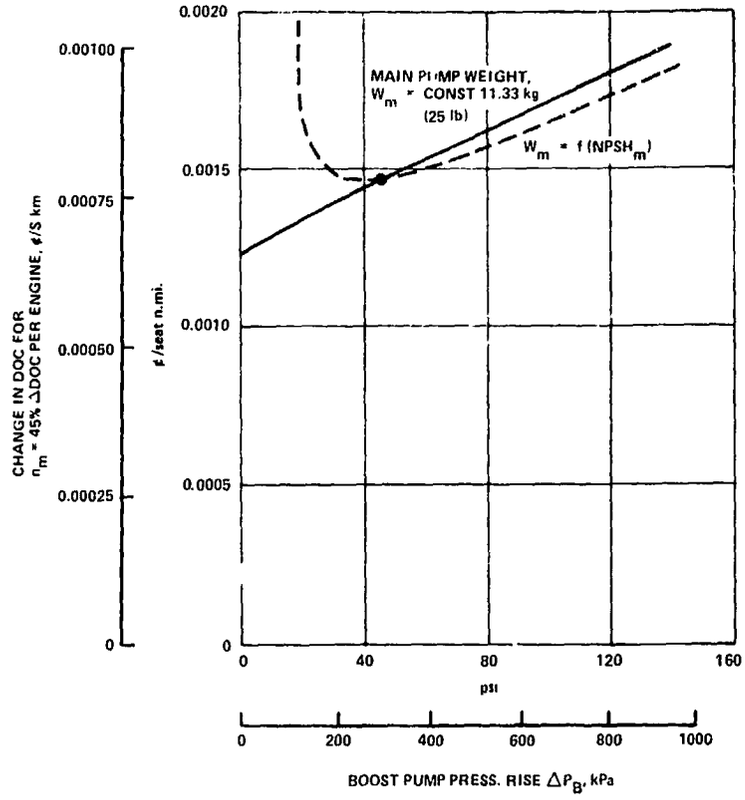

Figure 47. - Boost pump pressure rise effects.

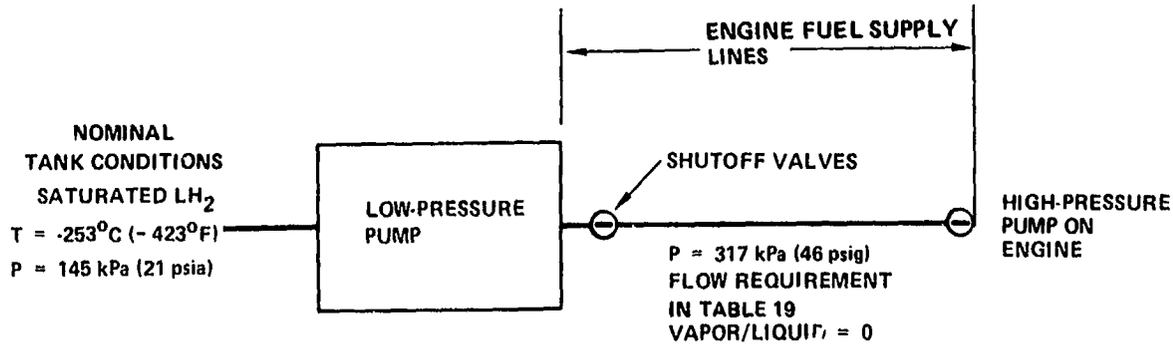

Figure 48. - Concept I schematic (tank-mounted low-pressure pump/engine-mounted high-pressure pump).

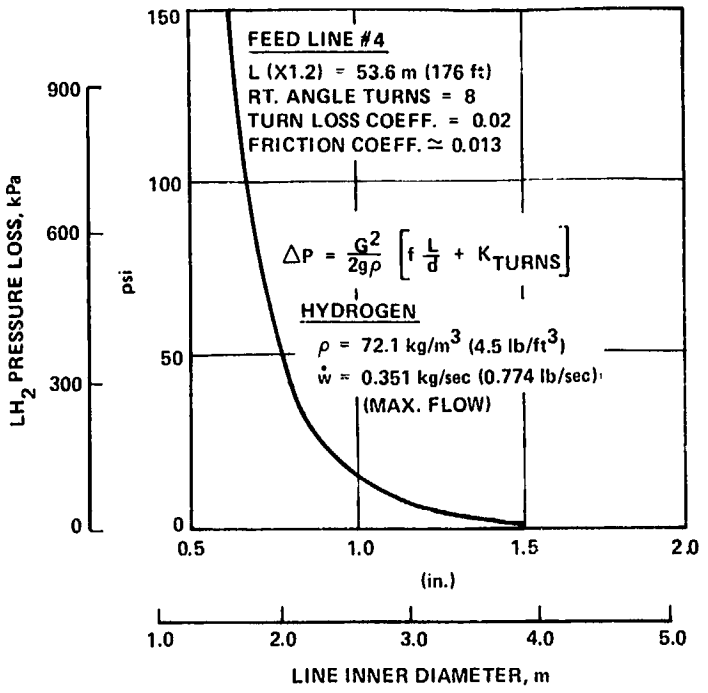

Figure 49. - LH_2 fuel feed line pressure loss.

Figure 50 shows the incremental ΔDOC determined from the sensitivity equation as a function of line diameter for the selected pump concept, determined in Section 5.1.2. A line diameter of 2.54 cm (1.0 inches) was determined to be optimal based upon this trade approach.

5.2.2 Insulation system comparison. - From the system optimization process described in Sections 5.1.2 and 5.2.1, a fuel-line inner diamter of 1.0 inch was chosen. Because the fuel to be pumped, LH_2, is cryogenic, the fuel lines must be insulated to prevent excessive heat input to, and consequent vaporization of, the fuel as it flows from the tanks to the engines, a distance of up to 48.8 m (160 feet). Two principal types of insulation systems were considered: vacuum and foam.

Where practical, vacuum insulation systems are usually utilized for ground-based cryogenic transfer systems, as the overall heat transfer can be minimized by means of an evacuated space filled with radiation shielding to control this mode of heat loss. The experience with vacuum-insulated systems for flight-weight systems is limited, but a significant drawback is found in manufacturing, installation, maintenance, and safety of the thin-walled tubing

necessary for a flight-weight system. On the other hand, to achieve the insulation properties of a vacuum system, foam-insulated lines must be relatively large and bulky. Foam systems can also degrade in performance over long periods of time. Thus, there is no clear-cut choice for the insulation approach. This section presents the results of the determination of the best present choice for insulation system. The approach incorporates consideration of both insulation properties and practical considerations such as weight, manufacture, maintenance, safety, etc.

5.2.2.1 Insulation requirements: Thermal insulation considerations are one factor in estimating the total feed-system weight. A primary requirement that was arbitrarily established for the proposed aircraft engine design was that the hydrogen vapor volumetric fraction should not exceed 0.5 at the engine inlet under any flow condition. This was a consideration affecting the design of the engine pump which reflects a limitation that allows up to one-half the cross-sectional area of the feed line to be gaseous hydrogen at any given instant. A second consideration relates to ground-hold conditions (i.e., zero H_2 flow) after initial line chilldown. The ground-hold condition will result in line venting and some fuel loss (boil-off) at various time intervals dependent on the insulation effectiveness. Excessive pressure in the line is prevented by thermal relief devices incorporated in the shutoff valves and a small hole in the pump check valve to allow venting into the fuel tank.

Various techniques have been developed for insulating cryogenic components. Some, such as those utilizing helium or nitrogen purges, do not appear suitable for aircraft feed line application. A vacuum jacket and/or closed cell type foam insulation appears suitable in terms of basic simplicity. A comparison of a typical foam insulation and a simple vacuum jacket in terms of heat leak rate is shown in Figure 51. It is apparent that the vacuum-jacket approach is superior in terms of minimizing heat leak rate. (Joints are not included).

Foam: The effect of line diameter (i.e., pressure drop) on required foam insulation thickness and total insulation weight is presented in Figure 52 for the condition $\dot{w}$ = 0.023 kg/sec (0.051 lb/sec). For the nominal 2.54 cm (1.0 in) line diameter, the total insulation weight (all four feed lines) is about 23 kg (50 lbs). Both the line and insulation weights are related to feed line diameter as shown previously. Since the line diameter determines hydrogen pressure drop, it is possible to relate the line and insulation weight to either the pump discharge pressure or pressure rise as shown in Figure 53. This approach in combination with a pump weight versus pressure rise curve permits direct determination of the minimum weight system, see Section 5.1.2.

The vacuum-jacketed line approach is superior to the foam insulation in terms of minimum heat leakage as noted previously in Figure 51. If the insulation system is a vacuum annulus only, the insulation weight is zero. If an aluminized mylar radiation shield is wrapped on the inner line, as is almost certainly necessary, the insulation weight is 0.104 kg/m (0.07 lb/ft), or 18.3 kg (40.3 lb) for 176 m (576 ft) total line length.

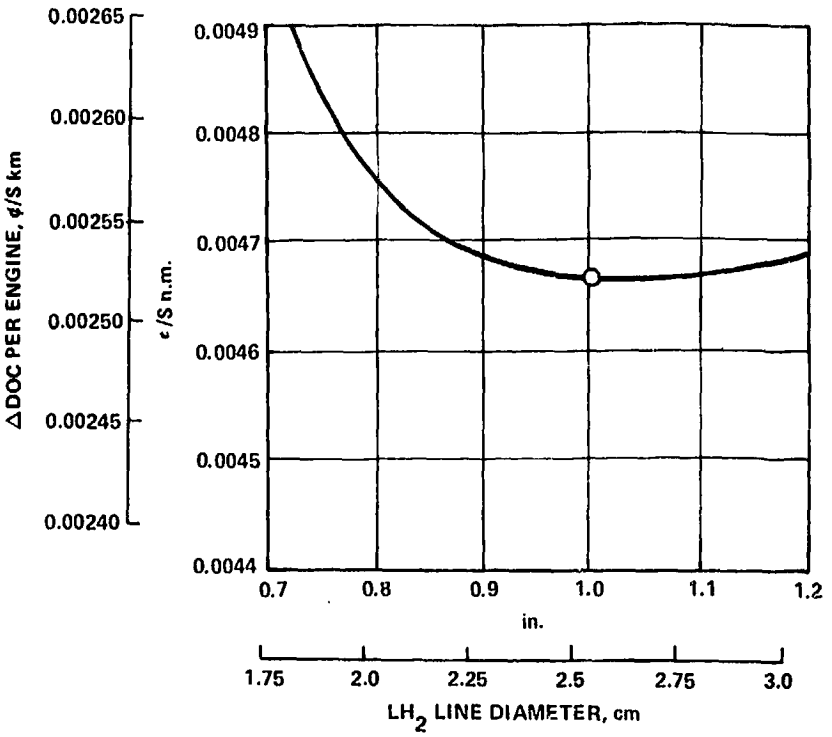

Figure 50. - Size optimization for engine fuel supply line.

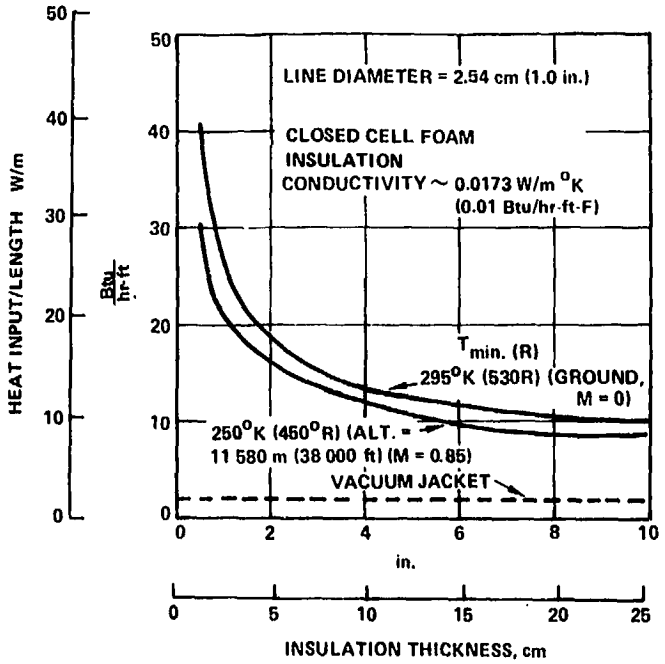

Figure 51. - Effect of insulation on heat leak rate.

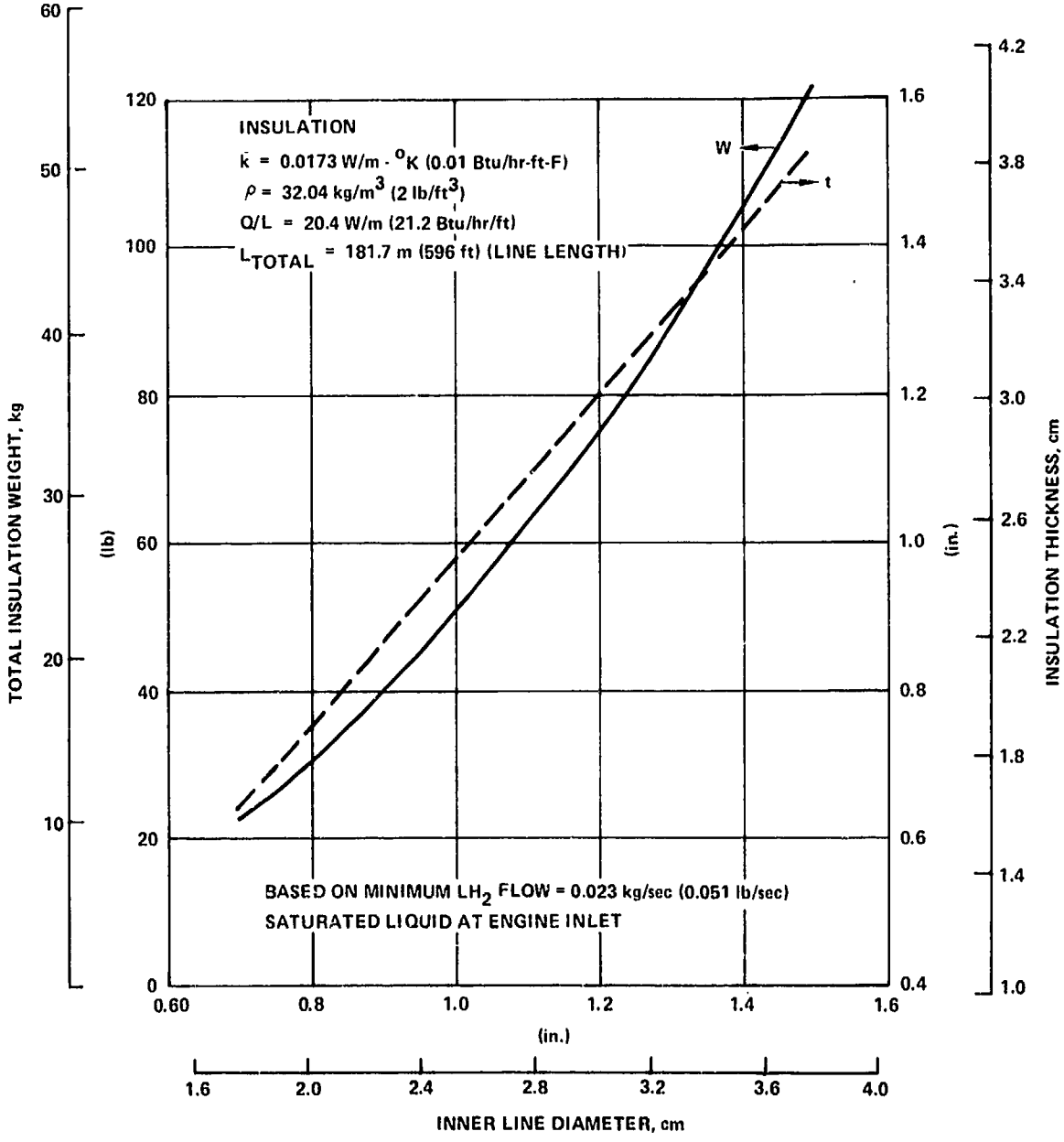

Figure 52. - Foam insulation requirements.

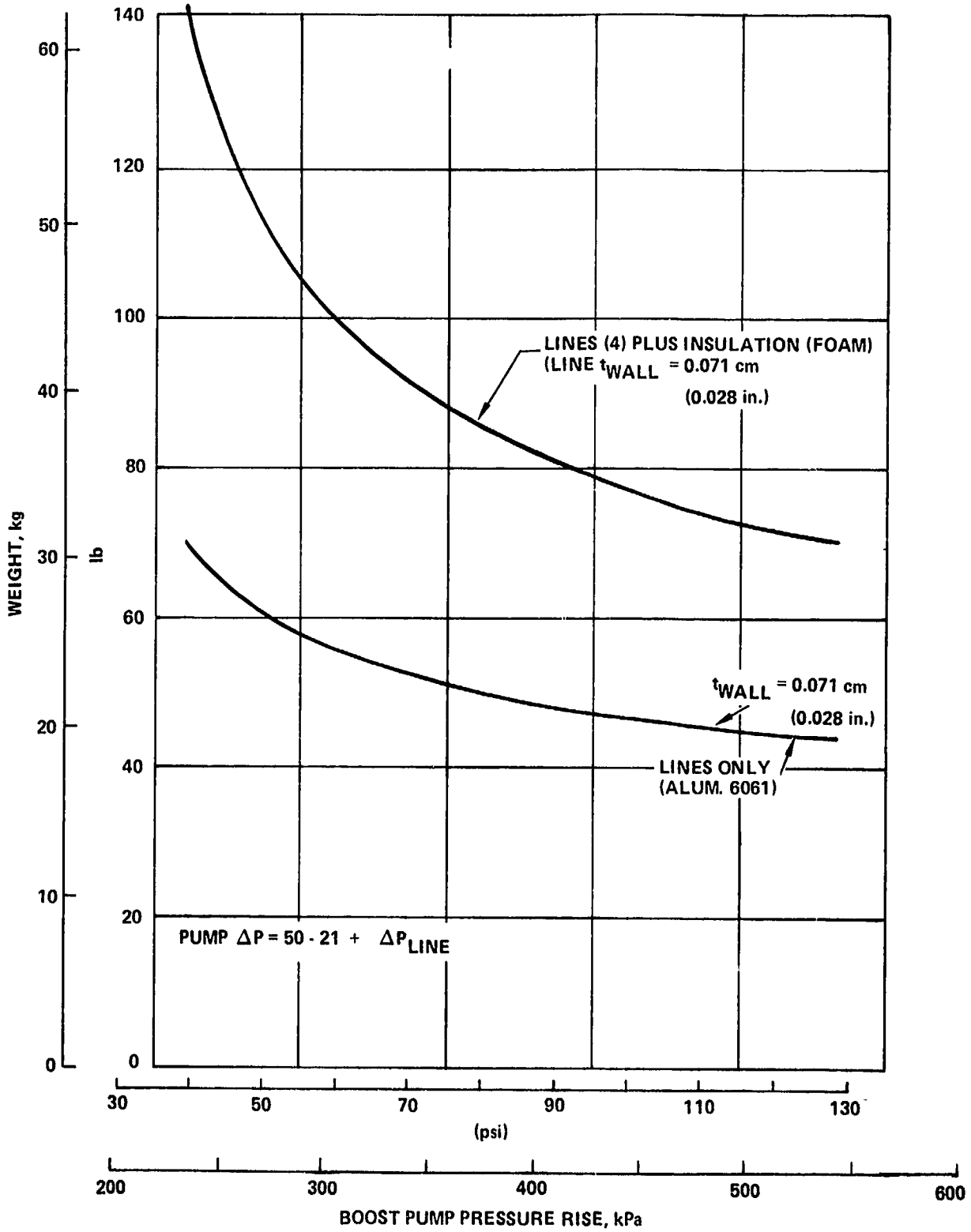

Figure 53. - Fuel feed line weight requirements.

5.2.2.2 Line configurations:

Vacuum jacket insulation: The inner line is wrapped with approximately 20 alternate layers of fiberglass cloth and aluminized mylar. The mylar acts as a radiation shield and the fiberglass prevents contact between the mylar sheets. Commercial manufacturers of cryogenic piping have found that vacuum insulated lines without radiation shields lose significant amounts of heat through radiative mechanisms. The space between the inner and outer lines is vacuum pumped to approximately 1 micron.

Line wall thickness calculated from flow pressure or minimum handling gage (Sec. 5.2.3) determines the tubing weights. However, the values chosen have been called into question during discussions with one manufacturer of cryogenic piping with whom the problem was discussed, CVI Corporation. CVI recommends somewhat thicker walls for three reasons: easier fabricability, easier repair, and greater structural strength. CVI suggested inner and outer wall thicknesses of 0.089 and 0.122 cm (0.035 and 0.048 in.) respectively, compared to Rocketdyne's estimates of 0.030 and 0.064 cm (0.012 and 0.025 in.). However, CVI's experience lies primarily in the area of nonflight weight systems produced without advanced welding techniques. CVI's general concern must be considered, however. Therefore, a recommended technology effort for subsequent work includes fabrication, testing, and repair of flightweight cryogenic lines to establish minimum wall thicknesses that may be utilized for an operating system.

It is expected that the greatest stress loadings will be experienced by the outer line. A technique for wrapping the outer line with a nonmetallic composite material reinforcement may allow simultaneous reductions in weight at a fixed strength level and also a backup insulation system. In a NASA-funded study, engineers at Martin-Marietta Corporation showed that serviceable cryogenic lines could be constructed by wrapping thin metallic tubing with glass-fiber reinforcement. The metallic tube carried the cryogenic fluid, while the wrapped reinforcement provided both strength and thermal insulation. If the outer vacuum jacket were wrapped with glass reinforcement, the single wrap could act both as a reinforcement and as a backup insulation.

Another option for the outer jacket is the use (for all or part of the outer jacket) of semi-flex line. This approach would eliminate differential thermal expansion problems.

Provision of a one micron vacuum in the vacuum annulus may be accomplished in either of two ways; first, each fuel line could consist of a single annulus extending the entire length of the line. This annulus would be pumped by an onboard vacuum pump or by periodic pumping by ground-based equipment. Alternatively, the annulus could be pumped down and sealed during assembly and repumped only if measurements indicated a vacuum leak. Second, the vacuum line could be built from independent stand-alone units. Again, the individual segments, or spools, could be pumped by onboard or ground-based pumps, or they could be pumped out and sealed when constructed.

The spool approach is preferred due to its greater reliability. In the case of a single vacuum annulus, a single large leak imposed by some accident during flight could conceivably disable that fuel line. Further, vacuum pumping of a thin annulus is very slow, requires a large pump, or may require an extensive network of pumping lines throughout the aircraft. For the spool approach, as discussed in Section 5.6, loss of vacuum on a single, 3.05 m (10 ft) spool will not cause vaporization of the fuel that passes through the spool. Thus, a single spool failure does not endanger the aircraft at any point of the flight profile.

Foam insulation: The foam insulation approach offers several distinct advantages compared to the vacuum approach principally in the areas of safety and reduction of technical complexity. From the standpoint of safety, foam insulation is not lost by catastrophic failure of spool sections, and the presence of the foam protects the inner fuel line from damage during handling and normal operations. Foam-insulated lines also present significant advantages in manufacturing and maintainability. Vacuum spool sections must be fabricated as complex double-concentric units and pumped at the fabrication or installation points. Construction for foam lines is much simpler: individual single tubes can be welded together and then covered by a foamed-in-place insulation. Repair is accomplished simply by cutting and removing the foam, repairing the inner line, and refoaming an insulation layer. Foam layers must be protected against the phenomenon of cryopumping, in which condensation of gases within the foam cells eventually degrades the insulation properties. Lightweight, metallic coverings can successfully protect against cryopumping problems. An additional advantage of foam is the elimination of one type of thermal expansion problem. For a concentric-tube vacuum insulation system, the differential contraction between the cold inner line and the warm outer line can be sufficient to damage the lines in the absence of a bellows in one of the lines to absorb the change in length. In current practice, no provision for differential thermal contraction is provided for foam-insulated lines, since the foam cells are sufficiently resilient to expand and compress to absorb the length change. Thus, the only thermal contraction which need be considered is the net length change of the metallic inner line. This effect is discussed in Section 5.2.3 below.

The disadvantages of foam are weight, fire resistance, and long-life embrittling. Foam is expected to be 25 percent heavier than a vacuum line on per foot basis, but the elimination of complex spool connections should essentially offset weight penalities. Care must be taken that the foams selected for use are resistant to burning in short, relatively intense hydrogen fires. Finally, many existing foams tend to become embrittled during long exposure to cryogenic temperatures. At the present time, no known foams are completely unaffected by such conditions. Long-life foam development programs are presently underway, and it is expected that by 1985 fully stable foams will be available.

It is concluded that a foam-insulated cryogenic piping system is the best choice for use in hydrogen-fueled aircraft. A further comparison of foam versus vacuum lines is presented in Sect. 5.6.2.

5.2.3 Design description. - This section includes discussion of materials for use in the fuel lines, thermal contraction, and weight.

5.2.3.1 Materials selection: Liquid hydrogen feed system materials which have been utilized successfully at Rocketdyne are summarized in Table 20. The cast aluminum alloy (Tens-50) and the highly alloyed stainless steel (A-286) materials are utilized mainly for fittings, valve bodies, or other complex shapes. The candidate materials for feed lines are the wrought aluminum (6061) alloy and 321 stainless steel. Use of a working-stress level equal to the lower value of either one-half of yield or one-fourth of ultimate strength results in the aluminum alloy having the highest strength-to-weight ratio. Because of its much lower thermal conductivity and thermal expansion characteristics, 321 stainless steel was chosen for the inner line. 6061 aluminum was used for the outer line.

5.2.3.2 Thermal contraction provisions: Two types of thermal contraction must be considered for lines which experience temperature changes from ambient to cryogenic temperatures. First, the overall length of the line may change, thereby affecting the system geometry and line-attachment provisions. This length change is on the order of 10×10^{-6} in/in/^{o}C, or 4.57 cm (1.8 in.) for a 15.24 m (50 ft) run of line cooled from ambient to cryogenic temperatures. Practically, this length change may be rendered harmless through the provision of sufficient bends in the line, a line-space envelope which allows the normal portion of the bend to absorb the length change elastically, and compliant mounting provisions (such as a cable-tray type of approach to supporting the fuel lines). Bellows might be provided where necessary, but normal practice has shown that the provisions suggested above are sufficient under ordinary operating conditions.

The second type of thermal contraction problem is the differential thermal expansion between the inner and outer lines. When the inner is cooled from ambient to cryogenic temperature and the outer line remains at essentially ambient temperature, differential thermal strains may be developed. For the case of foam-insulated lines, current practice with long, large diameter lines in the Space Shuttle has shown that thermal strains are accommodated without any need for special provisions such as bellows. Vacuum-insulated lines, on the other hand, generally require some type of mechanical strain-absorbing element such as a bellows. In addition, special configurations of foam-insulated lines may require large-deflection capability, so bellows arrangements were investigated for this application. Rocketdyne has extensive experience in cryogenic-line applications for rocket engines, such as the

TABLE 20. - CANDIDATE MATERIALS FOR LIQUID HYDROGEN APPLICATION, 217.2°C (-423°F)

Material	Density kg/cm^3 (lb/in^3)	Yield Stress kPa (psi)	Ultimate Stress kPa (psi)	*Working Stress kPa (psi)
Tens-50 Aluminum - Cast	0.0027 (0.096)	372 317 (54 000)	455 054 (66 000)	113 763 (16 500)
6061 Aluminum - Wrought	0.0027 (0.096)	317 159 (46 000)	413 685 (60 000)	103 421 (15 000)
321 Stainless Steel	0.0079 (0.286)	296 475 (43 000)	1 310 004 (190 000)	148 237 (21 500)
A-286 Stainless Steel Machined	0.0079 (0.287)	896 318 (130 000)	1 365 162 (198 000)	341 290 (49 500)
*Working Stress = Lower value of either 1/2 yield or 1/4 ultimate stress				

Space Shuttle Main Engine. The general approach for insulation in the engine system is to apply foam over exposed lines, joints, valves, etc., wherever possible. Because the engine operates intermittently and then at very high fluid-flow rates, more efficient insulation approaches were rejected due to weight or complexity. A prime purpose for covering the exposed surface is preclusion of formation of LOX that could lead to an engine fire, and foams are effective in this role.

At some locations, however, foams cannot be used. The rocket engine is gimballed, and the cryogenic transfer lines must incorporate sufficient flexibility to permit several degrees of rotation. The bellows units are double walled with insulation provided by a vacuum in the annulus. This vacuum is produced by pumping the annulus to 1 micron, backfilling with pure argon gas, and sealing. When cryogenic fluid flows in the lines, the argon liquifies and a vacuum is produced. To achieve 1 micron vacuum in a bellows unit that has many slowly pumping regions requires several days of laboratory pumping, and the approach chosen allows attainment of a good vacuum without requiring heavy on-board pumping equipment. All lines and bellows are welded wherever possible.

5.2.3.3 Fuel feed line weight: Minimum fuel line wall thickness can be estimated from the hoop stress produced by the contained fluid, using the relation:

$$t = \frac{Pd}{2\sigma_w}$$

where

t = wall thickness

P = internal pressure

σ_w = working stress

and prior experience for line fabricability. In the case of the selected concept which uses a tank-mounted boost pump, the hydrogen pressure levels are so low (approximately 317 kPa (46 psia)) as to result in unrealistically thin walls (approximately 0.003 - 0.008 cm (0.001 - 0.003 inches)) if only hoop stresses are considered. Rocketdyne manufacturing experience and Lockheed CL-400 experience indicate minimum wall thickness of 0.041 cm (0.016 inch) are required for practical considerations.

For the inner fuel-containment line, 321 stainless steel was chosen because of its thermal properties and because of ease of fabrication and welding, as well as proven structural integrity. 6061 aluminum was chosen for the outer line because of weight saving and compatibility with liquid hydrogen. Table 21 summarizes line-only and line-plus insulation weights. It is noted that the total weight of vacuum insulated line is only 4.5 kg (10 pounds), or 3.4 percent less than foam-insulated line.

TABLE 21. - LINE WEIGHT SUMMARY

	Weight per m (ft), kg (lb)	Total Feed System Weight per 182 m (596 ft), kg (lb)
Inner Line (0.016 Stainless Steel, 2.54 cm (1.0 in.) o.d.)	0.27 (0.18)	49 (107)
Outer Line (0.016 Aluminum, 10.16 cm (4 in.) o.d.)	0.34 0.23	62 (137)
Total	0.61 0.41	111 (244)
Insulation Weight		
Foam		23 (50)
Vacuum		18 (40)
Total Weights		
Foam		134 (294)
Vacuum		129 (284)

5.2.3.4 Fuel line summary: The selected fuel line configuration is summarized in Figure 54. Although vacuum insulation saves a small amount of weight in the fuel-line, the foam insulated line was selected due to safety, manufacturing, and repair considerations. In addition, an analysis was performed to determine the difference in cost which might be expected between a typical vacuum jacketed fuel line and a foam insulated design. It was found that the foam insulated line would cost only 62 percent as much as the vacuum design; $39 100 versus $62 700; thus adding another reason for selecting the foam insulation system.

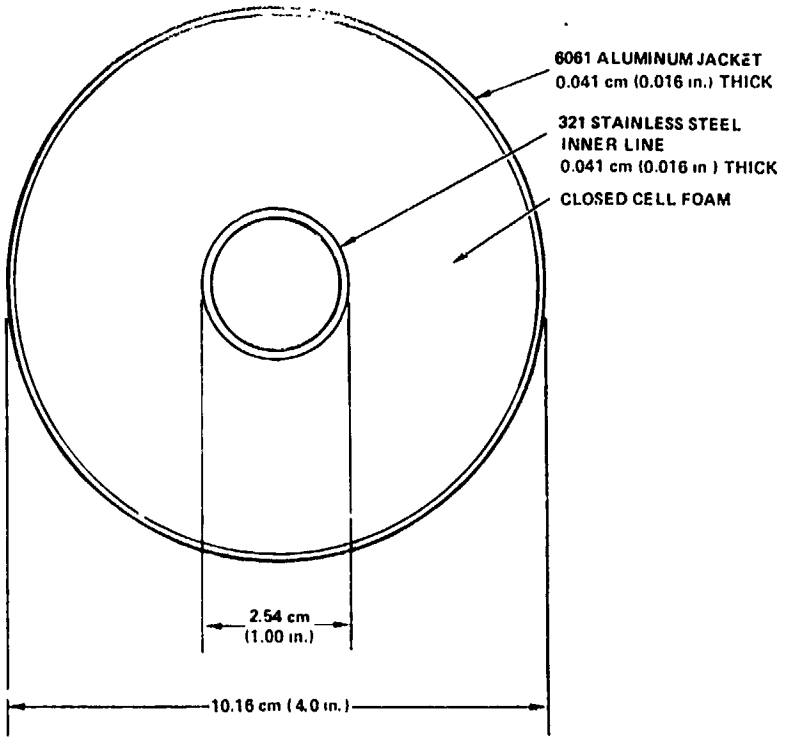

Figure 54. - Selected fuel-line configuration.

5.3 Boost Pump

In the fuel-system optimization effort (Sec. 5.1.2), it was determined that the boost pump should provide a minimum 317 kPa (46 psi) boost over the entire range of fuel-flow, as specified in the schedule of Table 19. The objective of the boost pump design effort was to select the most attractive pump within this constraint and other design requirements detailed in

Sec. 5.3.1. This pump should not only attain minimum incremental ΔDOC, but it should also be amenable to long-life and easy maintenance in airline operations. It has been determined that two- or three-stage centrifugal pumps operating at speeds up to 36 000 rpm are the leading candidates for this application. However, there is no data for the operation of this or any other type of flight-weight pump in liquid hydrogen for times approaching the 8000 hours desired for airline operations. Development of long-life, reliable cryogenic pumps of this type appears to rest on development of satisfactory bearings.

5.3.1 Design requirements. - The design philosophy for the boost pump system is based upon the premise that a single pump failure shall not compromise aircraft safety. In addition, aircraft operators are reluctant to ground an aircraft if one boost pump in any of its fuel tanks is incapable of being operated. In accordance with this philosophy, each tank in the hydrogen-fueled subsonic transport will incorporate a minimum of three boost pumps. The justification for this conclusion is discussed in the following paragraphs.

Although hydrocarbon-fueled aircraft can takeoff and climb to cruise altitudes with boost pumps inoperative most of the time, hydrogen-fueled aircraft engines would flameout if the boost pumps failed, due to vaporization in the line with loss of pressure. Hence, the boost pump system must entail a redundancy which precludes loss of thrust from any engine in the event of pump failure immediately after the aircraft becomes airborne. During takeoff and initial climb, this philosophy dictates that one tank supplies one engine and that two pumps in each tank must be operated simultaneously. Thus, with two pumps operating, a single boost pump failure just after takeoff could not cause a loss of engine thrust. The redundancy requirement further dictates that no two pumps within a given fuel tank can be supplied electrical power from the same source.

The above requirements indicate that each pump must be capable of supplying fuel at the pressure and flowrate required by one engine at the maximum flow condition which occurs during sea level climb operation. To permit engine performance growth without the necessity of redesigning the engine pumps, a margin of 10 percent excess capacity has been specified in the pump functional requirements. A draft of a general functional requirement specification for a pump system is shown in Table 22.

TABLE 22. - FUNCTIONAL REQUIREMENTS

Title:	Pump, Fuel Boost, tank-mounted, Plug-in Motor Driven
1.	Scope
	This document defines the functional requirements for a submerged, motor driven, liquid hydrogen fuel boost pump. The pump shall have provisions for quick removal and replacement from the tank without having to remove fuel, plumbing, or electrical wiring from the aircraft.
2.	Applicable Documents
	(to be added)
3.	Requirements
3.1	Ports
3.1.1	Discharge - The discharge port shall be a four bolt flange type sized for one inch tubing.
3.1.2	Pressure Sensing - Pressure sensing bosses shall be provided at each pump for sensing discharge pressure.
3.2	Lubrication - The pump and its driving motor shall be lubricated with a system compatible with hydrogen.
3.3	Pump Housing - A pump housing shall be provided which permits removal of the pumping element and driving motor without requiring that fuel be removed from the tank during the operation.
3.4	Check Valves - Check valves shall be provided in the inlet and discharge passages of the pump housing such that no fuel leakage can occur when the pump elements are removed.
3.5	Thermal Relief - The pump discharge check valve shall have a small hole vented to the tank to provide thermal relief.
3.6	Electrical -
3.6.1	Power - The pump motors shall be "Y" connected and shall be rated for continuous duty at 115/200 volts, 3 phase, 400 Hertz, or as an alternate, 270 Vdc power.
3.6.2	Power Consumption - The power consumption shall be optimized for the cruise operation.

TABLE 22 - Concluded.

3.6.3 Electrical Connection - The electrical connection between the removable element and the pump housing shall be automatically disconnected concurrently with removal of the pumping element and the motor subassembly.

3.7 Performance -

3.7.1 Fluid - The pump shall be compatible with liquid hydrogen fuel.

3.7.2 Operating Pressures - The pump inlet and discharge pressures shall be in accordance with the requirement of Figure ___

3.7.3 Flowrate - The pump flow requirements shall be as dictated by Figure ___.

3.7.4 Environment - The pumping element, housing and driving motor shall be capable of operating in an environment established by the presence of liquid hydrogen stored at a pressure of 145 kPa (21 psia) absolute.

3.7.5 Priming - The pumping element shall be capable of priming itself if initially filled with gaseous hydrogen at start up.

3.7.6 Maximum Pressure - The maximum pressure output of the pump under any condition shall be compatible with the limitations of the engine systems.

3.8 Reliability -

3.8.1 MTBF - The mean time between failures per element shall not be less than 2500 hours using the definition:

$$\text{MTBF} = \frac{(\text{Cumulative Flight Hours})\ (\text{No. of Units/Aircraft})}{\text{Cumulative Number of Chargeable Failures}}$$

3.8.2 TBO - The scheduled time between overhauls shall not be less than 8000 flight hours.

3.8.3 Shelf Life - The unit shall have a shelf life of not less than 5 years with a capability of immediate service.

3.8.4 Safety - Safety concepts and design features shall be incorporated in the pump and drive design. The pump shall be capable of operating dry in a hydrogen gas environment without hazard.

3.9 Pump Mounting Attitude - The pump assembly shall be mounted vertically with the pump inducer located at the low point in the storage tank.

During cruise, when fuel flowrates and the hazard resulting from engine flameout are considerably reduced, each pump must be capable of supplying two engines by means of crossfeed for added redundancy and to reduce electrical power requirements if the operator chooses.

Boost pump performance requirements were determined from the flow-pressure requirements of Table 19 and as a result of the concept selection trade described in Section 5.1.2. The flow-pressure schedule is an unusually wide range from the standpoint of throttling of the pump output, and this factor has influenced pump selection considerably. The performance of the boost pump must be matched to that of the engine-mounted main pump since no engine-to-tank return line is provided in the hydrogen aircraft. The boost pump must provide a minimum NPSP of 3.4 kPa (0.5 psi) to the engine-mounted pump with minimum weight and power consumption.

Other design requirements are determined from the intended mission of the pump system within the aircraft. The pump must be designed for long life, 8000 hours being the baseline goal. The bearings must operate in LH_2 or, alternatively, an acceptable thermal isolation system must be found. The pump drive must operate on available aircraft power systems. Several candidates were considered, but the choices soon narrowed to electrically driven pumps. For the evaluation performed here, two aircraft electrical systems were considered. Present conventional systems utilize 400 cycle power. It is projected that by 1995 commercial aircraft may utilize 270 volt dc power systems, which have considerable advantages for aircraft applications. Both of these electrical systems were considered, and the details are given in Section 5.3.3. The tank-mounted boost pump must be safe in operation and easily maintainable. The manufacturing costs should be as low as possible consistent with meeting other operating needs. Finally, the boost pump must meet all general requirements of FAR 25.

5.3.2 Candidate pump types. - Four basic candidate pump types were considered: inducer, vane, piston, and centrifugal. In preliminary calculations, tandem row inducer pump designs were shown to have the lowest values of ΔDOC. However, at the minimum flow condition (flight idle at 11 582 m (38 000 ft) and M = 0.85), they did not deliver enough pressure rise to meet the specified main pump NPSP (pressure above vapor pressure) requirement of 3.4 kPa (0.5 psi). This pressure rise might have been met by using the wide range, tandem row inducer design along with 50 percent flow recirculation around the motor-boost pump unit. However, this would result in a pump inlet vapor volume fraction that might be too high for the pump to operate because an inducer pump cannot pump two-phase flow if the inlet flow coefficient is too far off design. This, in combination with the fact that such a design would have to approach an unstable operating condition (which occurs in an axial pump that is operated at too low a flow) in order to meet the NPSP requirement, resulted in a decision to use a pump design with a wider operating range capability.

Positive displacement pumps would have design rotational speeds less than 10 percent of those of centrifugal or inducer pumps and, therefore, would be

too heavy for this particular combination of head rise and volume flowrate. Included in this positive displacement category are piston pumps and vane pumps. Additionally, positive displacement pumps typically have large surface areas that require some lubrication. This requirement would likely reduce operating life significantly, since liquid hydrogen is not a good lubricant. For these reasons, vane and positive displacement pumps were not considered further. The only remaining candidate is the centrifugal pump, with its wide operating range, forgiving stall characteristic, and relatively small lubrication requirement. Constant-speed and variable-speed centrifugals were evaluated as to ability to meet flow requirements and ΔDOC minimization. This evaluation is described in detail in Section 5.3.4.

For centrifugal pumps that are designed for maximum efficiency, the performance characteristics are shown parametrically in Figure 55 for design point operation (sea level climb at M = 0.38) and Figure 56 for minimum flow operation (flight idle at 11 582 m (38 000 ft) and M = 0.85). It is apparent that stage numbers and design speeds can be varied over wide ranges to give whatever combination of characteristics is desired.

From Figure 55, it is apparent that, in this rotational speed range (less than 40 000 rpm to obtain an inlet diameter greater than 1 inch so as to pass the flow), multistaging is necessary in order to operate down to shutoff (P_m > 345 kPa (50 psi)). With these high efficiency types of designs, operation down to shutoff is possible if the stage specific speed is greater than about 3000. However, this may be done at a stage specific speed of only 1150 by designing specifically to obtain a wide operating range. This is achieved at the expense of approximately a 14 point penalty in efficiency. It may be concluded that simplicity can be achieved at the expense of performance. Since both objectives are of interest here, wide range designs as well as high-efficiency designs were investigated.

5.3.3 Candidate pump drive systems. - Hydraulic, engine bleed air, and electrical pump drives were initially considered. Preliminary calculations showed that the fluid line and system weights necessary for the first two choices for use with remotely-located tank-mounted boost pumps were prohibitively high so that the choice was narrowed to an electrical drive. The aircraft electrical system may be either the standard 400 cycle ac system or a 270 volt dc system that has shown promise for future aircraft applications. Special controls are required if variable speed is to be used, whereas they are not if constant speed (which requires pump operation nearly down to shutoff) is to be used.

Brushless motors were assumed for the 270 volt dc case. The weights of these motors are shown in Figure 57 along with the weights of the corresponding electronic equipment required to operate a brushless motor over infinite ranges of torque and speed. In Figure 58 these motor and electronic equipment weights are summed to give the overall brushless motor assembly weights. For this brushless motor data, four additional assumptions were made: (1) the stator is hydrogen cooled to reduce resistance and, consequently, size

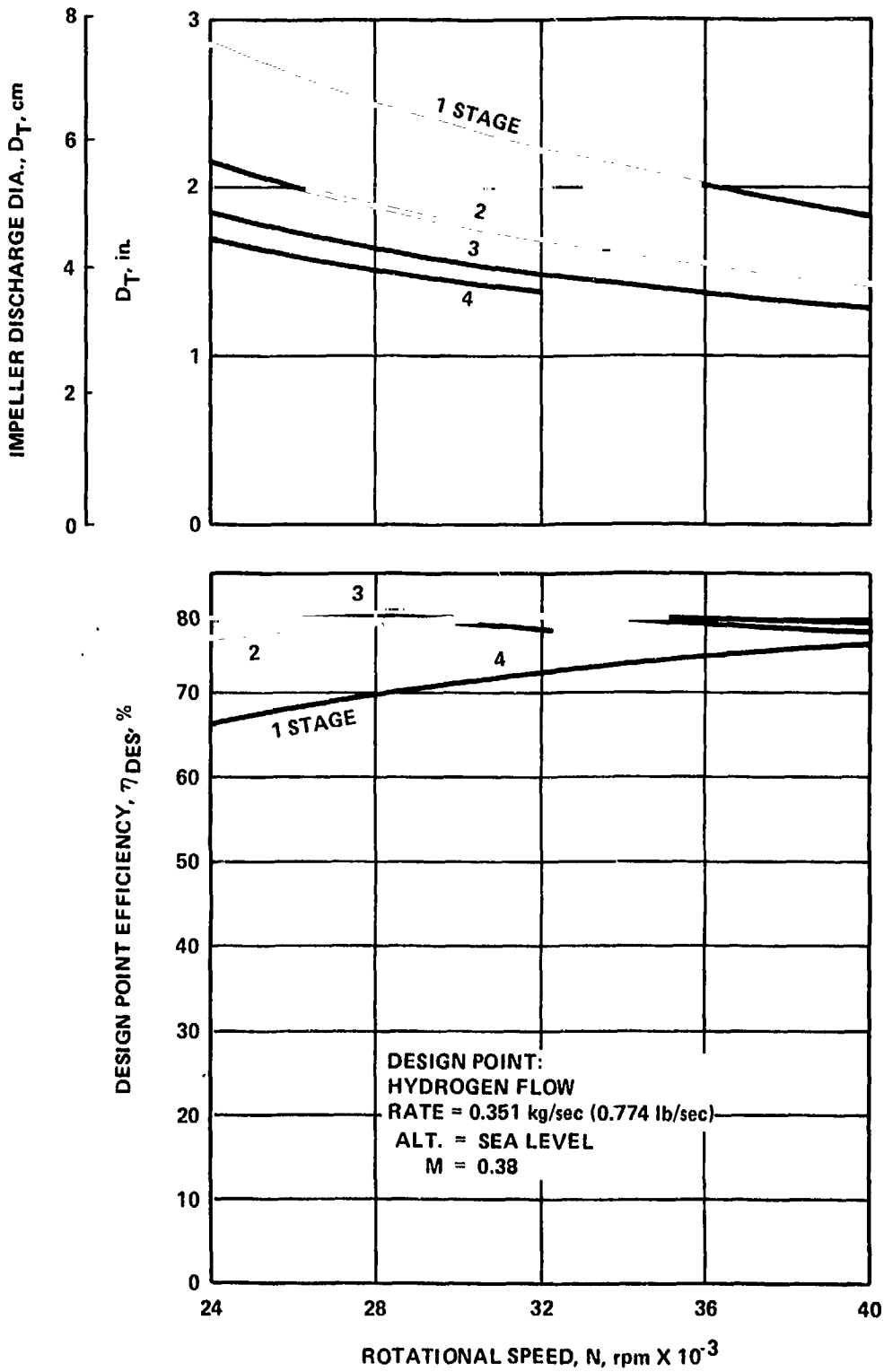

Figure 55. - Design point performance for centrifugal pumps designed for maximum efficiency.

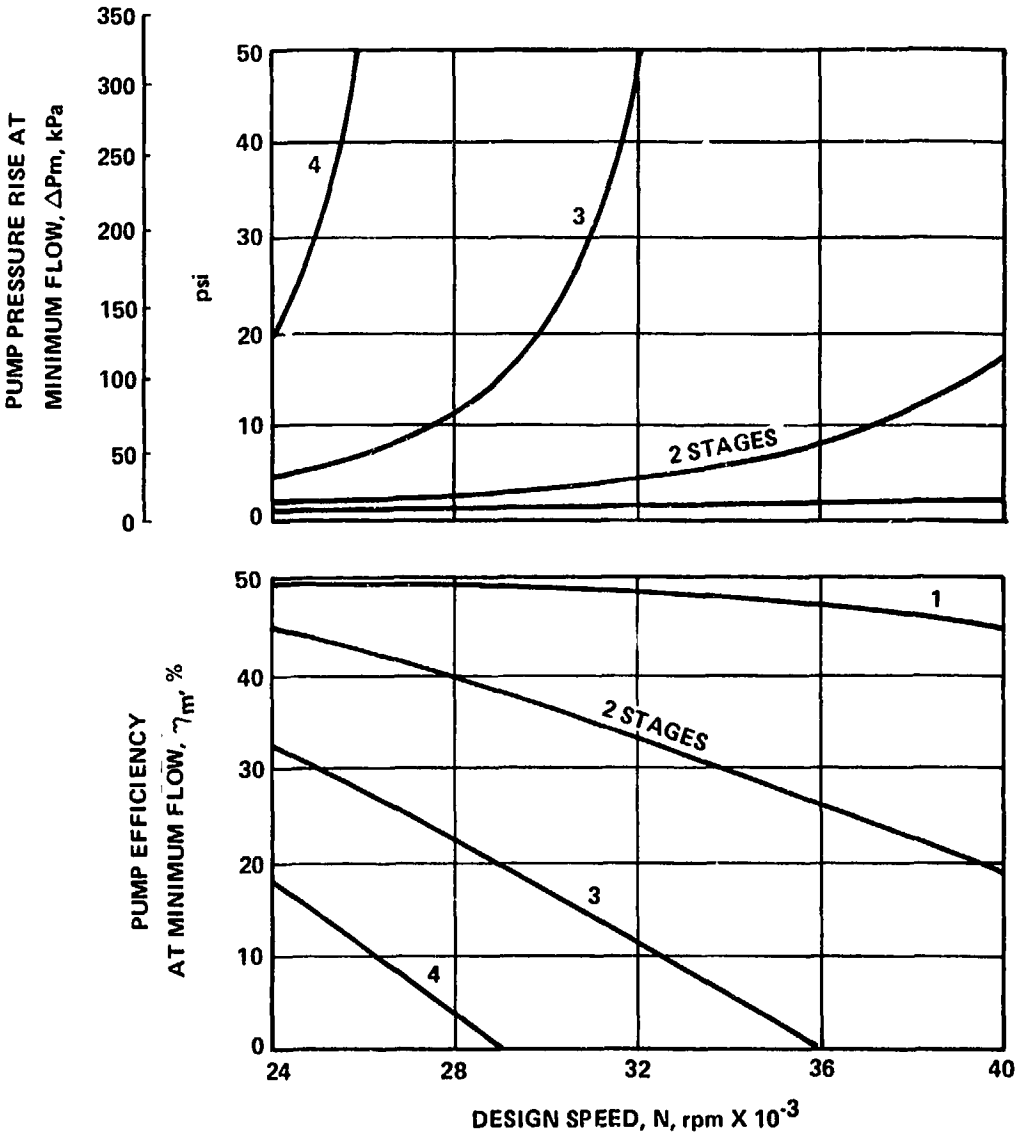

Figure 56. - Off design performance for centrifugal pumps designed for maximum efficiency.

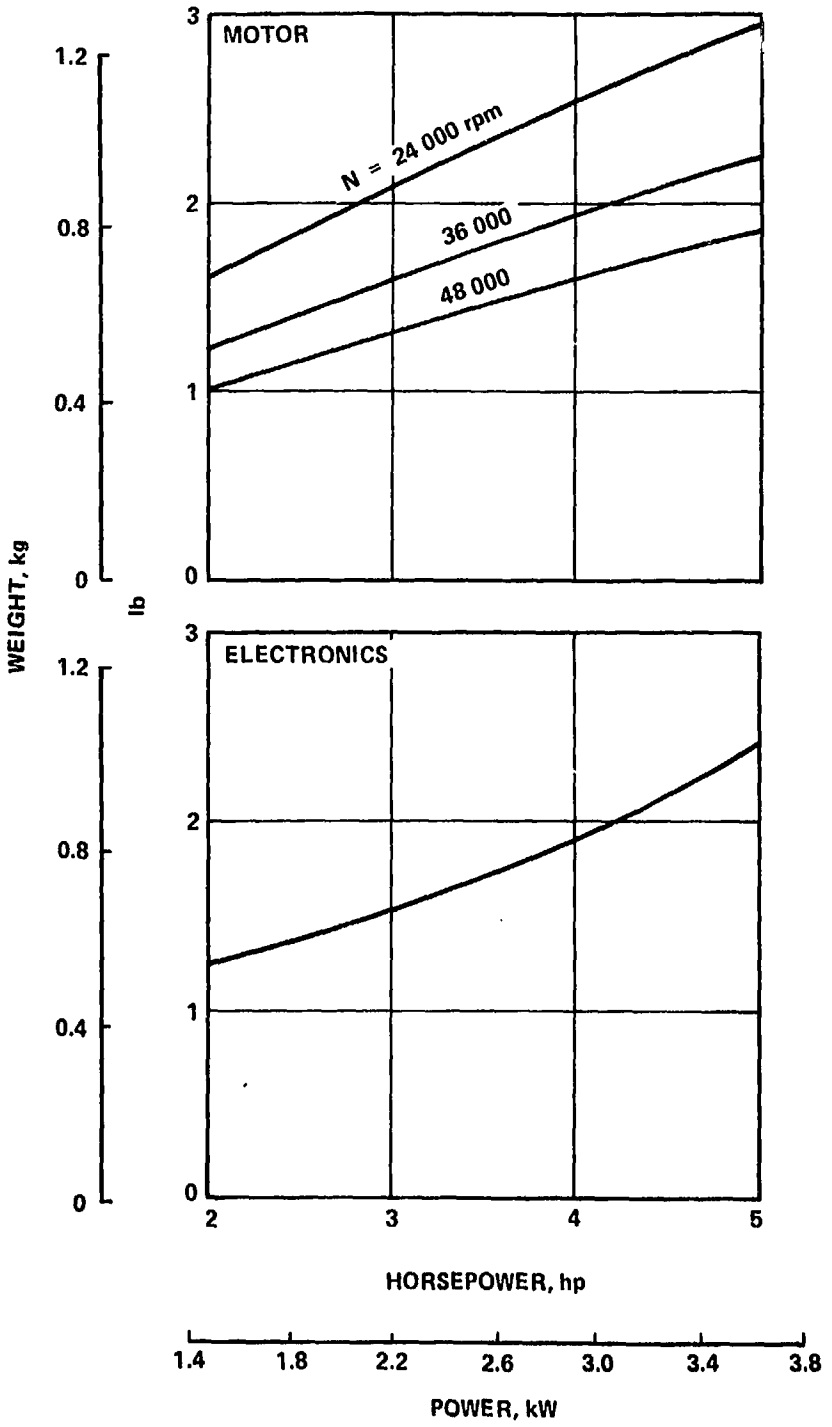

Figure 57. - 270 V brushless dc motor weight breakdown.

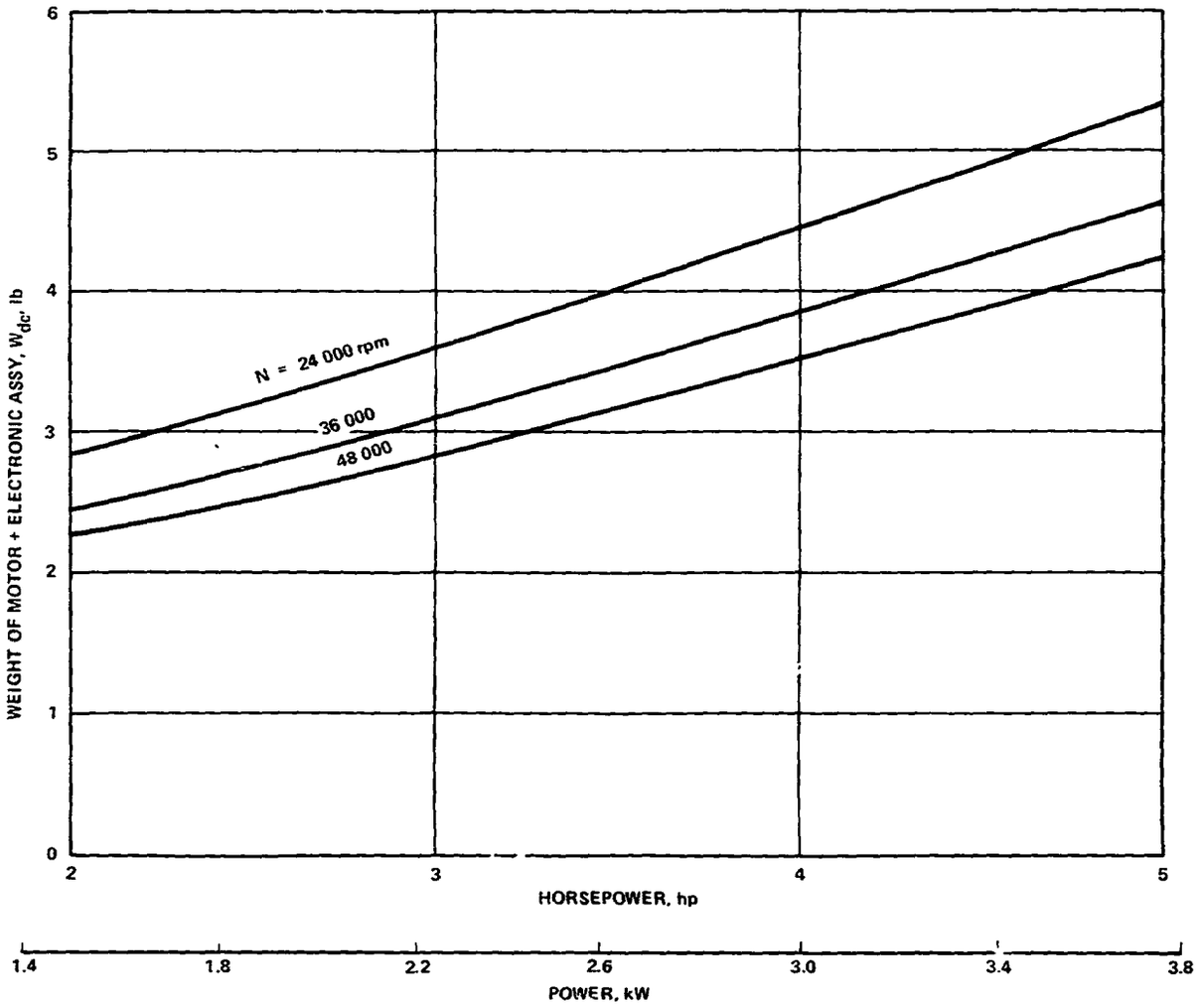

Figure 58. - 270 V brushless dc motor weights - includes weight of electronic assembly.

and weight, (2) there is no fluid in the air gap between the rotor and the stator, (3) hydrogen cooling does not result in any hydrogen vaporization, and (4) electromagnetic interference is suppressed to existing military standards. Regarding these assumptions, it must be noted that keeping the hydrogen out of the air gap may be difficult to achieve and, in fact, may not even be desirable. Further investigation and, possibly, some technology efforts are required to establish the proper approach.

For 400 cycle ac motors, the weights for 24 000 rpm, 2 pole, constant speed motors are shown in Figure 59. If variable speed is desired, a rather large inverter weight must be added. This is also shown in Figure 59. Finally, the efficiencies of these motors are shown in Figure 60. Due to the electronic equipment losses, a brushless dc motor is slightly less efficient than a constant speed ac motor. However, if an inverter is used to make the AC motor variable speed, the large losses in the inverter drop the overall efficiency more than 10 percentage points. This is also shown in Figure 60.

5.3.4 Boost pump and drive candidate evaluation. - In order to evaluate candidate pumps, alternates must first be sized to meet specified flow conditions.

5.3.4.1 Pump sizing: The pump inlet diameter requirement in the tank was determined from isentropic equilibrium expansion (from a saturated liquid) curves for hydrogen (Figure 61) and the maximum hydrogen flowrate per engine of 0.351 kg/sec (0.774 lb/sec). The resulting line size requirements are shown in Figure 62 as a function of tank vapor pressure and pump inlet vapor volume fraction (assuming the flow has reached equilibrium). As shown, a one-inch diameter hole will pass the flow at a low vapor fraction for a tank vapor pressure of 145 kPa (21 psia). Since this is about as small a pump inlet as is practical from a manufacturing standpoint, this value was used throughout the pump selection procedure.

5.3.4.2 Pump selection: Seven pump-drive combinations were investigated. As shown in Table 23 three were analyzed with ac motors and four were analyzed with dc motors. Within each motor category, two of the combinations used constant speed motors because there are two methods for obtaining throttling down to shutoff; (1) using a single stage, wide range pump (which has a lower efficiency), and (2) using a multistage, high efficiency pump. The other combination within each motor category used a variable speed motor and, since variable speed reduces the required number of stages, a high efficiency type pump.

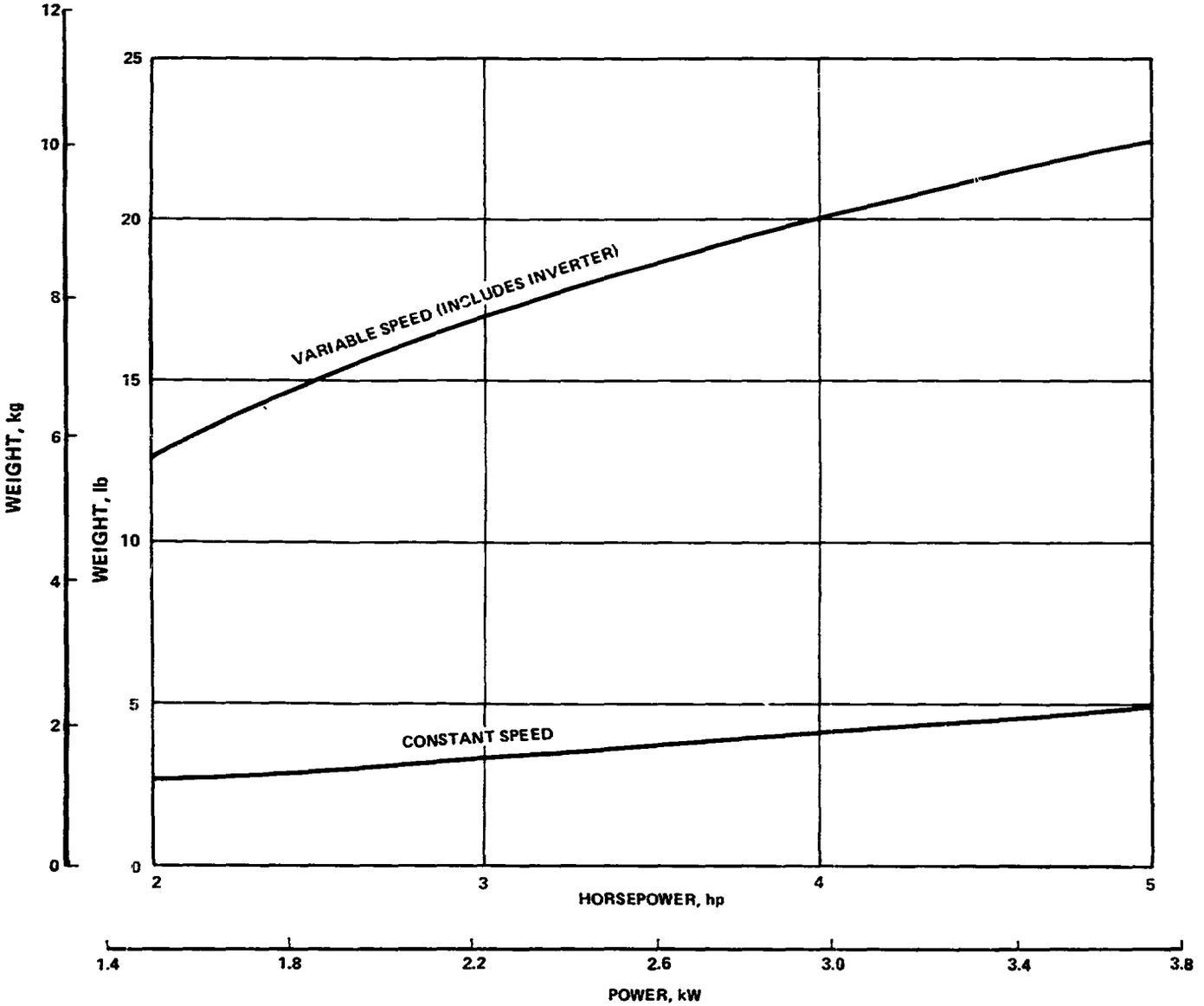

Figure 59. - 400 Cycle ac motor weights - 24 000 rpm, 2 pole.

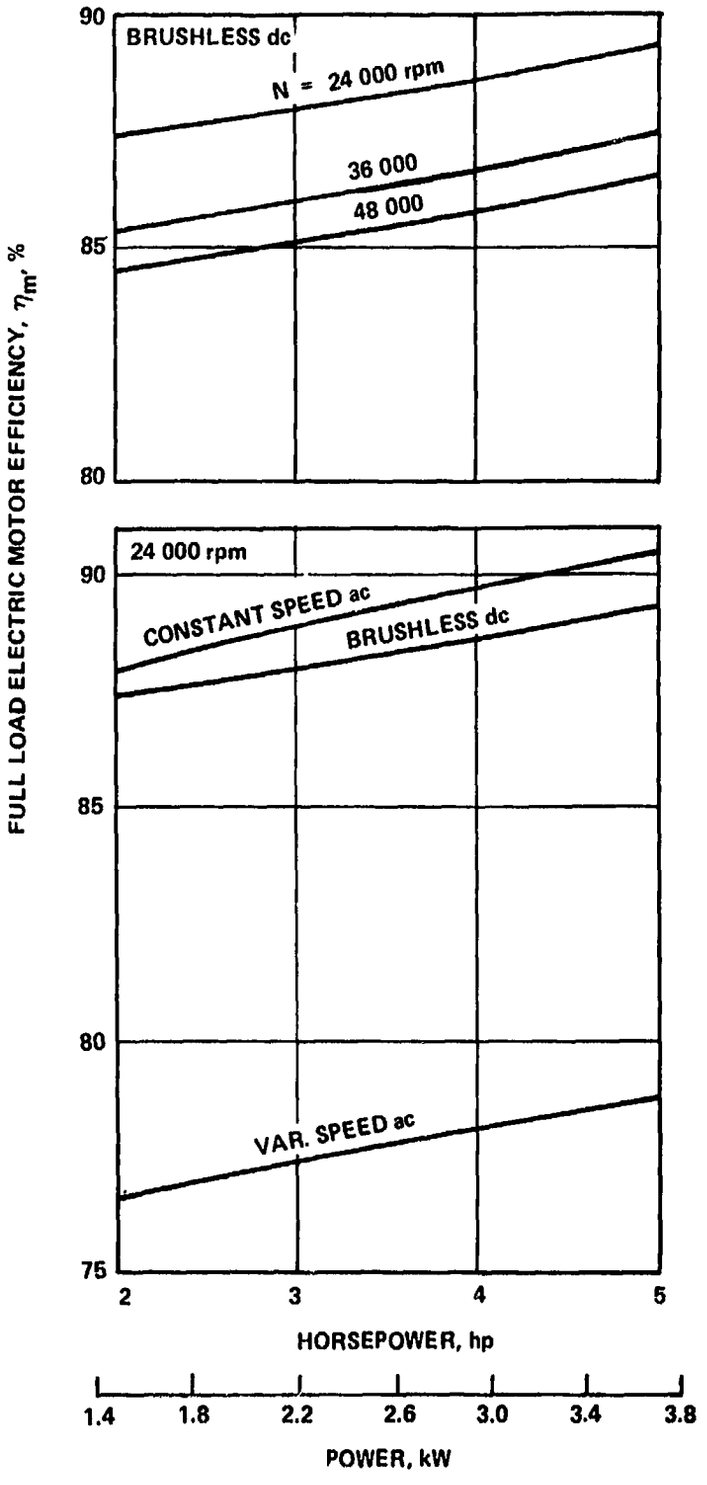

Figure 60. - Electrical motor efficiencies at full load.

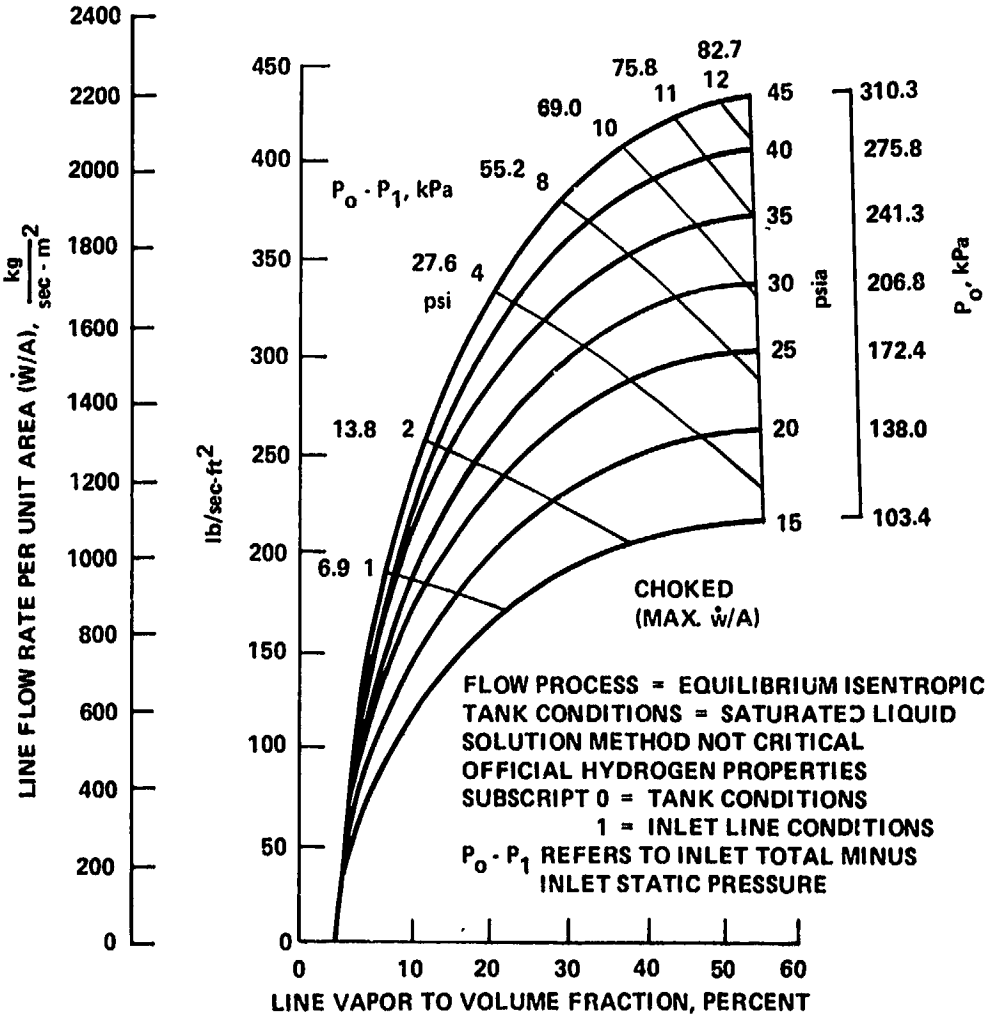

Figure 61. - Zero NPSH pumping capability requirements for hydrogen.

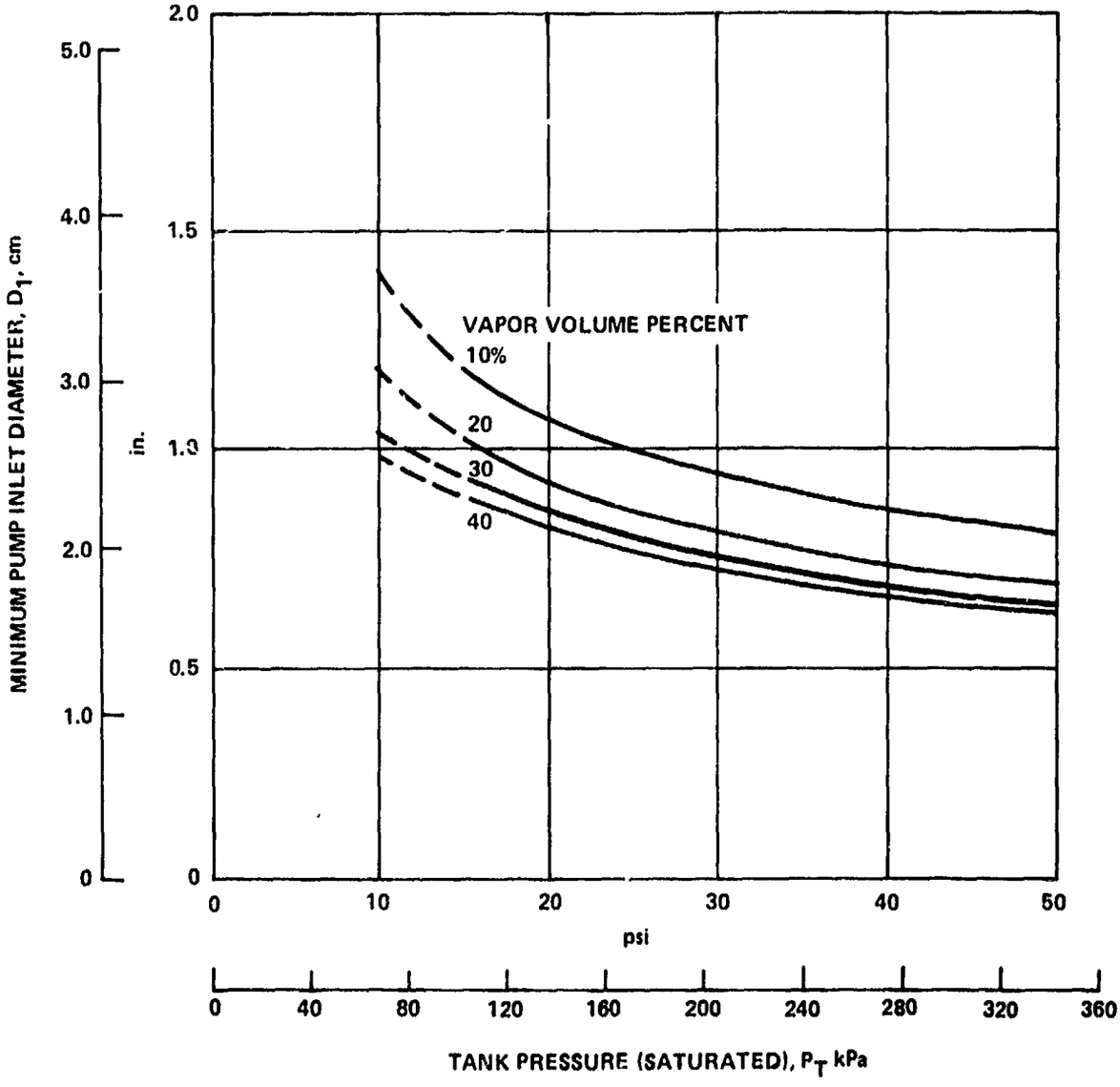

Figure 62. Boost pump inlet diameter requirements.

TABLE 23. BOOST PUMP CANDIDATE SUMMARY
(SI UNITS)

	Configuration	1	2	3	4	5	6	7
General	Speed	Const	Const	Var	Const	Const	Var	Var
	Current	400 Hz ac	400 Hz ac	400 Hz ac	270 Vdc	270 Vdc	270 Vdc	270 Vdc
	Sync with Source Current	Yes	Yes	@ Design	No	No	No	No
	No. of Pump Stages	1	5	3	1	3	2	3
	Freq Conv/Speed Control	No/No	No/No	Yes/Yes	Yes/No	Yes/No	Yes/Yes	Yes/Yes
Weights (kg)	Boost Pump	4.37	1.17	1.28	0.95	0.51	0.68	0.51
	Boost Motor	1.91	1.36	1.34	0.73	0.68	0.73	0.68
	Frequency Conv.	0	0	5.78	0.73	0.65	0.65	0.65
	Total Boost	6.28	2.53	8.41	2.41	1.84	2.06	1.84
	Line	13.3	13.3	13.3	13.3	13.3	13.3	13.3
	Main Pump	11.3	11.3	11.3	11.3	11.3	11.3	11.3
	Total (3 Boost)	43.47	32.24	44.08	31.12	29.49	30.16	29.49
Design (Max power -S.L. Climb @ M = 0.38)	Flow, $\dot{w}$, kg/sec	0.351	0.351	0.351	0.351	0.351	0.351	0.351
	Pressure rise, ΔP, kPa	317	317	317	317	317	317	317
	Speed, N, rpm	24 000	24 000	24 000	40 000	36 000	33 000	36 000
	Pump η, percent	50	78	79	64	78	78	78
	Motor η, percent	90	89	77	86	86	86	86
	Electrical, kW	3.50	2.28	2.58	2.86	2.36	2.34	2.36
Cruise (M = 0.85 @ 11 582 m)	Flow, $\dot{w}$, kg/sec	0.132	0.132	0.132	0.132	0.132	0.132	0.132
	Electrical, kW	2.64	1.72	0.55	2.16	1.78	0.50	0.48
	Main pump, kW	14.2	14.2	14.2	14.2	14.2	14.2	14.2
Min Flow (Flt Idle @ 11 582 m and M = 0.85)	Flow, $\dot{w}$, kg/sec	0.023	0.023	0.023	0.023	0.023	0.023	0.023
	Pressure rise, ΔP, kPa	427	427	34	427	427	34	110
	Speed, N, rpm	24 000	24 000	6850	40 000	36 000	9410	18 000
	Pump η, percent	6.4	9.9	32	8.2	9.9	32	18
	Motor η, percent	88	87	28	82	82	42	76
	Electrical, kW	2.48	1.63	0.13	2.04	1.69	0.08	0.26
ΔDOC, c/S km*		0.00085	0.00072	0.00082	0.00075	0.00071	0.00069	0.00069

* on a per engine basis

TABLE 23. Concluded.
(U.S. Customary Units)

	Configuration	1	2	3	4	5	6	7
General	Speed	Const	Const	Var	Const	Const	Var	Var
	Current	400 Hz ac	400 Hz ac	400 Hz ac	270 Vdc	270 Vdc	270 Vdc	270 Vdc
	Sync with Source Current	Yes	Yes	@ Design	No	No	No	No
	No. of Pump Stages	1	5	3	1	3	2	3
	Freq Conv/Speed Control	No/No	No/No	Yes/Yes	Yes/No	Yes/No	Yes/Yes	Yes/Yes
Weights (lb)	Boost Pump	9.64	2.58	2.83	2.10	1.12	1.50	1.12
	Boost Motor	4.20	3.00	2.95	1.60	1.49	1.60	1.49
	Frequency Conv	0	0	12.75	1.62	1.44	1.44	1.44
	Total Boost	13.84	5.58	18.53	5.32	4.05	4.54	4.05
	Line	29.3	29.3	29.3	29.3	29.3	29.3	29.3
	Main Pump	25.0	25.0	25.0	25.0	25.0	25.0	25.0
	Total (3 Boost)	95.84	71.08	97.18	68.6	65.01	66.5	65.01
Design (Max power -S.L. Climb @ M = 0.38)	Flow, $\dot{W}$, lb/sec	0.774	0.774	0.774	0.774	0.774	0.774	0.774
	Pressure Rise, ΔP, psi	46	46	46	46	46	46	46
	Speed, N. rpm	24 000	24 000	24 000	40 000	36 000	33 000	36 000
	Pump η, percent	50	78	79	64	78	78	78
	Motor η, percent	90	89	77	86	86	86	86
	Electrical hp	4.69	3.06	3.46	3.84	3.16	3.14	3.16
Cruise (M = 0.85 @ 38 000 ft)	Flow, $\dot{W}$, lb/sec	0.292	0.292	0.292	0.292	0.292	0.292	0.292
	Electrical hp	3.54	2.31	0.74	2.90	2.38	0.67	0.65
	Main Pump hp	19.0	19.0	19.0	19.0	19.0	19.0	19.0
Min Flow (Flt Idle @ 38 000 ft and M = 0.85)	Flow, W, lb/sec	0.051	0.051	0.051	0.051	0.051	0.051	0.051
	Pressure Rise, ΔP, psi	62	62	3	62	62	5	16
	Speed, N, rpm	24 000	24 000	6850	40 000	36 000	9410	18 000
	Pump η, percent	6.4	9.9	32	8.2	9.9	32	18
	Motor η, percent	88	87	28	82	82	42	76
	Electrical hp	3.33	2.18	0.17	2.74	2.27	0.11	0.35
ΔDOC (¢/Sn.mi.)*		0.00169	0.00138	0.00156	0.00142	0.00139	0.00129	0.00128

* on a per engine basis

As shown in the last data block (Minimum Flow) in Table 23, all the constant speed designs delivered a high pressure rise of 62 psi during minimum flow operation. This high pressure rise provides more than enough net positive suction pressure (NPSP, pressure above the vapor pressure) to meet the main pump requirements. However, with a variable speed boost pump, the boost pump speed can be adjusted so that the pump puts in only enough pressure (approximately) to meet the main pump NPSP requirements. As shown, this was assumed for the three variable speed cases (configurations 3, 6 and 7 in Table 23). This is also true during cruise. As a result, the boost pump power requirements are lower for the variable speed cases during off-design operation. However, in the analysis that was made, the main pump was assumed to be independent of the boost pump discharge pressure during cruise operation, as is also shown in Table 23. As a result, the main pump discharge pressure probably exceeds the cruise requirements for the cases in which a constant speed boost pump is used. In these constant speed boost pump cases, variable speed main pumps would have to be used in order to match with the boost pump during all modes of operation. In summary, exact matching between the boost and the main pumps can be achieved only if one of the two pumps has a speed that can be set independently.

As shown in Table 23, configuration 2 (a 5-stage pump driven by a constant speed motor) has the lowest direct operating cost (ΔDOC) of the ac driven candidates and configuration 7 (a 3-stage pump driven by a variable speed motor) is best for the dc candidates. Configuration 3, which has a variable speed ac drive, cannot compete with configuration 2 because the frequency converter required to obtain variable speed with ac is very heavy. This is not true with dc because the converter is much lighter for dc and because it is required for both constant and variable speeds. As a result, the variable speed drive (configuration 7) was the best with dc. Also shown is that the use of wide range, single stage pumps to obtain simpler configurations results in a decrease in pump efficiency and, consequently, an increase in operating cost. This is particularly true with ac where the lower design speed results in a lower single stage pump specific speed which, in turn, results in a greater pump efficiency penalty.

Because the minimum allowable boost pump pressure rise during minimum flow operation was originally unknown, several variable speed designs, each with a different pressure rise at the minimum flow condition, were analyzed to determine their pump and motor efficiencies during minimum flow operation. The results are summarized in Table 24. These data, in turn, were used in a heat transfer analysis to determine the resulting NPSP's delivered to the main pump. Of the candidates listed in Table 24, the one with the lowest ΔP minimum 34 kPa (5 psi) delivered 6.2 kPa (0.9 psi) NPSP to the main pump, which exceeds the requirement. All of the other designs had even higher NPSP's. As a result, all the variable speed configurations in Table 23 (configurations 3, 6 and 7) will meet the main pump NPSP requirements.

TABLE 24. - EFFECT OF PRESSURE RISE REQUIREMENT AT MINIMUM FLOW ON PUMP DESIGN AND MINIMUM FLOW PERFORMANCE

$\dot{w}_{min}$, kg/sec (lb/sec)	ΔP_{min}, kPa (psi)	Number of Stages	N_{des}, rpm	N_{min}, rpm	Pump η_{min}, %	Motor η_{min}, %	Elect. Power (min) kW(hp)
0.023 (0.051)	34 (5)	2	33 000	9 730	31	42	0.087 (0.116)
↓	69 (10)	2	37 200	15 060	24	55	0.17 (0.23)
	138 (20)	3	29 900	17 170	17	71	0.37 (0.50)
	207 (30)	3	31 000	21 900	14	77	0.63 (0.84)
	276 (40)	3	31 700	26 300	12	80	0.94 (1.26)
	110 (16)	3	36 000	18 000	12	76	1.69 (2.27)

Pump = Centrifugal Designed for Maximum Efficiency
Motor = Variable Speed, Brushless dc

5.3.5 Selected boost pump and drive system. - The selection of the final boost pump configuration is dependent on the engine pump and fuel control characteristics and is described in Section 5.6.

5.3.6 Boost pump mounting and changing tool. - An important part of this program has been to find a method by which the fuel pumps may be replaced quickly and safely, without requiring that the liquid-hydrogen fuel tank be drained. In this section, a configuration devised with this requirement in mind is described. Included are drawings and description of the physical configuration of the pump mounting, the method of changing the pump without draining the fuel tank, and a tool designed to accomplish the changing of the pump. Particular consideration has been given to ensuring the safety and reliability of the configuration and the method for changing the pumps.

Figure 63 shows the physical configuration of the pump mounting. Three pumps are placed on a single mounting unit. Since FAA regulations require that two pumps be operable for all takeoffs and landings, this choice allows continuation of missions where one pump has failed at some intermediate time. This capability is desirable, since all intermediate stops of a flight may not be equipped or convenient for changing a cryogenically cooled pump.

The pump and housing are shown in cross section in Figure 63. Each pump has its own inlet while the discharge is common for the three pumps. The pump cavity housing is roughly cylindrical with the inlet located at the bottom of the fuel tank, so that the fuel may be used entirely. Fuel enters at the pump inlet and passes through the inducer and three impellers and exits through a check valve into the fuel line leading to the engine. The check valve is provided to ensure that fuel will not be pumped in reverse direction through a pump(s) that is not operating.

The pump is contained within the housing by means of locking lugs. To change a pump the insulated panel covering all three pumps is removed and the pump changing tool shown in Figure 64 is secured to the pump housing external locking lugs. An "O" ring is provided to seal the tool to the pump lower housing surface. The helium lines are then attached to the pump changing tool, the GHe inlet valve and air escape valves opened and the changing tool (and new pump) purged of air. When this is completed, the GHe line is connected to the pump purge port located in the pump lower housing plate. The tool is then rotated 0.785 rad (45 deg) to disengage the lugs and the pump pulled down so that the pump inlet closure sleeve blocks the pump inlet thereby preventing the escape of the LH_2 in the tank. At this point the pump GHe purge valve is opened admitting GHe to the top of the pump, forcing the LH_2 trapped in the pump back into the tank via the small check valve and discharge passage in the pump housing. When this is complete, the operating handle is turned another 0.785 rad (45 deg) to disengage the closure sleeve locking lugs and the pump is completely withdrawn and placed on the carrier plate in the changing tool. The new pump is then moved into position by means of the carrier plate operating rod and the procedure reversed to replace the pump (no further purging is required however). The purging lines are then removed, the changing tool removed and the cover plate replaced. The fluid discharge and

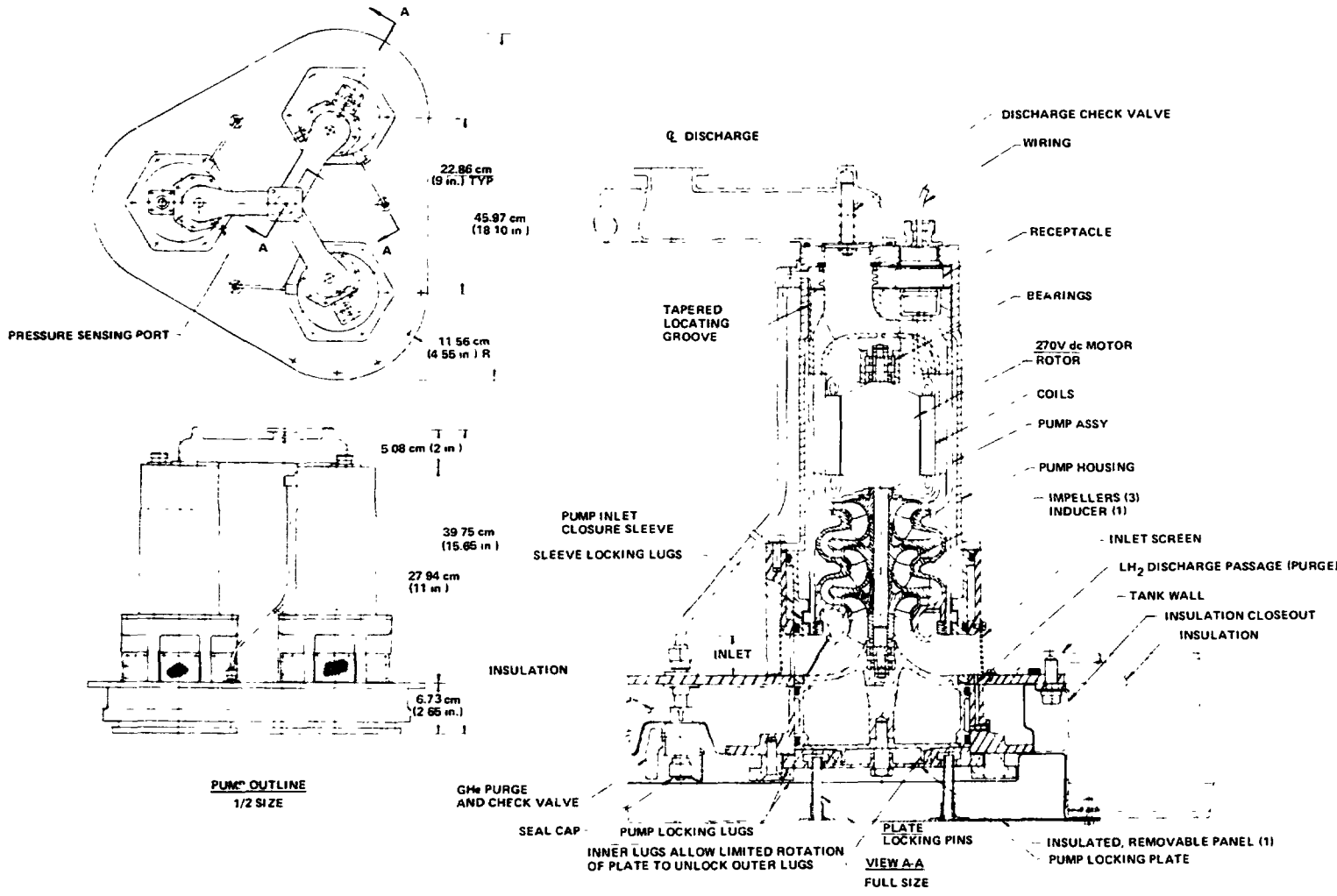

Figure 63. - Boost pump assembly and installation.

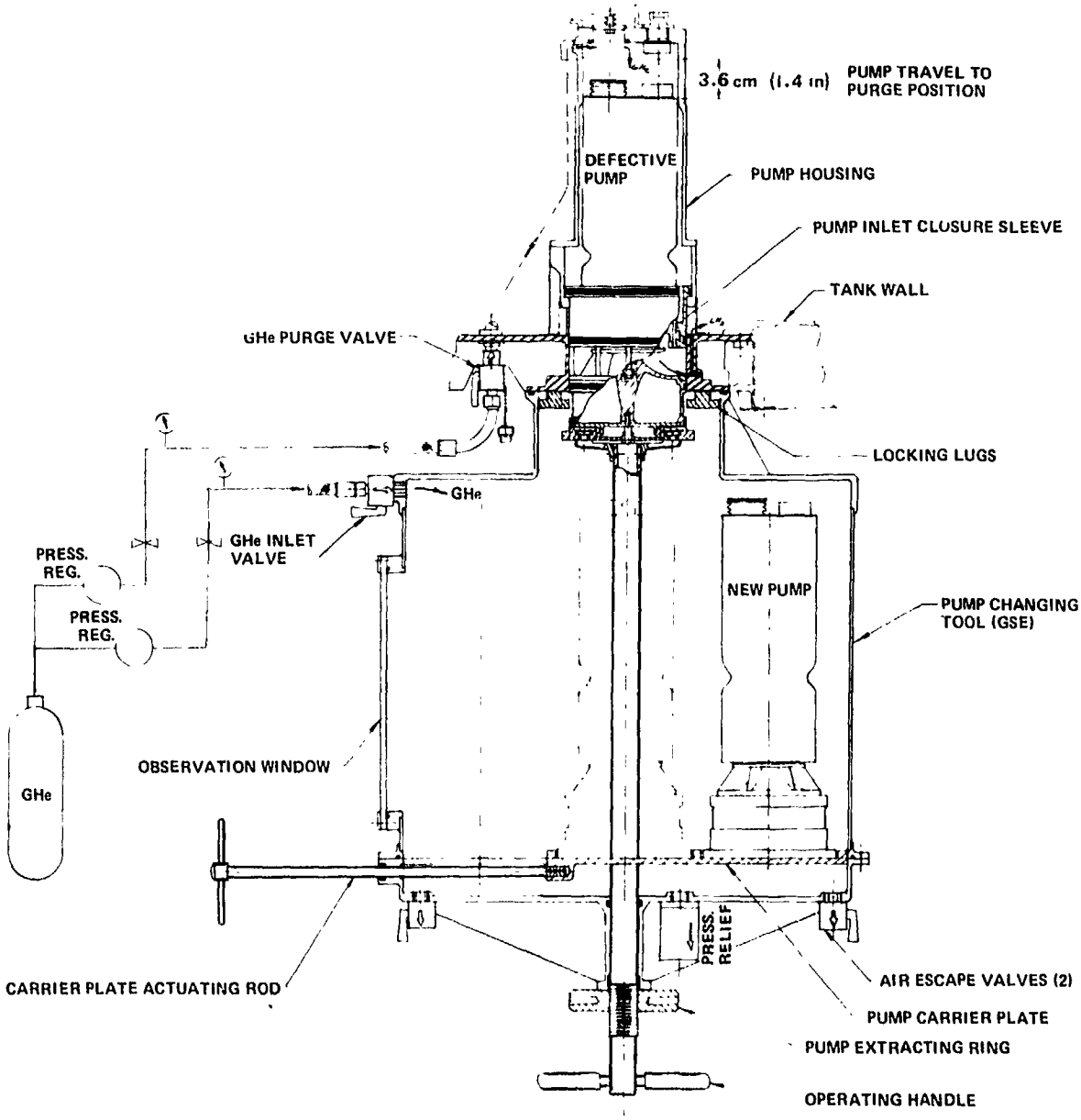

Figure 64. - Boost pump replacement concept.

electrical connections are made simultaneously during the final travel of the pump into its locked position. Since the new pump is warm and quickly cools to liquid-hydrogen temperature, the bellows-mounted seal is provided to absorb the thermal expansion of the pump during its temperature change. Such seals have proven effective on previous Rocketdyne pumps producing considerably higher pressure than the approximately 414 kPa (60 psi) maximum required here.

This approach to an easily replaceable pump unit has several advantages. Because both the pump cavity and the pump-changing tool are purged, there is no chance foreign matter such as particulates or vapor that might condense or freeze at liquid-hydrogen temperatures can find its way into the pump cavity, even if the pump changing operation is delayed with the pump cavity exposed. Second, the proposed approach ensures the safety of the mechanic who performs the operation. Should there be any failure during the pump-changing operation, the tool prevents the escape of hydrogen that might injure the mechanic or result in a hazardous condition. Third, the mechanism of the pump-changing tool, together with appropriate guides built into the pump cavity ensures that the replacement pump will be inserted into precisely the correct position to seal with the bellows-mounted seal. Finally because the replacement pump is protected inside the pump-changing tool, there is little chance of its being damaged prior to insertion. All handling of the pump itself may be accomplished within a controlled workshop environment rather than on the field.

It is estimated that a pump may be changed in 10-15 minutes by means of the approach described here, by one or two mechanics. Because the tool may be constructed of aluminum alloy, it should weigh on the order of 9.1 kg (20 lbs). Thus, the replacement pump and tool unit should weigh approximately 13.6 kg (30 lbs) and may be carried by a single person. However, a second person may be required to attach the tool to the lower side of the fuel tank, particularly if the access is in an awkward position. The tool will become cold as the pump-replacement operation is conducted through its contact with the cold pump and the tank. Thus, the mechanic must take the precaution of wearing gloves during the operation, but no other special protection is required.

5.4 Engine Fuel Pump

The engine fuel pump requirements are to provide a high pressure rise and to comply with the severe demands of air transport service while operating in the liquid hydrogen environment represented by a low net positive suction head (NPSH), cryogenic temperature, and low viscosity. This section discusses the implications of these requirements for the engine pump, presents the more significant design trade-offs, provides the results of a selected design approach, and recommends certain items for advanced technology development.

5.4.1 Design requirements. - The pump requirements start with the engine fuel flow and delivery pressure requirements which were developed in the engine study reported in Section 4.0. Table 25 presents a summary of the more significant operating conditions for the baseline engine, and tabulates the required fuel flow and fuel delivery pressure for each of these conditions. The engine LH_2 fuel pump is required to meet this set of requirements for engine fuel flow and delivery, with stable nonpulsating flow.

In order to avoid severely penalizing the engine fuel supply system which delivers LH_2 to the engine fuel pump, it is necessary that the engine pump not require an excessively high fuel inlet pressure. Based upon preliminary studies of the engine fuel supply system, it was agreed to consider the condition of a saturated liquid at 345 kPa (50 psia) as a definition of the state of the LH_2 at the engine high pressure pump inlet for design purposes. All subsequent pump investigation was based upon this assumed pump inlet condition for steady state operation. Other pump design requirements were the following:

- During starts, it was assumed that the engine pump may encounter significant vapor associated with heat soak into the aircraft fuel line, and that either this vapor would have to be vented, or some scheme would have to be established for passing it through the pump.
- Pump rotational speed was not constrained, except as it may be by the selected drive system.
- The pump should be designed to minimize aircraft DOC, associated with pump weight and required input power.
- The minimum time between overhaul (TBO) upon entry into air transport service was established at 1000 hours.
- Design for flight reliability and flight safety was an overriding requirement.
- Requirements for vapor venting, and pump thermal preconditioning, or other unusual operational constraints associated with the use of LH_2 fuel were to be eliminated or minimized.

5.4.2 Candidate pump types and selection of preferred concept. - Pump types which were considered to be potentially feasible for the proposed application were

- Centrifugal pumps, single or multistage
- Positive displacement piston pumps
- Positive displacement vane pumps.

TABLE 25. - SUMMARY OF BASELINE ENGINE OPERATING CONDITIONS

Operating Condition	Altitude, km (ft)	Mach No.	Thrust, daN (lb)	HP Spool Rotational Speed, rpm	HP Spool Rotational Speed, %	Fuel Flow, kg/sec (lb/sec)	Compressor Discharge Pressure, kPa (psia)	Sum of Heat Exchanger Pressure Drops, kPa (psid)	Injector and Metering Pressure Drop, kPa (psid)	Required Fuel Pressure, kPa (psia)
1. Ground Start	(0)	(0)	(0)	3 373	20.0	0.011 (0.024)	151.0 (21.9)	0.69 (0.1)	68.9 (10.0)	220.6 (32.0)
2. Ground Idle	(0)	(0)	(0)	10 456	62.0	0.044 (0.096)	579.2 (84.0)	5.5 (0.8)	68.9 (10.0)	653.6 (94.8)
3. Take-off	(0)	(0)	13 658 (30 706)	17 297	102.6	0.396 (0.874)	3 468.1 (503.0)	479.2 (69.5)	962.5 (139.6)	4 909.8 (712.1)
4. Take-off	(0)	0.40	9 116 (20 493)	17 316	102.7	0.411 (0.906)	3 606.0 (523.0)	513.7 (74.5)	1 034.2 (150.0)	5 155.2 (747.7)
5. Max. Climb	(0)	0.40	8 566 (19 258)	17 119	101.5	0.386 (0.851)	3 445.3 (499.7)	450.9 (65.4)	912.2 (132.3)	4 808.4 (697.4)
6. Start Cruise	10.67 (35 000)	0.85	2 910 (6 542)	16 886	100.1	0.166 (0.366)	1 516.2 (219.9)	74.5 (10.8)	168.9 (24.5)	1 759.5 (255.2)
7. Flight Idle	12.19 (40 000)	0.85	375 (842)	13 087	77.6	0.039 (0.086)	402.0 (58.3)	4.1 (0.6)	68.9 (10.0)	475.0 (68.9)

References 5 and 6 describe the preliminary development of a five cylinder piston pump for LH_2 service. This work demonstrated the feasibility of piston type pumps, but also highlighted the problems of leakage and life, and the necessity to operate at very low speed which resulted in a physically large pump for a given flow rate. Reference 7 reports similar work with a LH_2 piston type pump which was tested by the General Electric Co. In addition, Reference 7 reports that tests of a cryogenic vane pump were unsuccessful.

Because of these reported limitations of positive displacement pumps in the existing state of the art, and because centrifugal type pumps for LH_2 service have been relatively successful, the decision was made to concentrate the remainder of this limited investigation exclusively on the use of centrifugal type pumps. Further serious consideration of positive displacement LH_2 pumps for air transport service must be preceded by successful detailed investigation aimed at resolving the presently known design deficiencies of this type of equipment.

Both single and multistage centrifugal pumps were considered. The single stage pump represented the simplest design, whereas the use of multistages had the advantage of greater efficiency since it permitted the pump to operate at a more favorable specific speed.* In addition, the multistage pumps were smaller in diameter thus reducing the impeller thrust loads, and facilitating packaging. The following table shows the comparison of size and efficiency for various numbers of pump stages.

Number of Stages	Stage Ns	Impeller Dia cm (in.)	Estimated Efficiency %
1	257	13.4 (5.28)	50.5
2	432	9.5 (3.73)	60.2
3	585	7.7 (3.05)	66.0

Based upon this comparison, the 2 stage centrifugal design was selected as a reasonable compromise between design simplicity, pump efficiency, thrust load, and packaging feasibility. Subsequent work was based upon use of a two-stage design.

---

* Specific speed $Ns = \frac{N\,Q^{1/2}}{H^{3/4}}$ where N = rpm, Q = gallons per minute, H = head in feet

5.4.3 Candidate pump drive systems. - Four candidate pump drive systems were considered:

- Bleed air driven turbopump
- 270 Vdc electric motor driven pump
- Fixed ratio shaft driven pump
- Variable ratio shaft driven pump.

Figure 65a shows the bleed air driven turbopump system which was considered. The power source was high pressure bleed air extracted from the engine compressor. This was then ducted to a high speed air turbine and the flow to the turbine was modulated to an inlet valve. The air turbine was used to direct drive a centrifugal type LH_2 pump to provide LH_2 to the engine. One main advantage of this type of drive was the ease with which variations in pump speed could be obtained.

Another type of drive which was considered was based upon the recent development of high efficiency, 270 Vdc electric generators and motors having at once a capability for both high speed and variable speed. Control flexibility was a main advantage of this type of drive, if it should prove possible to design a system having a competitive weight. Figure 65b shows a schematic of a 270 Vdc pump drive system.

The simplest type drive which was considered was a fixed speed ratio shaft drive, using power extraction from the engine gearbox. This type drive is shown schematically in Figure 65c. The inability to vary the speed of the pump was seen as a possible major problem with this concept.

A variable speed mechanical drive can be used to obtain pump speed variation with a shaft driven system, and this scheme is shown in Figure 65d. Added mechanical complexity was seen as a possible major drawback for this approach.

The comparative evaluation of these drives is discussed in the next section.

5.4.4 Engine pump and drive candidate evaluation. - A trade-off analysis was conducted to select a preferred pump and drive system. In performing the analysis, engine operating conditions were first reviewed with particular reference to fuel delivery requirements as summarized on Table 25. Two conditions were selected as having particular significance in the pump drive trade-off analysis:

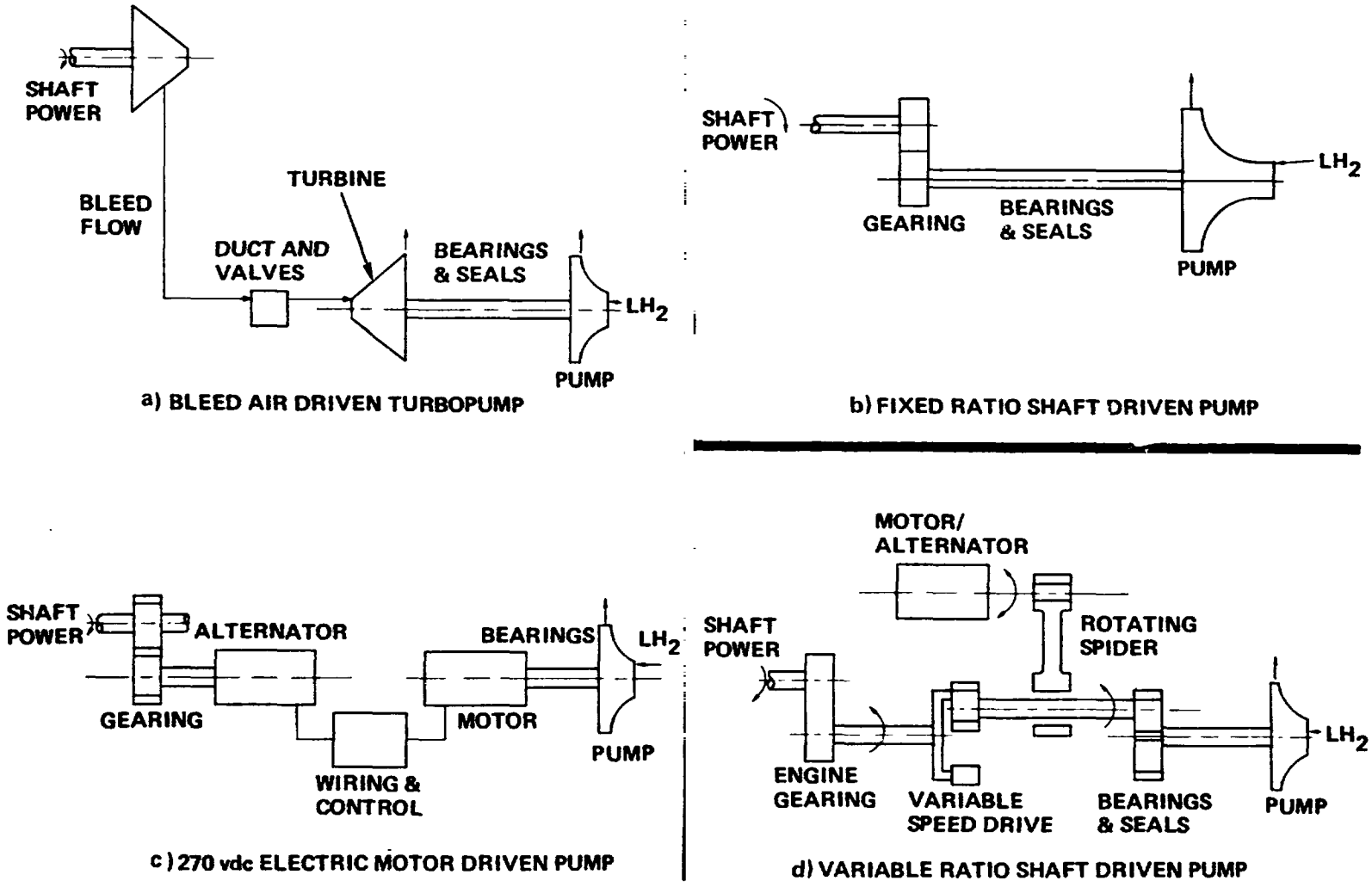

Figure 65. - Alternative engine pump drive concepts.

- Takeoff (Condition 4) was selected as one point for comparison, since it represented the maximum pump power requirement and hence would determine the drive weight.

- Start of cruise (Condition 6) was selected as another point for comparison, since it was typical of long term cruise operation, and would reflect the influence of pump drive overall efficiency on engine SFC.

The pump drives to be compared represent two basic types, variable speed ratio and fixed speed ratio. The first three candidate drive types, discussed in Section 5.4.3, had a variable speed ratio. The variable speed type has the advantage of permitting adjustment of the pump speed and resulting fuel delivery to more nearly match the engine requirements. This results in a reduction of required pump input power at off-design conditions, such as cruise. A fixed speed ratio pump drive does not permit such a speed adjustment and hence requires relatively greater power input during the off-design operation, when compared to the variable speed systems. Tables 26 and 27 show summaries of pump operating conditions for both the variable speed ratio drives and a fixed speed ratio drive.

These data were then used in developing weight estimates and power requirements for the various drive systems. The attached summary chart, Table 28, shows a comparison of the significant characteristics of the alternative pump drives. Drive system overall efficiency is presented for both takeoff and start of cruise conditions, and also the resulting required engine power extraction. System weights are shown. The change in DOC was calculated for the different systems, and is shown tabulated as a relative ranking. In addition, the various drives were ranked according to design simplicity, inherent reliability potential, and system cost.

In evaluating the results of trade-off analyses presented in this summary, it was decided that the delta DOC numbers developed for the start of cruise condition should be given relatively little weight since the absolute values were quite small. Primary significance was assigned to system design simplicity and inherent reliability potential, with system weight and cost considered next. On this basis, the fixed ratio shaft drive was selected as the preferred pump drive. The bleed air driven turbopump is considered to be the second most attractive alternative. The 270 Vdc system has the decided advantage of not requiring a shaft dynamic seal in the pump, but has the disadvantage of relatively high system weight. The variable speed ratio shaft drive has the disadvantage of mechanical complexity.

5.4.5 Pump bearing considerations. - The engine LH_2 fuel pump bearing system represents one of the key technical problems in the design of the overall system. The bearing system must be capable of operating at high rotational speeds (50 000 rpm); must be capable of carrying high loads, particularly high thrust loads under certain conditions; and must be compatible with the pumping of LH_2.

TABLE 26. - VARIABLE SPEED PUMP, SUMMARY OF OPERATING CONDITIONS

Operating Conditions (1)	Pump Speed Ratio, N/N_D	Fuel Flow kg/sec (lb/sec)	Fuel Flow l/min (gpm)	Required Fuel Pressure, kPa (psia)	Fuel Supply Pressure kPa (psia)	Required Pressure Rise kPa (psid)	Pump Pressure Rise kPa (psid)	Pump Flow Ratio,(3) W/W_D	Pump Efficiency %	Pump and Throttle Efficiency %	Pump Input Power kW (S hp)
1. Ground Start	0.295	0.011 (0.024)	10.7 (2.82)	220.6 (32.0)	482.6 (70.0)	-262.0 (-38.0)	182.7 (26.5)	0.136	37.0	---	0.09 (0.12)
2. Ground Idle	0.604	0.044 (0.096)	42.8 (11.3)	653.6 (94.8)	482.6 (70.0)	171.0 (24.8)	1 753.3 (254.3)	0.175	48.0	---	2.60 (3.49)
4. Take-off (2)	1.000	0.044 (0.906)	385.0 (101.7)	5 155.2 (747.7)	344.7 (50.0)	4 810.5 (697.7)	4 810.5 (697.7)	1.000	69.0	69.0	44.74 (60.0)
6. Start Cruise	0.975	0.166 (0.366)	155.6 (41.1)	1 759.5 (255.2)	344.7 (50.0)	1 414.8 (205.2)	4 569.8 (662.8)	0.415	58.0	18.0	20.43 (27.4)
7. Flight Idle	0.756	0.039 (0.086)	38.2 (10.1)	475.0 (68.9)	482.6 (70.0)	-7.6 (-1.1)	2 746.2 (398.3)	0.126	37.0	---	4.73 (6.34)

(1) See Table 25 "Summary of engine operating conditions" for further definition.

(2) Condition 4 was pump design point.

(3) Pump flow ratio includes speed correction for W_D

TABLE 27. - FIXED RATIO SHAFT-DRIVEN PUMP, SUMMARY OF OPERATING CONDITIONS

Operating Conditions (1)	Pump Speed Ratio, N/N_D	Fuel Flow kg/sec (lb/sec)	Fuel Flow ℓ/min (gpm)	Required Fuel Pressure, kPa (psia)	Fuel Supply Pressure kPa (psia)	Required Pressure Rise kPa (psid)	Pump Pressure Rise, kPa (psid)	Pump Flow Ratio,(3) w/w_D	Pump Efficiency %	Pump and Throttle Efficiency %	Pump Input Power kw (S.H.P.)
1. Ground Start	0.100	0.011 (0.024)	10.7 (2.82)	220.6 (32.0)	(290) (42)	-262.0 (-38.0)	48.3 (7.0)	0.265	55.2	---	0.015 (0.02)
2. Ground Idle	0.189	0.044 (0.096)	42.6 (11.3)	653.6 (94.8)	48..6 (70.0)	171.0 (24.8)	171.0 (24.8)	0.561	66.2	---	0.186 (0.25)
4. Take-off (2)	1.000	0.411 (0.906)	385.0 (101.7)	5 155.2 (747.7)	344.7 (50.0)	4 810.5 (697.7)	4 810.5 (697.7)	1.000	69.0	69.0	44.7 (60.0)
6. Start Cruise	0.542	0.166 (0.366)	155.6 (41.1)	1 759.5 (255.2)	344.7 (50.0)	1 414.8 (205.2)	1 414.8 (205.2)	0.745	67.2	67.2	5.46 (7.32)
7. Flight Idle	0.100	0.039 (0.086)	38.2 (10.1)	475.0 (68.9)	48..6 (70.0)	-7.6 (-1.1)	48.3 (7.0)	0.949	64.9	---	0.052 (0.07)

(1) See Table 25, "Summary of engine operating conditions" for further definition.

(2) Condition 4 was pump design point

(3) Pump flow ratio includes speed correction for k_p.

TABLE 28. - COMPARISON OF ALTERNATIVE DRIVES FOR ENGINE PUMP

	System Overall Efficiency (b)		Delta Engine Power kW (hp)		System Weight kg (lb)	Relative DOC Cruise	Relative Ranking (a)		
	Take-off	Start Cruise	Take-Off	Start Cruise			Simplicity	Reliability Potential	System Cost
Bleed Air Driven Turbopump	0.336	0.293	91.9 (123.2)	12.5 (16.8)	16.0 (35.3)	1.28	2	2	2
270 Vdc Electric Motor Driven Pump	0.429	0.418	72.0 (96.6)	8.8 (11.8)	18.7 (41.2)	1.10	3	2	3
Variable Ratio Shaft Driven Pump	0.502	0.488	61.5 (82.5)	7.5 (10.1)	18.3 (40.4)	1.00	4	3	3
Fixed Ratio Shaft Driven Pump	0.590	0.154	52.3 (70.2)	23.9 (32.0)	11.4 (25.2)	1.92	1	1	1

(a) Variation from 1 to 4, 1 being best.

(b) Includes engine to pump drive losses.

Rocket engine turbopumps have typically used rolling element bearings operating in LH_2. The LH_2 provides cooling but essentially no lubrication because of the very low viscosity; lubrication is provided by the use of teflon type separators, wherein the teflon transfers as a solid film lubricant to the rolling elements and races. These systems have demonstrated the required speed and load capability but have a demonstrated maximum life of about 10 hours, although extremely lightly loaded bearings have been run over 1000 hours. Therefore, if rolling element bearings operating in LH_2 are to be used in the engine LH_2 pump, it will be necessary to assure extremely light loading under all operating conditions.

Hydrostatic LH_2 bearings, and hybrid bearings consisting of a hydrostatic bearing used in combination with a rolling element bearing have been proposed and tested experimentally, but have not yet demonstrated the capability of meeting the engine fuel pump requirements.

Foil bearing systems have been tested by AiResearch with air and cryogenic helium, and appear to offer an attractive design alternative for LH_2 systems, although the loading would have to be controlled to a low value.

Industrial cryogenic turbomachines utilize oil lubricated bearings, both rolling element and plain journal bearing types, but require strict thermal control within the machine to prevent freezing the oil. However, the oil lubricated bearings have both high rotational speed capability, and substantial load carrying capacity.

Based upon these considerations, a preliminary selection of a bearing system was made for the proposed shaft driven pump described later. This system used an oil lubricated rolling element bearing at the shaft drive end of the pump. The bearing would receive oil from the engine gearbox and would operate at gearbox temperatures. Careful thermal design of the pump would be required to successfully use this design approach. The high load capacity of the oil lubricated bearing would be used to carry the pump thrust loads, which can be substantial under certain conditions of impeller seal wear and leakage. In addition, the oil lubricated bearing would carry the local radial loads at the shaft drive end of the unit. A foil type bearing (or rolling element alternative) was located between the two pump impellers and operated in the cryogenic hydrogen. With careful attention to dynamic and hydrodynamic balance, the loads on this bearing can be maintained at a suitable low value. It was considered that this hybrid approach offered the potential for meeting the engine LH_2 fuel pump bearing system design requirements, and it was recommended for advanced technology development.

5.4.6 Selected pump and drive system. -

5.4.6.1 General description: The selected engine high pressure pump is a two stage centrifugal design, and is shaft driven from the engine at a fixed speed ratio. The pump is designed to provide a flow of 387 ℓ/min (102 gpm) at a pressure rise of 4723 kPa (685 psid) with a design rotational speed of 50 000 rpm. At the design point, the required shaft power input is 50.5 kW (67.7 hp) and the required condition for the hydrogen at the pump inlet is 345 kPa (50 psia) minimum at 25°K (45°R) maximum. These limits correspond to saturated liquid (0 NPSH) at 345 kPa (50 psia). Table 29 provides a more detailed summary of the pump operating conditions and design characteristics.

Referring to the pump cross-sectional drawing shown in Figure 66, it may be seen that the pump rotating group consists of the two impellers and the shaft, fastened together with curvic couplings and an axial tie bolt. This construction is typical for modern, small, high speed turbomachines. The curvic couplings provide the required accuracy in alignment of the pump rotating parts and, in addition, can be made with convex-convex generated surfaces, thus reducing the surface contact area and increasing the resistance to conductive heat flow along the shaft. Minimizing the heat flow from the warm engine gearbox to the cryogenic end of the liquid hydrogen pump was an important design requirement.

A splined torsion drive shaft is used to connect the pump rotating group to the engine gearbox. The torsion shaft provides the torsional compliance necessary to isolate the gear tooth generated excitation from the inertia of the pump rotating group and, in addition, it provides additional resistance to conductive heat flow. As shown later in Figure 72, a fluid coupling is incorporated in the drive train in the engine gearbox. This is to permit the pump to be disengaged from a windmilling engine in the event of an in-flight shutdown.

The pump rotating group is carried in an oil lubricated ball bearing at the gearbox end, and in a foil type journal bearing running in hydrogen at the pump end. This bearing arrangement has a particular advantage in that the high load capacity oil lubricated bearing not only carries the radial load at the gearbox end of the pump, but also carries all of the axial thrust load, so that the foil bearing running in the cryogenic hydrogen at the impeller end of the pump is only required to carry the local radial load. With accurate dynamic balancing of the impellers, the magnitude of this local radial load can be kept relatively small. This provision for carrying the thrust load was an important consideration, since the possibility of encountering high thrust loads always exists for high pressure centrifugal pumps, for instance if a labyrinth type thrust balance seal were to develop an abnormally high leakage rate.

The ball bearing is a preloaded duplex pair carried in a ring type flexible mount. The flexible mount provides the necessary radial compliance to accommodate the greater than normal temperature range expected for this application and, in addition, provides some angular compliance for the shaft,

TABLE 29. - ENGINE MOUNTED, HIGH PRESSURE LH_2 PUMP CHARACTERISTICS

Conditions:		
Inlet Pressure	345 kPa	(50 psia) (Total Net)
Inlet Temperature	25.2°K	(45.4°R) (Saturated)
Discharge Pressure	5068 kPa	(735 psia)
Flow	386 ℓ	(102 gpm) (Liquid)
Design Data:		
No. of Stages		2
Total Head	7 509.7 m	(24 638.13 ft)
Speed		50 000 rpm
First Stage TSH (a)	70.6 m	(231.75 ft)
First Stage S_V (b)		10 000
Stage Specific Speed		431.5
Overall Efficiency		60.2%
Overall Power	50.5 kW	(67.7 hp)
Impeller Diameter	9.47 cm	(3.730 in.)
Impeller Reynolds No.		2.29×10^7
Impeller Eye Dia. First St.	2.50 cm	(0.985 in.)
Impeller Eye Dia. Second St.	2.22 cm	(0.875 in.)
Impeller Tip Width	0.14 cm	(0.055 in.)

(a) TSH = Thermal Suction Head

(b) S_V = Suction Specific Speed = $\dfrac{NQ^{1/2}}{(NPSH + TSH)^{3/4}}$

necessary to accommodate the radial compliance of the foil bearing at the pump end. The ball bearing pair is lubricated by a slight oil mist from the engine gearbox, and a drain-back port is provided to return any collected mist to the gearbox. Direct spray lubrication was not planned for this bearing and may be objectionable because of the possibility for very low operating temperatures. A dynamic shaft seal was provided to retain the oil mist in the gearbox, and an overboard drain was provided to accommodate any oil leakage from the seal.

Because the thrust bearing is some distance from the impellers in the selected bearing arrangement, there is some possibility for axial misalignment of the impeller and diffuser center lines. To accommodate this without a harmful degradation in pump performance, the impeller tip width was made somewhat larger than the diffuser entrance width.

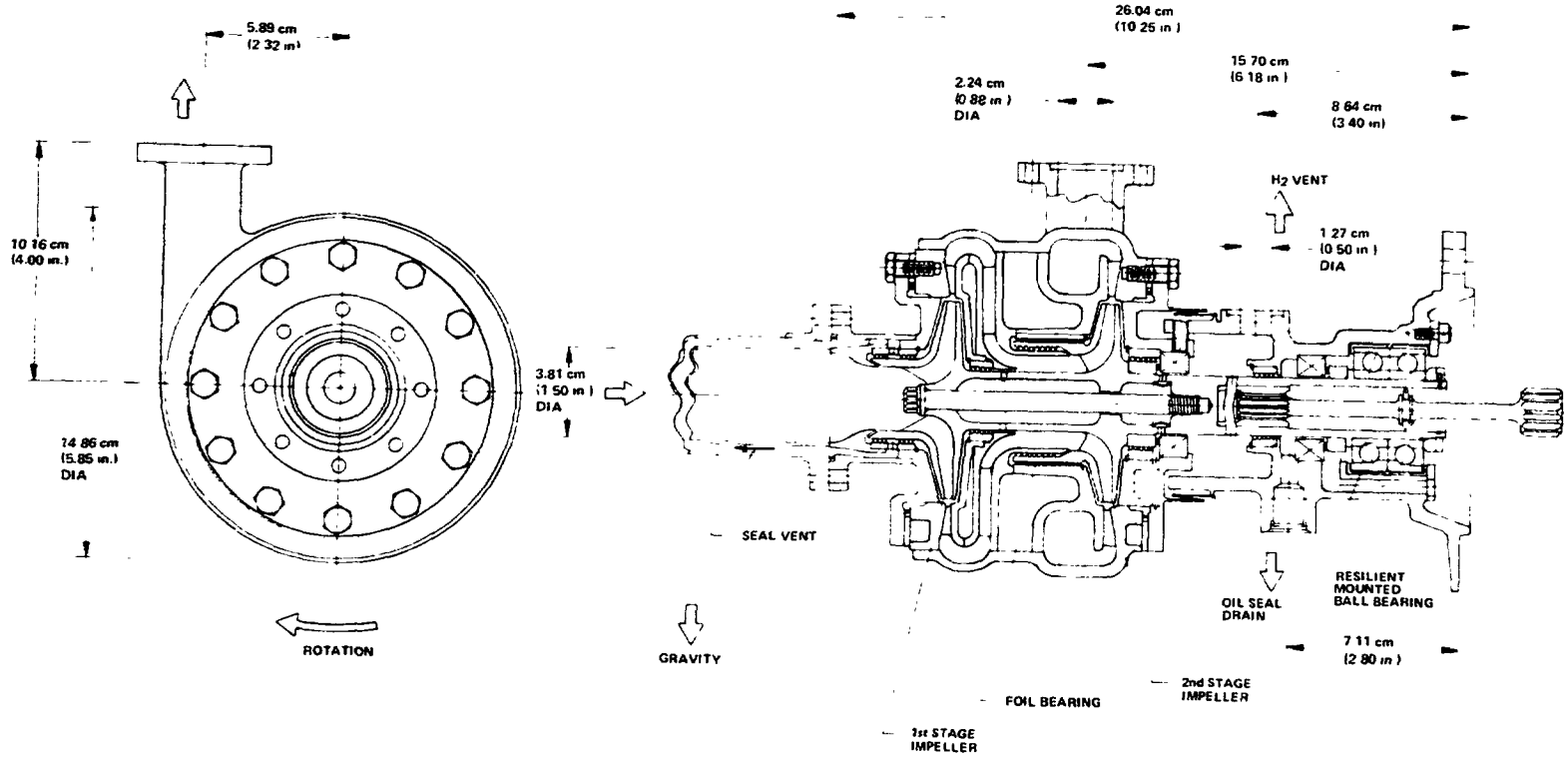

Figure 66. - Engine high pressure LH_2 pump.

The foil bearing located between the two pump impellers is an AiResearch proprietary design similar to the bearings used in a variety of other high speed turbomachines. The advantage of the foil bearing is that it offers the potential for a long service life in the cryogenic end of the pump where oil lubrication was not feasible. An alternative design approach was to use a rolling element bearing operating in the cryogenic hydrogen, in lieu of the foil bearing.

Labyrinth seals are used for controlling leakage and for obtaining thrust balance across the pump impellers. Referring to the cross-sectional drawing of Figure 66, it can be seen that the first stage impeller inlet labyrinth seal is vented to a location about six inches upstream of the pump inlet. This was done to minimize vapor flashing in the pump inlet, which would be detrimental to pump performance. The rear labyrinth seal for the second stage impeller is also vented, for the purpose of reducing the required design pressure of the hydrogen dynamic shaft seal. A hydrogen vent is provided in the housing to accommodate any leakage from the hydrogen dynamic shaft seal.

The pump inlet housing assembly is mounted to the bearing housing assembly by three radial pins. This arrangement facilitates radial contraction of the pump housing at cryogenic temperatures, and also reduces the conductive heat transfer. A thin gage convoluted seal is provided to preclude leakage. The pump assembly is mounted to the engine gearbox by a standard AND 20002 15.24 cm (6.00 in.) flange.

5.4.6.2 Materials: Materials selected for use in significant parts of the engine LH_2 pump were:

- Impellers - Inconel 718
- Diffuser housing - aluminum alloy
- Main housing - 300 series corrosion resistant steel
- Rolling element bearings - 400 C corrosion resistant steel
- Impeller shaft - Inconel 718
- Splined drive shaft - Nitralloy
- Oil seal assembly - carbon, 400 C corrosion resistant steel, and 300 series corrosion resistant steel.

5.4.6.3 Weight: The estimated total weight for the two stage shaft driven centrifugal pump was 5.9 kg (13.1 lb). This was obtained by detailed estimate of the weight of the individual components shown on the layout of Figure 66.

5.4.6.4 Performance: Performance maps showing pump head and efficiency as a function of pump flow and rotational speed are shown in Figure 67.

5.5 Fuel Control System

5.5.1 Design requirements. - The initial undertaking in the design of a fuel delivery and control system was to review the required functions, establish a list of inputs needed to perform those functions, and itemize the required output.

Functions of the engine fuel delivery and control system include:

- Provide the interface between the engine fuel supply system and the engine. The control system receives fuel from the engine fuel supply system within a limited range of thermodynamic states, and delivers this fuel to the engine in a condition which provides for efficient combustion, and at the proper flow rate for all engine operating conditions.

- Provide scheduling of compressor bleed valves used during starting, and compressor variable vane positions.

- Provide scheduling of other valves and/or ignition required during engine prestart conditioning, and starting, and shut-down.

Inputs to the engine fuel delivery and control system include:

Physical Inputs

- Fuel from the engine fuel supply system, provided in accordance with a flow schedule established by the engine fuel flow requirements, and in accordance with a minimum pressure schedule established by the engine high pressure pump suction performance limits.

- Electrical power from the aircraft system for use in the engine fuel delivery and control system electronic control, for use in operation of valves and actuators, and for possible use as a pump drive.

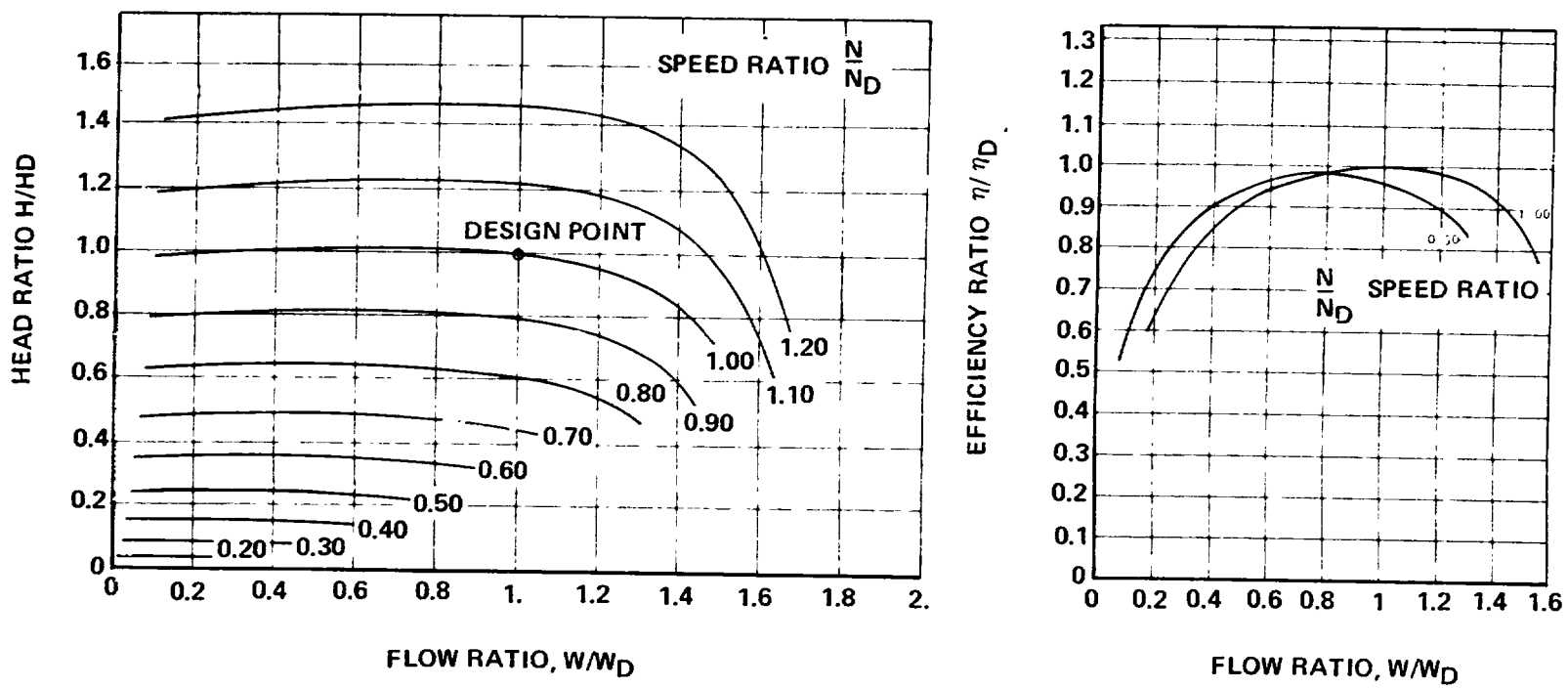

Figure 67 - Performance maps for two-stage centrifugal pump.

- Engine compressor bleed air for use in the engine compressor variable vane actuators, and for possible use as a fuel turbopump drive.

- Engine shaft power for possible use as a fuel pump drive.

- Heat for use in vaporizing and heating the hydrogen fuel, to be obtained from the aircraft environmental control heat load, from the engine turbine cooling air, and from the engine exhaust.

Informational Inputs

- Command signals, including

  Electrical system master switch
  Engine fuel system purge operation
  Engine start signal
  Engine power level setting
  Engine stop signal.

- Informational inputs from the engine, including

  Fan rotational speed
  Compressor rotational speed
  Compressor inlet total temperature
  Compressor inlet total pressure
  Compressor discharge total pressure
  Compressor variable guide vane and stator vane positions
  Low pressure turbine inlet total temperature, or exhaust gas total temperature.

- Informational inputs generated within the fuel delivery and control system, including

  Pump inlet housing temperature
  Pump discharge pressure
  Pump discharge temperature
  Pump rotational speed
  Fuel flowmeter rotational speed

Outputs from the engine fuel delivery and control system include:

Physical Outputs

- Fuel delivered to the engine combustor, in a condition which provides for efficient combustion, and at a proper flow rate for all engine starting, transient, and steady state operating conditions.

- Vent gas during cool down or purging operations.
- Pump shaft dynamic seal vent gas.

Informational Outputs

- Engine speed or thrust indication*
- Scheduling of compressor bleed valve
- Scheduling of compressor variable vane positions
- Signals for monitoring of fuel delivery and control system significant parameters, such as fuel pump rotational speed, control valve positions, etc.

5.5.2 Candidate concepts. - Candidate concepts for the fuel control system which were studied and evaluated were based on use of the following pump drive systems:

- Bleed air driven turbopump system
- 270 Vdc motor driven pump system
- Engine shaft driven pump system, fixed speed ratio
- Engine shaft driven pump system, variable speed ratio.

System schematics for these concepts are shown in Figures 68 through 71. In each of these systems, electronic control circuitry was used in conjunction with the fluid pumping and metering elements. This use of electronic circuitry is consistent with modern engine design technique and will probably be used exclusively on this class engine in the 1985 time period.

All of the schemes use a flow modulating and shut-off valve downstream of the heat exchangers to reduce the effect of heat exchanger capacitance in fuel system transient performance. A turbine type flowmeter is included for fuel flow measurement upstream of the flow modulating valve.

5.5.3 Selected system.

5.5.3.1 Description: Selection of the design of the fuel control system was dependent on the choice of drive for the engine fuel pump. With the selection of the fixed speed ratio engine shaft driven pump system as

* Other engine monitoring parameters are not considered part of the engine fuel delivery and control system.

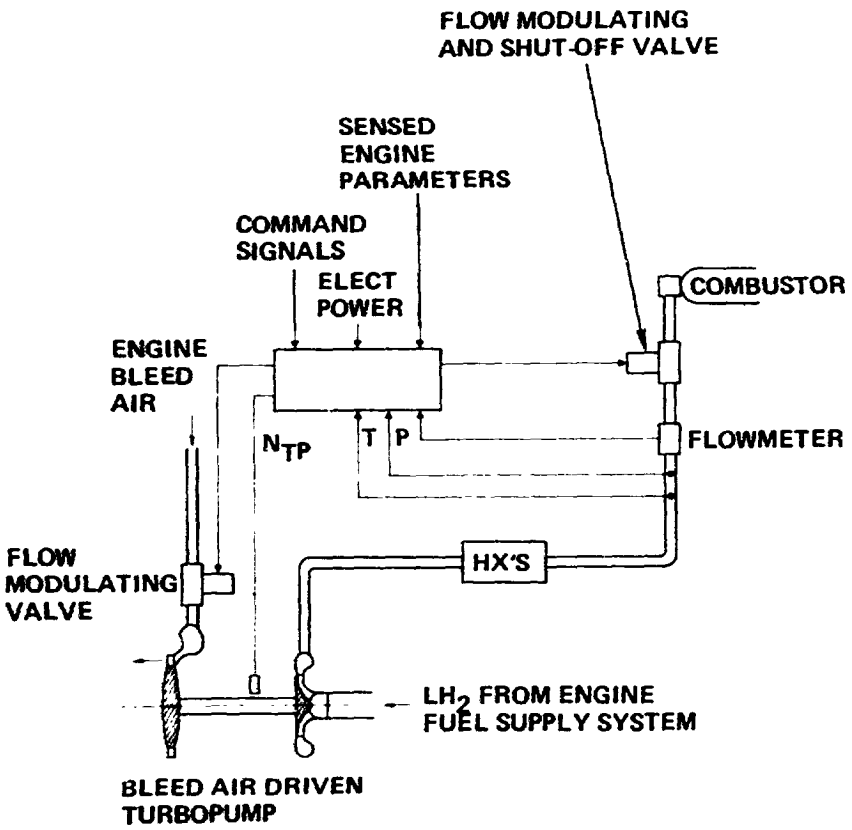

Figure 68. - Bleed-air driven turbopump system.

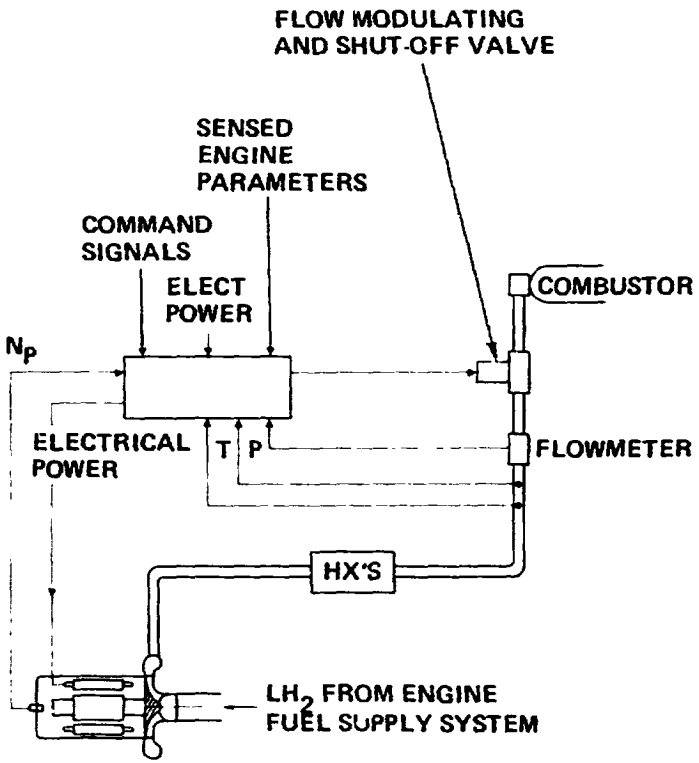

Figure 69. - 270 Vdc motor-driven pump system.

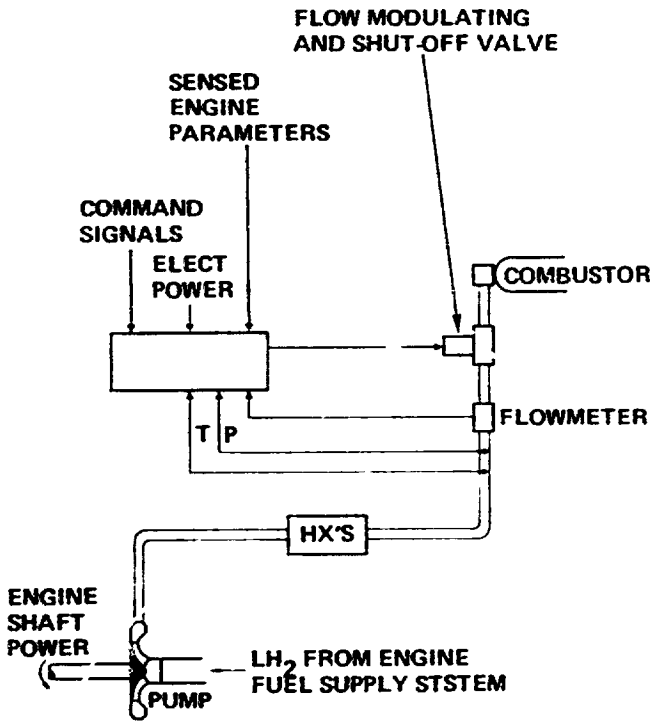

Figure 70. - Engine shaft-driven pump system, fixed speed ratio.

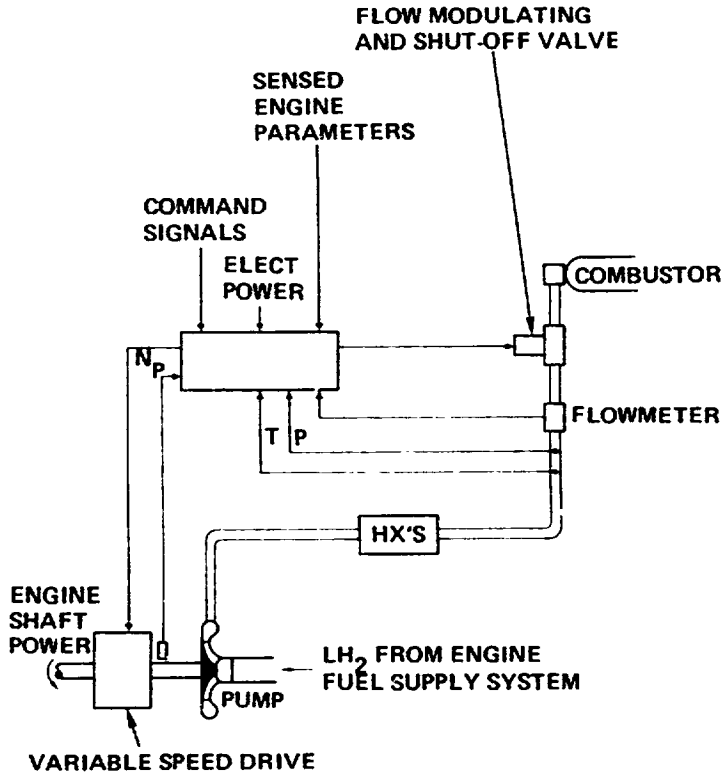

Figure 71. - Engine shaft-driven pump system, variable speed ratio.

discussed in Section 5.4.4, the control system represented in Figure 70 became the preferred concept. Figure 72 shows the actual design arrangement of the components in the overall aircraft system. A description of the operation of this system is discussed in the following section.

5.5.3.2 Control response considerations: With the design arrangement shown in Figure 70, the potential problems associated with the effects of the large heat exchanger volume capacitance and the H_2 fluid compressibility are minimized. It is expected that control response characteristics comparable to that of a conventionally fueled engine can be readily achieved. Note that particular attention will have to be paid to the design and development of the fuel flow modulating valve and the turbine type flowmeter.

5.6 Engine Fuel Supply System Final Design and Performance

The critical problem in the delivery of fuel from the tank to the engine is to ensure that the engine mounted pump is delivered a supply of liquid hydrogen at a pressure such that no significant amount of vapor is present (two-phase flow), although it is estimated that at low speeds the main pump could handle a vapor-to-volume fraction of approximately one half. This means that the heat added by the tank boost pump, motor, supply line, valves, etc., cannot exceed the fuel saturation enthalpy associated with the pressure at the engine pump inlet (zero net positive suction head). Since the heat added by the lines and system is proportional to the area of the line and inversely proportional to the flow rate, the lowest flow rate is the most critical. The heat added by the boost pump is proportional to the pressure rise but inversely proportional to the pump efficiency. A high pressure rise across the boost pump is desirable to suppress vaporization in the delivery system but the pump efficiency corresponding to the pressure rise must also be considered.

Another important consideration which influenced the system configuration and concept was the desirability of being able to use the hydrogen vapor in the delivery system during engine start. This would preclude the necessity for either having a long vapor return line back to the tank from the engine or providing a method to safely vent or dump the vapor. In addition, the residual vapor would then be useable in the engine. This could be accomplished by designing the engine fuel control system to handle vapor during the starting transient condition. The pressure required to insure fuel delivery to the engine and into the combustor could be supplied by the boost pump which is immersed in liquid. The increasing flow rate during acceleration from starting to ground idle would chill down the system so that liquid hydrogen would be available at the engine pump prior to reaching idle.

The above concept was pursued during the course of the study and was selected as the final approach described in the following sections.

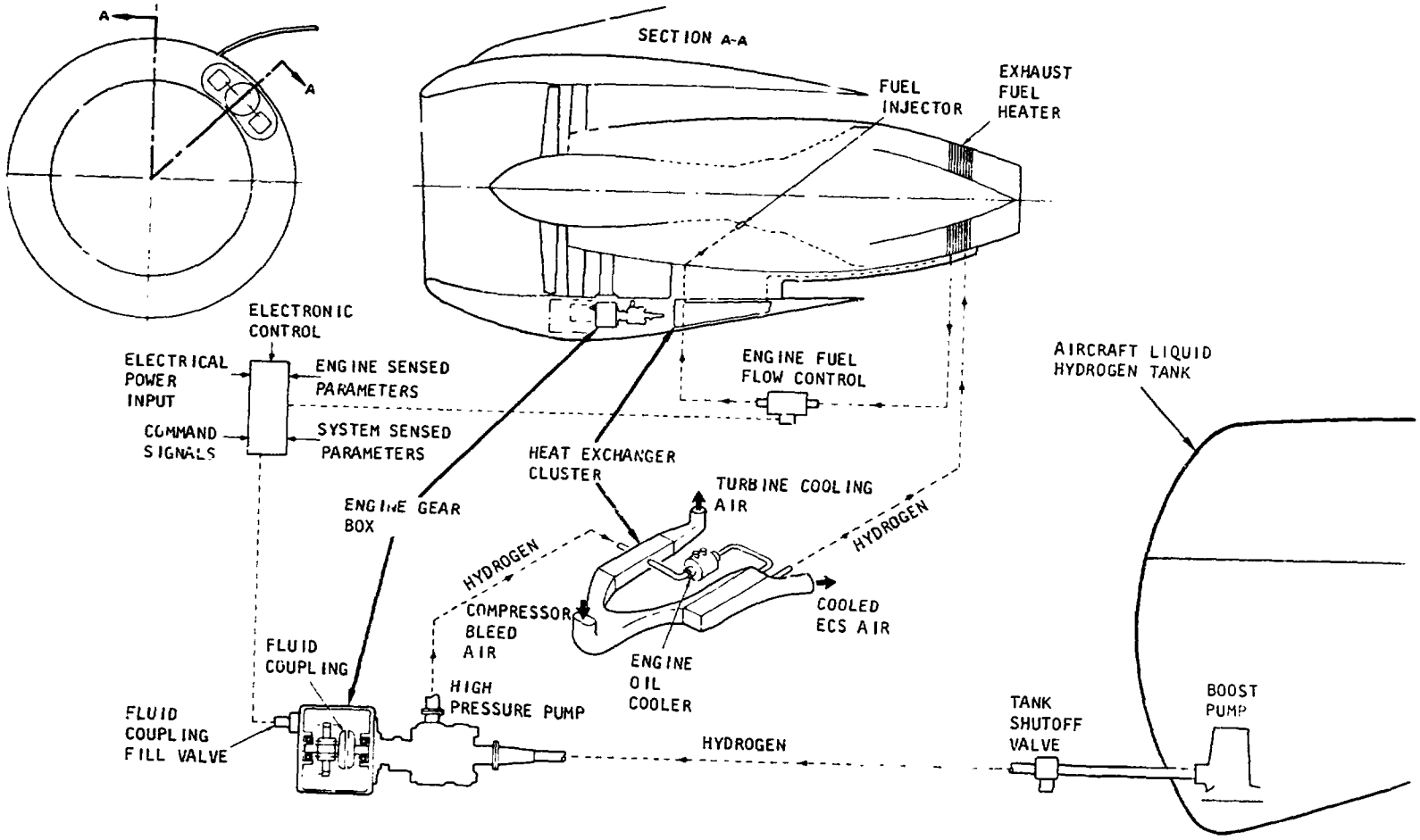

Figure 72. - LH_2 engine fuel delivery and control system.

5.6.1 Heat added to hydrogen. - During system operation, the liquid hydrogen temperature at the engine pump inlet will be higher than the tanked value due to heat inputs from the pump and (submerged) electric motor as well as heat input along the length of the fuel feed line. The primary concern is to ensure that the hydrogen vapor volumetric fraction never be greater than 0.5 at the engine pump inlet under all operating conditions. In actuality, it is desirable to ensure that some excess in engine delivered pressure compared to inlet saturation pressure is maintained. This excess pressure is usually referred to as net positive suction pressure (NPSP) and a minimum value of zero was specified for normal operations.

The hydrogen saturation pressure at the engine pump inlet can be obtained from the calculated fluid enthalpy at the inlet in conjunction with hydrogen property tables. The engine inlet pressure is simply the tank pressure plus the boost pump pressure rise minus the feed line pressure loss. Therefore, we have

$$NPSP = P_{ENG} - P_{SAT} = P_{TANK} + \Delta P_{PUMP} - \Delta P_{LINE} - P_{SAT} \tag{1}$$

The engine pump inlet enthalpy is equal to the hydrogen enthalpy at tanked conditions plus the enthalpy rise attributed to line, pump and motor heating, respectively:

$$h_{eng} = h_{TANK} + \Delta h_L + \Delta h_p + \Delta h_M \tag{2}$$

The enthalpy rise due to line heating Δh_L is determined simply from:

$$\Delta h_L = \frac{Q/L \cdot L}{\dot{w}_{H_2}} \tag{3}$$

The enthalpy rise due to pump heating is given by:

$$\Delta h_p = \Delta P \cdot \left[\frac{1}{\rho}\left(\frac{1}{\eta_p} - 1\right) + 0.0175\right] \tag{4}$$

which for liquid hydrogen with a density of 4.3 lb/ft^3 and using the proper conversion factors to obtain consistent units reduces to:

$$\Delta h_p = \Delta P \cdot \left[0.0412\left(\frac{1}{\eta_p} - 1\right) + 0.0175\right] \tag{5}$$

where ΔP is pump pressure rise (psi) and η_p is pump efficiency. The numerical factor 0.0175 accounts for compressibility effects on the hydrogen internal energy.

The fluid enthalpy rise due to the submerged electric motor inefficiency is given by:

$$\Delta h_M = \frac{550}{778} \frac{hp}{\dot{w}_{H_2}} \left(1 - \eta_M\right) \qquad (6)$$

where hp is motor horsepower and η_M is motor efficiency.

5.6.2 Final system selection. - The above relations, together with the line, joint, and valve heat leaks were used to determine conditions during the critical ground start of the engine. The boost pump selected to give maximum efficiency at low flows is a three stage, 270 volt dc driven centrifugal, variable-speed pump as shown in outline in Figure 73. This pump is the same as configuration 7 in Table 23.

The assumptions used in the analysis were:

- Starting flow rate is 0.011 kg/sec (0.024 lb/sec)
- The longest line run was used (tank #4 to engine #4)
- Compartment temperature = 54.4°C (130°F) at sea level
- One inch diameter stainless steel line
- Line is chilled down at engine start.

The objective was to compare foam versus vacuum insulation systems for the engine fuel supply line.

Since the in-service reliability of light weight vacuum jacketed line is unknown, but based on experience with static ground equipment is not expected to be very high, the foam jacketed concept was included in this analysis. The foam line consists of concentric tubes filled with 1.5 inches of closed cell foam with suitable bellows and connectors. Being a passive system, the consequences of a leak into the closed cell foam space will not, in the short term, increase the heat leak rate and it is expected to be more reliable and rugged overall.

The analysis was based on the boost pump and motor characteristics shown in Figure 74. Transient conditions during start are shown in Figure 75. Heat rejection to the fluid from the pump and motor as well as line, joint, and valve heat leaks, are included in the fuel temperature rise.

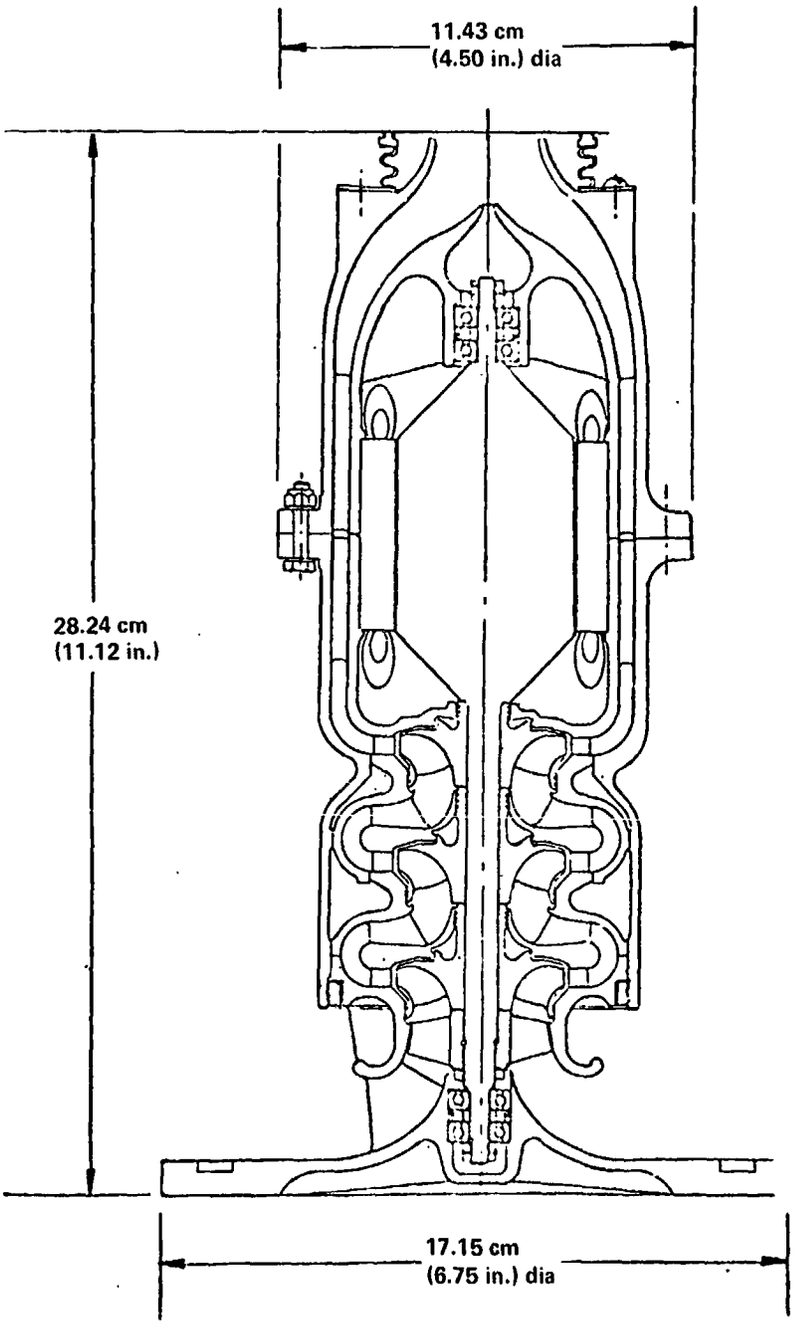

POWER	270 Vdc
PUMP WEIGHT	0.508 kg (1.12 lb)
rpm	36 000 max.
MAX. kW (hp)	2.36 (3.16)
SYSTEM WEIGHT	28.8 kg (63.5 lb)

3-STAGE, VARIABLE SPEED CENTRIFUGAL

Figure 73. - Selected LH_2 boost pump.

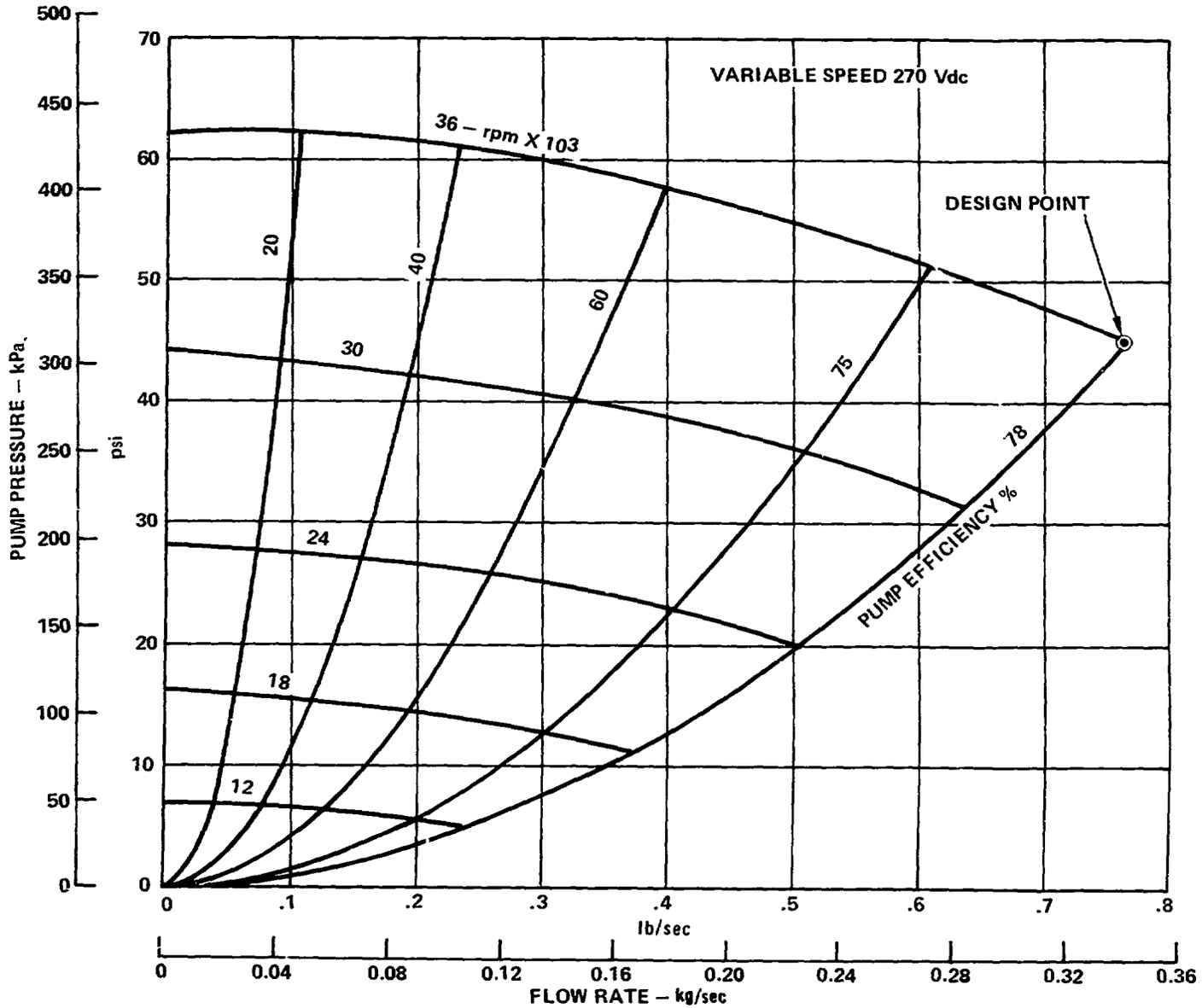

Figure 74. - Three-stage pump characteristics.

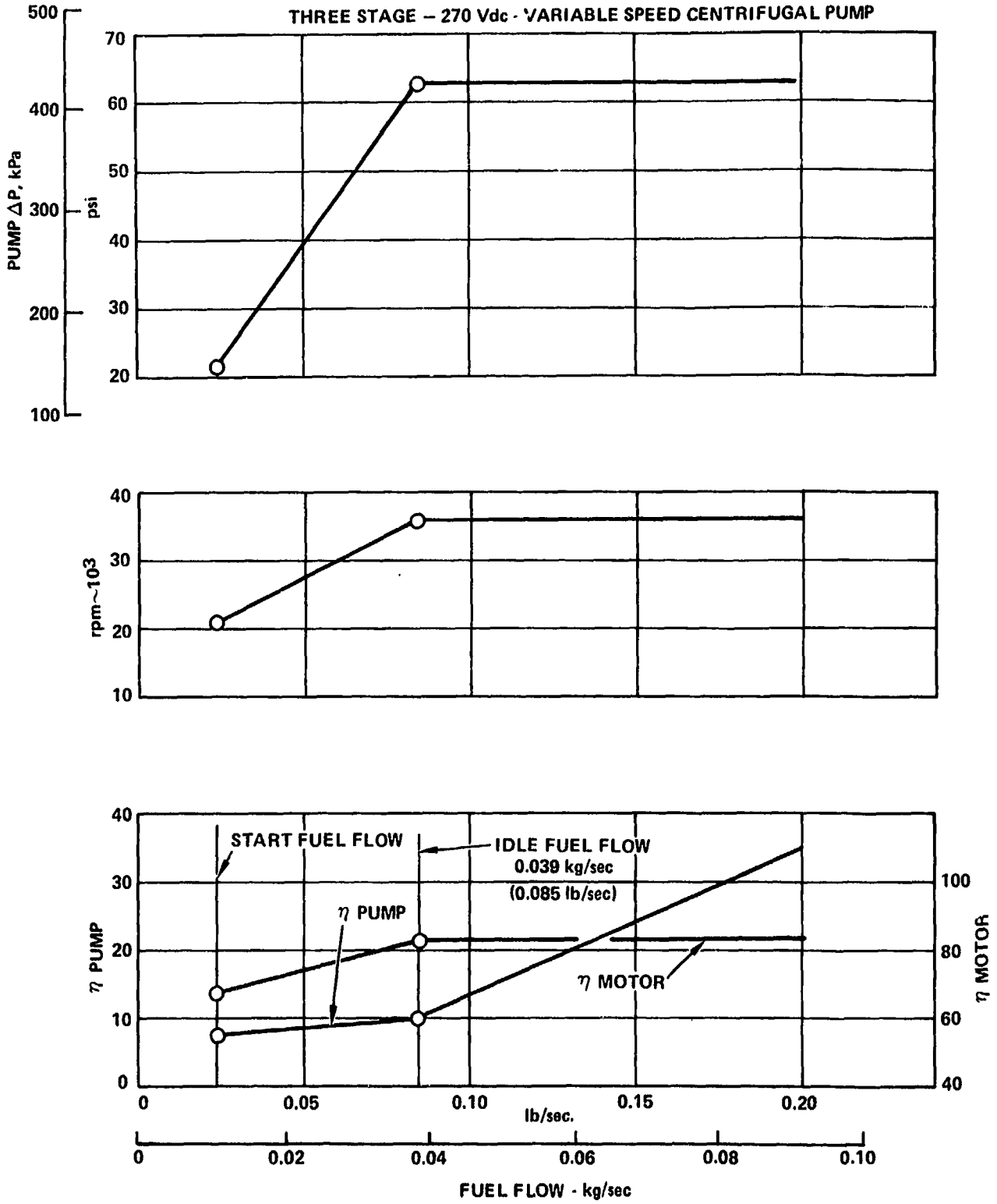

Figure 75. - Pump characteristics (transient).

Figure 76 shows the pump NPSP, V/L volume ratio, and percent of vapor at the pump inlet versus fuel flow. Also shown is the effect of GH_2 leakage into either 1 or 2 of the average 3 m (10 ft) long vacuum-jacketed line sections. Since it would not be reasonable to ground the airplane with a single vacuum leak, the assumption must be that a second leak could develop, either inflight or at a location where repairs were not possible. With this assumption, the performance of the foamed line is seen to be nearly identical to the vacuum line with a GH_2 leak in two 3m (10 ft) sections. Since the weight of the foamed line is only about 10-15 percent greater, it would appear that the foam concept is more attractive in safety, manufacturing, reliability, original cost and maintenance.

In the case of an unchilled vapor filled line, the engine acceleration to idle will take a longer time than with a chilled line since the engine will not accelerate until the engine pump receives liquid H_2 (V/L = 0). This time could be reduced by using the intertank transfer system to increase the boost pump flow rate.

5.6.3 Final system configuration. - The final system layout and details are shown in Figure 77. The lines are foam insulated and protected by an outer aluminum cover which would contain any H_2 leakage in the inner line. All components are purged and ventilated. An outer shroud (unpressurized) is provided where the fuel line runs through pressurized compartments. The motors and actuators of all shutoff and crossfeed valves can be removed without disturbing the line itself. Pump replacement can be done with LH_2 fuel in the tank. (See Section 5.3.6).

5.6.4 Engine operational procedures. - The procedures and requirements for operation of the engine, and its fuel delivery and control system, are as follows:

- Initial Condition

  Engine is stopped

  Electrical system is de-energized

  Engine fuel flow control valve is closed

  Tank shut-off valve is closed

  Boost pump is not running

  Entire fuel system down stream of the liquid hydrogen tank has reached a soak temperature of 311°K (560°R). The system is full of hydrogen gas at a temperature of 311°K (560°R), and the pressure has relieved to the 145 kPa (21 psia) tank pressure through a reverse flow check valve in the tank shut-off valve.

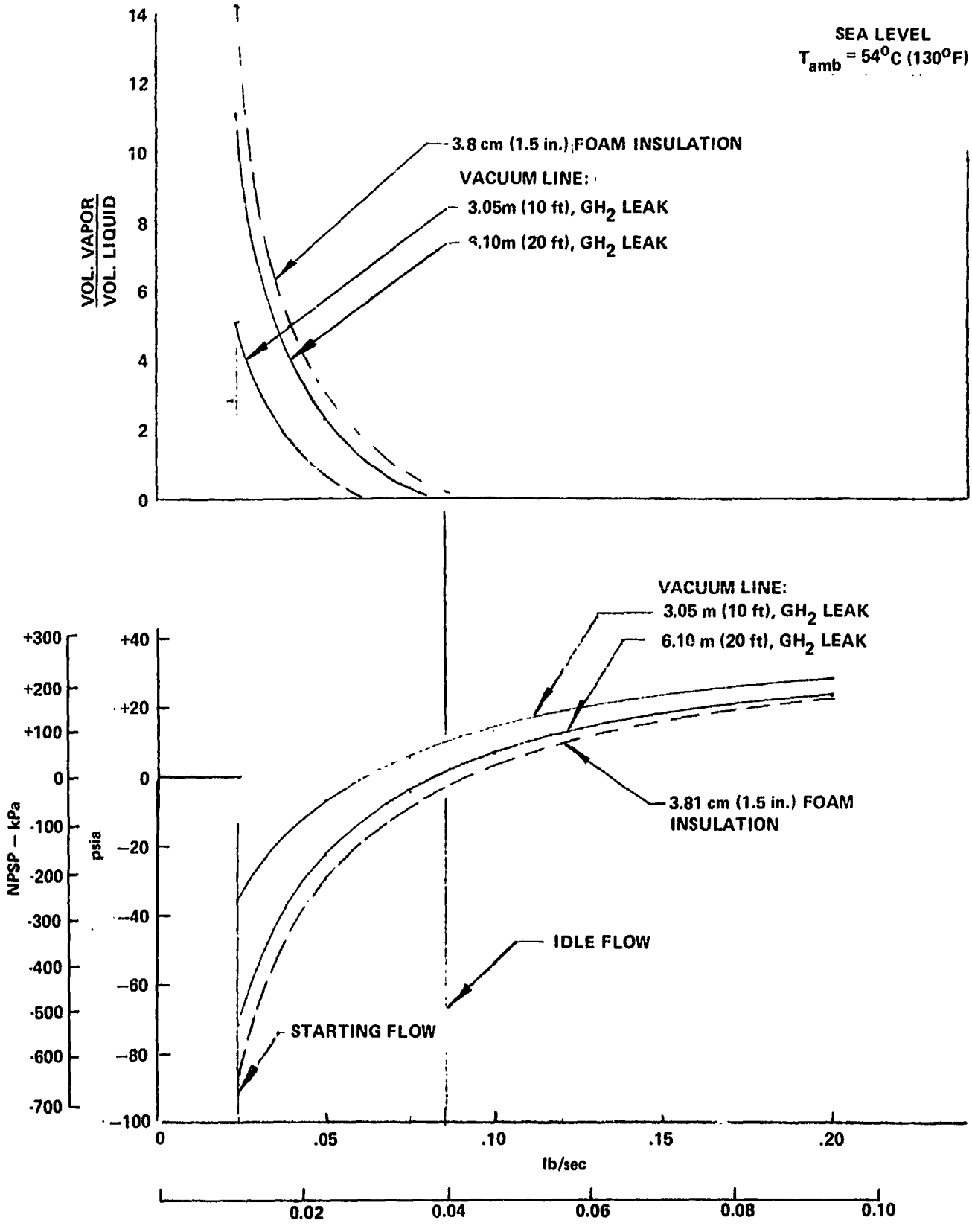

Figure 76. - Engine pump inlet conditions.

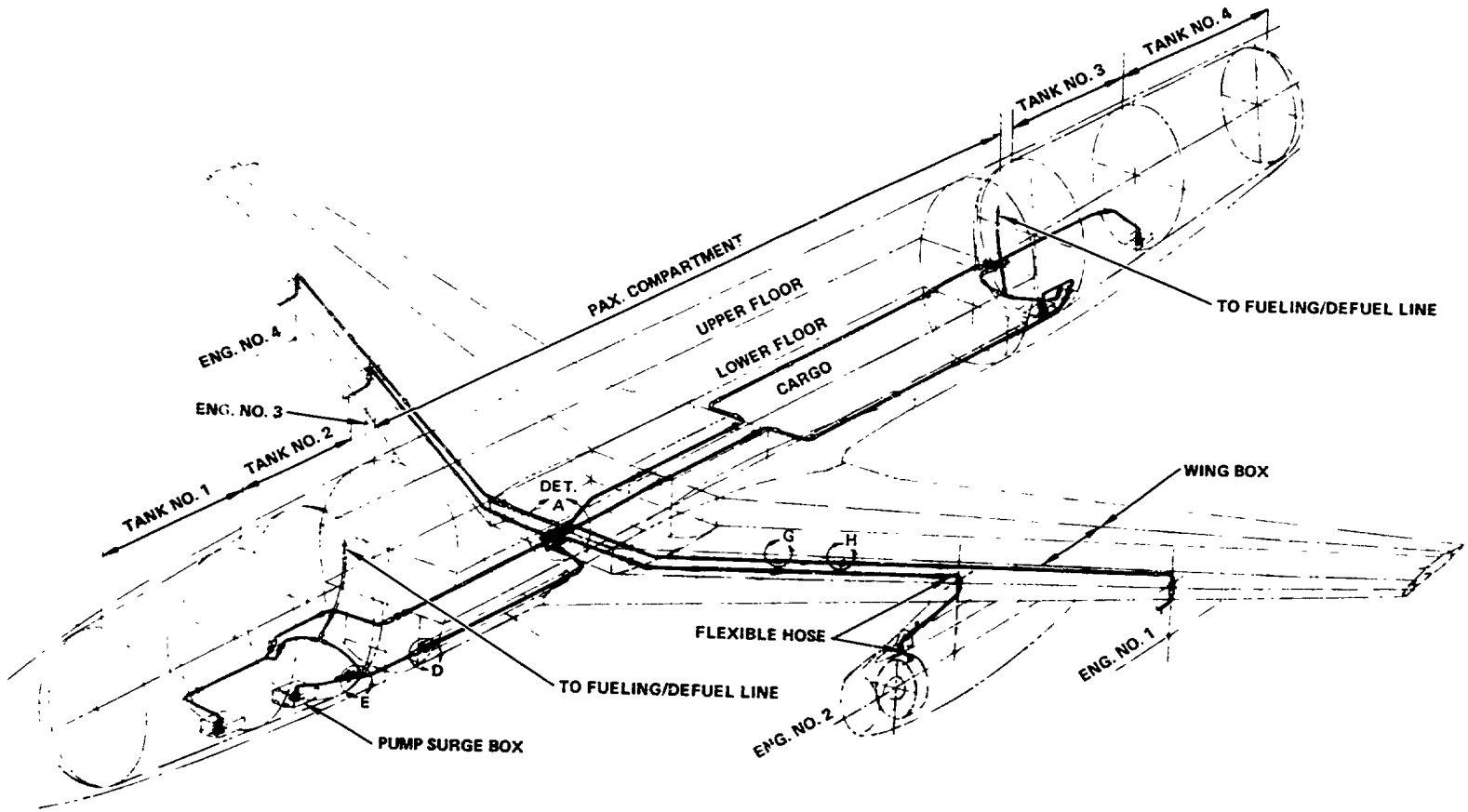

Figure 77. - Engine fuel supply system.

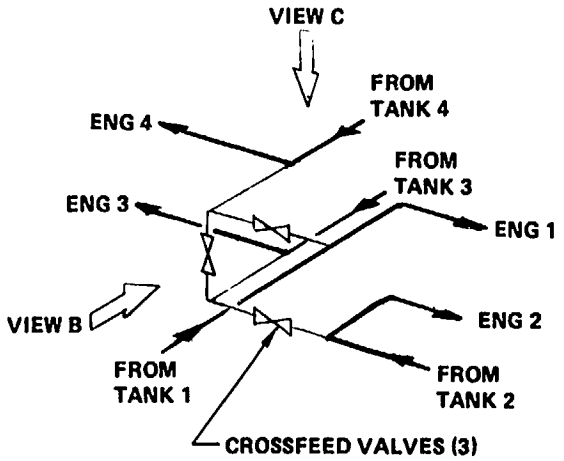

DET. A – CROSSFEED VALVE SCHEMATIC

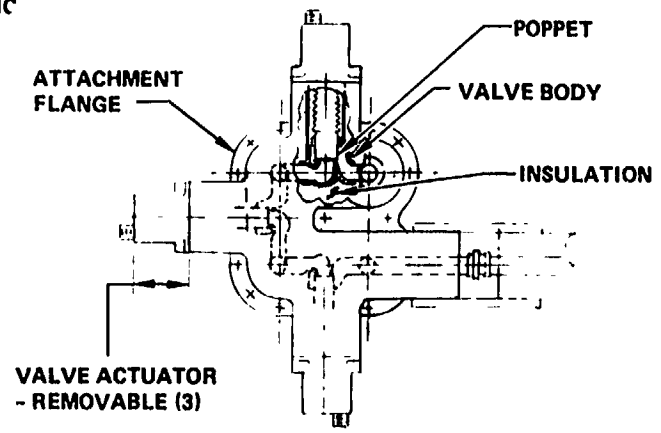

VIEW B
CROSSFEED VALVE ASSY - INSTALLATION

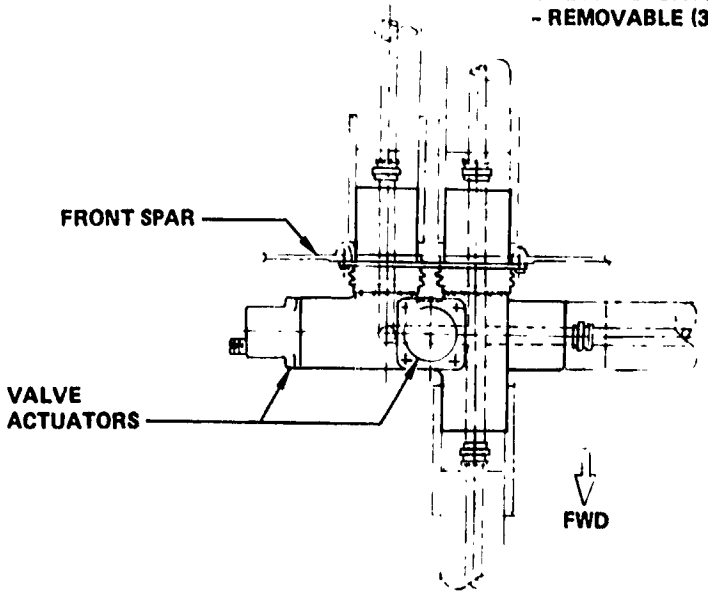

VIEW C
CROSSFEED VALVE ASSY.

Figure 77. - Continued.

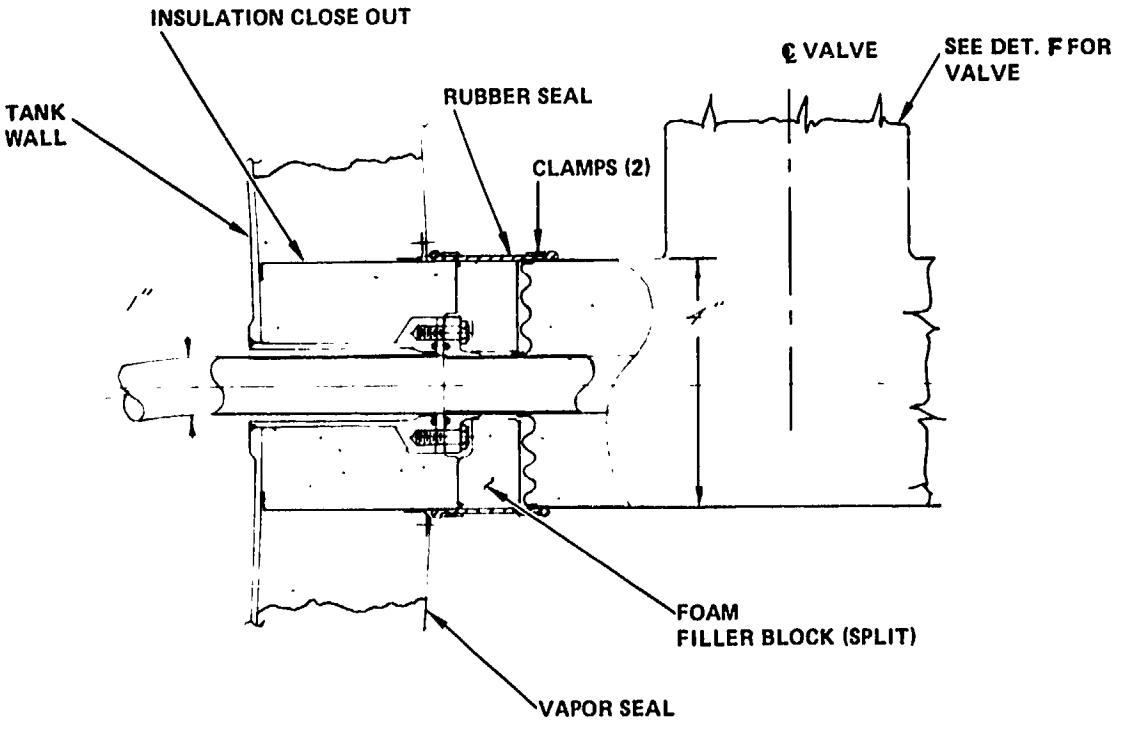

DET. E – TANK FTG AND VALVE INSTL.

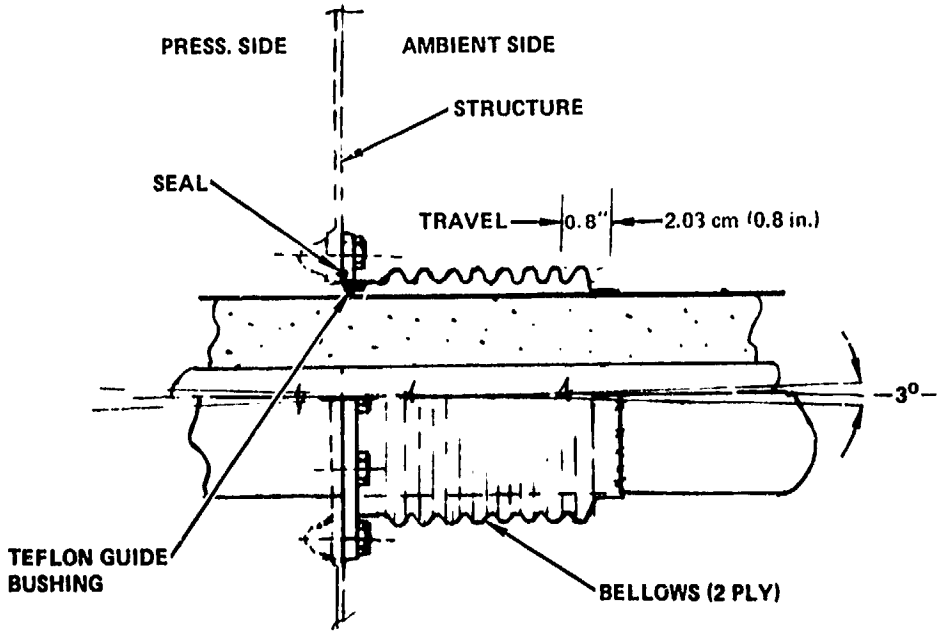

DET. D – BULKHEAD FTG. – FLEXIBLE

Figure 77. - Continued.

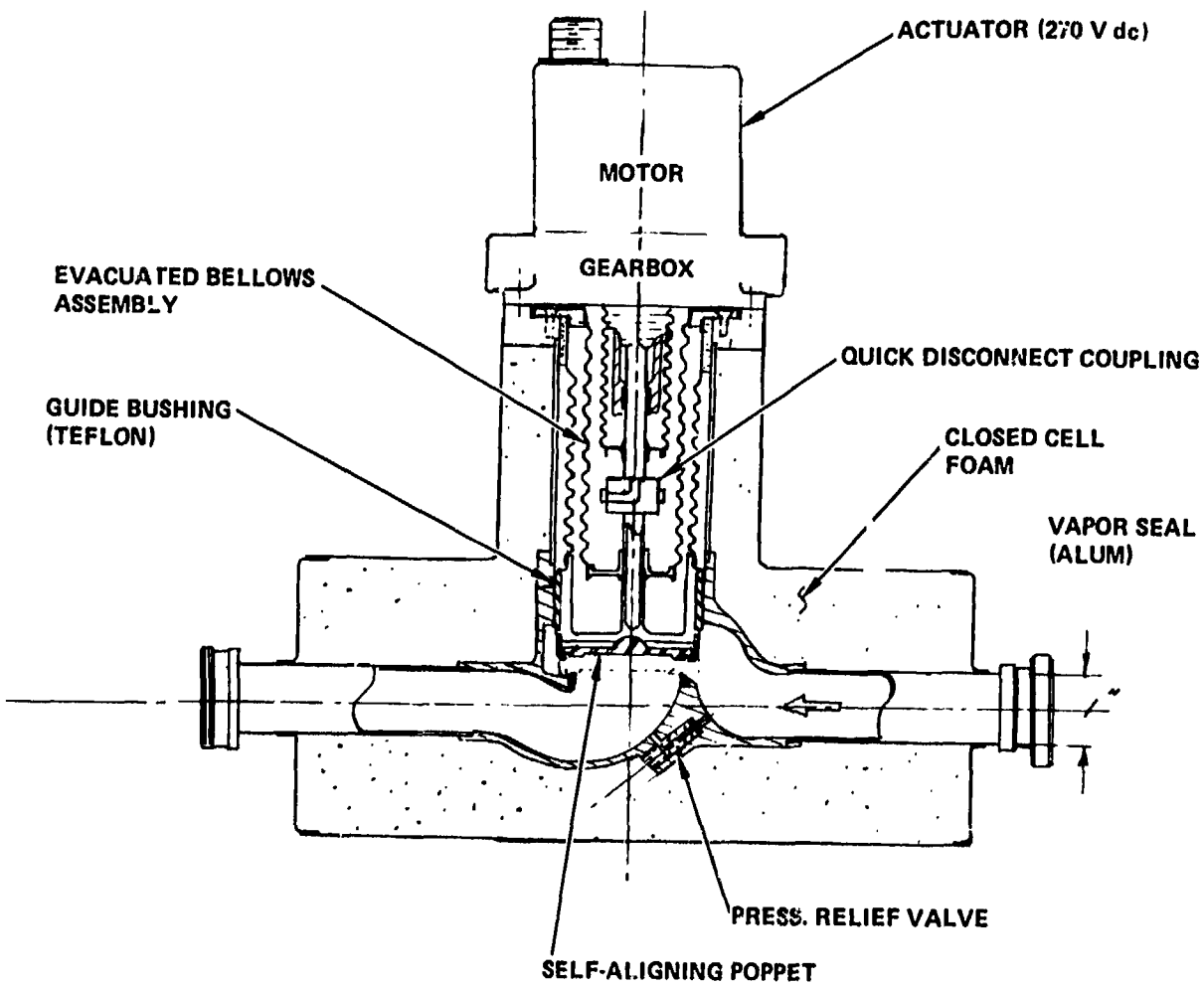

DET. F – TANK ISOLATION VALVE

Figure 7. - Continued.

- Start Procedure

  Energize engine electrical system. This automatically opens the high pressure pump drive fluid coupling fill valve. The valve latches open and will remain open until electrically energized to close.

  Open tank shut-off valve.

  Start boost pump. Since the boost pump inlet is immersed in liquid hydrogen, the boost pump will pressurize the hydrogen gas in the line up to the engine fuel flow control valve to approximately 290 kPa (42 psia).

  Start cranking engine. Engine oil pressure develops during cranking, and fills the high pressure pump fluid drive coupling thus driving the pump.

  At 10 percent speed, turn on ignition, move throttle to idle position and the engine fuel flow control valve starts the admission of fuel to the engine fuel injector.

  Engine cranking continues until the engine is self-sustaining, and then the cranking is terminated.

  Engine continues acceleration to idle speed.

  Continue operation at idle speed until chill-down of the engine high pressure pump is completed. The time required for chill-down is approximately one minute. After chill-down of the engine high pressure pump is completed, normal engine operations may be commenced.

- Ground and Flight Operation

  System responds to command inputs in a manner similar to that of a conventional Jet A-fueled turbofan engine.

- Shut Down

  Reduce engine speed to idle.

  Move throttle to idle cut-off.

  De-energize engine electrical system. This automatically energized the high-pressure pump drive fluid coupling fill valve to close. The valve latches close, and will remain closed after the electrical system is de-energized. With the valve closed, the fluid drive coupling drains, disconnecting the pump drive.

  Turn off boost pump.*

  Close tank shut-off valve.

*Because the engine pump interstage bearing operates in the hydrogen working fluid and is dependent upon it for cooling, and in the case of the foil bearing is dependent upon it for load carrying ability, it is desired to maintain boost pump pressure until after the engine pump fluid coupling has disconnected. This time delay in turning off the boost pump can be short, perhaps 10-15 seconds.

- Procedure After Aborted Ground Start

  Turn off ignition.

  Crank engine for a predetermined time to ventilate engine and remove any hydrogen vapor.

  Determine reason for aborted start and take corrective action if required.

  Start engine using normal start procedure.

- Procedure for In-Flight Shut Down

  Reduce engine speed to idle.

  Move throttle to idle cut-off.

  De-energize engine electrical system. This automatically energizes the high-pressure pump drive fluid coupling fill valve to close. With the valve closed, the fluid coupling drains permitting the fuel pump to stop, although the engine may be windmilling at moderately high speed.

  Turn off boost pump.

  Close tank shut-off valve.

- Procedure for In-Flight Start

  Open tank shut-off valve.

  Start boost pump.

  Energize engine electrical system. This automatically energizes the high-pressure pump drive fluid coupling fill valve to open. Since the engine is windmilling, oil pressure is available and the coupling fills thus driving the pump at windmilling speed.

  Initiate ignition.

  Move throttle to idle position.

  When engine is started and operating normally at flight idle, move throttle to the desired power setting.

5.7 Technology Development Required

The study of the engine fuel supply system identified and brought into focus various areas of risk in the technology where advances in the state of the art are either necessary or highly desirable to facilitate the timely and economic development of a full scale system. This section lists the more significant of these technical risk items, and presents recommendations regarding appropriate advanced development.

5.7.1 Engine fuel pump. - The engine high-pressure pump bearing system is a major technical risk item requiring advanced development. The current state of the art in advanced high pressure LH_2 pumps has evolved mainly from the development work which has been done on rocket engine turbopumps. As a result of this work, the problems of designing for pump performance (head, flow range, and suction performance), and also the problems of mechanical design and materials selection for cryogenic service, have been adequately resolved and may be considered state of the art.

However, all rocket engine components inherently have a very short mission duty cycle. This has resulted in very short specified life requirements, even for reusable equipment such as Space Shuttle, where the main engine design life requirement is 10 hours and 100 missions. On the other hand, air transport equipment such as that being considered in this study, is at the other end of the life requirements spectrum, with airliner utilization running to 10 hours a day operation, equipment overhaul periods of 5000 hours minimum being common, and equipment service life of 40 000 hours being typical.

This vast difference in life requirements poses a specific problem in that the rocket engine turbopump bearing technology is not transferable since the bearing systems developed for rocket engine turbopumps can only meet the very short life requirements and do not have the inherent potential for development of the long life capability required for air transport service. This limitation of life development potential is well demonstrated by the vast amount of work which has been necessary to achieve even the limited life required for rocket turbopump applications.

For these reasons, it is considered that the most critical problem in the development of a high-pressure LH_2 pump suitable for airline service is the pump bearing system, and it is recommended that the newer approaches described in this report be investigated.

It should be noted that these comments apply only to the bearings of the high-pressure LH_2 pump, which are relatively highly loaded and which operate at high rotational speed. The very lightly loaded bearings of a LH_2 fuel boost pump, which run at lower rotational speed, can probably be developed adequately for airline service as a further evolution of the existing design approach, using rolling element bearings and separators having a dry lubricant capability.

It is recommended that engine high-pressure pump bearing system advanced development be undertaken, and that such advanced development start with the preliminary design of an engine high pressure pump in sufficient depth to establish the bearing requirements. This would then be followed by design, fabrication, and feasibility testing of a bearing system having the objective of meeting these requirements. Initial bearing tests would be in a bearing test rig, followed by tests in an actual pump.

5.7.2 Engine fuel control system. - Operation of the cryogenic hydrogen fuel control system presents several new problems such as starting with the supply line full of vapor, the necessity for extremely rapid chill down of the engine high pressure pump, the probable necessity to control the flow of fuel in both the vapor and liquid states, and the presence of significant volume capacitance in the fuel system combined with the use of the relatively compressible H_2 fuel. These new problems suggest the desirability of analysis and computer simulation of the selected engine fuel delivery and control system, to verify performance capability including flow, pressure, and thermal transients. Following analysis and computer simulation, fabrication and test of a breadboard system would be highly desirable.

5.7.3 Overall system. - It is desirable to make a preliminary investigation of systems interactions involved in utilizing H_2 as a heat sink for cabin air conditioning, engine oil cooling, engine stator vane and rotor blade cooling, in combination with the engine exhaust fuel heating concept. This may be done by computer simulation, and particular attention should be paid to identifying critical off-design conditions.

6. FUEL SUBSYSTEMS

The aircraft fuel subsystems, illustrated schematically in Figure 78, consist of all fuel-oriented systems up to the interface at the engine fuel control system. These systems cover the functions of storing fuel, fueling/defueling, supplying fuel to the engine and auxiliary power unit (APU), transferring fuel, pressurizing/venting, jettisoning, and purging and/or inerting systems. These systems are discussed in the following paragraphs.

6.1 Fuel Tank Arrangement

Fuel is stored in thermally insulated tanks located within the fuselage. There are four separate tank compartments, corresponding to the number of engines, in accordance with the convention that each engine be fed from an independent source during takeoff and landing. They are numbered sequentially beginning at the forward end of the airplane. Tanks 1 and 2 are located between the flight station and the forward end of the passenger compartment. Tanks 3 and 4 are located aft of the passenger compartment. Each tank has a nominal usable fuel capacity of 6985 kg (15 400 lb) of LH_2. Tanks 1 and 2 in the forward storage area are separated by a bulkhead which isolates the liquid fuel in each of the tanks. However, a vent system which is common to both tanks maintains an equal ullage pressure on both sides of the bulkhead. Tanks 3 and 4 are separated by a similar bulkhead in the aft fuselage area.

6.2 Fueling and Defueling

A fueling system shown in Figure 79 is provided which interfaces with the airport ground supply through two adapters located at the aft end of the fuselage below the vertical tail. Liquid hydrogen is supplied to the fueling adapter (Appendix B, Figure B-2) and displaced hydrogen gas from the aircraft fuel tanks is returned to the airport liquefaction facility for recycling by means of the vapor recovery adapter (Figure 80). A 5-inch vacuum-insulated fueling manifold conveys fuel to Tanks 2, 3, and 4, reducing to a 3-inch manifold between Tanks 1 and 2. Fuel is discharged into each tank by means of a perforated fueling manifold located near the bottom of the tank below the normal reserve fuel level. The perforations are sized to maintain a low discharge velocity to minimize turbulence in the bulk liquid.

The fuel level control system consists of a shutoff valve (Figure 79) actuated by a signal from a level sensor which terminates flow to each tank when it is full. When a given flight requires less than full tanks, the shutoff valves are actuated by a signal initiated by bugs on the tank fuel quantity indicators, located in the aircraft flight station, which have previously been set at the desired fuel quantity. The fuel quantity can also be selected at the refueling panel in the tail (Figure 79).

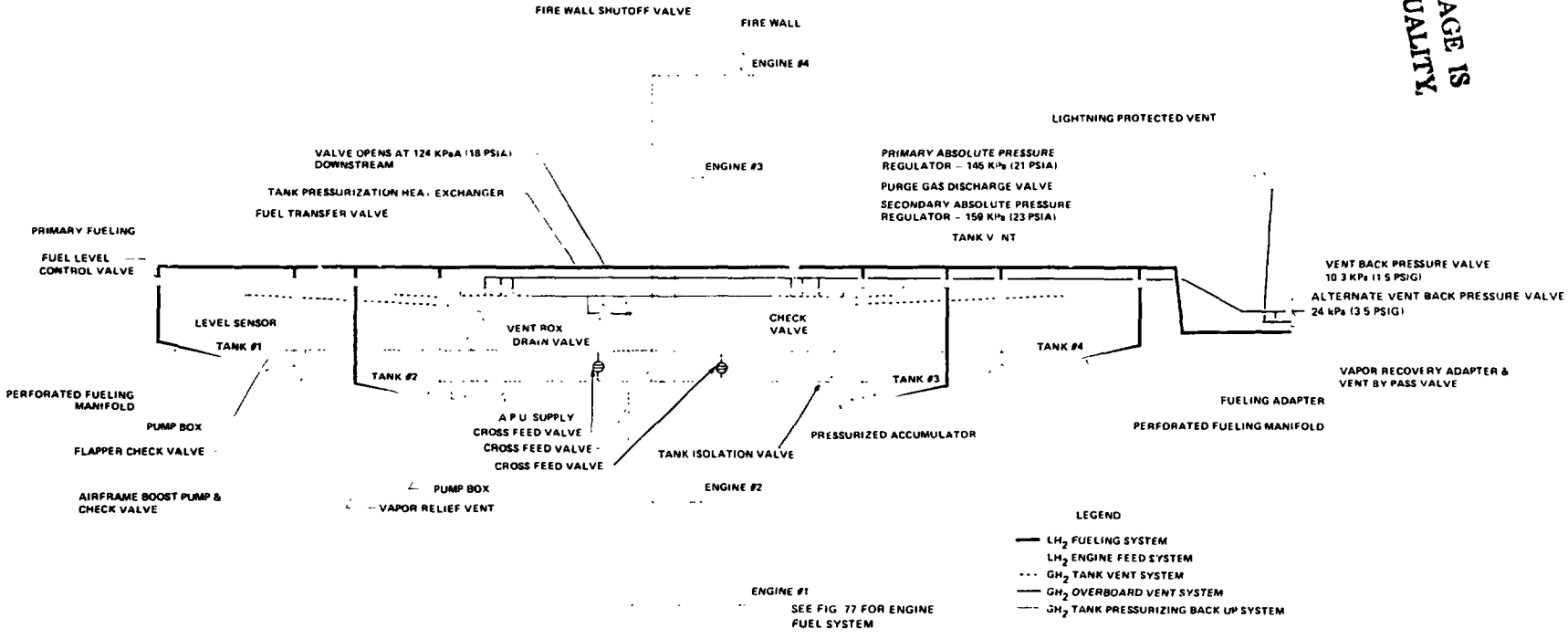

Figure 78. - Aircraft fuel system schematic.

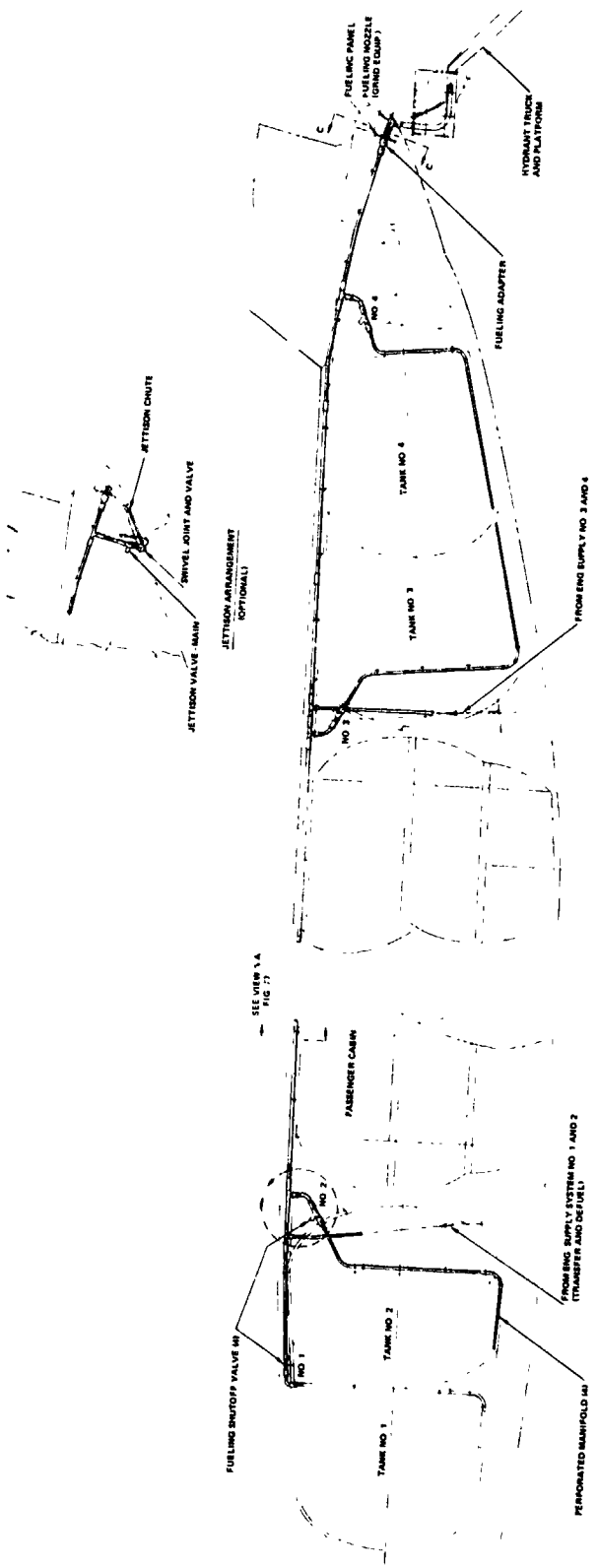

Figure 79. - Layout-fueling/defuel system.

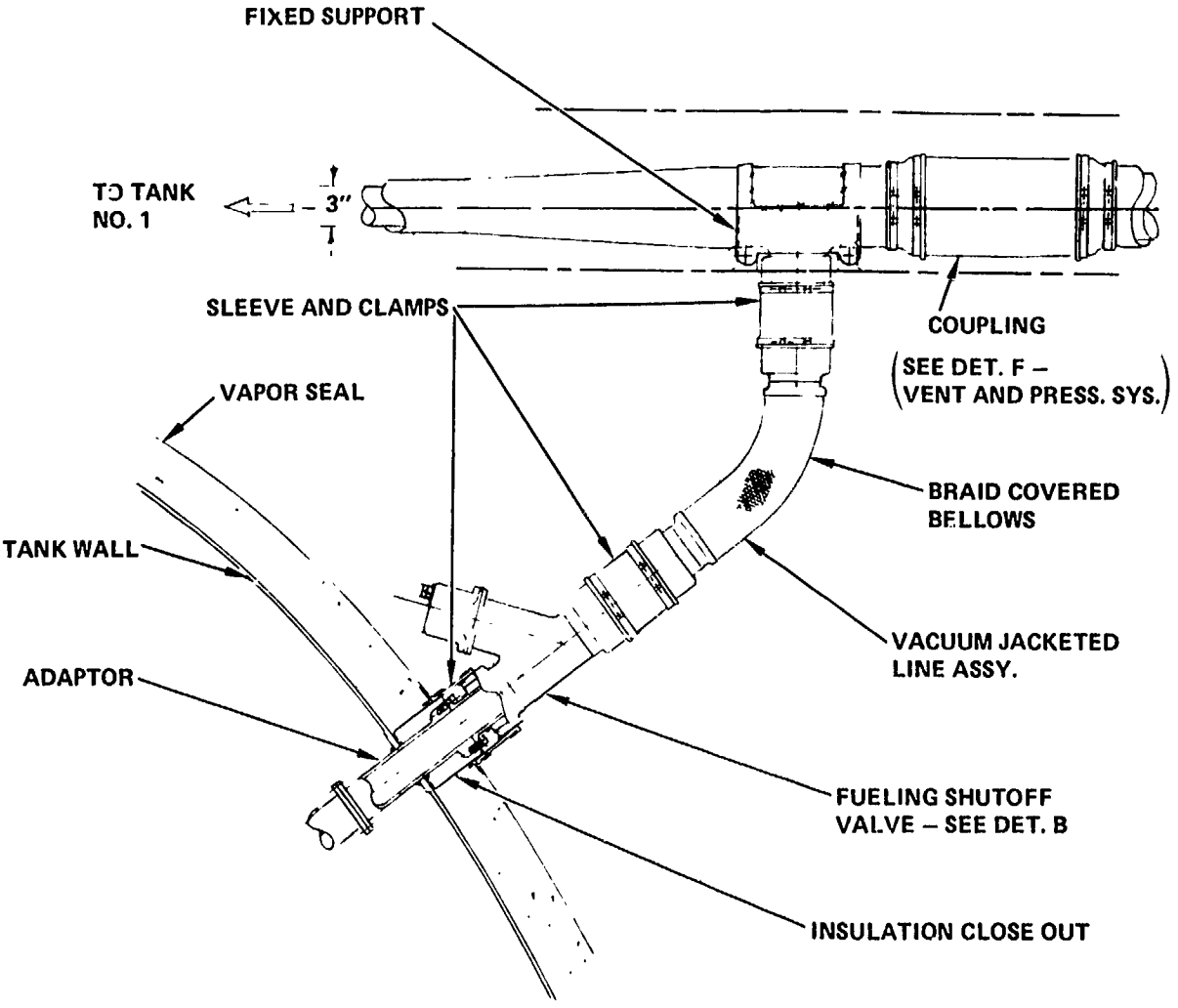

DET. A – FUELING VALVE INSTL.

Figure 79. - Continued.

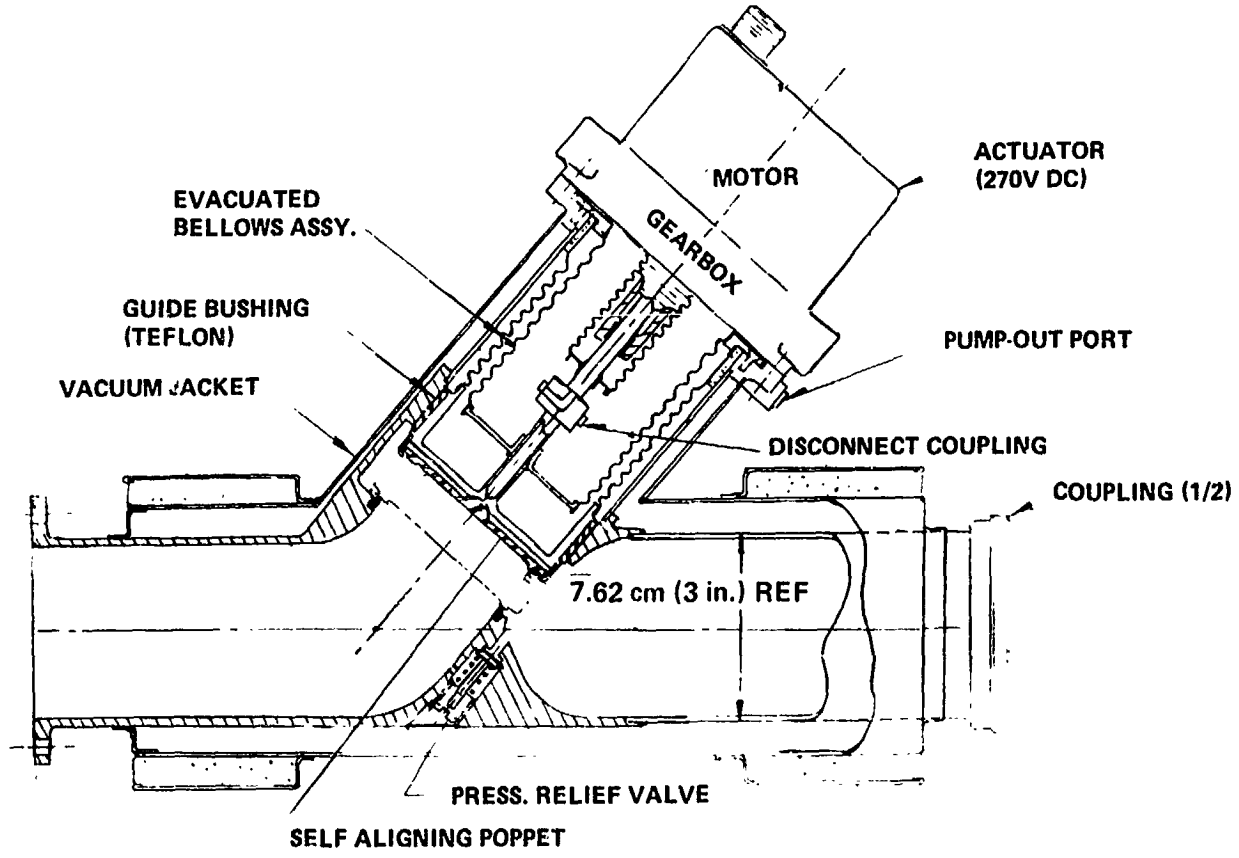

DET. B – FUELING SHUTOFF VALVE

Figure 79. - Continued.

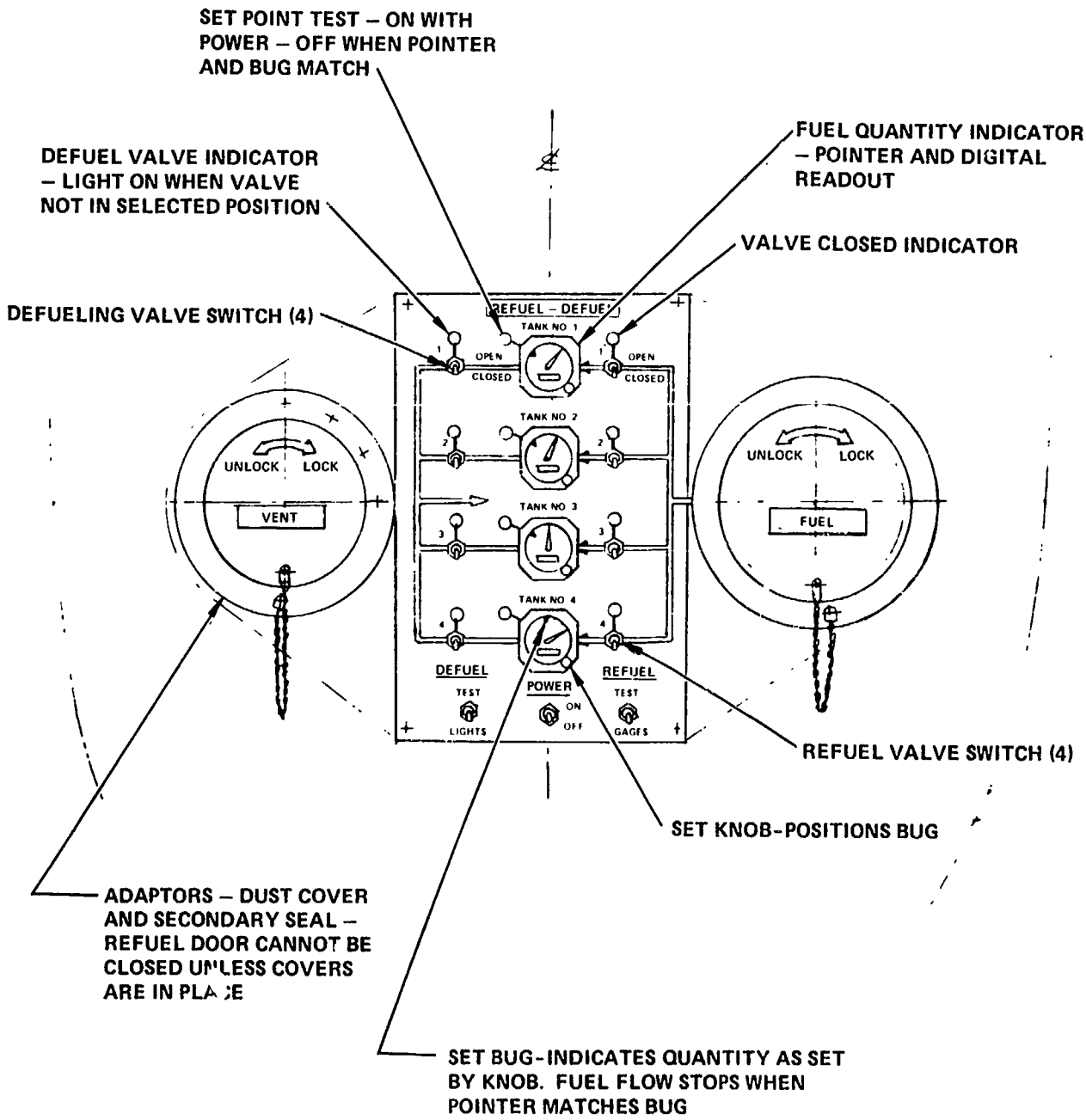

VIEW C-C – REFUEL PANEL

Figure 79. - Concluded.

Vapor released during the fueling operation flows through the absolute tank pressure regulators (Figure 79) into the common vent line where it is diverted to the vapor recovery adapter by means of a vent bypass valve built into the adapter and operated by the actuating linkage of the adapter (See Figure 79). The absolute pressure regulators prevent flashing of the fuel by maintaining the tank pressure above the saturation pressure of the delivered fuel.

The fuel tanks are protected from overpressurization in the event that a shutoff valve fails to close when the tank is full by limiting the ground system delivery pressure (Reference 2) and by sizing the vent lines to allow liquid hydrogen overflow through the vent system to the vapor recovery adapter.

Defueling is accomplished with both fueling and vapor recovery adapters connected to the airport defueling facility (Reference 2). The fuel transfer and refueling line tank isolation valves are then opened and the fuel level control valves are closed. Operation of the tank boost pumps will start the defueling operation. To maintain tank pressure above outside ambient, some heat may have to be added to the stored hydrogen by means of the fuselage-mounted tank pressurization heat exchanger which utilizes a calrod heating element to convert liquid hydrogen to gas. The tanks may be defueled individually or simultaneously.

6.3 Engine Fuel Supply

The engine fuel supply system is shown in Figure 77. Each engine is normally supplied fuel from its identically numbered fuel tank. In the event of engine failure, fuel from the tank which normally supplies the failed engine can be made available to the operating engines by a crossfeed system. However, the crossfeed system is not required for aircraft center of gravity control as will be discussed in 7.2, Operational Requirements of the Liquid Hydrogen Fuel System. A significant feature is the location and arrangement of the crossfeed valves. They are contained in one assembly for convenience in servicing and also to preclude long sections of transfer lines which would contain vapor and could result in engine flameout when switching from direct to crossfeed.

Lines leading to the engines are located in the wing box for protection and isolation. The lines are foam insulated within a protective metal outer tube. Evacuated double bellows lines with an outer braided cover are used where required for flexibility.

A surge box located at the low point in each fuel tank houses three boost pumps which supply fuel to each engine. The surge box traps fuel in the vicinity of the pumps to minimize unusable fuel, and to ensure its availability during unusual transient maneuvers. The present design utilizes a presurized accumulator downstream of the pump check valves to preclude engine starvation if the fuel migrates to the top of the surge box during negative or zero g flight.

The reasons for selection of a three-pump system rather than the two-pump arrangement used in conventional hydrocarbon-fueled aircraft are discussed in 5.3.1.

6.4 Auxiliary Power Fuel Supply

The APU is supplied liquid fuel, normally from Tank No. 2, but available from any tank by crossfeed. During the initial APU startup, before electrical power is available to the tank-mounted boost pumps, it is expected that the normal tank pressure 145 kPa (21 psia) will preclude the need for a separate APU tank-mounted boost pump. It is also possible that an external combustion engine may be a feasible method of driving an APU. This represents a change from a statement in Reference 1 which had indicated that the APU might operate on boiloff hydrogen. More detailed studies showed that this was impractical because of the wide variation in boiloff rates, and also because of the high compressor power required to raise the gas to conventional APU combustor pressure.

6.5 Fuel Transfer

Fuel transfer between tanks can be accomplished by opening the appropriate fuel transfer valves and fuel level control valves while operating the tank boost pumps. A fuel transfer system is incorporated to preclude trapping of fuel in any tank should the feed line tank isolation valve fail in the closed position. The effect of this type of failure on center of gravity travel is discussed in 8.3.3, Fuel Management.

6.6 Fuel Jettison

Inasmuch as this airplane meets the climb requirements of FAR 25.1001 (b) and (c) with full fuel load, a fuel jettison system is not legally required. However, some situations can be postulated in which a jettison system might be desirable. For example, if a wheels up landing is anticipated fuel could be jettisoned to reduce the landing speed. Assuming a full fuel load and climb to 3048 m (10 000 ft) the time to jettison fuel down to the reserve level would be approximately 1.4 hours. The jettison arrangement could be as shown on sheet 1 of Figure 79.

6.7 Tank Vent and Pressurization System

The forward pair of tanks and the aft pair of tanks have separate pressurization and vent systems but share a common overboard vent system downstream of the pressure regulators (see Figure 80). The tanks are maintained at an absolute pressure of 145 kPa (21 psia) by a primary absolute pressure regulator located just downstream of the point where the vent line emerges from each pair of tanks. A secondary pressure regulator set at an absolute pressure of 159 kPa (23 psia) is mounted in parallel with the primary regulator to protect the tank from excessive pressure in the event of failure of

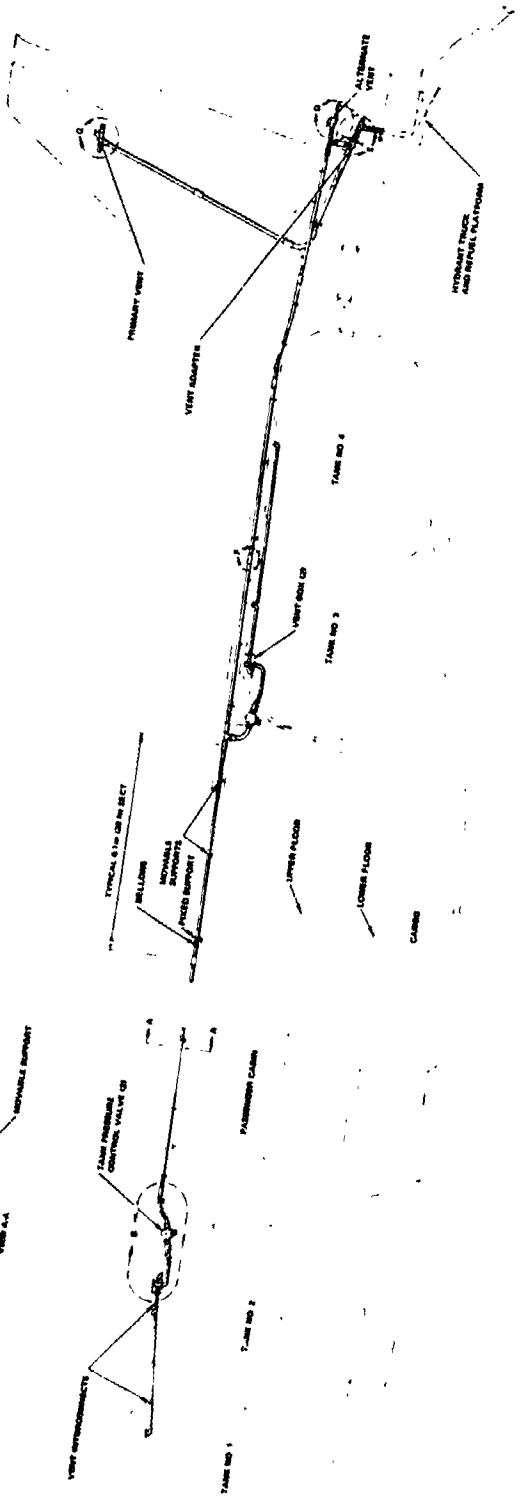

Figure 80. - Layout-vent and pressurization system.

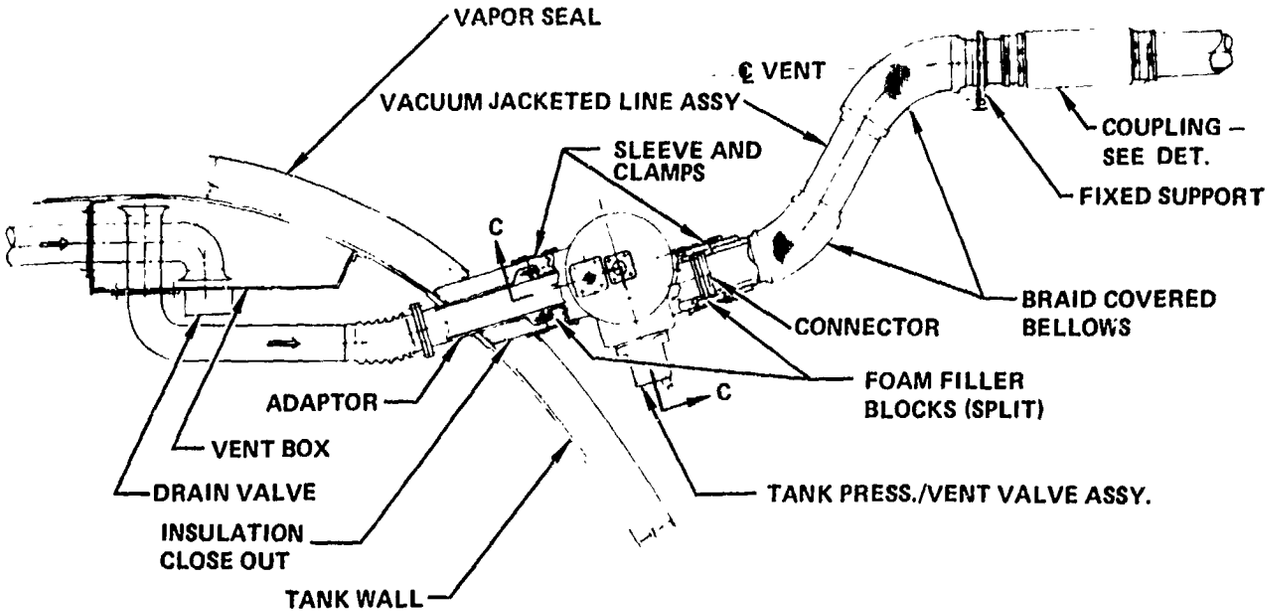

DET. B – TANK PRESSURE CONTROL VALVE INSTL.

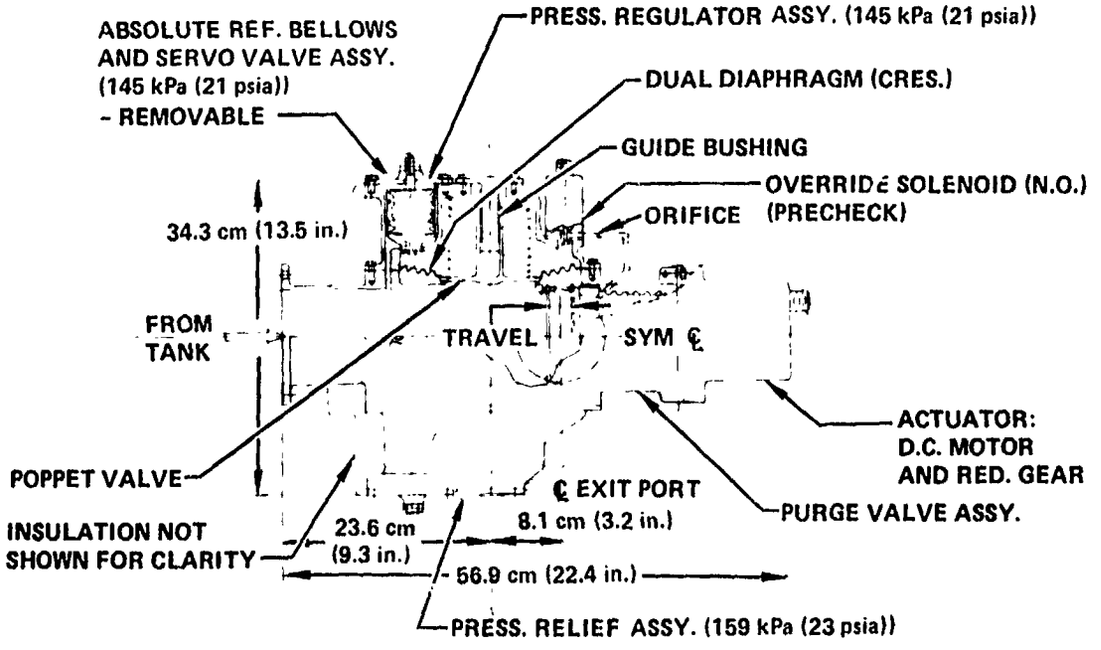

VIEW C-C – PRESS. CONTROL VALVE

Figure 80. - Continued.

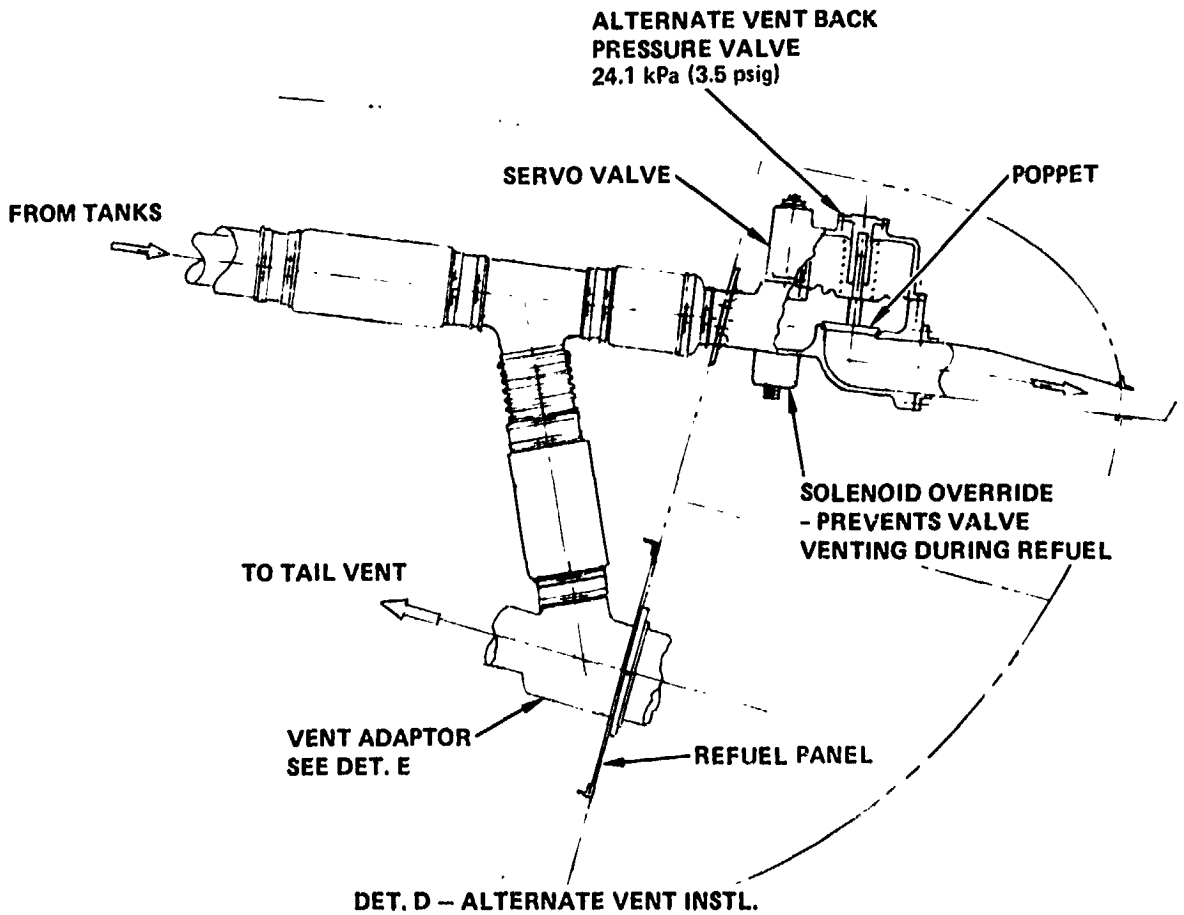

Figure 80. - Continued.

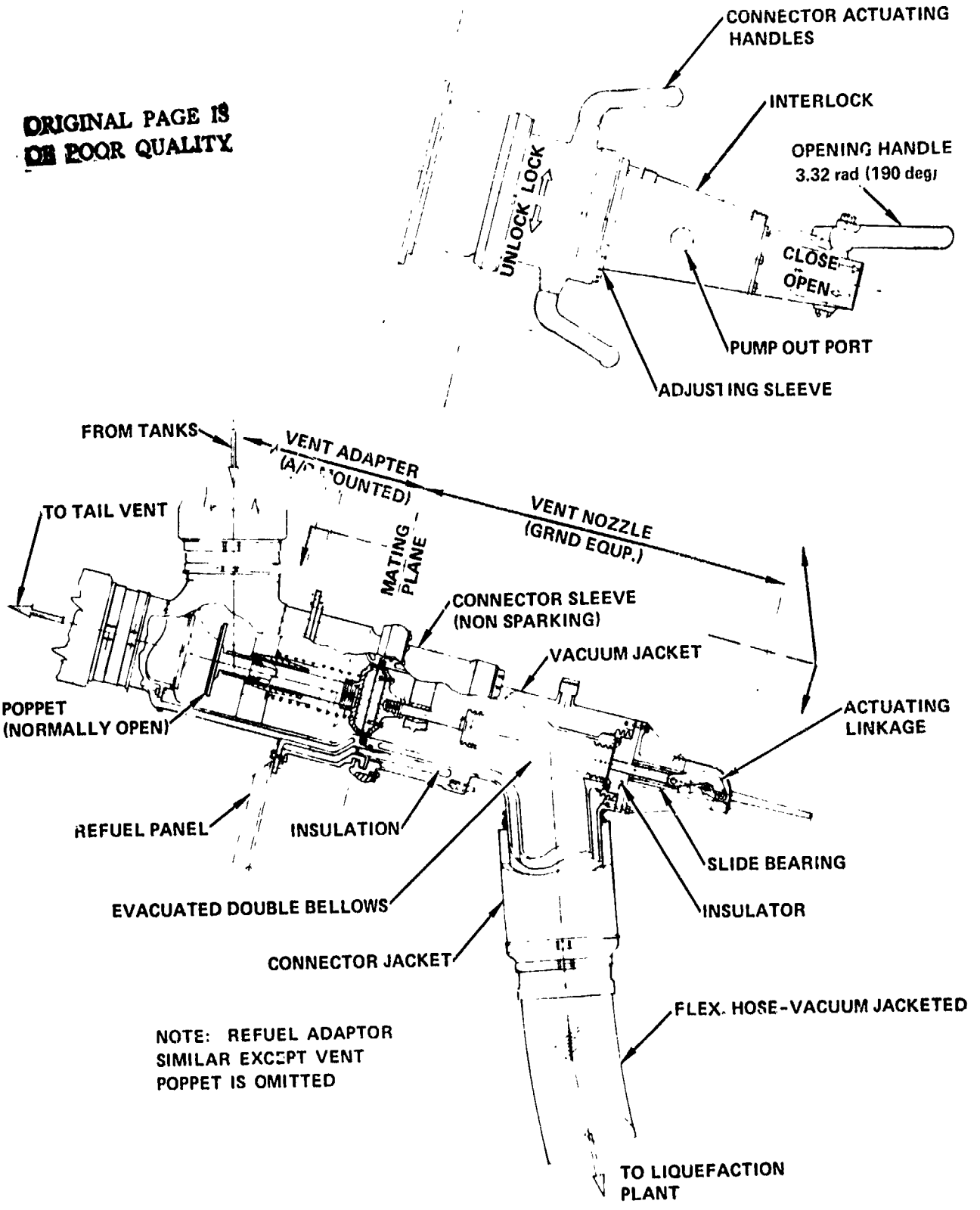

DET. E – VENT NOZZLE AND ADAPTOR

Figure 80. - Continued.

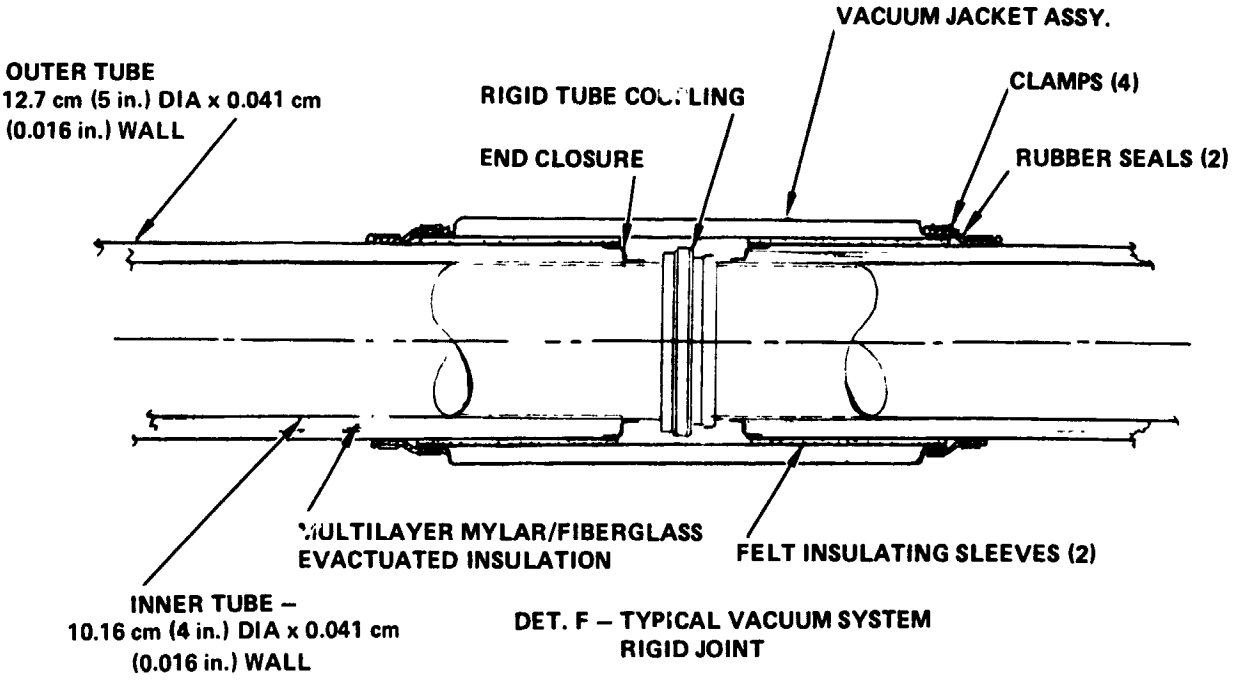

DET. F – TYPICAL VACUUM SYSTEM
RIGID JOINT

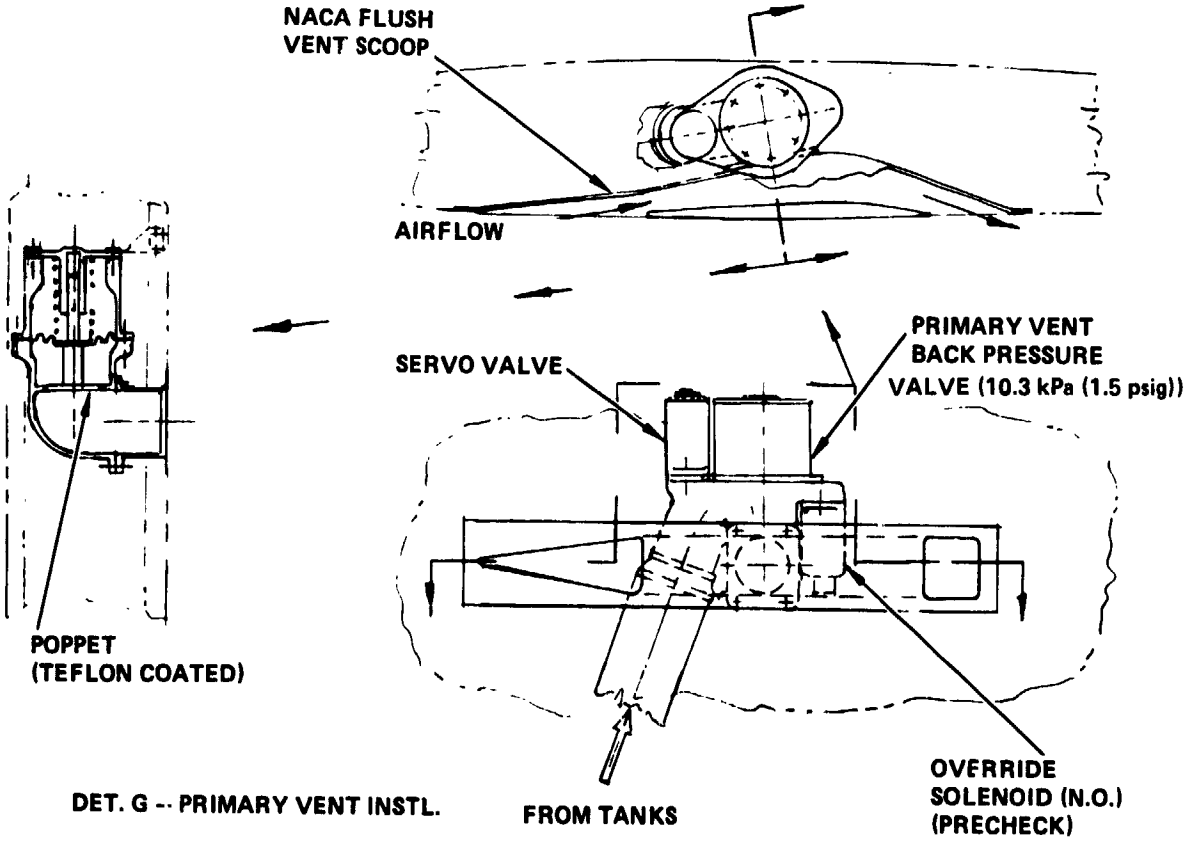

DET. G -- PRIMARY VENT INSTL.

Figure 80. - Concluded.

C-2

the primary regulator. A purge gas discharge valve for use during the initial tank fill and during tank purging for repair or inspection completes the valve assembly at this location. If the tank absolute pressure drops below 124 kPa (18 psia) when the boost pumps are operating, as might happen, for example, if a takeoff is attempted immediately after the tanks are filled with subcooled hydrogen, a backup absolute pressure regulator allows liquid flow normally supplied from Tank No. 4 to be evaporated at the fuselage-mounted tank pressurization heat exchanger. Tank pressures are, thus, always maintained above the minimum level.

Vent boxes located within Tanks 2 and 3 act as liquid traps to preclude liquid from passing overboard through the common vent line. A drain valve at the bottom of each trap allows the liquid fuel to drop down into the tank below when the fuel level is below the float in the drain valve. Each vent box communicates with the tank it serves through a single vent line with its inlet in the ullage bubble above the point of intersection of the fuel surfaces for maximum pitch attitude extremes with full fuel tanks. This represents the simplest and most reliable vent design. If detailed aircraft attitude studies reveal that no single inlet location will always be void of liquid fuel, an alternative design is available which incorporates two inlets in each vent line. The inlet which is remote to the vent box would be open at all times and the inlet near the vent box would be closed by means of a float-operated vent valve when under fuel but open when not covered by fuel. The added complexity of this system is to be avoided if possible since it places moving components within the fuel tanks which would ultimately require maintenance.

The common vent line downstream of the absolute pressure regulators serves a dual purpose. In flight, gas relieved through the pressure regulators is conveyed through the vent line to a lightning-protected overboard vent mounted in the vertical stabilizer. The overboard vent assembly includes a servo operated back-pressure valve set at 10.3 kPa differential (1.5 psig) to prevent air from being drawn into the vent where it could constitute a hazard. During fueling operations, the common vent serves as a means to recover large quantities of boiloff gases by routing them back to the vapor recovery adapter so that they can be recycled by the airport hydrogen liquefaction and distribution system. In the event of the failure of the primary vent an alternate servo operated vent set at 24.5 kPa (3.5 psig) is located in the tail cone area (Figure 80). This valve is closed by an override solenoid to prevent opening during fueling.

6.8 Nitrogen Inerting System

An investigation was made to determine the characteristics of a GN_2 inerting system which might be required to inert the space surrounding the nonintegral fuel tank (candidate A), and the engine supply system down to and including the engine pump and fuel control. The ground rules established for this study were:

1. The purge system is a flight dispatch item and must have dual redundancy in all functional aspects.

2. The quantity of N_2 carried must be sufficient to meet the most severe of the following: (a) one flight of 10 190 km (5500 n.mi.) + alternate destination + ground hold, or (b) two flights of 4050 km (2187 n.mi.) with ground hold and diversion to an alternate destination.

3. The minimum purge space pressure must be at least 1 psig above ambient to preclude ingestion of air due to local flight pressures above ambient free stream.

4. Leakage rates through fuselage structure based on improved L-1011 production aircraft experience.

5. N_2 purge system must prevent air ingestion during maximum emergency rate of descent.

6. N_2 to be stored as a liquid.

The most difficult aspect of the analysis was to predict what leakage might occur in a service aircraft. As a starting point the functional test procedure (FTP) required of all production L-1011's was reviewed. This requires that after blocking all valves, vents, and drains, the air leakage should not exceed 39 kg/min (87 lb/min) with a cabin differential pressure of 48 to 55 kPa (7 to 8 psi). Correcting this rate for leakage area, one psi differential and N_2 properties and temperatures, it was calculated that approximately 4990 kg (11 000 lb) of N_2 would be required for the 10 190 km (5500 n.mi.) flight profile. Since this is not reasonable, discussions were held with the L-1011 test personnel as to how this leakage might be reduced. The conclusion was that since much of the L-1011 leakage was due to the many door and window seals, feed-thrus, and hidden holes in structure, that in the LH_2 aircraft, with minimal access doors and careful attention to sealing of holes, this rate might be reduced to 10 or 15 percent. For purposes of this analysis, the 10 percent value was assumed.

A schematic of the system is shown in Figure 81. Cabin discharge air is used to heat the cryogenic LN_2.

The significant surface areas and volumes are:

	Surface Area m^2 (ft^2)	Vol. m^3 (ft^3)
Forward LH_2 tank compartment	216.7 (2333)	80.8 (2854)
Aft LH_2 tank compartment	220.6 (2375)	71.8 (2536)
Engine supply purge jacket (including engine pump and fuel control)	41.1 (442)	2.8 (99)
Total	478.4 (5150)	155.4 (5489)

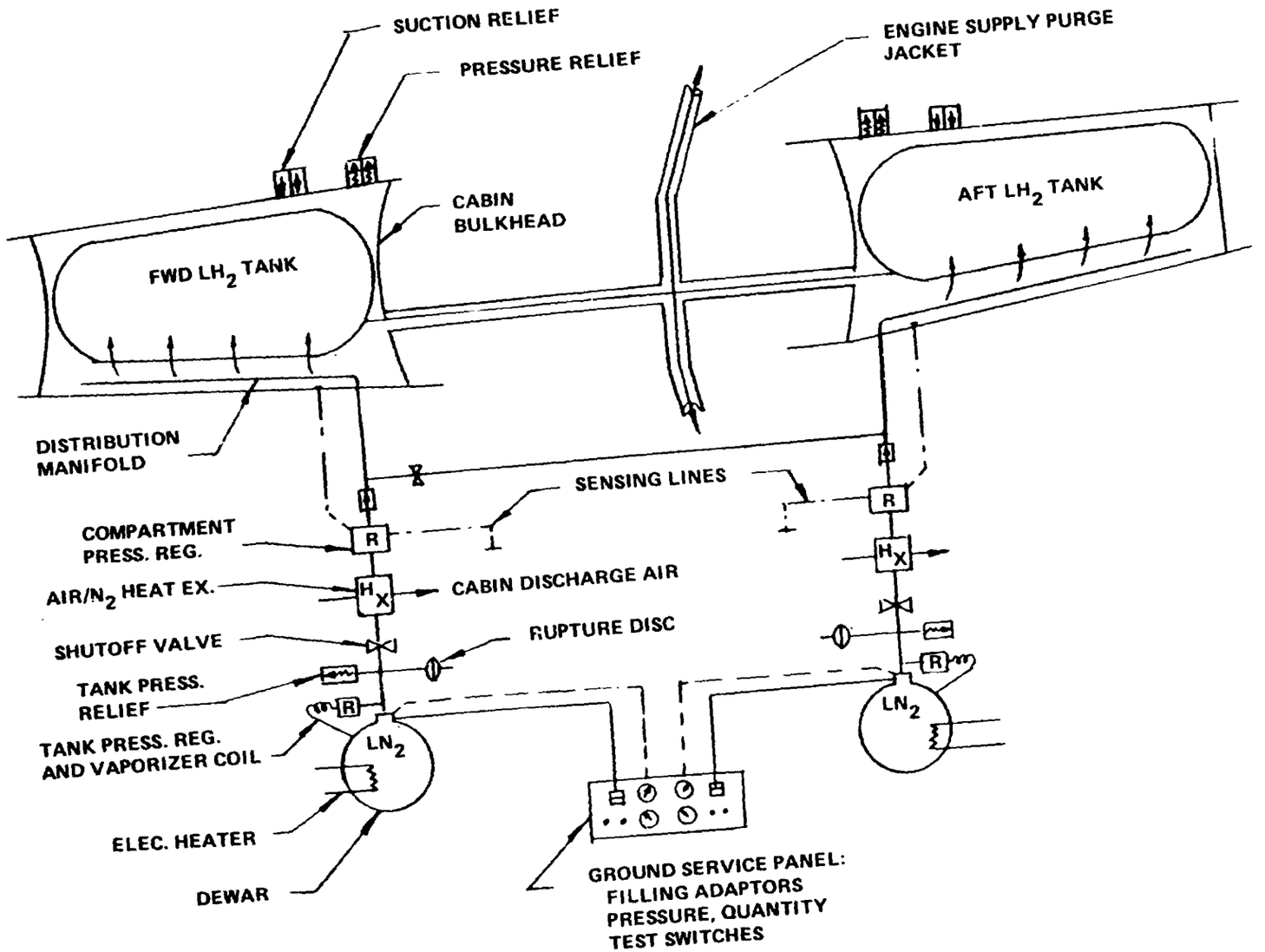

Figure 81. - N_2 purge system schematic.

Comparison of the mission profiles showed that the two 4050 km (2187 n.mi.) trips constituted the more severe requirement with regard to quantity of N_2 because of the more frequent climbs and descents. N_2 venting is required on climb with subsequent replenishment being necessary on descent. On this basis the following weights were estimated for the system:

LN_2 Required:

Compartment charging	838.7 kg	(1849 lb)
Leakage	467.2	(1030)
Residual N_2	32.2	(71)
Total	1338.1 kg	(2950 lb)

System Weights:

LN_2 Dewars (60 psig)	117.0 kg	(258 lb)
Equipment	45.4	(100)
Plumbing and shrouds	179.6	(396)
	342.0 kg	(754 lb)
+ 10 percent contingency	34.5	76)
Total System	376.5 kg	(830 lb)
+ LN_2	1338.1	(2950)
Total installed system + gas	1714.6 kg	(3780 lb)

The effect on DOC (assuming the LN_2 costs nothing since it is required for H_2 liquefaction) is equivalent to an increase of 1.53 percent in the baseline value of 0.99¢/s.km (1.8334¢/seat n.mi.). This is clearly undesirable, not only for the direct economic penalty, but also from the point of view of logistics and servicing.

An alternate concept was also examined in which the compartments are held at a constant absolute pressure. This saves the quantity of N_2 required for charging and recharging but increases the leakage so that the first quantity of LN_2 required is 1252 kg (2760 lb), almost as much as before. Further structural penalties would result from designing the tank compartments to withstand this pressure.

If the internal pressure differential could be reduced to 3.45 kPa (1/2 psig) the total system weight would be 1556 kg (3430 lb), a 9 percent reduction. The 3.45 kPa (1/2 psi) might be marginal, however, in preventing air ingestion under certain flight conditions.

The approach selected for the final candidate fuel containment systems A, B, C, and D consists of air purging and compartment ventilation where applicable, together with the leak detection at purge exits. This approach is further described in 8.6.1. N_2 inerting is used, however, in the flexible foam outer insulation layers of candidates no. 3 and no. 4 as described in 8.6.2.

The need for active inerting and choice of a final concept is dependent on service experience with an actual LH_2 fuel system in a developmental aircraft program.

6.9 Technology Developments Required

To establish the most promising fuel system design will require component and system design evaluations followed by detailed laboratory developmental testing. Areas in which this effort should be concentrated include the following:

6.9.1 Negative "g" operation. - The availability of fuel to the tank boost pumps must be assured at all times to prevent engine starvation. The present design proposes a pressurized accumulator downstream of the boost pumps. Other methods, such as double-ended boost pumps, should be investigated inasmuch as they may be lighter in weight and more reliable than the proposed accumulators.

6.9.2 Engine starting without boost pumps operating. - If the airplane is to be self-supporting, the engines and/or the APU must be capable of being started without the aircraft fuel tank boost pumps operating. Hence, the minimum inlet fuel pressure for starting the engines and/or the APU should be determined and compared to available pressure at the engine/APU inlet as a result of fuel tank pressurization.

6.9.3 Float-operated valve development. - Because of the low density of liquid hydrogen and permeability of most materials when subjected to hydrogen, the design of a float presents problems in sizing and material selection. The feasibility of floats to operate shutoff valves or switches should be investigated at an early date since they offer the simplest and most reliable method of sensing liquid levels.

6.9.4 Fuel quantity gauging. - A neutron radiation fuel gauge should be investigated for fuel quantity gauging. Neutrons will pass through the walls of the fuel tank quite easily and yet are attenuated proportionately to the density of the hydrogen they pass through. This would allow the gauging components to be placed external to the tank.

As an alternate, capacitance gauging is feasible and has been used in LH_2 but would require the insertion and support of long probes at multiple locations in each tank.

6.9.5 APU concepts - It is also desirable to make a preliminary investigation of of APU concepts for the H_2 fueled aircraft, including investigation of the utilization of H_2 boiloff as the fuel. This investigation would center around study of the feasibility of using the external combustion concept to facilitate the utilization of H_2 boiloff.